

EFFECTS OF MEMBRANE ACTION ON THE ULTIMATE STRENGTH  
OF REINFORCED CONCRETE SLABS

A thesis presented for the  
degree of Doctor of Philosophy in Civil Engineering  
in the University of Canterbury,  
Christchurch, New Zealand.

by

D. C. HOPKINS

1969

# ACKNOWLEDGEMENTS

I gratefully acknowledge the assistance that I have received during the course of this project and extend my thanks to:

Professor H.J. Hopkins, Head of Department, for his general supervision and guidance.

Professor R. Park for his valuable assistance and continued encouragement throughout the project and for his helpful advice during the preparation of this thesis.

Members of the academic staff, particularly Dr A.J. Carr, for their assistance.

Mr H.T. Watson, and members of the technical staff, particularly Messrs J. Sheard and N. Prebble, for their assistance with experimental work.

The University Grants Committee for financial assistance in the form of a Postgraduate Scholarship and a research grant.

Certified Concrete Limited for their assistance in making the model floor.

Mrs J.M. Keoghan for typing the manuscript.

Finally, I wish to thank my wife for her encouragement and assistance at all times.

## SUMMARY

This thesis describes an investigation of the effects of membrane action on reinforced concrete slabs, particularly the implications of allowing for compressive membrane action in the design of slab and beam floors.

An examination of the minimum reinforcement requirements of a rectangular slab reveals that high design live loads are required before the benefits of membrane action can be fully exploited. Studies of the effect of compression on the flexural capacity of a reinforced concrete section and of the effect of membrane action on a clamped circular slab with elastic lateral restraint at the circumference are undertaken. These show that lightly reinforced, thick slabs with high concrete strength will benefit most from compressive membrane action in practical situations, and that if the surround is flexible, tensile membrane action will be evident at the stage when the ultimate load of the slab is reached.

The effects of compressive forces in the panels on the design of the supporting beams is studied. It is shown that some beams are required to resist considerable tension and that membrane action may have considerable effect on

the torsion induced in the edge beams. A design method is derived to deal with beams subject to tension.

An investigation is then made of the lateral restraint provided at the edges of an interior panel by the surrounding panels, considered to be of elastic, homogeneous material.

An experimental study of a quarter-scale, nine-panel slab and beam floor was conducted. The equations derived by Park for the ultimate strength of slabs with compressive membrane action were used to design the floor. The membrane action was assessed as sufficient to double the Johansen ultimate load of the centre panel. A smaller enhancement was allowed for in the centre-edge panels and none was allowed for in the corner panels. The centre spans of all beams were designed to carry the tension induced by the compressive membrane forces in the panels.

Results of fourteen load tests on this model floor are analysed with particular reference to the effects of membrane action. Satisfactory behaviour at service load was observed and the floor sustained the predicted ultimate load before failure of the centre panel. The measurement of concrete and steel strains at critical sections revealed the presence of compressive membrane forces in the centre panel and tensions in the beams that were of the order expected.

A comparison of the volumes of steel reinforcement required in the model floor indicated that design including



compressive membrane action brings no advantage except when the additional steel that is required to resist the tensile forces induced in the beams can also be used to resist moments due to earthquake or other lateral loading of the structure.

It is concluded that allowance for membrane action in design would be of small benefit for normal slab and beam floors and would be of greatest use when very high loads are imposed on slabs with high lateral restraint at the edges.

## NOTATION

$a, a'$	Depths of the equivalent rectangular stress blocks at the ultimate flexural capacity of sections in regions of positive and negative moment respectively.
$A$	Gross area of a section.
$A_s, A'_s$	Areas of tension steel in slab or beam sections subject to positive and negative moment respectively.
$b$	Breadth of a rectangular section and of the web of a T- or L-section.
$b_f$	Breadth of flange of a T- or L-section.
$c'_c$	Force in concrete per unit length of a hogging moment yield line.
$d, d'$	Distances from the top of a section to the centroids of the tension steel, for positive and negative moments respectively.
$d_n$	Depth of the neutral axis of a section, measured from the compression face.
$D$	Overall depth of a beam or slab.
$e$	Strain - subscripts used are defined by Figures 7.7 and E.1.
$E$	Young's modulus.
$f_y$	Yield stress of steel reinforcement.
$f'_c$	Cylinder strength of concrete in compression.
$f_{ct}$	Tensile fracture stress of concrete.
$F$	Enhancement of the load capacity of a reinforced concrete slab due to membrane action, i.e., $F$ = the ratio of the ultimate load with membrane action to that calculated by Johansen's yield line theory.

$F_{max}$	Maximum attainable enhancement factor for a reinforced concrete section.
$F^*$	Average enhancement of the moment capacities of slab sections along yield lines necessary to produce a load enhancement of $F$ .
$G$	Shear modulus of concrete considered as an elastic, homogeneous material.
$i_s, i_L$	Ratios of hogging to sagging yield moments due to steel in the short and long directions of a slab.
$i_1, i_2$	Particular values of $i_s$ and $i_L$ .
$J$	Subscript denoting the value of a quantity at the Johansen ultimate load.
$k_1, k_2, k_3$	Constants defining the stress block for concrete in compression as proposed by Hognestad <u>et al.</u> (20)
$L_x, L_y$	Clear span plan dimensions of a rectangular slab in the $x$ and $y$ directions.
$m, m'$	Yield moment capacities, per unit length, along sagging and hogging moment yield lines respectively - taken as the moment of internal steel and concrete forces about the mid-depth of the slab.
$M, M'$	Moments at beam sections at mid-span and support, taken as the moment of internal actions taken about the mid-depth of the beam.
$m_J, M_J$	Values of $m, M$ at the Johansen ultimate load.
$M_{EQ}$	Value of $M$ due to earthquake loading only.
$M_{tmax}$	Maximum torsional moment in a beam.
$s$	Spacing of bars in slabs, or stirrups in beams.
$T_x, T'_x$	Tensions induced in an $x$ -direction beam due to compressive membrane action in the panels, i.e., the difference between the steel tension and concrete forces at a beam section in the span and at a support respectively (except as used in Appendix A).
$T_1 \dots T_6, T_B, T'_B, T''_B$	Also used to denote tension in beams.

$T_m$	The maximum torque in an edge beam supporting the square slab of Figure 4.4.
$u$	Cube strength of concrete in compression.
$v$	Volume of steel in a slab.
$V'_u$	Shear to be taken by stirrups.
$w$ or $w_M$	Ultimate load per unit area of slab with membrane action.
$w_J$	Johansen ultimate load per unit area of slab.
$W$	The sum of in-plane loads acting along each half of each edge of a surround.
$x, y$	Rectangular co-ordinates in a horizontal plane.
$\delta_F, \delta_S \dots$	Vertical deflection at points F, S...
$\Delta$	Lateral deflection of slab surround.
$\epsilon'_x, \epsilon'_y$	Ratios of the effective outward movement of the edge of a surround to the half span of the slab.
$\lambda_1, \lambda_2$	Parameters defining the length of top steel as in Figure 2.1.
$\mu$	(a) In Chapter 2: Ratio of the sagging yield moment, $M_x$ , in the x-direction to that in the y-direction, $M_y$ . (b) In Chapters 5 and 7 and in Appendix A: Poisson's ratio.
$\phi$	Capacity reduction factor as used in ACI 318-63.
<u>Notes:</u>	(i) Other symbols are defined in the text, generally by Equations or Figures and apply only to one Chapter. (ii) The notation used in Chapter 3 is defined in Figures 3.1 and 3.3 and within the text of the Chapter. Main symbols used are:
$K$	A measure of the flexibility of the restraining springs at the circumference.
$M_r, M_\theta$	Moments, per unit length, in the radial and circumferential directions respectively.

$M_o, M'_o$	Moment capacities per unit length of sagging and hogging moment yield lines respectively when no membrane forces exist at the section.
$q, q_J, q_M$	Intensities of the uniform load - in general, at the Johansen load, and at the enhanced load.
$Q_J, Q_M$	Total loads on the circular slab.
$Q_r$	Shear force, per unit length, at a radius, $r$ .
$T_o$	Force in the tension steel after yield.
$T_\theta, T_r$	Net tensions, per unit length, in the circumferential and radial directions.
$w$	Deflection of a point on the slab.
$w_o$	Deflection at the centre of the slab.

## CONTENTS

	Page
CHAPTER 1	INTRODUCTION AND SCOPE OF WORK
1.1	Introduction . . . . . 1
1.2	Object and Scope of Work Performed . . . . . 7
CHAPTER 2	MINIMUM STEEL REQUIREMENTS IN RECTANGULAR SLABS SUPPORTED ALONG ALL FOUR EDGES . . . . . 11
CHAPTER 3	A STUDY OF THE EFFECT OF MEMBRANE FORCES ON A REINFORCED CONCRETE SECTION AND ON A CIRCULAR SLAB WITH PARTIAL LATERAL RESTRAINT AT THE EDGES
3.1	Enhancement of the Moment Capacity of a Reinforced Concrete Section . . . . . 24
3.2	The Effect of Membrane Action on a Clamped Circular Slab Supported and Laterally Restrained at its Circumference 31
CHAPTER 4	THE EFFECT OF PANEL MEMBRANE ACTION ON THE DESIGN OF SUPPORTING BEAMS
4.1	Summary . . . . . 56
4.2	Determination of Beam Moments . . . . . 56

CHAPTER 4.3	The Effect of Panel Membrane Action on Torsion in Supporting Beams . . . . .	70
4.4	Discussion and Conclusion . . . . .	77
CHAPTER 5	STIFFNESS OF SURROUNDS FOR SQUARE SLABS	
5.1	Introduction and Summary . . . . .	79
5.2	Method of Analysis and Cases Considered . . . . .	80
5.3	Displacements of the Loaded Edges . . . . .	83
5.4	Stresses in the Surround . . . . .	86
5.5	Deep Beam Approximation . . . . .	86
5.6	Conclusions . . . . .	92
CHAPTER 6	DESIGN AND CONSTRUCTION OF A MODEL SLAB AND BEAM FLOOR	
6.1	Introduction . . . . .	95
6.2	General Design Basis and Specific- ations . . . . .	99
6.3	Design of Floor Panels . . . . .	102
6.4	Design of Beams . . . . .	109
6.5	Construction . . . . .	111
6.6	Material Properties and Final Slab Dimensions . . . . .	117
CHAPTER 7	INSTRUMENTATION AND TEST PROGRAMME	
7.1	Instrumentation . . . . .	122
7.2	Test Programme . . . . .	131
7.3	Reduction and Processing of Raw Data . . . . .	134

CHAPTER 8	TESTS ON THE PERFORMANCE OF THE METHOD USED TO CALCULATE SECTION ACTIONS	
8.1	Summary . . . . .	148
8.2	Tests on Special Control Specimens . .	148
8.3	The Effect of Variation in Strain Readings . . . . .	159
CHAPTER 9	BEHAVIOUR OF THE NINE-PANEL MODEL FLOOR DURING THE TEST PROGRAMME	
9.1	Summary . . . . .	163
9.2	Test by Test Description of Floor Behaviour . . . . .	168
9.2.1	Tests 101, 102, 105 and 106 . .	168
9.2.2	Tests 103 and 108 . . . . .	170
9.2.3	Tests 104 and 109 . . . . .	171
9.2.4	Tests 107, 110 and 111 . . . . .	172
9.2.5	Test to Failure of Floor as A Whole . . . . .	181
9.2.6	Test to Failure of Outer Panels . . . . .	190
9.3	Examination of Aspects of Floor Behaviour . . . . .	196
9.3.1	Deflections . . . . .	196
9.3.2	Strains . . . . .	203
9.3.3	Cracking . . . . .	209
9.3.4	Reactions . . . . .	213



	Page
9.3.5 Moments . . . . .	216
9.3.6 Membrane Action Effects . . . . .	232
CHAPTER 10 DISCUSSION OF TEST RESULTS	
10.1 Summary . . . . .	253
10.2 Discussion of Test Results . . . . .	253
10.3 Conclusions . . . . .	262
CHAPTER 11 A COMPARISON OF THE REINFORCING STEEL REQUIREMENTS OF THE MODEL FLOOR, DESIGNED WITH AND WITHOUT ALLOWANCE FOR MEMBRANE ACTION	
11.1 Introduction and Summary . . . . .	266
11.2 General Basis of Comparison . . . . .	267
11.3 Comparison of Steel Volumes . . . . .	269
11.4 Discussion . . . . .	271
11.5 Conclusions . . . . .	278
CHAPTER 12 GENERAL CONCLUSIONS	
12.1 Conclusions from Work Performed . . . . .	280
12.2 Suggestions for Further Research . . . . .	284
APPENDIX A DESIGN CALCULATIONS	
A.1 Park's Equations for the Ultimate Loads of Panels . . . . .	288
A.2 Design of Panels . . . . .	291
A.3 Design of Beams . . . . .	299
APPENDIX B MATERIAL PROPERTIES AND SLAB DIMENSIONS	

	Page
APPENDIX B.1 Concrete Properties . . . . .	305
B.2 Steel Properties . . . . .	306
B.3 Slab Dimensions . . . . .	308
APPENDIX C DETAILS OF LOAD INCREMENTS FOR THE TEST ON THE NINE-PANEL FLOOR . .	312
APPENDIX D REDUCED DATA FROM SLAB TEST	
D.1 Deflections . . . . .	314
D.2 Reactions . . . . .	321
D.3 Strains . . . . .	324
APPENDIX E COMPUTER PROGRAMME DESCRIPTION . . .	346
APPENDIX F RESULTS OF TESTS ON CONCRETE SLAB STRIPS . . . . .	350
REFERENCES . . . . .	355

## CHAPTER 1

### INTRODUCTION AND SCOPE OF WORK

#### 1.1 INTRODUCTION

In the calculation of the ultimate loads of two-way reinforced concrete slabs, the yield line theory due to Johansen<sup>(2)</sup> has been widely adopted. This theory does not include the effect of forces in the plane of the slab and under-estimates the ultimate loads of slabs when in-plane compressive forces are present because the compression enhances the ultimate moment of resistance of the section. In the common case of a lightly reinforced slab the large shift of the position of the neutral axis which occurs with cracking, causes a tendency for the edges of the slab to move outward as the slab deflects further. If the edges are restrained against outward movement, compressive forces are induced in the plane of the slab. The resulting enhancement of the load carrying capacity of the slab may be thought of as due to the enhancement of the moment capacities of the yield sections, or to an arching or doming effect in the slab as a whole.

Ockleston<sup>(3,4,5)</sup> has reported on tests on interior panels of a full scale slab and beam floor for which the

ratios of experimental ultimate load to predicted Johansen load (= enhancement factor) were greater than 2.5. The fact that Ockleston showed that this large increase could be accounted for by the development of in-plane compression has stimulated considerable research, both experimental and theoretical, into the phenomenon of membrane action in reinforced concrete slabs.

Powell<sup>(6)</sup> tested small scale rectangular slabs (36" x 20.57" x 1.286") with equal percentages of steel, top and bottom, in both directions. Experimental results revealed enhancement factors between 1.61 (for 1.53% reinforcement) to 8.25 (for .25% reinforcement).

Wood<sup>(7)</sup> tested three square panels (68" x 68" x 2.25) cast monolithically within a stiff reinforced concrete surround and obtained enhancement factors of 4.38 (for .25% reinforcement top and bottom) and 10.9 (for .25% steel on the bottom only).

In addition, Wood<sup>(7)</sup> analysed two cases of an isotropically reinforced, circular slab taking membrane action into account and assuming rigid-plastic materials. The first case was a simply supported slab with bottom reinforcement only, and the analysis gave a curve of enhancement factor versus load which rose parabolically from 1.0 at zero deflection until a central tensile membrane region started to spread outwards from the centre. The load continued to rise, almost linearly, with further

increase in central deflection as the growing tensile membrane was supported by a diminishing outer region under high compression. In the second case of a clamped circular slab, fully restrained against rotation and horizontal movement at the circumference, the assumption of rigid-plasticity gave maximum enhancement at zero deflection, with the slab in a state of maximum compression everywhere.

The enhancement at zero deflection was clearly an over-estimate of the collapse load of the corresponding real slab which deflects appreciably before full plasticity occurs. On the basis of a comparison of the maximum enhancement factor predicted by his theory with experimental values obtained in his own tests and those of Thomas<sup>(1)</sup>, Ockleston and Powell, Wood proposed reduction factors to be used in assessing the practical load carrying capacities of slabs for which conditions of restraint can be relied upon to induce compressive membrane forces.

Because one possible mode of collapse of a square slab involves only the enclosed circle, Wood's analyses applied well to square (or nearly square) slabs.

Analysis of other cases of unrestrained slabs made by Morley<sup>(18)</sup>, Kemp<sup>(17)</sup>, Sawczuk<sup>(37)</sup>, Taylor<sup>(14)</sup> and Hayes<sup>(19)</sup> have shown similar trends in slab behaviour to that of Wood's analysis of a simply supported circular slab. All analyses show that unrestrained slabs require large deflections to develop a useful degree of enhancement. The more

general case involving lateral restraint at the boundaries has more practical significance and has received considerable attention. Restrained slabs pose problems, especially in rectangular slabs with the lack of symmetry in the conditions of lateral edge restraint. The complexity of this situation has led researchers to study first the problem of a one way slab or slab strip, restrained at its ends. The related geometry of vertical deflections, neutral axis depths and outward movement of the ends forms the basis of these analyses.

Christiansen<sup>(10)</sup> related outward spread of the edges, movement of the restraining medium and elastic and plastic shortening of the slab to obtain the vertical deflection at which arching action provided greatest assistance. This theory showed good agreement with tests on four one way slabs tested by Christiansen but extension of the theory to two-way slabs was not carried out in detail.

Similar geometrical relationships were used by Liebenberg<sup>(8,9)</sup> in developing a theory for a restrained beam or slab strip, paying particular attention to the effect of the stress-strain relationship for concrete. Laboratory tests on restrained slab strips were performed to test the theory and to determine the values of empirical constants involved in it. Although favourable comparisons of theory and experiment were obtained, the empirical nature of the theory made its extension to the general case

of a two-way slab difficult.

More recently, Gurfinkel<sup>(16)</sup> has developed a computer programme to analyse simply supported beams with eccentric end restraint using the computed moment-curvature characteristic of the beam elements subject to axial compression. No experimental results were obtained to test the accuracy of the theoretical approach but the analysis is amenable to refinement and extension.

Park<sup>(11,12,13)</sup> has developed a theory for two-way slabs with membrane action to cover rectangular slabs restrained against horizontal movement and rotation along three or four edges. For the purposes of analysis the slab was envisaged as a series of strips running in both the long and short directions. The effect of outward movement of the edges and elastic creep and shrinkage strains was taken into account in relating the geometry of the deflected strips, the neutral axis depths and the magnitude of the membrane forces induced. Expressions were derived for the ultimate loads of the panels using virtual work analysis and an empirical value of central deflection at ultimate load.

Park tested 45 small scale rectangular slabs (60" x 40") in a very stiff surrounding frame. Slabs varied in thickness from 1.0" to 2.0", boundary conditions included either three or four edges laterally restrained and some tests were carried out with sustained loading.

Reinforcement ratios ranged from zero to 2.4 per cent and membrane action enhancement was considerable.

Park compared the ultimate loads of the slabs in his tests and those of Wood and Powell with very satisfactory results.

Brotchie, Jacobsen and Okubo<sup>(15)</sup> reported on tests on artificially restrained square slabs of 15" span. Thicknesses varied from 3" to  $\frac{3}{4}$ ", bottom steel of 0, 1.0, 2.0 per cent was provided and no top steel was used. Extremely high loads were sustained due to enhancement by membrane action. In some tests, load cells were incorporated in the restraining frame and the relationship between load and membrane force was obtained. Experimental results were compared with those of a theory derived on the assumption of rigid-plastic materials using the geometry of the yield line pattern and it was concluded that the increased load capacity and the improved behaviour produced by membrane action was sufficiently large and sufficiently predictable to warrant serious consideration in design. Further studies on the practical and economic implications of membrane action were suggested.

The experimental results of Powell, Wood, Park and Brotchie, Jacobsen and Okubo have shown that very large enhancement factors can be obtained for slabs, artificially restrained, against lateral movement at the boundaries.

The results of the full scale test carried out by



Ockleston reveal that considerable enhancement of load is available in practical situations. Further evidence of this nature is to be found in the report by Liebenberg<sup>(9)</sup> on tests on 50 panels of a full scale reinforced concrete building. Panels, both interior and exterior, were tested under three- or two-point loading and enhancement of the load carrying capacity was observed in all cases. Tests on a model floor at the University of Illinois<sup>(24)</sup> revealed enhancement by membrane action. The floor as a whole failed at 547 psf with a torsional failure of the spandrel beams. The central panel alone was then loaded to failure at 829 psf, an enhancement on the Johansen load of 1.94 and it appears that if the other panels and the supporting beams had been suitably designed, the whole floor could have sustained this high load.

Thus, in the practical situations where membrane action has been observed, not all panels of the floors have been loaded simultaneously to the enhanced load and consequently the beams have not been loaded to capacity.

The aim of the work described in this thesis is to investigate the feasibility of designing panels of multi-panel slab and beam floors to allow for membrane action and to investigate the structural and economic implications of such a procedure.

## 1.2 OBJECT AND SCOPE OF WORK PERFORMED

As an initial part of the study of the economy

resulting from, and the feasibility of, designing slabs allowing for membrane action, the conditions leading to minimum reinforcement content in an orthotropically reinforced concrete slab without membrane action are studied. Variables studied include the coefficient of orthotropy, the ratio of hogging to sagging yield moments and the regions of load intensity for which the minimum steel requirements of codes of practice govern the amount of steel placed.

The effects of compression on the ultimate moment capacity of a singly reinforced concrete section are then examined in so far as these determine the maximum enhancement factor attainable in slabs of uniform thickness with passive edge restraint.

This study is followed by an extension of Wood's analysis of a clamped circular slab of rigid-plastic material<sup>(7)</sup>. The analysis is extended to include elastic edge restraint, unequal top and bottom reinforcement and the tensile membrane range. Results of the extended theory are compared with tests on laterally restrained square slabs.

In a multi-panel slab and beam floor when membrane action exists in the panels, tensions are induced in the beams. The effect of this beam tension on the flexural capacity of the beam is examined and a design method derived.

The presence of membrane forces normal to the edge of the supporting beams, particularly edge beams is studied with particular reference to the torsion induced in the beams.

Of particular importance in the assessment of the effects of membrane action enhancement in reinforced concrete slabs is the outward movement at the edges of the slab. For an interior panel of a multi-panel slab and beam floor, the amount of lateral movement occurring at the edges is dependent upon the stiffness of the surrounding panels with respect to in-plane forces. A surround of elastic, isotropic material is analysed using a plane stress finite element computer programme. Data on the edge movements and stresses in the surround is obtained. Because this analysis is slow, the accuracy of considering the sides of the surround as deep beams is investigated. Direct determination of the surround movement would be of great assistance in developing a theory involving the interaction of the edge forces due to panel membrane action and the outward movement of the surround.

To test the feasibility of designing floors with allowance for membrane action, Park's existing theory is used to design a nine-panel model floor. Panels are designed with allowance for compressive membrane action enhancement and the beams designed to carry the tensions induced. The behaviour of the floor as a whole, of the

centre panel, and of the beams is of particular interest in this experimental study with respect to both serviceability and ultimate strength.

Electrical resistance strain gauges were used to measure membrane forces in the panels and tensions in the beams. A study of the accuracy and sensitivity of the method used to measure these forces includes laboratory tests on control specimens.

Behaviour of the model floor is examined with particular reference to the effects of membrane action on serviceability, cracking, deflections, strain levels, the ultimate strength of the floor as a whole and the levels of membrane compression in the panels and tensions in the beams.

A comparison of the total steel volume requirements of the model floor is made between the design method used and design without allowance for membrane action. The use of steel provided in the beams for earthquake moments to resist the tension induced by membrane action is studied as part of this comparison.

Finally, general conclusions are drawn from the results of the studies made and topics for further research are discussed.

## CHAPTER 2

### MINIMUM STEEL REQUIREMENTS IN RECTANGULAR SLABS SUPPORTED ALONG ALL FOUR EDGES

#### 2.1 INTRODUCTION

As a preliminary to studying the effects of membrane action on the behaviour of reinforced concrete slabs, conditions required to give the minimum steel in a rectangular slab were investigated. The following study was restricted to slabs in which top and bottom reinforcement were uniformly spaced and the ratio of hogging to sagging yield moment was equal along opposite edges. The dimensions and properties of the slab considered are shown in Figure 2.1 (a) and (b). The eight possible collapse patterns of this slab are shown in Figure 2.1(c) to (j). Patterns (c), (d), (e), and (f) all involve a central sagging yield line parallel to the  $L_y$  direction, whereas patterns (g), (h), (i), and (j) have this central yield line running parallel to the  $L_x$  direction and although the latter appear less likely to occur, they cannot be disregarded.

All patterns were considered in the following analysis in which the values of  $\mu$ ,  $i_1$ ,  $i_2$ ,  $\lambda_1$ ,  $\lambda_2$  were varied for a slab of given  $L_y/L_x$  ratio. In each case the volume of

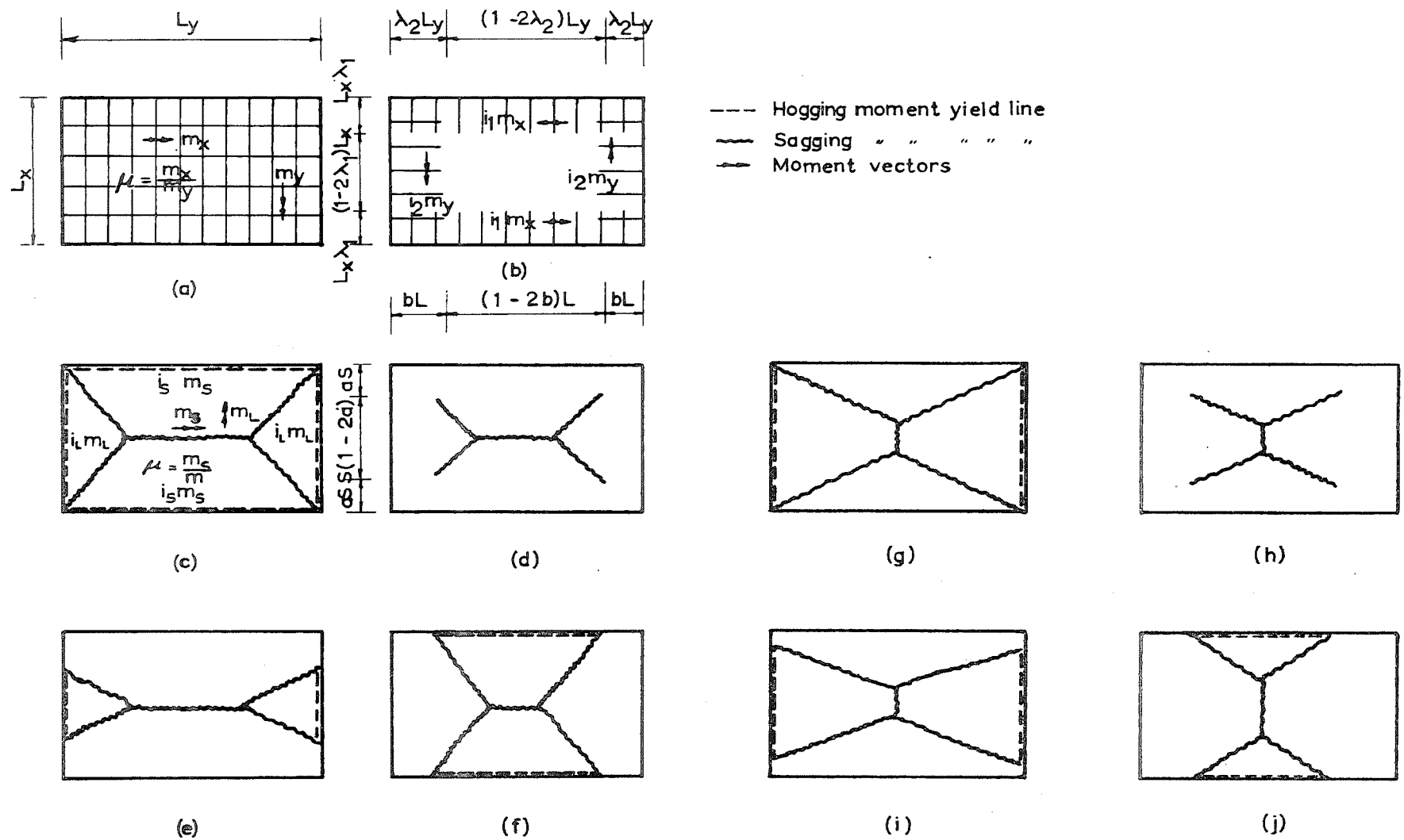


FIGURE 2.1 RECTANGULAR SLAB AND POSSIBLE FAILURE MECHANISMS

steel required for the slab was calculated and the conditions giving minimum steel volume were determined. As a result, optimum values of  $i_1$  and  $i_2$  were found; values of  $\lambda_1$ ,  $\lambda_2$  were related to  $i_1$ ,  $i_2$ ; and  $\mu_e$ , the most economical coefficient of orthotropy was determined as dependent upon  $L_y/L_x$ ,  $i_1$  and  $i_2$ .

In many cases, especially when  $\mu_e$  took high values, minimum reinforcement conditions were seen to govern.

## 2.2 VOLUME OF STEEL IN SLAB

For a lightly reinforced section, the moments per unit width are given by:

$$\begin{aligned} m_x &= A_{sx} f_y (d_x - a/2) & a &= A_s f_y / .85 f'_c \\ m_y &= A_{sy} f_y (d_y - a/2) & & \dots(2.1) \end{aligned}$$

similar expressions resulting for the hogging yield moments. For very lightly reinforced sections the value of 'a' is small relative to  $d_x$  or  $d_y$  and for the purposes of studying minimum steel requirements it may be assumed that  $d_x = d_y$ .

It is therefore reasonable to assume that  $m_x$  and  $m_y$  vary directly with the area of steel,  $A_s$ , in exactly the same manner. Therefore, in general,  $A_s = km$  where  $k$  is a constant incorporating  $d_x$  and  $f_y$ .

The volume of steel,  $V$ , is then given by

$$V = k L_x L_y m_y (1 + \mu) + 2k L_x L_y m_y (i_1 \lambda_1 / \mu + i_2 \lambda_2) \dots(2.2)$$

(bottom steel)                      (top steel)

### 2.3 COLLAPSE MODES OF SLAB

Figures 2.1(c) and (d) show the two most probable collapse modes.

In (c) full hogging moments are developed around the edges of the slab and full sagging yield moments developed along the sagging yield lines as shown.

In (d) the portion of the panel without top reinforcement fails as a simply supported slab of reduced span lengths. Collapse patterns (e), (f), (g), (h), (i), (j) were not considered at this stage, but it will be shown that the conditions imposed by modes (c) and (d) require little or no modification when the other patterns are considered.

The collapse load of mode (c) may be shown to be <sup>(7)</sup>,

$$w_c = \frac{24 m_y \mu^2 (1 + i_1)}{L_x \left( \frac{L_x}{L_y} \right)^2 \left[ \sqrt{\frac{1+i_1}{1+i_2}} + 3\mu \left( \frac{L_y}{L_x} \right)^2 - \sqrt{\frac{1+i_2}{1+i_1}} \right]^2} \dots (2.3)$$

and since mode (d) is a special case of (c) for which  $i_1 = i_2 = 0$ ,  $L_x = (1-2\lambda_1)L_x$ ,  $L_y = (1-2\lambda_2)L_y$ :

$$w_d = \frac{24 m_y \mu^2}{L_x \left( \frac{L_x}{L_y} \right)^2 \frac{(1-2\lambda_1)^4}{(1-2\lambda_2)^2} \left[ \sqrt{1 + 3\mu \frac{(1-2\lambda_2)^2 L_y^2}{(1-2\lambda_1)^2 L_x^2}} - 1 \right]^2} \dots (2.4)$$

The minimum length of top steel may be obtained by equating  $w_c = w_d$ . The resulting relationship between  $i_1$ ,  $i_2$ ,  $\lambda_1$



and  $\lambda_2$  is

$$\frac{(1-2\lambda_1)^2}{(1-2\lambda_2)} \left[ \sqrt{1 + 3\mu \left(\frac{L_y}{L_x}\right)^2 \frac{(1-2\lambda_2)^2}{(1-2\lambda_1)}} - 1 \right] =$$

$$\sqrt{\frac{(1+i_2)}{(1+i_1)^2}} \left[ \sqrt{1 + 3\mu \left(\frac{L_y}{L_x}\right)^2 \frac{(1+i_1)}{(1+i_2)}} - 1 \right] \quad \dots(2.5)$$

Comparison of similar terms on the left and right sides of Equation 2.5 gives:

$$\frac{(1-2\lambda_1)^2}{(1-2\lambda_2)} = \sqrt{\frac{(1+i_2)}{(1+i_1)^2}} \quad \dots(2.6)$$

$$\text{and} \quad \frac{(1-2\lambda_2)^2}{(1-2\lambda_1)} = \frac{1+i_1}{1+i_2} \quad \dots(2.7)$$

Equating values for  $(1-2\lambda_1)^2$  given by each of 2.6 and 2.7 gives:

$$\frac{(1-2\lambda_2)}{(1+i_1)} \sqrt{1+i_2} = \frac{(1-2\lambda_2)^2 (1+i_2)}{(1+i_1)} \quad \dots(2.8)$$

which reduces to:

$$1-2\lambda_2 = \frac{1}{\sqrt{1+i_2}} \quad \dots(2.9)$$

and similarly

$$1-2\lambda_1 = \frac{1}{\sqrt{1+i_1}} \quad \dots(2.10)$$

Thus  $\lambda_1$  and  $\lambda_2$  may be determined if  $i_1$  and  $i_2$  are known.

#### 2.4 MOST ECONOMICAL COEFFICIENT OF ORTHOTROPY, $\mu_e$

The value of  $\mu$  which gives the least volume of steel in the slab may be determined by setting  $\frac{\partial V}{\partial \mu} = 0$ .

From Equation 2.2:

$$V = k L_x L_y m_y (1 + \mu + 2 i_1 \lambda_1 \mu + 2 i_2 \lambda_2) \quad \dots (2.2a)$$

$$\text{and } m_y = \frac{w L_x^2 \left(\frac{L_y}{L_x}\right)^2 t^2 (1 - 2 \lambda_1)^4}{24 \mu^2 (1 - 2 \lambda_2)^2} \quad \text{from Equation 2.4.}$$

$$\text{in which } t = \sqrt{1 + 3\mu \left(\frac{L_y}{L_x}\right)^2 \frac{(1 - 2 \lambda_2)^2}{(1 - 2 \lambda_1)^2}} - 1 \quad \dots (2.11)$$

For differentiation with respect to  $\mu$ , values of  $i_1$ ,  $i_2$ ,  $L_x$ ,  $L_y$  will be constant and therefore substitution for  $m_y$  in Equation 2.2a gives:

$$V = K \left[ \frac{t^2}{\mu^2} (1 + 2 i_2 \lambda_2) + \frac{t^2}{\mu} (1 + 2 i_1 \lambda_1) \right]$$

$$\therefore \frac{1}{K} \frac{\partial V}{\partial \mu} = (1 + 2 i_2 \lambda_2) \left( \frac{2t}{\mu^2} \frac{\partial t}{\partial \mu} - \frac{2t^2}{\mu^3} \right) + (1 + 2 i_1 \lambda_1) \left( \frac{2t}{\mu} \frac{\partial t}{\partial \mu} - \frac{t^2}{\mu^2} \right) \quad \dots (2.12)$$

= 0 for minimum V.

Now from Equation 2.11:

$$t^2 + 2t = 3\mu \left(\frac{L_y}{L_x}\right)^2 \frac{(1 - 2 \lambda_1)^2}{(1 - 2 \lambda_2)^2}$$

$$\therefore \frac{\partial t}{\partial \mu} = \frac{3\mu}{2(t+1)} \left(\frac{L_y}{L_x}\right)^2 \frac{(1 - 2 \lambda_1)^2}{(1 - 2 \lambda_2)^2}$$

Substitution for  $\mu$  and  $\frac{\partial t}{\partial \mu}$  in  $\frac{\partial V}{\partial \mu} = 0$  gives

$$t+1 = 3 \left(\frac{L_y}{L_x}\right)^2 \frac{(1 + 2 i_2 \lambda_2)(1 - 2 \lambda_1)^2}{(1 + 2 i_1 \lambda_1)(1 - 2 \lambda_2)^2} - 1$$

which is the condition for minimum volume.

Substitution for  $t+1$  from Equation 2.11, squaring, and collecting terms leads to the result:

$$\mu_e = \frac{3\left(\frac{L_y}{L_x}\right)^2 \left(\frac{1-2\lambda_2}{1-2\lambda_1}\right)^2 - 2\left(\frac{1+2i_1\lambda_1}{1+2i_2\lambda_2}\right)}{\left(\frac{1+2i_1\lambda_1}{1+2i_2\lambda_2}\right)^2} \dots (2.13)$$

which corresponds to the result stated by Wood<sup>(7)</sup>. The validity of Equations 2.3 to 2.13 is limited to the range of  $i_1$  and  $i_2$  values for which the collapse mode is of the form shown in Figure 2.1(c). In particular, the central sagging yield line must be parallel to  $L_y$ . For the symmetrical rectangular slab under consideration, this condition is fulfilled if  $\mu \geq \left(\frac{L_x}{L_y}\right)^2 \left(\frac{1+i_2}{1+i_1}\right)$ .

## 2.5 MOST ECONOMICAL VALUES OF $i_1$ and $i_2$

The values of  $i_1$  and  $i_2$  which give the least volume of steel could be determined by differentiation of Equation 2.2 but this is difficult and tedious and a simple computer programme was written to investigate the effects of  $i_1$  and  $i_2$  on the steel volume.

For each  $L_y/L_x$  ratio steel volumes were calculated for a range of  $i_1$  and  $i_2$ . For each combination of  $i_1$  and  $i_2$ ,  $\mu_e$  was calculated before the volume of steel was computed.

In all cases the combination of  $i_1 = i_2 = 2.0$  gave minimum volume. For a square slab, the differentiation of

the volume expression with respect to  $i$  ( $= i_1 = i_2$ ) does, in fact, give  $i = 2.0$  for minimum steel.

For  $L_y/L_x \approx 1.0$  greatest economy is thus achieved if  $i_1 = i_2 = 2.0$ , provided  $\mu_e$  can be attained.

## 2.6 EFFECT OF OTHER COLLAPSE MODES

### (i) Modes (c), (d), (e), and (f)

By considering modes (e) and (f) as special cases of mode (c) it may be shown that, provided  $\lambda_1$  and  $\lambda_2$  are calculated from Equations 2.9 and 2.10, modes (c), (d), (e), (f) have identical collapse loads for any given value of  $\mu$ .

### (ii) Modes (g), (h), (i), (j)

Since these bear the same relation to each other as (c), (d), (e), (f), the collapse loads of patterns (g), (h), (i), (j) are identical. It is thus necessary to find the regions of  $L_y/L_x$ ,  $i_1$  and  $i_2$  for which the latter modes have a lower collapse load than the former. To achieve this the loads of each set were computed for a range of  $L_y/L_x$ ,  $i_1$  and  $i_2$  ( $\lambda_1$  and  $\lambda_2$  were calculated using Equations 2.9 and 2.10; the coefficient of orthotropy,  $\mu$ , was always set at  $\mu_e$  as given by the particular values of  $L_y/L_x$ ,  $i_1$  and  $i_2$ ). Under these conditions, modes (g), (h), (i), (j) governed only when  $L_y/L_x$ ,  $i_1$  and  $i_2$  were such that mode (c) was not valid initially for the calculation of  $\mu_e$ . By considering the case when the collapse pattern

consists of diagonal yield lines, it may be shown that the initial collapse mode is valid if the value of  $\mu_e$  calculated therefrom (Equation 2.13) satisfies

$$\mu_e \geq \left(\frac{L_x}{L_y}\right)^2 \frac{(1+i_2)}{(1+i_1)} \quad \dots(2.13a)$$

Only in exceptional cases will this condition not be satisfied since for economy  $i_1 \approx i_2$  and  $\mu_e \approx 3\left(\frac{L_y}{L_x}\right)^2 - 2$

i.e.  $\mu_e$ , increases with  $L_y/L_x$  while its minimum allowable value decreases.

The analysis of modes (c) and (d) will therefore provide sufficient check unless Equation 2.13a is not satisfied.

## 2.7 PRACTICAL IMPLICATIONS AND LIMITATIONS

For a slab of chosen  $L_y/L_x$ , three parameters were investigated for a range of  $i_1$  and  $i_2$  values in order to assess the practical usefulness of Equation 2.13. The parameters investigated were: (i) the most economical coefficient of orthotropy; (ii) the volume of steel required in the slab; and (iii) the range of load and  $i$  values for which minimum reinforcement requirements do not govern.

### (i) Variation of Most Economical Coefficient of Orthotropy

The variation of  $\mu_e$  with  $i_1$  and  $i_2$  was determined for

a given  $L_y/L_x$  ratio by using Equation 2.13. Values of  $i_1$  and  $i_2$  between 0 and 3.0 were used. For each combination,  $\lambda_1$  and  $\lambda_2$  were determined by Equations 2.9 and 2.10 and  $\mu_e$  calculated. Values of  $\mu_e$  were plotted on an  $i_1$  vs  $i_2$  graph and contours of equal  $\mu_e$  drawn in the regions where the value of  $i_2$  did not invalidate the assumed failure mechanism.

Figure 2.2 shows these graphs for  $L_y/L_x = 1.0$  and  $2.0$ .

### (ii) Variation of Steel Volume

In this investigation the value of  $\mu_e$  was calculated and used to find the values of  $m_x$  and  $m_y$ . The value of  $m_y$  was found from Equation 2.4 and the percentage of steel,  $p$ , calculated using the equation  $pd^2f_y = m$ , based on the assumption that the depth of the rectangular stress block,  $a$ , is zero.

From 2.4

$$\frac{m_y}{f'_c d^2} = \frac{w \left( \frac{L_x}{d} \right)^2}{24 f'_c} \left( \frac{L_x}{L_y} \right)^2 \frac{1}{\mu^2} \frac{(1-2\lambda_1)^4}{(1-2\lambda_2)^2} \dots (2.4b)$$

in which  $\frac{w \left( \frac{L_x}{d} \right)^2}{24 f'_c} = W_R$  is a convenient non-dimensional measure of the load which, for the purposes of this investigation, was kept high so that minimum reinforcement conditions were not encountered in the range of values of  $i$  and  $L_y/L_x$  investigated. From the values of percentage steel volume calculated for each combination of  $i_1$  and  $i_2$ , contours of equal volume were plotted for valid regions on

FIGURE 2.2 VARIATION OF  $\mu_e$

21

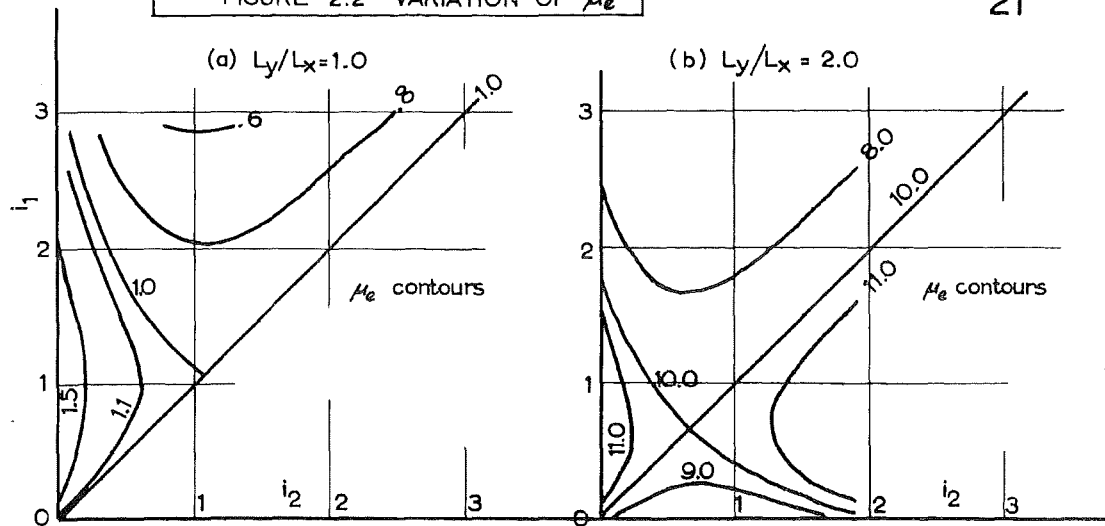


FIGURE 2.3 VARIATION OF STEEL VOLUME

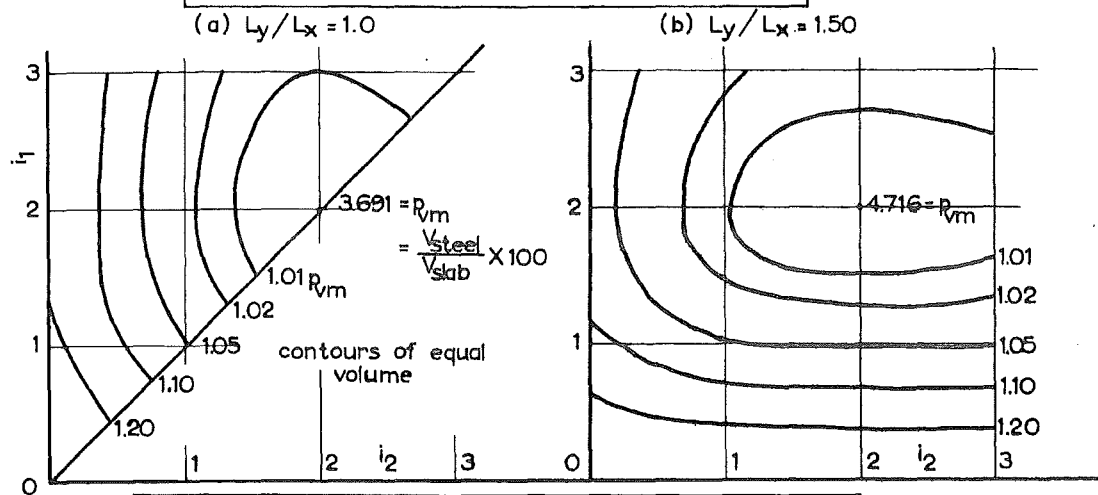
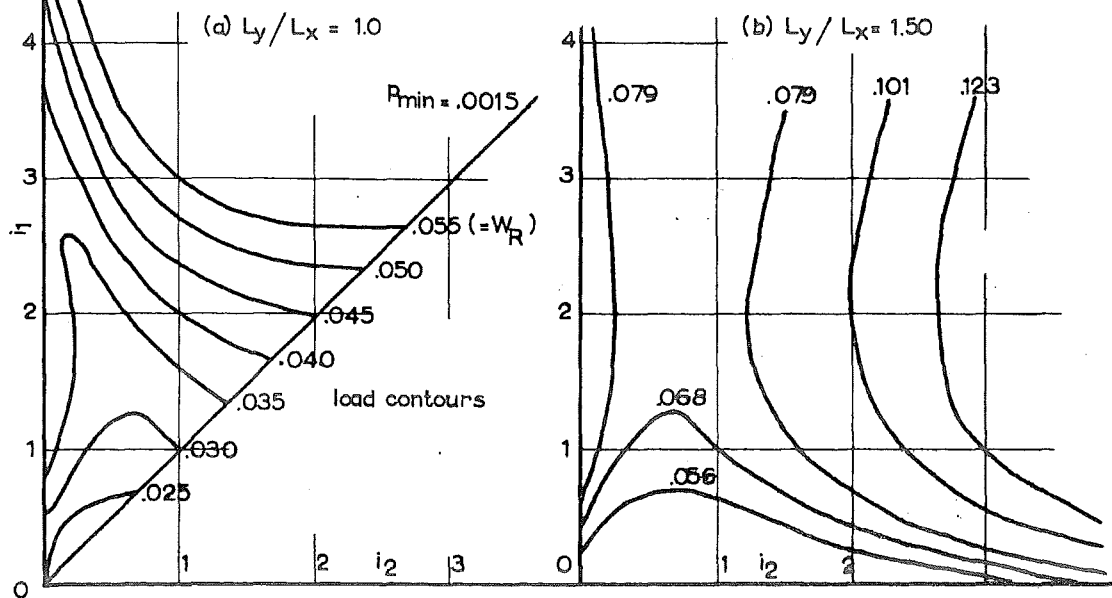


FIGURE 2.4 MINIMUM REINFORCEMENT BOUNDARIES



the  $i_1$  vs  $i_2$  graphs. Figure 2.3 shows these contours for  $L_y/L_x = 1.0$  and  $1.5$ .

(iii) Minimum Reinforcement Restriction Imposed by Codes of Practice

For each value of  $L_y/L_x$ , a range of load parameters was used, for each of which the contour on the  $i_1$  vs  $i_2$  diagram was found which marked the boundary beyond which minimum reinforcement restrictions would govern.

The steel percentage was calculated on the basis described in (ii) above. In all cases  $\mu_e$  was calculated before  $m_y$  and  $p$ .

Figure 2.4 shows contours of equal  $W_R$  for  $L_y/L_x = 1.0$  and  $1.5$ . The minimum steel percentage allowed in these figures was .15 per cent as in the British Code of Practice CP114.

## 2.8 DISCUSSION

Figures 2.2, 2.3 and 2.4 show clearly the effect of the various parameters.

The value of  $\mu_e$  is not affected greatly by change in  $i_1$  and  $i_2$  values particularly in relation to the effect of increase in  $(L_y/L_x)$  ratio. The large increase in  $\mu_e$  with increase in  $L_y/L_x$  reduces the steel requirement in the long direction and hence far greater loads are necessary in rectangular slabs to avoid minimum reinforcement conditions



when the value of  $\mu_e$  is used. To illustrate the interpretation of  $W_R$  values, consider a slab with  $(L_x/d) = 30$ ,  $f'_c = 4000 \text{ lb/in}^2$ . The ultimate load,  $w$ , is then  $106.9W_R$  psi which for  $W_R = .025$  is 2.67 psi or 374 psf. Comparison of these values with Figure 2.4 shows just how often minimum steel will govern.

When minimum reinforcement conditions do not apply, the volume of steel may be seen to vary considerably with  $i_1$  and  $i_2$  for a given  $L_y/L_x$ . For the very minimum conditions of  $i_1 = i_2 = 2.0$ , increase in  $L_y/L_x$  requires more steel per unit volume of slab. The advantages of using a value of  $i_1$  in the region of 2.0 are clear from inspection of Figure 2.3 and, for slabs with  $L_y/L_x > 1.0$ , a decrease in  $i_2$  from the position,  $i_1 = i_2 = 2.0$ , brings smaller penalties than a decrease in  $i_1$ . Penalties for decreasing  $i_2$  from this point are relatively less for a slab with  $L_y/L_x > 1.0$ , but it is clear that use of  $i_1 > i_2$  should be preferred.

It may be concluded that although minimum reinforcement conditions will govern in many cases, values of  $m_x/m_y = \mu_e$  and  $i_1 \approx i_2 \approx 2.0$  will give greatest economy where these conditions can be achieved. Furthermore, it is apparent that variation from this optimum does not increase the volume of steel greatly but an increase in  $i_2$  may result in appreciable change in minimum reinforcement conditions for slabs with  $L_y/L_x > 1.0$ .

## CHAPTER 3

### A STUDY OF THE EFFECT OF MEMBRANE FORCES ON A REINFORCED CONCRETE SECTION AND ON A CIRCULAR SLAB WITH PARTIAL LATERAL RESTRAINT AT THE EDGES

#### 3.1 ENHANCEMENT OF THE MOMENT CAPACITY OF A REINFORCED CONCRETE SECTION

##### 3.1.1 Introduction

The enhancement of the load carrying capacity of reinforced concrete floors by compressive membrane action is due to the enhancement of the moment capacity measured about the mid-depth of the sections along the yield lines. For any singly reinforced section there is a limit to the factor by which the application of compression enhances this moment capacity. The amount of reinforcement in the section has the greatest effect on this maximum factor and in the following sections, the effect of reinforcement and other variables on the maximum attainable enhancement factor is examined.

##### 3.1.2 Yield Locus for a Singly Reinforced Section

By examining the conditions at ultimate, on a singly reinforced section, a failure locus may be obtained

relating the moment and axial compression.

Consider the section as in Figure 3.1(a) and having a tensile stress,  $f_y$ , in the steel and a rectangular stress block for the concrete, as shown in Figure 3.1(c).

With the notation as in Figure 3.1, noting that the moment of forces is taken about the mid-depth of the section:

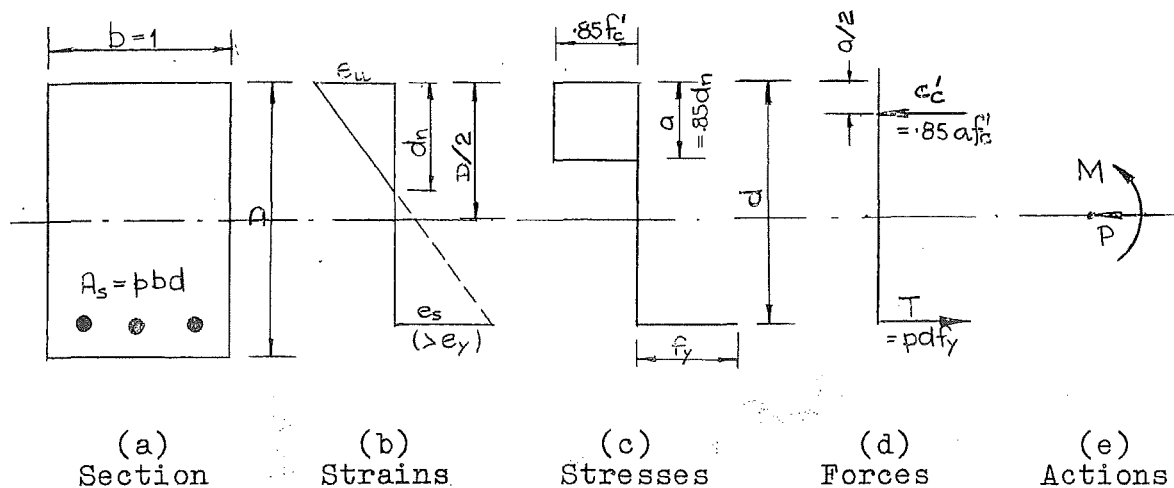


FIGURE 3.1. SECTION NOTATION.

$$P = .85f'_c \cdot a - pdf_y \quad \dots(3.1)$$

$$M = .85 f'_c \cdot a \cdot (D/2 - a/2) + pdf_y (d - D/2) \quad \dots(3.2)$$

and if the moment about the mid-depth for  $P = 0$  is denoted  $M_0$ , then  $M_0 = pdf_y(d - pdf_y/1.7f'_c)$  and  $T_0 = pdf_y$ .

Elimination of 'a' from Equations 3.1 and 3.2 gives the yield locus as

$$M/M_0 = 1 + g(P/T_0) - h(P/T_0)^2 \quad \dots(3.3)$$

in which

$$g = (.5D/d - 2t)/(1-t) \quad \dots(3.3a)$$

$$h = t/(1-t) \quad \dots(3.3b)$$

$$t = pf_y/(1.7 f'_c) \quad \dots(3.3c)$$

For  $M/M_o$  to be a maximum,  $\frac{dM}{dP} = 0$ , which gives

$$(P/T_o) = 2g/h \quad \dots(3.4)$$

$$\text{and } F_{\max} = (M/M_o)_{\max} = 1 + g^2/4h \quad \dots(3.5)$$

where  $F_{\max}$  is the maximum attainable enhancement factor, and is a function of  $t$  and  $D/d$  only.

### 3.1.3 Relationship Between $t$ , $D/d$ and $F_{\max}$

The relationships between  $F_{\max}$ ,  $D/d$ ,  $p$ , and  $f_y/f'_c$  may be shown on one graph.

Considering the relationship between  $F_{\max}$ ,  $t$  and  $D/d$ , Equation 3.5 gives

$$F_{\max} = 1 + \frac{(.5D/d - 2t)^2}{4(1-t)t}$$

the solution for which is

$$t = \frac{[2F_{\max} - (2 - \frac{D}{d})] - \sqrt{[2F_{\max} - (2 - \frac{D}{d})]^2 - F_{\max}(\frac{D}{d})^2}}{4F_{\max}} \quad \dots(3.6)$$

Therefore  $t$  may be plotted against  $F_{\max}$  for a given  $D/d$ . From Equation 3.3(c) it is clear that ' $t$ ' may also be plotted against  $f_y/f'_c$  to give a straight line of slope =

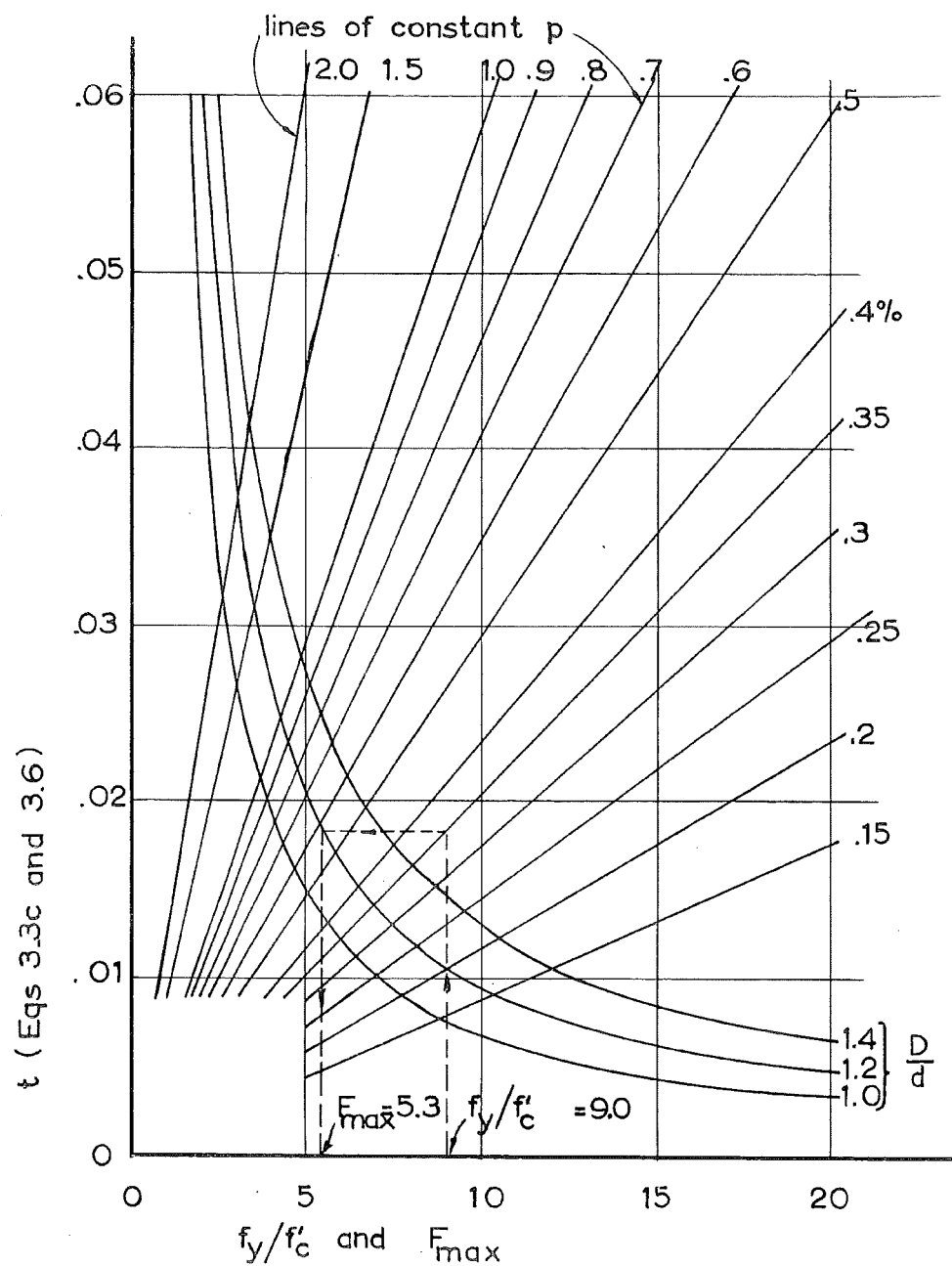


FIGURE 3.2 MAXIMUM ENHANCEMENT FACTOR

$p/1.7$ .

The plots of  $f_y/f'_c$  and  $F_{max}$  (horizontal axis) against  $t$  (vertical axis) are shown in Figure 3.2. The maximum attainable enhancement factor for a given  $f_y/f'_c$ ,  $D/d$  and  $p$  is determined by following the appropriate vertical line corresponding to  $f_y/f'_c$  until the desired straight line for  $p$  is met at an ordinate  $t_1$ . The point with ordinate  $t_1$  on the appropriate curve of constant  $D/d$  has an abscissa equal to the maximum attainable enhancement factor. This process is shown on the figure for  $f_y/f'_c = 9.0$ ,  $D/d = 1.20$  and  $p = .003$ , to give  $F_{max} = 5.3$ .

#### 3.1.4 Condition That Steel Will Yield at Maximum Enhancement

In the above analysis it was assumed that the steel strain,  $e_s$ , exceeded the yield strain,  $e_y$ , at all times. The situation giving least steel strain is that when maximum moment enhancement is reached. This is when the depth of the rectangular stress block,  $a = .5D$  since any increase of 'a' beyond  $.5D$  would reduce the moment about the mid-depth. When  $a = .5D$ ,  $d_n = D/1.7$  and consideration of similar triangles on the strain diagram (Figure 3.1(b)) yields

$$e_s = e_u (1.7(d/D) - 1) \quad \dots(3.7)$$

If the modulus of elasticity of the steel,  $E_s$ , =  $30 \times$

$10^6$  psi, then  $e_y = f_y/30 \times 10^6$  and for yield to take place  $e_s > e_y$ . This requires

$$30 \times 10^6 e_u(1.7(d/D)-1) > f_y \quad \dots(3.8)$$

For  $e_u = .0033$ , the following conditions result if yield is to occur:

$$D/d = 1.0, f_y \geq 70,000 \text{ psi}$$

$$D/d = 1.1, f_y \geq 54,500 \text{ psf}$$

$$D/d = 1.25, f_y \geq 36,000 \text{ psi}$$

Thus for most mild steels in sections with values of  $D/d \geq 1.2$  the condition of  $a = .5D$  does not invalidate the assumption that the tension steel is yielding.

### 3.1.5 Discussion and Conclusion

The variation of  $F_{\max}$  with  $f_y/f'_c$ ,  $D/d$  and  $p$  is summed up in Figure 3.2. Quantitative data as to the reduction of  $F_{\max}$  with increase in  $p$ , the increase in  $F_{\max}$  with increase in  $D/d$ , and the reduction of  $F_{\max}$  with increase in  $f_y/f'_c$  may be obtained therefrom. This diagram serves also as a compact qualitative description of the factors influencing the enhancement of the moment capacity of the section. It is clear from Figure 3.2 that to obtain the highest enhancement factor, any design should aim at:

- (i) A low value of  $f_y/f'_c$ , which would be best

achieved by increasing the concrete strength since it is the concrete which is providing the enhancement.

(ii) A high value of  $D/d$  gives a large enhancement factor. However, a high value of  $D/d$  would cause a reduction in stiffness and in the absolute value of the unenhanced moment,  $M_o$ . Other factors such as crack widths dictate that minimum cover to the tension steel is preferable and the  $D/d$  value would thus be fixed within close limits.

(iii) A low reinforcement content. This requirement is the most critical. The low reinforcement content of reinforced concrete slabs leads to the enhancement of their load carrying capacities due to self-induced compression on the sections when the outer edges are restrained from moving laterally outward. This greater enhancement for lower slab reinforcement is not due entirely to the fact that greater enhancement of the moment capacity of a section is available. The tendency for the edges to spread outwards as the slab deflects is greater for lightly reinforced slabs since the neutral axis is nearer the compression face of the concrete. The benefit gained from this effect is not apparent in the figure.

Finally, it must be remembered that for slabs, the attainment of the maximum available enhancement will be impossible in practice if the net compression is provided



by passive restraint against lateral movement, since the lateral movement and vertical deflection will impose the condition that  $a < D/2$ . However, in cases where the net compression is actively applied it is possible that 'a' may equal (or even exceed)  $D/2$ .

### 3.2 THE EFFECT OF MEMBRANE ACTION ON A CLAMPED CIRCULAR SLAB SUPPORTED AND Laterally RESTRAINED AT ITS CIRCUM-FERENCE

#### 3.2.1 Introduction and Summary

Wood<sup>(7)</sup> has dealt with the effect of membrane action on uniformly loaded circular slabs, both clamped and simply supported. Exceptionally high enhancement factors were obtained for the clamped slabs since Wood assumed that the concrete and steel were rigid-plastic materials and the lateral movement of the edges was zero. This resulted in a load-deflection curve which fell from a maximum at zero deflection. In this section the extension of Wood's treatment to include finite movement at the edges and the case of unequal top and bottom reinforcement is described. The results obtained compare well with some available test data for very stiff surrounds and the load-deflection curve exhibits an algebraic maximum.

For more flexible surrounds, the commencement of a tensile region at the centre occurred before this maximum was reached and special consideration of this case was

required.

In this case it was found that the conditions at the edge of the slab could not be defined explicitly, requiring an assumption to be made regarding the relationship between the radius of the tensile membrane and the membrane force at the perimeter. This enabled a load-deflection relationship to be determined after the tensile membrane began but its validity is questionable because the assumption of rigid-plastic materials became inaccurate when the surround stiffness was low, and particularly when the tensile membrane started before a maximum load was attained.

It is pertinent to point out, before proceeding, that the conical collapse mechanism of a circular slab of radius  $R$  applies also to the case of a square slab of side  $2R$ , and for a uniformly distributed load, the Johansen loads are identical. The results of the following analysis will therefore apply equally well to square panels.

### 3.2.2 Analysis of a Uniformly Loaded Circular Slab With Finite Surround Stiffness

The slab of Figure 3.3 was analysed. Top and bottom steel is isotropic, the bottom steel covering the whole area while the top reinforcement extends only as far into the slab as is necessary. A conical collapse mode was assumed, the geometry of which is shown in Figure 3.3(b).

The support conditions allowed no deflection or

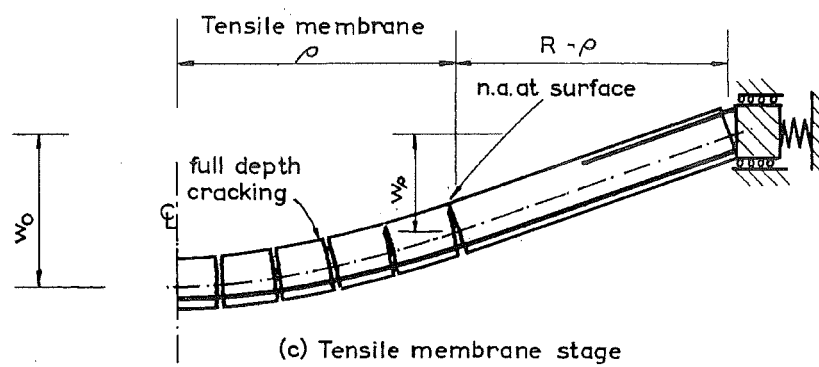
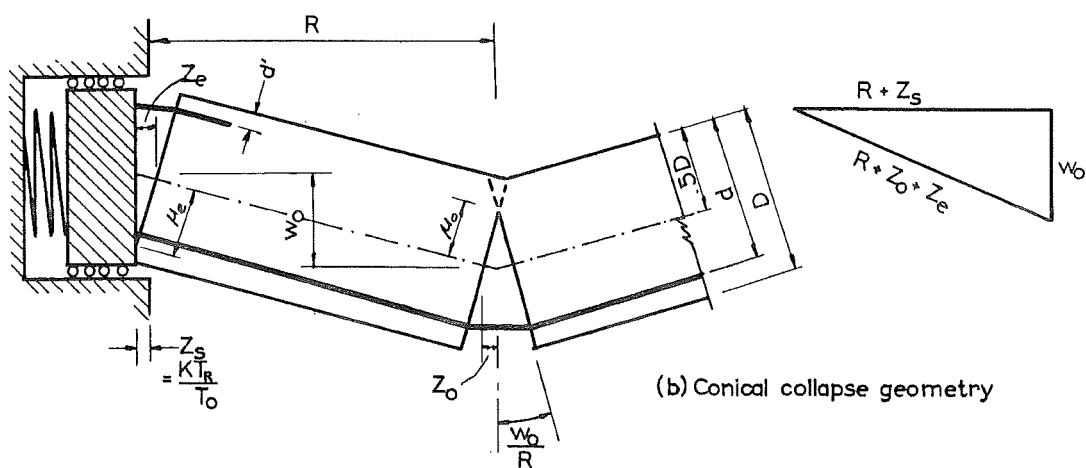
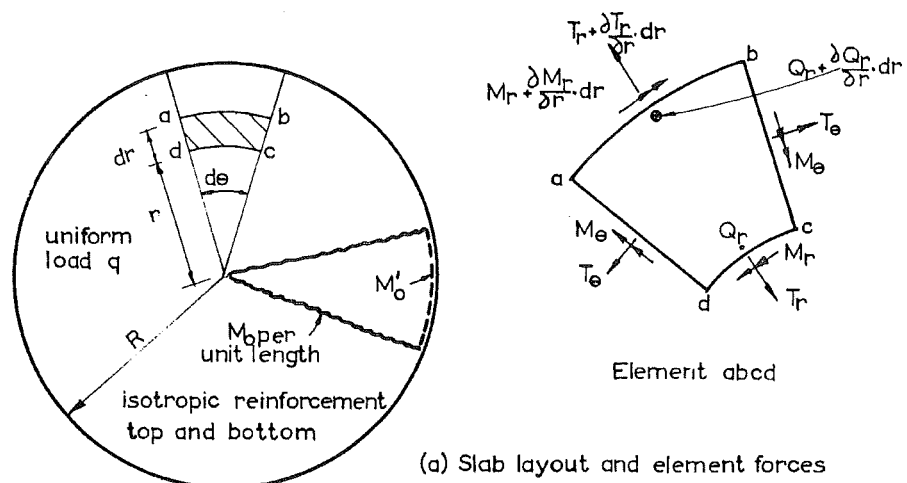


FIGURE 3.3 CIRCULAR SLAB NOTATION

rotation but the edge of the slab could move outward against the springs of flexibility  $K$  per unit length of circumference.

By considering the strain rates of the conical collapse mechanism, it may be shown<sup>(7)</sup> that the distance,  $\mu_\theta$ , from the mid-depth to the neutral axis at a point along a sagging moment yield line at a distance,  $r$ , from the centre is given by

$$\mu_\theta = \mu_0 - 0.5w_0 r/R \quad \dots(3.9)$$

Forces on an element of the slab are shown in Figure 3.3(a) from which it may be seen that symmetry requires that no variation of forces with  $\theta$  is possible.

Equilibrium of this element gives:

$$\frac{d}{dr}(rQ_r) + \frac{d}{dr}(rT_r \frac{dw}{dr}) = -qr \quad \dots(3.10)$$

$$\frac{d}{dr}(rT_r) - T_\theta = 0 \quad \dots(3.11)$$

$$\frac{d}{dr}(rM_r) - M_\theta - rQ_r = 0 \quad \dots(3.12)$$

Equations 3.10 and 3.12 combine to give

$$\frac{d^2}{dr^2}(rM_r) - \frac{dM_\theta}{dr} + \frac{d}{dr}(rT_r \frac{dw}{dr}) = -qr \quad \dots(3.13)$$

In all the above equations  $w$  = deflection at radius  $r$  and for this conical collapse is given by

$$w = w_0(1-r/R) \quad \dots(3.14)$$

By considering the yield locus it is possible to relate  $\mu_s$  to the applied compression on the section.

The yield locus (Equation 3.3) is

$$(M/M_0) = 1 + g(P/T_0) - h(P/T_0)^2 = f(M, P) \quad \dots(3.3)$$

and it may be shown by considering the strain components (curvature and extension) resulting from travel from one point to another on the yield locus, that

$$|\mu| = - \frac{\partial f}{\partial P} / \frac{\partial f}{\partial M} \quad \dots(3.15)$$

From equation 3.3

$$|\mu| = gM_0/T_0 - 2hM_0P/T_0^2 \quad \dots(3.16)$$

Combination of Equations 3.9 and 3.16 for the radial yield lines gives:

$$\mu_e = \mu_0 - .5w_0r/R = gM_0/T_0 - 2hM_0P_e/T_0^2$$

from which

$$P_e/T_0 = (g/2h - \mu_0 T_0 / (2hM_0)) + w_0 T_0 r / (4hM_0 R) \quad \dots(3.17)$$

$$= A + Br \quad \dots(3.17a)$$

where A and B are constants for a given  $w_0$ .

Substitution for  $(P_e/T_0)$  from Equation 3.17 in Equation 3.3 gives

$$M_e/M_0 = (1 + gA - hA^2) + (gB - 2hAB)r - hB^2r^2 \quad \dots(3.18)$$

$$= A_1 + B_1 r + C_1 r^2 \quad \dots(3.18a)$$

Since  $T_\theta = -P_\theta$ , Equation 3.11 becomes

$$\frac{d}{dr}(rT_r) = -(A+Br)$$

from which  $\frac{T_r}{T_o} = -(A + \frac{Br}{2}) \quad \dots(3.19)$

Substitution for  $M_\theta$  and  $T_r$  in Equation 3.13 gives:

$$\frac{M_r}{M_o} = \frac{r}{2} \left( B_1 - \frac{w_o T_o A}{2RM_o} \right) + \frac{r^2}{3} \left( C_1 - \frac{w_o T_o B}{2RM_o} \right) + A_1 - \frac{qr^2}{6M_o} \quad \dots(3.20)$$

which is a condition imposed by equilibrium and strain rates due to conical collapse.

Now at the hogging moment yield line the reinforcement percentage will normally be different and the yield locus may be expressed as

$$M/M_o' = 1 + g'(P/T_o') - h'(P/T_o')^2 \quad \dots(3.3^*)$$

At the edge  $M = M_R$ ,  $T_R/T_o' = (T_R/T_o)(T_o/T_o')$  and

$$M_R/M_o' = -(1 - g'T_R/T_o' - h'(T_R/T_o')^2) \quad \dots(3.21)$$

The Johansen load of the slab may be shown to be

$$Q_J = \pi R^2 q_J = 6 \pi (M_o + M_o') \quad \dots(3.22)$$

Equations 3.21 and 3.20 may be combined by equating values of  $M_R/M_o$  to give

$$\frac{qR^2}{6M_0} = A_1 + \frac{B_1 R}{2} + \frac{C_1 R^2}{3} - \frac{w_0 T_0 A}{2M_0} - \frac{w_0 T_0 BR}{6M_0} - \frac{M_R}{M_0} \dots (3.23)$$

and the enhancement factor is

$$F = (qR^2/6M_0) \cdot (M_0/(M_0 + M'_0)) = Q_M/Q_J$$

and in Equation 3.23:

$$A = \frac{g}{2h} - \frac{\mu_0 T_0}{2hM_0}, \quad B = \frac{w_0 T_0}{4hM_0 R} \quad \text{from Equation 3.17,}$$

$$A_1 = 1 + gA - hA^2$$

$$B_1 = gB - 2hAB$$

$$C_1 = -hB^2$$

$$\frac{M_R}{M_0} = \left( \frac{M_R}{M'_0} \right) \cdot \left( \frac{M'_0}{M_0} \right) = - \frac{M'_0}{M_0} \left( 1 - g' \left( \frac{T_R}{T'_0} \right) - h' \left( \frac{T_R}{T'_0} \right)^2 \right)$$

Thus Equation 3.23 may be used to determine  $Q_M/Q_J$  for a given  $w_0$  provided  $\mu_0$  can be expressed in terms of known quantities. This may be done by considering the geometry of the conical collapse (see Figure 3.3(b)). The outward movement of the edge is  $Z_s = -KT_R/T_0$  and the slope length along the slab mid-depth is  $R + Z_0 + Z_e$ . At collapse

$$(R + Z_s)^2 + w_0^2 = (R + Z_0 + Z_e)^2 \dots (3.24)$$

But  $Z_e = \frac{\mu_0 w_0}{R}$ ,  $Z_0 = \frac{\mu_0 w_0}{R}$  for small  $\frac{w_0}{R}$  so that Equation 3.24 becomes

$$\left(\frac{w_o}{R}\right)^2 (\mu_o + \mu_e)^2 + 2 w_o (\mu_o + \mu_e) - w_o^2 + 2 R K \left(\frac{T_R}{T_o}\right) - \left(K \frac{T_R}{T_o}\right)^2 = 0 \quad \dots (3.25)$$

and from Equation 3.16:

$$|\mu_e| = (M'_o/T'_o)(g' + 2h'(T_R/T_o)(T_o/T'_o)) \quad \dots (3.26)$$

$T_R/T_o$  may be found from Equation 3.19 and substituted in 3.26 to give

$$\begin{aligned} \left(\frac{\mu_e}{D}\right) &= \frac{(1-d')}{d} \left(\frac{\mu_o}{D}\right) + \frac{g'}{k} - \frac{g(1-t)}{k(1-t')} - \frac{1}{4} \frac{(1-d')}{d} \left(\frac{w_o}{D}\right) \quad \dots (3.27) \\ &= C_o \left(\frac{\mu_o}{D}\right) + C_2 \end{aligned}$$

In which

$$k = \frac{(D/d)}{(1-t)}, \quad k' = \frac{D/(1-d')}{(1-t')}, \quad t = p f_y / (1.7 f'_c)$$

Now from 3.19:

$$\begin{aligned} (K/D)(T_R/T_o) &= (K/D)(k/2h)(\mu_o/D) - (K/D)(g/2h) - \\ (K/D)(w_o/D)/8h &= C_3(\mu_o/D) + C_4 \quad \dots (3.28) \end{aligned}$$

Substitution of Equations 3.27 and 3.28 in Equation 3.25 yields a quadratic equation in  $(\mu_o/D)$ , relating it to known quantities to a given deflection,  $w_o$ ; viz.

$$\begin{aligned} \left(\frac{\mu_o}{D}\right)^2 \left[ \left(\frac{w_o}{R}\right)^2 (1+C_o)^2 - C_3^2 \right] &+ 2 \left(\frac{\mu_o}{D}\right) \left[ \frac{C_2}{D} (1+C_o) \left(\frac{w_o}{R}\right)^2 + \left(\frac{w_o}{D}\right) (1+C_o) + \frac{R C_3}{D} - \frac{C_3 C_4}{D} \right] \\ &+ \left(\frac{C_2}{D}\right)^2 \left(\frac{w_o}{R}\right)^2 + 2 \left(\frac{w_o}{D}\right) \left(\frac{C_2}{D}\right) - \left(\frac{w_o}{D}\right)^2 + \frac{2 C_4 R}{D^2} - \left(\frac{C_4}{D}\right)^2 \quad \dots (3.29) \end{aligned}$$

Equations 3.29 and 3.23 may thus be used in turn to find  $Q_M/Q_J$  for a given  $(w_o/D)$  ratio in a slab of known



properties, and load-deflection curves may be obtained for varying lateral restraint conditions for which  $(\mu_o/D)$  does not exceed .5 at the centre.

After  $(\mu_o/D)$  exceeds .5 at the centre, a tensile membrane forms from the centre and although the equilibrium equations still apply to the remaining conical portion, the relationship between the radius of the tensile membrane region and  $(T_R/T_o)$  is not explicit. A load-deflection relation for this region was obtained by assuming a relation between the two.

#### CONDITIONS AFTER PLASTIC MEMBRANE COMMENCES AT THE CENTRE

When  $\mu_o/D$  exceeds .5 the foregoing analysis is invalidated, and conditions become more complex since the geometry may no longer be used to ascertain  $T_R/T_o$  explicitly. However, in order to obtain a continuous curve, an approximate analysis was made. Wood's analysis of a simply supported slab<sup>(7)</sup> may be followed but without the condition that the radial tension,  $T_R$ , is equal to zero at the edge.

Wood shows that:

$$P_e/T_o = A + Br \text{ for the conical portion}$$

$$\text{in which } B = (T_o/4hM_o)(w_p/(R-\rho)) \quad \dots(3.30)$$

for a tensile membrane extending to a radius  $\rho$  from the

centre and a slab deflection,  $w_\rho$ , at the junction between tensile membrane and the outer cone (Figure 3.3(c)).

Since  $P_e/T_o = -1$  at  $r = \rho$ ,  $A = -1 - B\rho$ .

From Equation 3.11

$$T_r/T_o = -A - Br/2 + C/r$$

and the condition that  $T_r/T_o = 1$  at  $r = \rho$  gives  $C = \frac{-B\rho^2}{2}$ .

The condition at the edge of the slab is then

$$T_R/T_o = 1 - B(R - \rho)^2/2R \quad \dots(3.31)$$

Equating values of B from Equations 3.30 and 3.31 relates  $w_\rho$  and  $\rho$ :

$$w_\rho = (8hM_o/T_o)(1 - T_R/T_o)/(1 - \rho/R) \quad \dots(3.32)$$

Integration of Equation 3.10 gives

$$rQ_r + rT_r \frac{dw}{dr} = \frac{-qr^2}{2} + C_o$$

but  $Q_r = 0$  at  $r = \rho$ ,  $T_r = T_o$  at  $r = \rho$  and  $\frac{dw}{dr} = w_\rho/(R - \rho)$

so that  $C_o$  may be found, and

$$Q_r = \frac{-qr}{2} + \frac{T_r w_o}{(R - \rho)} + \frac{q\rho^2}{2r} - \frac{\rho w_o T_o}{r(R - \rho)} \quad \dots(3.33)$$

Equilibrium of radial moments for the cone gives

$$\frac{d}{dr}(rM_r) - M_\theta - rQ_r = 0 \quad \dots(3.12)$$

and since  $P_e/T_o = A + Br$  where A and B are constants for a

given value of  $p$ ,  $M_e$  may be expressed using the yield locus:  $M_e/M_o = A_1 + B_1 r + C_1 r^2$  where  $A_1$ ,  $B_1$  and  $C_1$  are directly related to  $B$ .

Integration of 3.12 with the condition that  $M_r/M_o = 1 - g - h$  at  $r = \rho$  finally results in:

$$\frac{qR^2}{6M_o} \left( 1 - 3\left(\frac{\rho}{R}\right)^2 + 2\left(\frac{\rho}{R}\right)^3 \right) = \left( A_1 + \frac{B_1 R}{2} + \frac{C_1 R^2}{3} \right) + \left( \frac{\rho}{R} \right) \left( A_1 + \frac{B_1 \rho}{2} + \frac{C_1 \rho^3}{3} \right) + \frac{\rho}{R} (1 - g - h) + \frac{w_p T_o}{2M_o} \left( 1 - \frac{\rho}{R} \right) - \frac{BR}{6} \frac{w_p T_o}{M_o} \left( 1 - \frac{\rho}{R} \right)^2 - \frac{M_R}{M_o} \dots (3.34)$$

Equation 3.34 expresses  $q$  in terms of known quantities and the unknown  $T_R/T_o$ .

At the start of the tensile membrane,  $\rho/R = 0$  and since  $A = -1$  at this stage Equations 3.23 and 3.34 are identical.

After the central tensile net has formed, the outward movement of the edges of the slab becomes indeterminate.

Equation 3.32 shows that for a chosen value of  $\rho/R$ ,  $w_p$  may be calculated if  $T_R/T_o$  is known. The relationship between  $T_R/T_o$  and  $\rho/R$  assumed was

$$\left( \frac{T_R}{T_o} \right)_{\rho/R} = \left( \frac{T_R}{T_o} \right)_{\rho/R=0} \left( 1 - \frac{\rho}{R} \right) \dots (3.35)$$

This gave satisfactory results but is not the only possible solution. Three other possible variations were investigated, viz:

$$\left(\frac{T_R}{T_0}\right)_{\rho/R} = \left(\frac{T_R}{T_0}\right)_{\rho/R=0} \left(1 - \frac{\rho}{R}\right) + \frac{\rho}{R} \quad \dots(3.36)$$

$$\left(\frac{T_R}{T_0}\right)_{\rho/R} = \left(\frac{T_R}{T_0}\right)_{\rho/R=0} \quad \dots(3.37)$$

$$\left(\frac{T_R}{T_0}\right)_{\rho/R} = \left(\frac{T_R}{T_0}\right)_{\rho/R=0} \left(1 - \left(\frac{\rho}{R}\right)^3\right) + \left(\frac{\rho}{R}\right)^3 \quad \dots(3.38)$$

The difference between these assumptions is shown in Figure 3.4 from which it may be seen that the difference is least for low surround stiffness but Equations 3.35 and 3.36 give similar results for the whole range of  $K/D$  values. Equations 3.37 and 3.38 imply a low rate of fall-off in  $T_R/T_0$  with increase in  $\rho/R$  and do not give consistent results throughout the range of surround stiffness.

However, when the tensile region forms, the assumption of rigid-plasticity of the concrete does not apply accurately and Equation 3.35 is sufficient to describe behaviour of the slab after the tensile membrane starts.

### 3.2.3 EFFECT OF VARIATION OF SLAB PARAMETERS ON THE BEHAVIOUR OF THE SLAB

The above analyses enable the determination of the load-deflection relationship of a circular slab under uniform load. Simple computer programmes were written to obtain this relationship for slabs of varying properties.

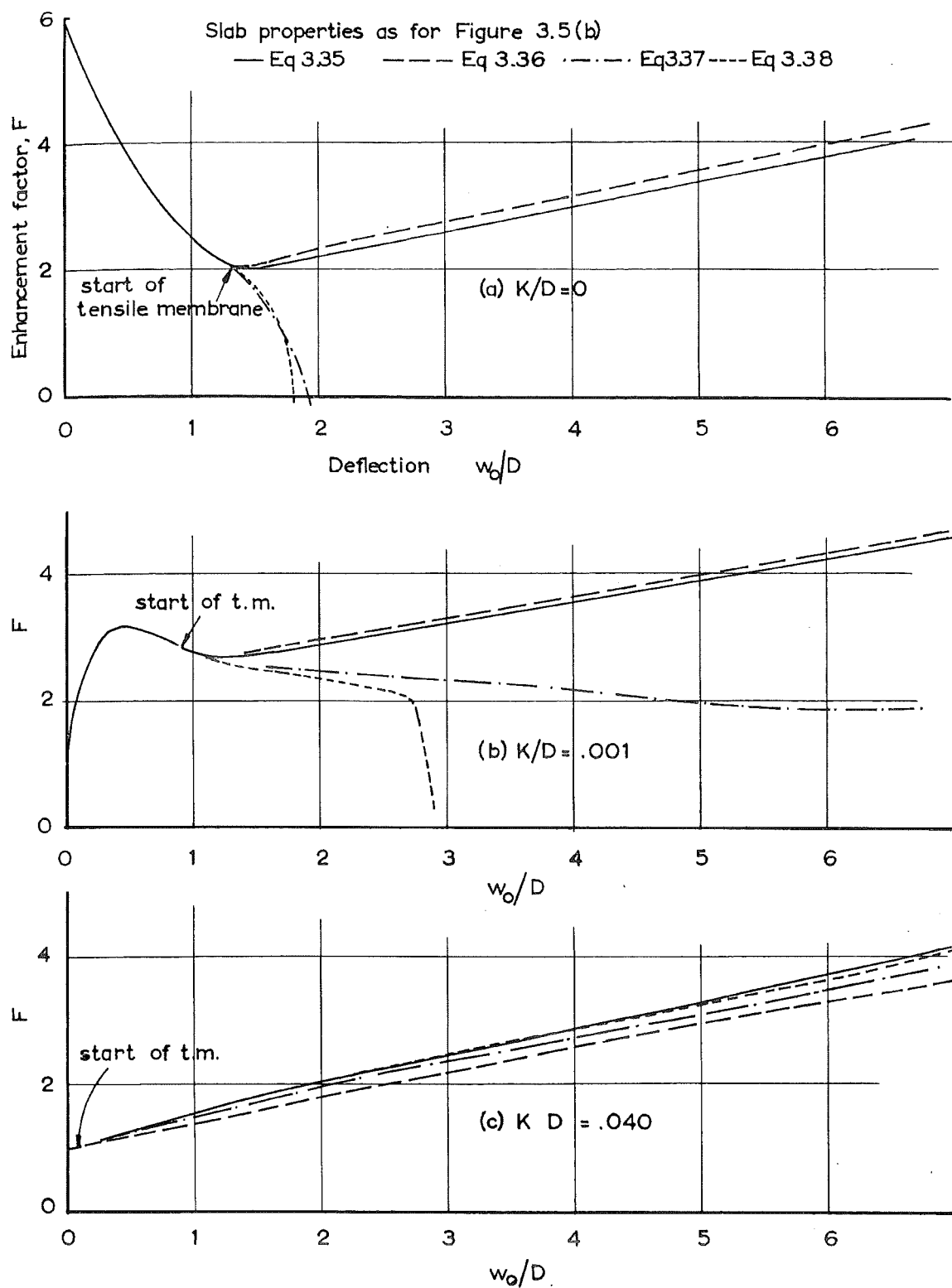


FIGURE 3.4 COMPARISON OF TENSILE MEMBRANE EQUATIONS

The variables investigated were:

$R/D$  = ratio of radius to depth of slab

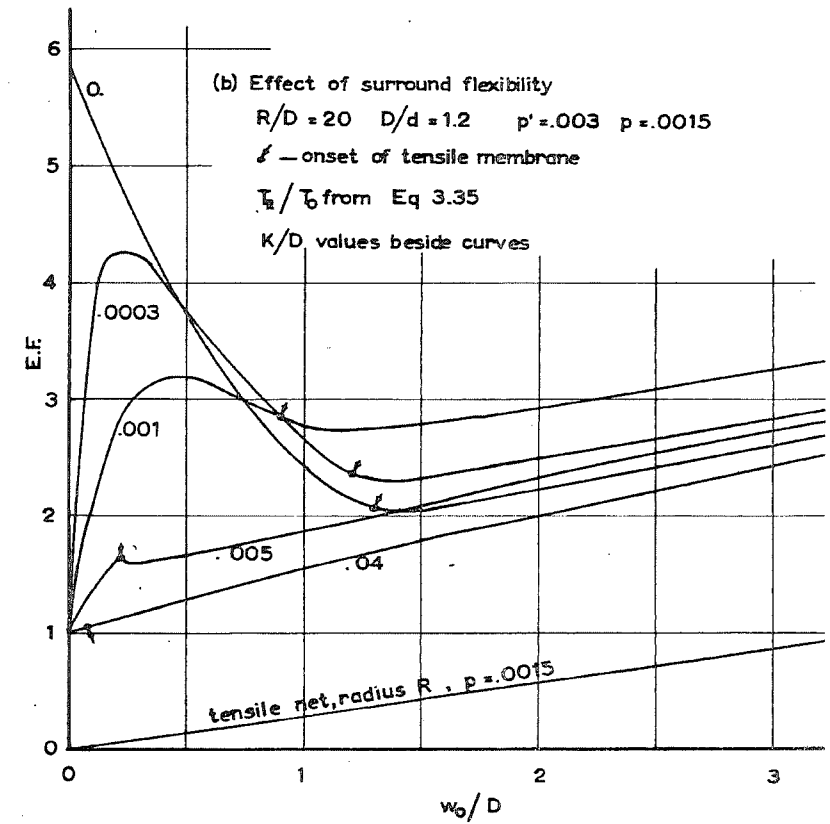
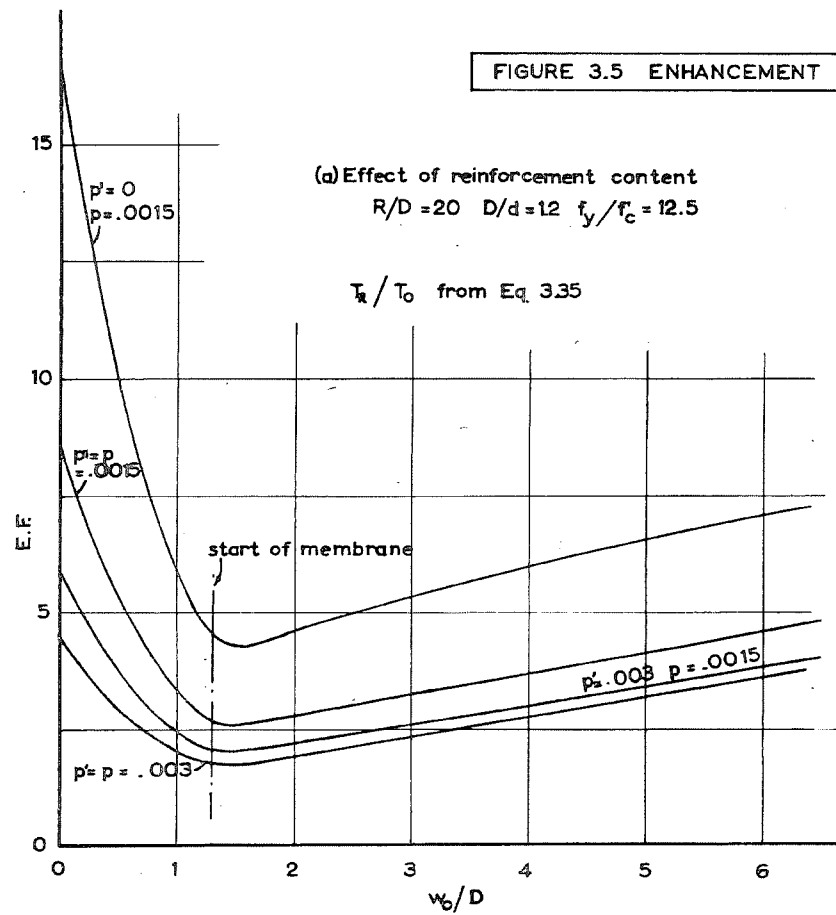
$K$  = measure of surround flexibility

$p', p$  = reinforcement ratios in the top and bottom of the slab.

Figure 3.5(a) shows the load-deflection relationships obtained for varying steel percentages, top and bottom. All the curves in this figure show a maximum enhancement at zero deflection.

In Figure 3.5(b), the effect of surround flexibility is illustrated both in its effect on the maximum enhancement and on the deflection at which this occurs. The values of surround flexibility shown are for  $K/D$  where  $K$  is the inward movement of the surround due to a radially inward force  $p.d$  per unit length of circumference.

The initial slope of these curves is smaller for increasing  $K/D$  and the deflection at which zero slope occurs increases with  $K/D$ . However, as the flexibility of the surround is increased, a stage is reached beyond which the tensile membrane starts at the centre ( $\mu_0/D > .5$ ) before zero slope is attained. Note that the case for which  $K/D = .04$  is tending to the solution for no lateral restraint.



### 3.2.4 Comparison With Some Experimental Results

#### 3.2.4.1 Summary and Introduction

Equation 3.23 was used to compare the load-deflection relationships of two sets of experimental results obtained from tests on square slabs restrained at the edges. These were two slabs tested by Wood<sup>(7)</sup> with all edges restrained by a monolithically cast edge beam and two slabs tested at M.I.T. by Brotchie, Jacobson and Okubo<sup>(15)</sup> in which the separately cast specimens were placed within a rigid surrounding frame. Because the collapse mechanism and the collapse loads of square and circular slabs are nearly identical, Equation 3.23 could be expected to give good results in comparison with these experimental results. Only a simple and approximate assessment of surround flexibility could be made in each case.

Agreement between the calculated and required surround flexibilities was good for the lightly reinforced, slender slabs tested by Wood. In the more heavily reinforced, thicker slabs tested at M.I.T. sensitivity to change in surround flexibility was not as great and, in general, the flexibility required to reproduce the experimentally determined enhancement was greater than that given by the approximate analysis.

#### 3.2.4.2 Properties of the Slabs Used in Comparison

The properties of the slabs are summarised in Table 3.1.



Table 3.1. Slab properties.

<u>Authority</u>	<u>Mark</u>	<u>Dimensions</u> (Inches)	R/D	$p'$ %	$p$ %	D/d	$f_y/f_c^*$
Wood	FS12	68 x 68 x 2.25	15.1	0	.25	1.24	7.17
Wood	FS13	68 x 68 x 2.25	10.0	.25	.25	1.24	8.80
M.I.T.	46	15 x 15 x .75	10.0	0	1.0	1.34	10.95
M.I.T.	48	15 x 15 x .75	10.0	0	2.0	1.34	12.31

\* On the assumption that  $f_c' = .8u$

#### 3.2.4.3 Assessment of Surround Flexibility

Surround flexibility was defined as the outward movement of the surround under a force of  $pdf_y (=T_o)$ . For circular slabs this is uniform around the circumference but for square slabs this is not so. To assess the surround flexibility of the square slabs of Table 3.1, the maximum deflection of a side of the surround was computed using Equations 5.3, 5.4, 5.8 and 5.6. These gave the outward movement of the surround due to bending, shear and axial deformation of the surround. The effective surround stiffness will be further reduced by shortening of the loaded slab under compressive membrane forces. Thus, the total surround stiffness was assessed by summing the outward movement of the surround under  $T_o$  and the shortening of a strip of slab of unit width under a force  $T_o$ . The slab strip shortening was calculated on the basis of an uncracked concrete section. Thus in this comparison the

value of  $K/D$  for a circular slab was assumed to be represented by the maximum effect occurring in the case of a square slab. Summaries of the assessment of surround stiffness are given below.

(i) Wood's Slabs<sup>(7)</sup>

The section of the surrounding beams used for these tests is shown in Figure 3.5. The yield stress of the reinforcement was 33,800 psi and the modulus of elasticity of the concrete was assumed to be  $3.5 \times 10^6$  psi.

$$\therefore T_o = p d f_y = 153 \text{ lb/in}$$

The force,  $W$ , on half the surround span was therefore 5200 lb.

Assuming a modular ratio of 10.0, the equivalent area of concrete in the surround section was  $270 \text{ in}^2$  and the moment of inertia =  $6140 \text{ in}^4$ . The equivalent plain concrete surround was taken as  $t \times b$  such that  $t \cdot b = 270 \text{ in}^2$ ;  $tb^3/12 = 6140 \text{ in}^4$ . Whence  $t = 16.4 \text{ in}$ ,  $b = 16.5 \text{ in}$ . Therefore in Equations 5.3, 5.4, 5.8, 5.6;

$$\frac{a_x}{b_x} = 2.07, \quad k = .183$$

Thus:

$$\Delta_e \cdot \frac{tE}{W} = 2.07, \quad \Delta_s \cdot \frac{tE}{W} = 3.56, \quad \Delta_B \cdot \frac{tE}{W} = 6.28$$

The slab strip shortening over half the span is  $\frac{PL}{EA} = \Delta_{ss}$

$$= 6.61 \times 10^{-4}.$$

$$\text{Now, } K/D = (\Delta_e + \Delta_s + \Delta_B + \Delta_{ss})/D = 7.69 \times 10^{-4}$$

$$\text{for } W = 5200, t = 16.4, E = 3.5 \times 10^6 \text{ psi.}$$

(ii) M.I.T. Slabs<sup>(15)</sup>

For these slabs, the steel surrounding frame was as shown in Figure 3.6 and in addition the continuous slabs were 29" x 29" overall, giving a 7" concrete surround. Only a very approximate assessment of surround movement was made since slab strip shortening formed the bulk of the total surround flexibility. The steel yield stress was 60,000 psi, and for two per cent of steel:

$$T_o = pdf_y = 673 \text{ lb/in.}$$

Under this force the outward movement of the steel portion only of the surround was computed. The slab strip shortening,  $\Delta_{ss}$ , was  $19.3 \times 10^{-4}$  in,  $\Delta_{ss}/D = 25.6 \times 10^{-4}$ . The final values of  $K/D$  for the one per cent and two per cent reinforcements were made up as follows:

	p = 1%	p = 2%
K/D due to ) surround ) deformation)	$1.0 \times 10^{-4}$	$2.0 \times 10^{-4}$
K/D due to ) slab strip ) shortening )	$12.8 \times 10^{-4}$	$25.6 \times 10^{-4}$
Total K/D	$13.8 \times 10^{-4}$	$27.6 \times 10^{-4}$

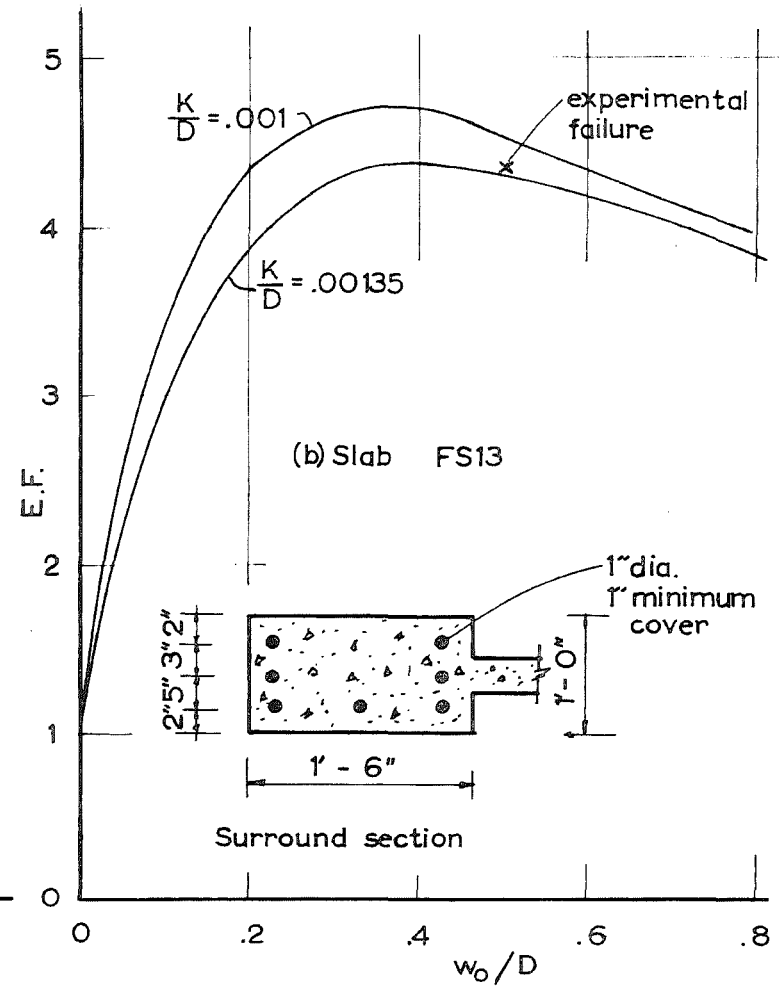
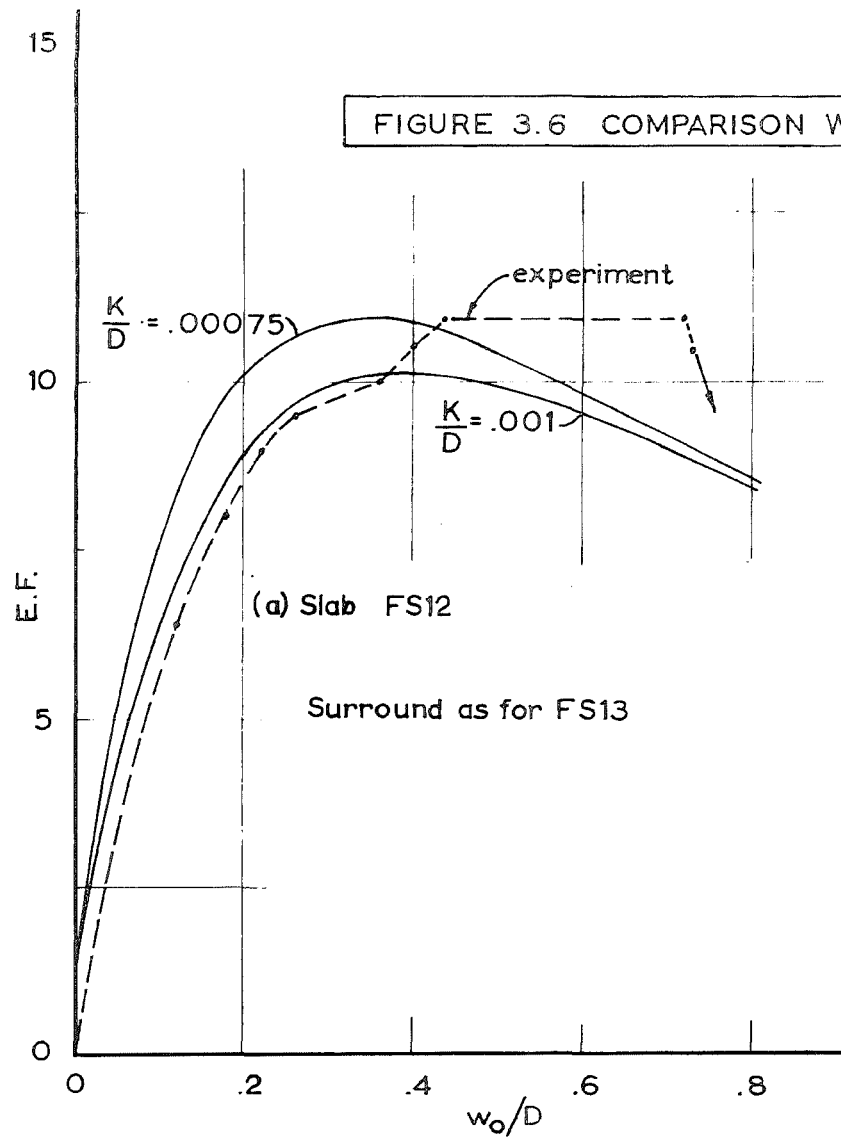
#### 3.2.4.4 Comparison of Load-Deflection Curves

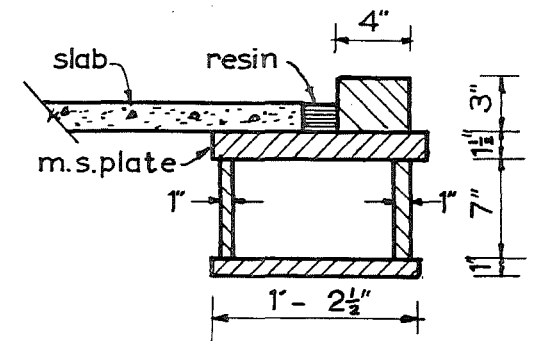
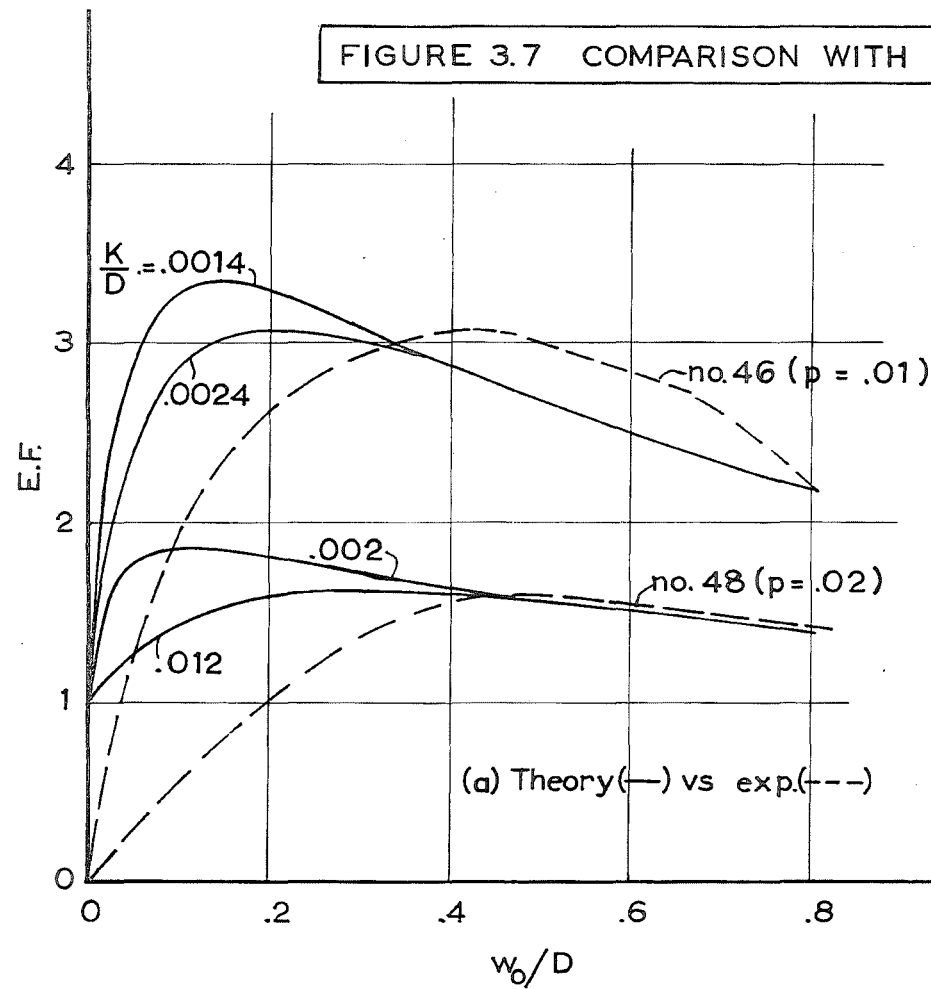
For Wood's Slab FS12<sup>(7)</sup> a value of  $K/D$  of .0007 gave a maximum load slightly in excess of the experimentally determined load (see Figure 3.6(a)). The value of .001 for  $K/D$  underestimated the maximum load but follows the experimental curve very closely up to an enhancement factor of 10. These values of  $K/D$  which give good agreement with the experiment compare well with the value of .000769 arrived at by approximate analysis.

Slab FS13 failed when the ratio of deflection to depth was 0.5 and the load 4.38 times the Johansen load. The value of  $K/D = .000769$  overestimated the load considerably and even the value .001 which gave good agreement in FS12 was an overestimate for FS13 (see Figure 3.6(b)). A value of .0013 gave closest agreement.

Figure 3.7(a) shows the two experimentally determined curves for the  $\frac{3}{4}$ " thick M.I.T. slabs. For one per cent reinforcement a value of  $K/D = .0026$  gave the correct maximum load while  $K/D = .00138$ , computed from slab strip shortening, overestimated the maximum load by approximately 10 per cent. For two per cent reinforcement a value of .012 was required as against .00276 calculated which had overestimated the collapse load by 18 per cent. The falling branches of both sets of theoretical curves agree well with those determined experimentally and overall similarity of shape is good.

FIGURE 3.6 COMPARISON WITH WOOD'S SLABS





(b) Support condition and surround section (approx. dimensions only)

### 3.2.5 Discussion and Conclusion

In the analytical approach presented, the effect of finite lateral stiffness of the slab surround was successfully taken into account. The load-deflection curves were similar to those obtained experimentally, especially where enhancement factors were large. Crushing of the concrete caused a divergence of the theoretical and experimental curves after a maximum had been reached.

This greater similarity at large enhancement factors is attributable, in part, to the effect of the assumption that the materials were rigid-plastic. The deflection at an enhancement factor of 1.0 was always zero and in cases of low enhancement, this departure from actual behaviour was relatively large.

Although the analysis does not strictly hold for the situation, it is interesting to note that better agreement is obtained when the theoretical curve is shifted bodily so that the experimental and theoretical deflections are equal at an enhancement factor of 1.0.

For an immovable surround, the enhancement factor was a maximum at zero deflection, the maximum value varying only with the section properties in accordance with the findings of Section 3.1.2. When the surround stiffness was finite, the maximum enhancement factor attained was governed, not only by the section properties, but by the ratio of span to depth of the slab and the stiffness of

the surround.

The reduction in the maximum load with increase in surround flexibility was to be expected but the equations derived provide a means of assessing the maximum enhancement.

The early onset of the tensile membrane at the centre could not be expected in practice: the assumption that the materials are rigid-plastic caused an underestimate of this deflection in the same way as it caused the underestimate of the deflection at which the enhancement factor was 1.0. However, the slopes of the load-deflection curves indicate the degree of enhancement which would be available.

For reinforcement ratios greater than .01 the relative effect of membrane action was small. Although such slabs are less sensitive to increase in surround flexibility than more lightly reinforced slabs, lateral restraint brings only small rewards.

The assessment of the equivalent surround flexibility,  $K/D$ , requires careful study. In addition to the effects considered, the following are of importance:

- (a) Shrinkage of the slab away from the surround
- (b) Creep deformation of surround and slab
- (c) Cracking of the elements comprising the surround
- (d) Deflection just prior to the onset of compressive membrane action.



The effect of these factors could well account for the discrepancies evident in the comparison with tests.

Clearly, in the design of a slab with allowance for membrane action enhancement, the surround flexibility should be overestimated by an amount dependent upon the sensitivity of the slab in question to the change in surround flexibility.

## CHAPTER 4

### THE EFFECT OF PANEL MEMBRANE ACTION OF THE DESIGN OF SUPPORTING BEAMS

#### 4.1 SUMMARY

The presence of compressive membrane forces in the panels of a slab and beam floor affects the flexural and torsional capacity of the supporting beams due to the axial tension and lateral loads applied to them. For this situation, a method of determining the beam moments is developed which is similar to methods used when membrane action is not considered. A method of allocating flexural steel to the critical sections of a T-beam subject to axial load and moment is then developed on the basis of ultimate strength theory.

Finally, the effects of panel membrane action on the torsion induced in the spans of supporting beams are examined.

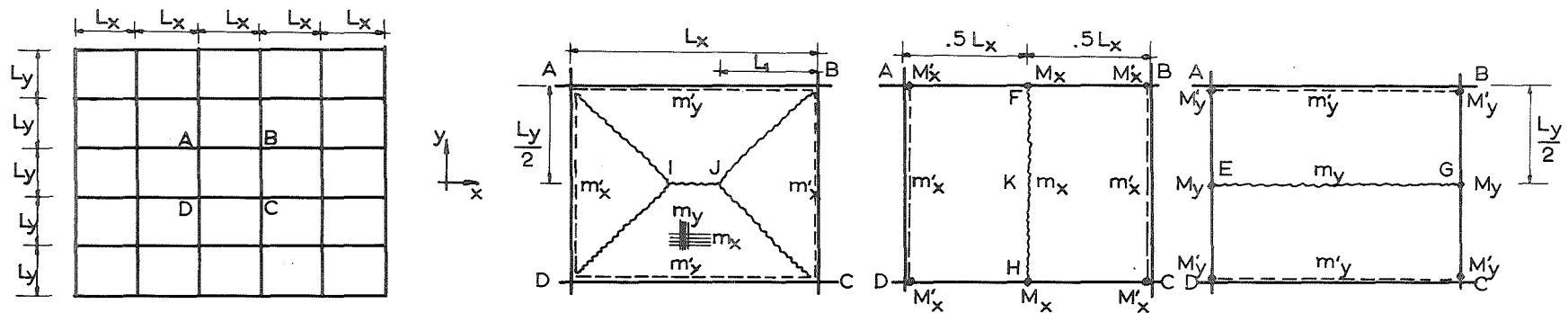
#### 4.2 DETERMINATION OF BEAM MOMENTS

Consider a typical interior panel of a slab and beam floor (Figure 4.1(a)). Let this panel be orthotropically reinforced with equal intensities of hogging moments along

opposite edges (Figure 4.1(b)). The quantities  $m_x$ ,  $m_y$ ,  $m'_x$ ,  $m'_y$  represent the average moments per unit width, acting about the mid-depth of the slab section.

The yield line pattern shown in Figure 4.1(b) applies to the case when no membrane forces are present. Compressive membrane forces will enhance the load carrying capacity of the panel. If it is assumed that the presence of membrane forces does not alter the plan geometry of the collapse mechanism or introduce nodal forces at I or J then the collapse mechanism of Figure 4.1(b) may be used to determine the collapse load of the panels when membrane action is considered.

Consider the design of a floor including the effect of membrane action. From the design of the panel (e.g. by the theory due to Park<sup>(11)</sup>) the distribution and magnitude of the membrane forces along a yield line would be known and hence the values of  $m'_x$ ,  $m'_y$ ,  $m_x$ ,  $m_y$  could be calculated. The magnitude and line of action of the resultant of the membrane forces acting on a yield line may be determined. The resultant forces are shown in Figures 4.1(f), (g), (h), (i) and (j). In Figures (f) and (g) it has been assumed that the distribution of  $c_x$  along KF is the same as that along IA. That these two resultants have the same line of action in the vertical direction results from the assumption that the slab elements are planar between yield lines.



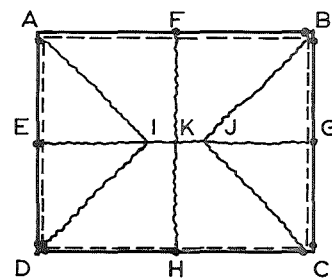
(a) floor layout

(b) panel mechanism

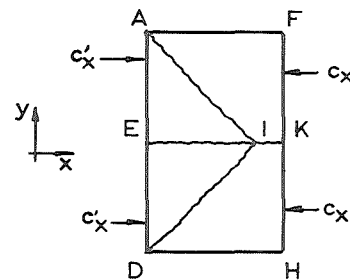
(c) x-direction

(d) y-direction

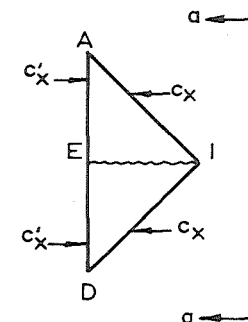
Beam mechanisms



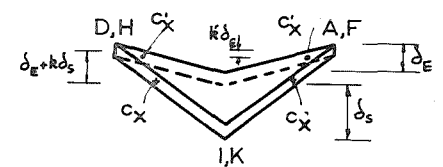
(e) composite mechanism



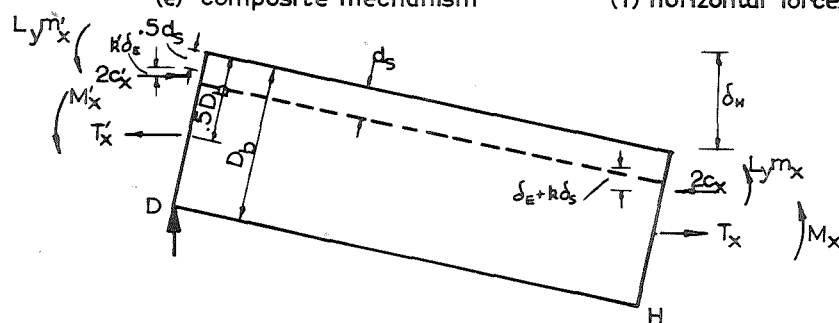
(f) horizontal forces



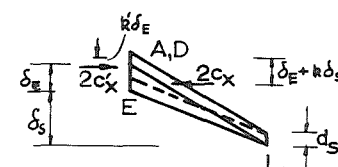
(g)



(h) view aa



(i) beam and slab element



(j) elevation

FIGURE 4.1

The possible beam collapse mechanisms (Figure 4.1 (c), (d)) must be guarded against by the provision of suitably strong beams. If the panels are designed allowing for membrane action enhancement, the beams must be designed to carry moments induced by the enhanced load together with the tensions induced in them by the compressive membrane forces in the panels on either side.

If the beams are not designed for both these effects, the beam collapse mechanisms will form first. At least, then, the beams must be so designed that both panel and beam mechanisms form simultaneously, as in Figure 4.1(e). This composite mechanism will form when the panel and beam mechanisms each have the same ultimate load. It is important to note that, when membrane action is considered, compression will be present along the slab yield lines HF and EG of Figure 4.1(c) and (d). Analysis of the composite mechanism with membrane action may follow closely that applicable to this case when membrane action is not considered. This similarity is best seen when both analyses are performed together, as below. Let the Johansen load be  $w_J$  and the enhanced load  $F.w_J$ . For the panel mechanism, moment equilibrium about AD for portion AID gives, at Johansen load,

$$\frac{w_J L_y \cdot L_1^2}{6} = L_y (m_{xJ} + m'_{xJ}) \quad \dots(4.1)$$

and for AIJB, moment equilibrium about AB gives

$$w_J L_y^2 \left( \frac{L_x}{8} - \frac{L_1}{6} \right) = L_x (m_{yJ}' + m_{yJ}') \quad \dots(4.2)$$

From which  $w_J$  and  $L_1$  may be determined for known  $m_{xJ}'$ ,  $m_{yJ}'$ ,  $m_{xJ}$ ,  $m_{yJ}$ .

For the beam mechanism in Figure 4.1(c), there is no shear along FH and moments about AD for AFHD gives

$$M_{xJ}' + M_{xJ} = \frac{w_J L_x^2 L_y}{8} - L_y (m_{xJ}' + m_{xJ}) \quad \dots(4.3)$$

and similarly for the mechanism of Figure 4.1(d)

$$M_{yJ}' + M_{yJ} = \frac{w_J L_y^2 L_x}{8} - L_x (m_{yJ}' + m_{yJ}) \quad \dots(4.4)$$

When membrane action is considered in design, the forces  $c_x'$  and  $c_x$  are not zero and their effect is to enhance the yield moments. The secondary effect of the variation of the level of the lines of action of these forces must be considered. At a load of  $Fw_J$  we get:

$$\frac{Fw_J L_y L_1^2}{6} = L_y (m_x + m_x') - 2c_x (\delta_E + k \delta_S - k' \delta_E) \quad \dots(4.5)$$

since  $c_x' = c_x$ , and for AIJB:

$$Fw_J L_y^2 \left( \frac{L_x}{8} - \frac{L_1}{6} \right) = L_x (m_y + m_y') - 2c_y (\delta_F + k \delta_S - k'' \delta_F) \quad \dots(4.6)$$

and for the beam mechanism in Figure 4.1(c) referring to Figure 4.1(i) and taking  $T_x = T_x'$  we have from moments about D:

$$M'_X + M_X = \frac{Fw_J L_X^2 L_Y}{8} - L_Y(m'_X + m_X) - T_X(\delta_H) \\ + 2c_X(\delta_H + \delta_E + k\delta_S - k'\delta_E) \quad \dots(4.7)$$

Combination of Equations 4.1 and 4.5 gives

$$L_Y(m'_X + m_X) = FL_Y(m'_{XJ} + m_{XJ}) + 2c_X(\delta_H + \delta_E + k\delta_S \\ - k'\delta_E) \quad \dots(4.8)$$

Substituting 4.8 into 4.7:

$$M'_X + M_X = \frac{Fw_J L_X^2 L_Y}{8} - FL_Y(m'_{XJ} + m_{XJ}) - 2c_X(\delta_H + \delta_E + k\delta_S \\ - k'\delta_E) - T_X\delta_H + 2c_X(\delta_H + \delta_E + k\delta_S - k'\delta_E) \\ \therefore M'_X + M_X = F \left[ \frac{w_J L_X^2 L_Y}{8} - L_Y(m'_{XJ} + m_{XJ}) \right] - T_X\delta_H$$

and using Equation 4.3 we get the relation

$$M'_X + M_X = F(M'_{XJ} + M_{XJ}) - T_X\delta_H \quad \dots(4.9)$$

Although the term,  $T_X\delta_H$ , does help in reducing the total free moment from the directly factored Johansen load sum, it is reasonable and conservative to neglect its contribution in this case.

Thus when membrane action in the panels is taken into account the sum of the beam moments may be obtained by using the normal methods employed when membrane action is not present, provided the load used is the enhanced panel load.

For continuous slab and beam floor systems, Park<sup>(22)</sup> has shown that, except for panels with unsupported exterior edges, the sum of the beam moments,  $M'_x + M_x$ , is the same whether calculated by analysis of the beam collapse mechanisms or by application of a load distribution to the beam equivalent to the adjacent trapezoidal segments of the slab. If the term,  $T_x \cdot \delta_H$ , of Equation 4.9 is ignored, then it follows that this interrelation will also apply for cases with membrane action.

The beams must also be designed to accommodate the tensions induced. At a support section the forces in concrete and steel must sum to

$$M'_x + T'_x \text{ and at mid-span to } M_x + T_x.$$

The value of  $T'_x = T_x = 2c'_x = 2c_x$  will be known from panel design but, so far, only the sum of  $M'_x + M_x$  has been found and the ratio of  $M'_x$  to  $M_x$  needs to be determined.

In cases without membrane action the ratio of  $M'_{xJ}$  to  $M_{xJ}$  may be found by consideration of the flexural stiffness of the beams with due allowance being made for moment redistribution within acceptable limits.

When membrane action is allowed for, two further aspects must be considered before the ratio of support to mid-span moment is found:

- (i) Dependence upon moment redistribution would lead to large deflections in the beams at ultimate load which could adversely affect the development of



membrane action in the panels of the floor. It is therefore recommended that special care should be taken to minimise moment redistribution.

(ii) The effect of tension on the beam moments is important. The beam moments have been defined as acting about the mid-depth where the net tension is taken to act. But the tension in the beams is due to slab compression acting near the level of the mid-depth of the slab which will normally be above the mid-depth of the beam.

This is equivalent to the application of a tension at the mid-depth of the beam plus a hogging moment (see Figure 4.2(a) and (b)).

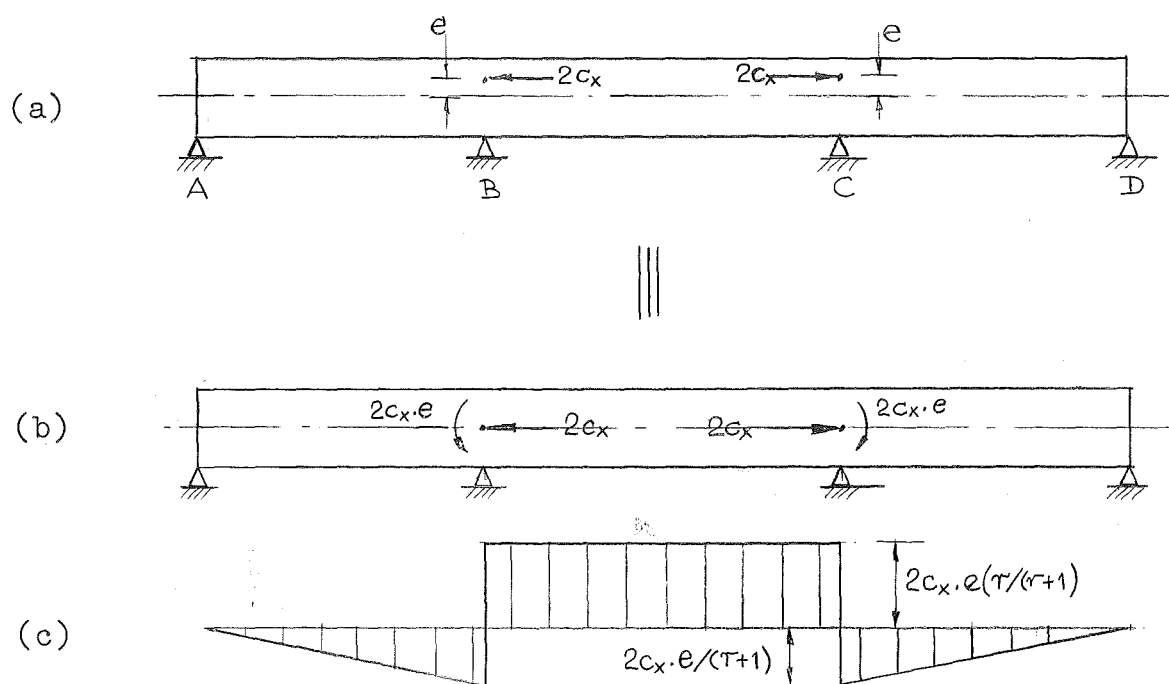


FIGURE 4.2. EFFECT OF COMPRESSIVE FORCES ON BEAM MOMENTS.

In Figure 4.2(a) the sum of the compressive forces,  $2c_x$ , in the panels on either side of the beam span, BC, have been shown applied at a distance,  $e$ , above the mid-depth of the beam. This is the manner in which the beam tension is applied in a slab and beam floor and Figure 4.2(b) shows the equivalent actions at the mid-depth of the beam. The tension is now applied at the mid-depth and in no way affects the moments about the mid-depth of the beam. The couples  $2c_x \cdot e$  do affect these moments, in fact producing a bending moment diagram of the shape shown in Figure 4.2(c) in which  $r$  is the ratio of the flexural stiffness of the spans ( $K_{CB}:K_{CD}$ ). Thus, if the amount of moment redistribution is to be kept to a minimum, when membrane action is considered, account should be taken of this effect.

The moments at the supports and at mid-span due to vertical loads only will be in the same ratio for any load. More particularly, the moments due to the Johansen load ( $M'_{xJ}$  and  $M_{xJ}$ ) will be in the same ratio as those due to the enhanced load (denoted  $M'_{xV}$  and  $M_{xV}$ ). Thus for an enhancement of load equal to  $F$ ,

$$M'_{xV} = F M'_{xJ}, M_{xV} = F M_{xJ}$$

When the effect of tension is added then

$$M'_x = F M'_{xJ} + 2c_x \cdot e \frac{r}{(r+1)} \quad \dots(4.10)$$

$$M_x = F M_{xJ} - \frac{2c_x \cdot e \cdot r}{(r+1)} \quad \dots(4.11)$$

Since the values of  $e$ ,  $r$ ,  $c_x$ ,  $F$ ,  $M'_{xJ}$ ,  $M_{xJ}$  will be known,  $M'_x$  and  $M_x$  may be found. The effect of membrane action on the relative proportions may be calculated, being dependent upon the values of  $c_x$ ,  $e$  and  $r$ .

Flexural steel may be allocated to the sections according to the ultimate strength method. Since the neutral axis will be near the compression face the sections can be designed on the assumption that the neutral axis is in the flanges and the effect of "compression" steel is negligible.

For the support section A of Figure 4.3(a), consideration of moment and force equilibrium gives:

$$T'_x = A'_s f_y - .85 f'_c a' b \quad \dots(4.12)$$

$$M'_x = A'_s f_y \left( \frac{D}{2} - d' \right) + .85 f'_c a' b \left( \frac{D}{2} - \frac{a'}{2} \right) \quad \dots(4.13)$$

Eliminating  $a'$  from these equations and making the resulting equation non-dimensional yields

$$\begin{aligned} \frac{1}{1.7} \left( \frac{p' f_y}{f'_c} \right)^2 - \left[ \frac{D}{d} - \frac{d'}{d} + \frac{2T'_x}{1.7 f'_c b d} \right] \left( \frac{p' f_y}{f'_c} \right) \\ + \frac{T'_x}{f'_c b d} \left( \frac{D}{2d} + \frac{T'_x}{1.7 f'_c b d} \right) + \frac{M'_x}{f'_c b d^2} = 0 \end{aligned} \quad \dots(4.14)$$

and similarly at mid-span, C,

$$\frac{1}{1.7} \left( \frac{b}{b_f} \right) \left( \frac{p f_y}{f'_c} \right)^2 - \left[ 1.0 + \frac{2T'_x}{1.7 f'_c b d} \left( \frac{b}{b_f} \right) \right] \left( \frac{p f_y}{f'_c} \right) + \frac{T'_x}{f'_c b d} \left( \frac{D}{2d} + \frac{T'_x}{1.7 f'_c b d} \left( \frac{b}{b_f} \right) \right) + \frac{M}{f'_c b d^2} = 0 \quad \dots(4.15)$$

Equations 4.14 and 4.15 are readily solved and show the effect of tension on the longitudinal steel requirements.

#### Influence of "Compression" Steel

The presence of steel near the compression face of the concrete has only a secondary effect on the capacity of the section. That this is so may be illustrated by considering the effect of its placement, after the section has been designed to include tension steel only. Compression steel may be above, below or at the depth of the neutral axis as given by tension steel design.

When placed at the neutral axis depth it has no effect. When placed in the compressive strain zone, this steel is in compression and the force introduced increases the moment about the mid-depth, but decreases the tension. When it is placed in the tensile strain region the moment reduces but the tension increases.

The conclusion that the compression steel has little effect on the capacities of the critical sections at ultimate load does not imply that its placement in the beam is of little value. Apart from serving to increase the ductility of high moment sections, its presence will substantially improve the tension carrying capacity of sections subject to low moment. In cases where the moment about the mid-depth of the section is zero, it is clearly

necessary to provide sufficient longitudinal steel in the section to carry the tension  $T'_x$  and this steel should be approximately evenly distributed between top and bottom faces of the beam.

The effect of tension on the reinforcement required at the two sections was investigated under the following conditions:

- (i)  $M'_x + M_x = \text{constant}$
- (ii)  $M'_x/M_x$  varied
- (iii)  $T'_x$  was varied in magnitude.

For each combination, the quantities  $(p'f_y/f'_c)$  and  $(pf_y/f'_c)$  were calculated.  $T'_x$  was applied in two different ways:

- (a) at the mid-depth of the beam so that it had no effect on the values of  $M'_x$  or  $M_x$
- (b) at a distance,  $e$ , from the mid-depth such that

$M'_x$  and  $M_x$  were modified according to:

$$M'_x (\text{modified}) = M'_x (T'_x = 0) + T'_x \cdot e$$

$$M_x (\text{modified}) = M_x (T'_x = 0) - T'_x \cdot e$$

Variation of  $pf_y/f'_c$  and  $p'f_y/f'_c$  with  $T'_x$  is shown in Figure 4.3(b).

In the range plotted, both  $p$  and  $p'$  increase approximately linearly with  $T'_x$  for both positions of application.

For no eccentricity,  $p$  rises more steeply than  $p'$  but the reverse is the case when  $T'_x$  is applied at  $.25d$  above the mid-depth of the negative moment section.

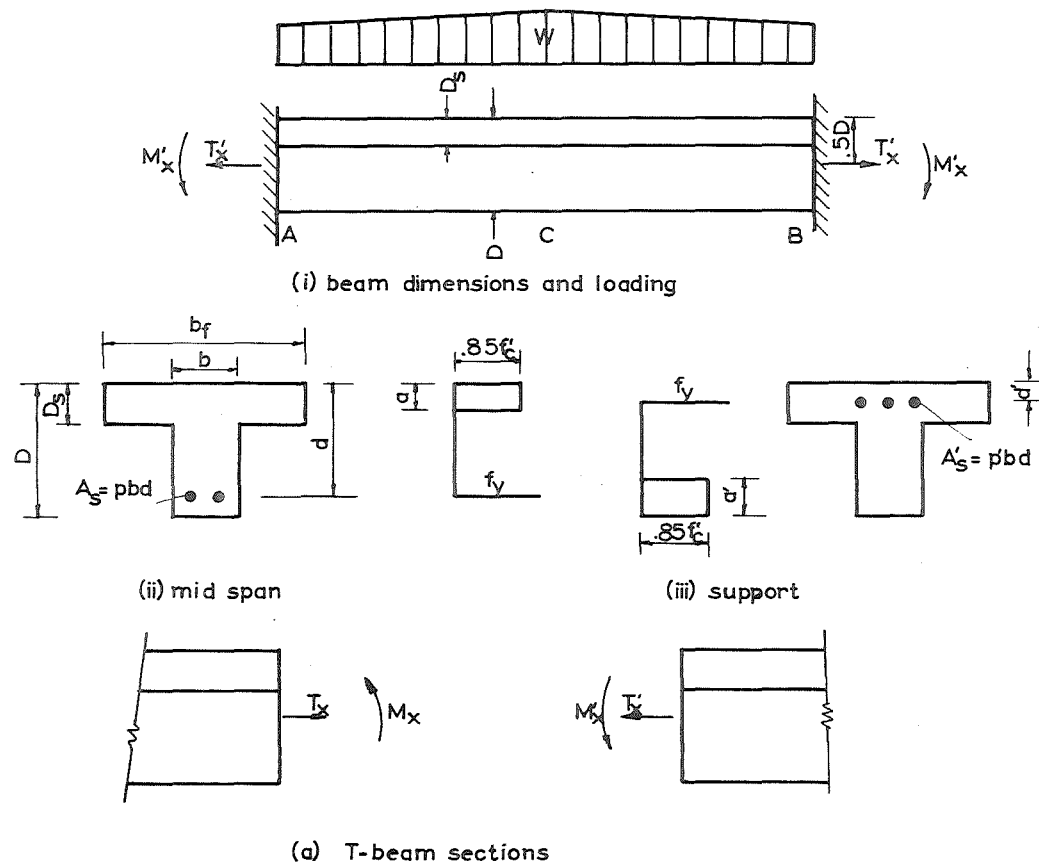
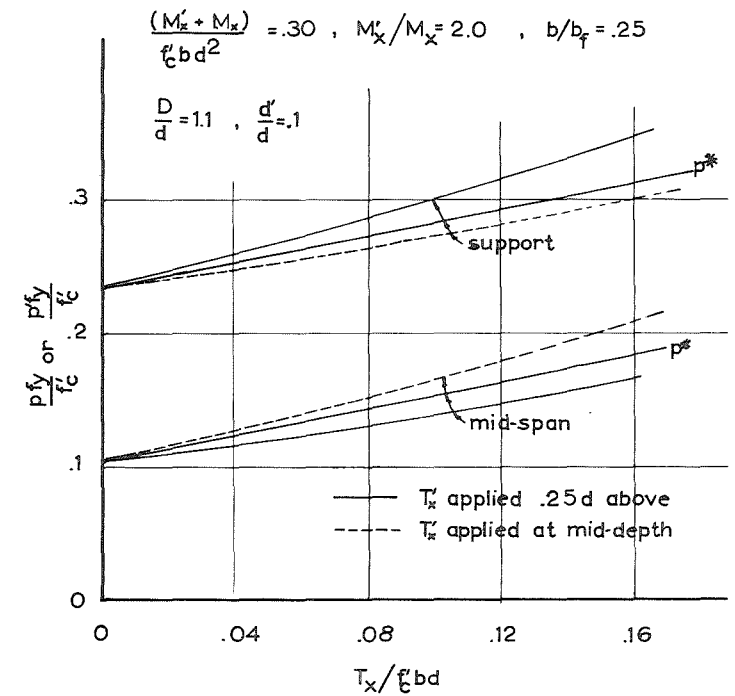


FIGURE 4.3 DESIGN OF BEAMS FOR TENSION

(b) effect of tension on steel requirements



It is interesting to compare the rates of rise of  $p$  and  $p'$  in this case with their rates of rise when no moment is applied. For this latter case

$$T'_x = 2 p^* b d f_y \quad \dots(4.16)$$

where  $p^*$  is the percentage of steel placed at both the top and bottom of the section.

$$\text{Hence, } \frac{p^* f_y}{f'_c} = \frac{T'_x}{2 f'_c b d} \quad \dots(4.17)$$

The variation of  $p^*$  is shown on Figure 4.3(b). Comparison of this with the curves when moment is present shows that the variation of total steel percentage is almost identical but at each of the critical sections the amount of extra steel required follows the variation of  $p^*$  rather than the  $2p^*$  required at a section on which no moment acts.

Two important conclusions may be drawn from Figure 4.3(b), viz:

- (a) The variation of steel percentage with tension is approximately linear.
- (b) The rate of increase in the total extra steel required when tension acts on a section is less when moment is also acting. Maximum extra steel is required when no moment acts and is given by Equation 4.17.

Hence the extra steel required in the whole beam to accommodate the tension will be less than that required for

a simple tie member.

### 4.3 THE EFFECT OF PANEL MEMBRANE ACTION ON TORSION IN SUPPORTING BEAMS

#### 4.3.1 Introduction

In designing an edge panel of a slab and beam floor system by yield line theory the torsional resistance provided by the exterior beams may be put to good use by placing steel in the top of the slab sections along the edge supported by these beams and relying on the full development of hogging yield moments in assessing the ultimate load of the panel. The edge beam would be required to take the torsion induced. The presence of compressive membrane action in the panel may affect the magnitude of this torsion in two ways:

In cases where the edge beams are stiff enough to withstand the lateral forces induced by compressive membrane action forces in the panel, these forces will induce a torsional moment in the beams unless they act through the shear centre of the beam.

In addition, the low torsional stiffness of the edge beams requires large rotations of the slab segments and before these take place, membrane forces may develop in other regions of the slab so that the full development of hogging yield moments along the exterior edges of the panel is not required.



Both of these effects are discussed in the following sections.

#### 4.3.2 Torsion Induced by Membrane Forces at the Edge of the Panel

This case is illustrated by considering the square, isotropically reinforced slab supported by beams around its perimeter as shown in Figure 4.4(a) and (b).

At the ultimate load the hogging yield moment will develop at the beam-slab junction and if  $m_J$  and  $m'_J$  are the enhanced hogging and sagging yield moments, the Johansen load given by the pattern of Figure 4.4(a) is

$$w_J = 24m_J(1+i)/L^2 \quad \dots(4.18)$$

When membrane action causes enhancement of this load to  $w_M = F.w_J$  it is reasonable to assume that both  $m$  and  $m'$  are enhanced by  $F^*$  giving  $m = F^*m_J$  and  $m' = iF^*m_J$ . Note that  $F^*$  will normally be greater than  $F$  (see Equation 4.5).

The maximum torsional moment in the beams will occur at the sections at the beam junctions, being the sum of the torsional moments induced by the actions of Figure 4.4(b) taken over half the length of the beam. Taking the general case in which membrane action enhances the Johansen load by  $F$ , the maximum torque  $T_m$  is given by

$$T_m = \sum_{L/2} (sb/2) + \sum_{L/2} (iF^*m_J) - \sum_{L/2} (c'_c - t'_y)(D/2 - D_s/2 - d_u) \quad \dots(4.19)$$

and since  $\sum_{L/2}^{<}(s) = \frac{w_M L^2}{8}$ ,  $m_J$  and  $(c'_c - t'_y)$  are constant along the edge,

$$T_m = .5L(Fw_J Lb/8 + iF^* m_J - (c'_c - t'_y)(D/2 - d_u - D_s/2)) \dots (4.19a)$$

For no enhancement:

$$im_J = t'_y(D_s/2 - d') + c'_c(D_s/2 - c'_c/1.7f'_c) \dots (4.20)$$

Denoting  $c'_c/.85f'_c = a$ , and noting that  $c'_c = t'_y$  for no enhancement, Equation 4.20 becomes:

$$im_J = t'_y(D_s - d' - a/2) \dots (4.20(a))$$

For a moment enhancement of  $F^*$  we have

$$iF^* m_J = t'_y(D_s/2 - d') + c'_c(D_s/2 - a/2) \dots (4.21)$$

and substitution for  $im_J$  from 4.20(a) gives

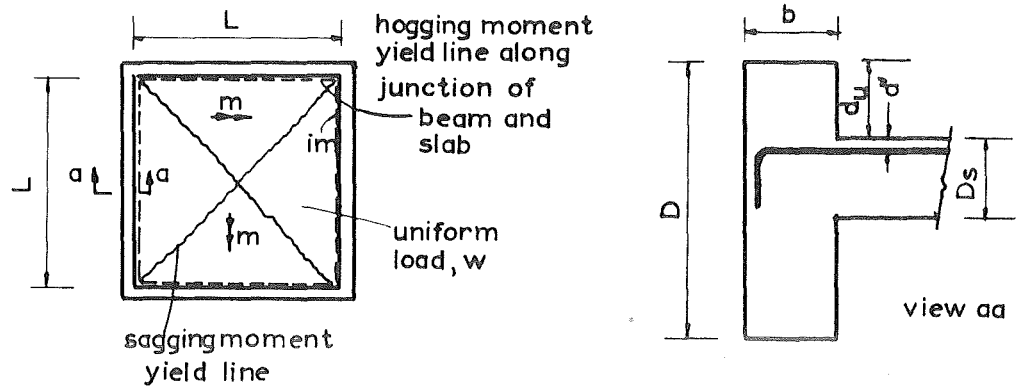
$$c'_c = t'_y(2F^* - 1 - 2d'/D_s(F^* - 1) - F^* a/D_s)/(1 - a/D_s) \dots (4.21(a))$$

which may be substituted in 4.19(a). Using Equations 4.18 and 4.21 to express all quantities in terms of  $im_J$  and assuming that 'a' does not vary, Equation 4.19(a) becomes

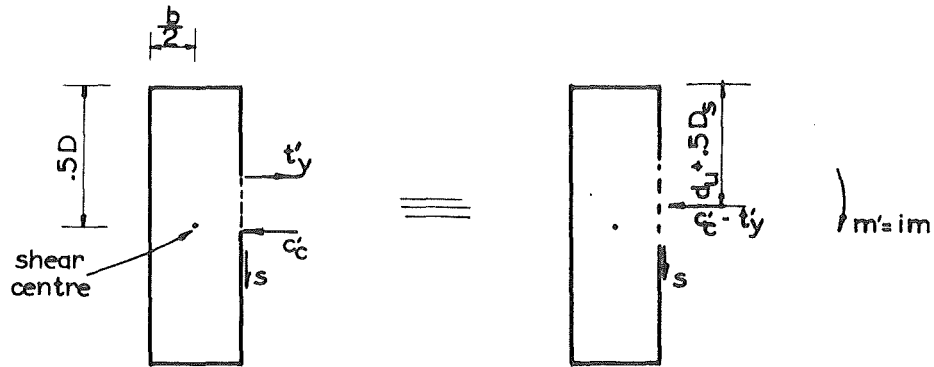
$$T_m = Fim_J \frac{L}{2} \left[ \frac{F^*}{F} + 3\left(\frac{b}{L}\right) \cdot \frac{(1+i)}{i} - \frac{2(F^* - 1)(D/2 - d_u - D_s/2)}{(1 - a/D_s)} \right] \dots (4.22)$$

$$= iFm_J L/2 (1 + A + B) \dots (4.22(a))$$

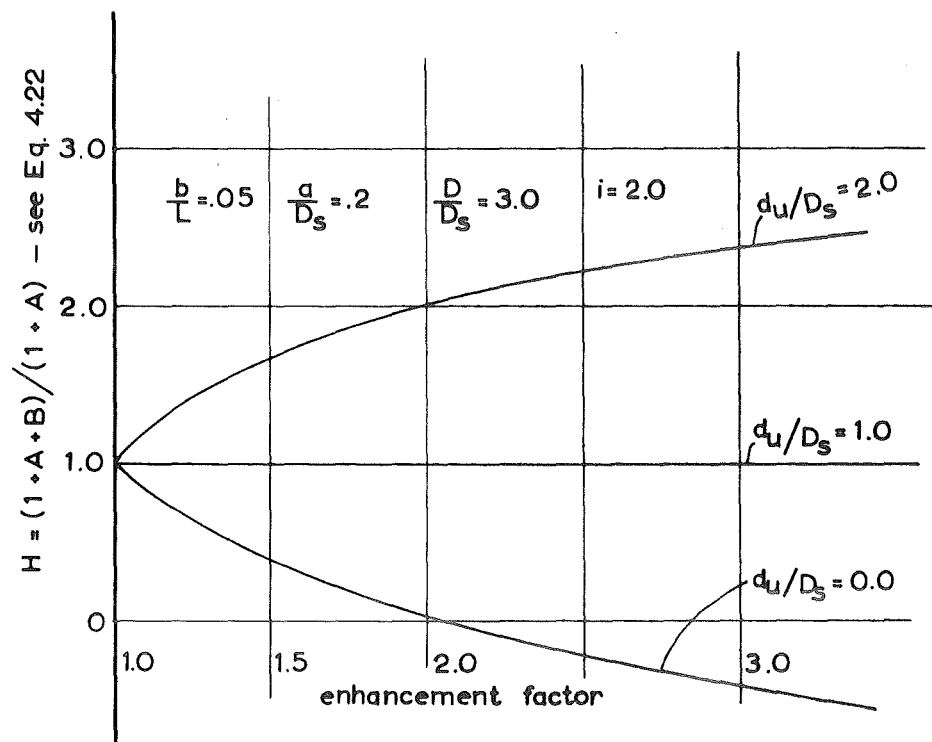
Now, without enhancement ( $F = 1$ ),  $B = 0$  and the maximum



(a) slab, and beam junction dimensions



(b) actions per unit length of beam



(c) effect of membrane action on maximum torque

FIGURE 4.4 TORSION IN EDGE BEAMS

torque is  $im_J L/2(1+A)$  as would normally be the case. However, once membrane action enhancement takes place the position of the slab centroid with respect to the shear centre of the beam becomes important. This effect is taken into account by the term B and the magnitude of this effect may be conveniently determined by calculating the ratio,  $H = (1+A+B):(1+A)$ , for various F values and beam-slab junctions. The results of these calculations for a typical beam are given below.

#### Calculation of the Ratio H

Example beam.

$$\frac{b}{L} = .05, \quad \frac{a}{2D_s} = .1, \quad i = 2.0, \quad \frac{D}{D_s} = 3.0$$

Assuming  $F^* = F$ .

$$\text{Therefore } 1+A = 1.225, \quad 1+A+B = 1.225 - 2.5 \frac{(F-1)(1-\frac{d_u}{D_s})}{F}$$

<u>Load Enhancement Factor</u>	<u>Values of <math>H = (1+A+B)/(1+A)</math></u>		
<u>F</u>	$d_u/D_s=0$	$d_u/D_s=1.0$	$d_u/D_s=2.0$
1.0	1.00	1.00	1.00
1.25	.59	1.00	1.41
1.50	.32	1.00	1.68
2.0	-.02	1.00	2.02
2.5	-.23	1.00	2.23
$\infty$	-1.05	1.00	3.05

These values are plotted on Figure 4.4(c).

The effect of change in  $d_u/D_s$  is understandably large and changes sign when the mid-depth of the slab coincides with the mid-depth of the beam. The reduction in maximum torsion is remarkable when the top of the slab is flush with the top of the beam.

#### 4.3.3 Conclusion

Design of a slab such as in Figure 4.4 to include the effects of membrane action would require the beams to be designed for a laterally outward load in addition to the normal vertical load. Placement of the slab flush with the beam at the top would offset this additional requirement by reducing the torsion induced in the beams. In the more general case in which lateral restraint is provided by surrounding panels and the supporting beams the effect on the beams would not be as great. The surrounding panels would take most of the lateral force and the nett lateral force on the beam would be smaller. Less effect on lateral bending and torsion would result.

Nevertheless, the high sensitivity of the maximum torque, even at low enhancement factors, indicates that consideration of this behaviour is important in many cases.

#### 4.3.4 Suppression of Hogging Yield Moment Development Along Exterior Edges of Panels in Which Membrane Action is Present

In designing edge panels to develop full hogging

moments along the exterior edges, only the torsional strength of the edge beam need be sufficient for this to occur ultimately. In the case of panels which may develop membrane compressive forces which enhance the load capacity of the panel, the full development of the exterior edge hogging yield moments may not be required. In the test to destruction on a model nine-panel reinforced concrete slab and beam floor described in Chapter 9, the steel strains along the exterior edges of the edge panels were well below yield values at the predicted ultimate load and a reduction in the edge beam torsion was evident. The presence of compressive membrane forces normal to the edge would account for the reduction in torsion, and, because membrane action is not purely an ultimate phenomenon, the value of the restraining moment could have been enhanced above that which the level of steel strains would normally imply.

However, the capacity of the edge beams to resist lateral force was not high and an alternative mechanism was sought.

Recently,<sup>(39)</sup> it has been reported that the torsional stiffness of a reinforced concrete beam reduces remarkably when cracking occurs. It is clear then that large twisting deformations of the beam would be required before the full yield moment could be developed and the slab element would have to rotate even further to create the differential movement necessary for the development of the yield moment.

No attempt was made to analyse this case but the observed behaviour during the test suggested that membrane action in other regions of the edge panels provided assistance in carrying the load before sufficient slab deformation could occur to develop the hogging yield moments along the exterior edges. Torsional moments in the edge beams computed on the basis of the full development of these hogging yield moments could thus considerably overestimate the true values.

#### 4.4 DISCUSSION AND CONCLUSION

It is clear that membrane action in panels will affect the flexural and torsional steel requirements of beams.

The method of determining beam tensions is a simplification but values of beam section actions resulting provide adequate strength and a realistic distribution of moment between mid-span and support sections.

The equations derived to determine the flexural reinforcement at critical sections of a T-beam subject to moment and axial tension require some qualification in that at sections of the beam at which the moment is zero, a sufficient amount of longitudinal steel must be placed to take the tension. Furthermore, at the critical sections it is necessary to check that the neutral axis lies within the section.

Because of the likely adverse effect of beam deform-

ations on the development of panel membrane action it would be wise to ensure the beam collapse mechanisms do not occur before the panel mechanism.

The effect of compressive membrane action on the torsion induced in the supporting beams is clearly considerable, and worthy of consideration in design. For the case in which membrane forces acting normal to the edge beam reduce the torsion, any advantage so gained could be offset by any extra provision required for biaxial bending of the beams.

However, in cases where membrane action may exist in other regions of the edge panels it is likely that the torsion for which the edge beams would normally be designed will not be attained. This latter effect, or even the combination of the two effects discussed could provide an instance in which the neglect of membrane action leads to the overdesign of edge beams for torsion.



## CHAPTER 5

### STIFFNESS OF SURROUNDS FOR SQUARE SLABS

#### 5.1 INTRODUCTION AND SUMMARY

The degree to which compressive membrane action enhances the load carrying capacity of a reinforced concrete slab depends principally on the lateral stiffness of the elements providing restraint against outward movement of the slab edges.

For interior panels of a multi-panel slab and beam floor, this restraint is provided by the panels surrounding the one in question. Thus when the interior panel exhibits compressive membrane action, the surrounding panels are subject to in-plane forces. The surrounding elements may therefore be considered as a flat slab with in-plane loads applied normal to the edges of a central hole which corresponds in size to the panel exhibiting compressive membrane action.

In order to obtain some measure of the variation of surround stiffness with the size of the outer panels, slabs of elastic, isotropic, homogeneous materials were analysed. The study was restricted to the consideration of a square slab with a square central hole.

A library computer programme employing the finite element method for the solution of plane stress problems was used to calculate the deflections of the loaded edges and the stresses within the surround.

Because the rigorous plane stress analysis required large computational effort an alternative method of computing the edge deflections was sought. Consideration of each edge of the surround as a deep beam proved very satisfactory in this respect. The rapid computation of edge displacements would permit extension of theories such as that due to Park<sup>(11)</sup> to include interaction of the edges of surround and slab.

## 5.2 METHOD OF ANALYSIS AND CASES CONSIDERED

The dimensions and properties of the slab considered in this study are shown in Figure 5.1(a). Due to symmetry it was necessary to analyse only the portion ABCDEF with boundary conditions as in Figure 5.1(b). For each surround shape, three separate load distributions were applied to the edges, BC and CD, each of the same total load. The shapes of these distributions (see Figure 5.1(c)) were chosen as representative of the possible distributions of membrane forces along the edges of a square interior slab.

Analysis was carried out using an existing computer programme for solving plane stress problems by the finite element method based on a quadratic strain triangle<sup>(21)</sup>.



Each of the portions ABCF and CDEF was divided into 160 triangular elements as in Figure 5.2. Loads were applied to nodal points in the y direction along BC and in the x direction along CD.

The study was limited to cases in which  $a_x = a_y$  and  $b_x = b_y$ . In the first series, the slab was of uniform thickness throughout and four cases were considered with  $a_x/b_x$  taking the values: .5, 1.0, 1.5, 3.0.

To investigate the effect of supporting beams, the case of  $a_x/b_x = 1.5$  was analysed with a thick band along BC and CD. The dimensions of this band are shown in Figure 5.2. The symmetrical shape was required because a two-dimensional stress system was being analysed, and the tapering thickness across the second row of elements was necessary to avoid stress discontinuity at the element boundaries.

For each surround under each load the following quantities were determined at each nodal point.

- (i) The normal stresses and strains in the x and y direction.
- (ii) The shear stress and strain in the x or y direction.
- (iii) The maximum and minimum principal stresses.
- (iv) The maximum shear stress.
- (v) Displacements in the x and y direction.

For reasons outlined under 5.1, displacements of the

loaded edges were of particular interest in the context of membrane action and it is these that receive greatest attention in the following sections.

### 5.3 DISPLACEMENTS OF THE LOADED EDGES

Although stress concentration at the re-entrant corner, B, cast doubt on the accuracy of computed stresses near this point, the use of small elements in this region ensured that its effect on stresses at other points was very small, and the effect on deflections even less.

In Figure 5.3 the displacements in the y direction of the edge BC of the surrounds are shown. The quantity,  $n = \frac{\Delta t E}{W}$ , expresses this movement in non-dimensional form.  $\Delta$  = deflection of the edge,  $t$  = thickness of slab,  $E$  = modulus of elasticity of slab material,  $W$  = total load applied normal to the edge BC ( = one half of total load applied to one edge of the interior hole).

Hence the deflection,  $\Delta$ , of the edge may be obtained from

$$\Delta = nW/tE \quad \dots(5.1)$$

Features to note in Figure 5.3 are

- (a) The small difference between load cases (i) and (ii).
- (b) The large difference between load case (iii) and load case (i).

- (c) The ratio of maximum deflection (at B) to deflection at C is greater for low values of surround width.
- (d) Deflections along the edge are remarkably constant for load case (iii), especially for  $a_x/b_x = 1.0$  and  $1.5$ .
- (e) The maximum deflection falls off rapidly as  $a_x/b_x$  is decreased from  $3.0$ , but the change in maximum deflection when  $a_x/b_x$  is decreased from  $1.0$  to  $0.5$  is very small.

Figure 5.4 shows that load case (iii) has less sensitivity to change in  $a_x/b_x$  than load case (i) and gives a clear indication that decrease in  $a_x/b_x$  lower than  $1.0$  brings little increase in surround stiffness. The effect of increasing the surround width is further lessened when the results of Chapter 3 are recalled, viz., an increase in surround stiffness does not produce a proportionate increase in the enhancement factor.

(f) The effect of including the thicker edge beam on the maximum deflection is plotted in Figure 5.4. In both load case (i) and load case (iii) its inclusion is equivalent to increasing the surround width. However, this effective increase in width was less than could have been achieved by using the same amount of extra material to increase the surround width directly. This situation

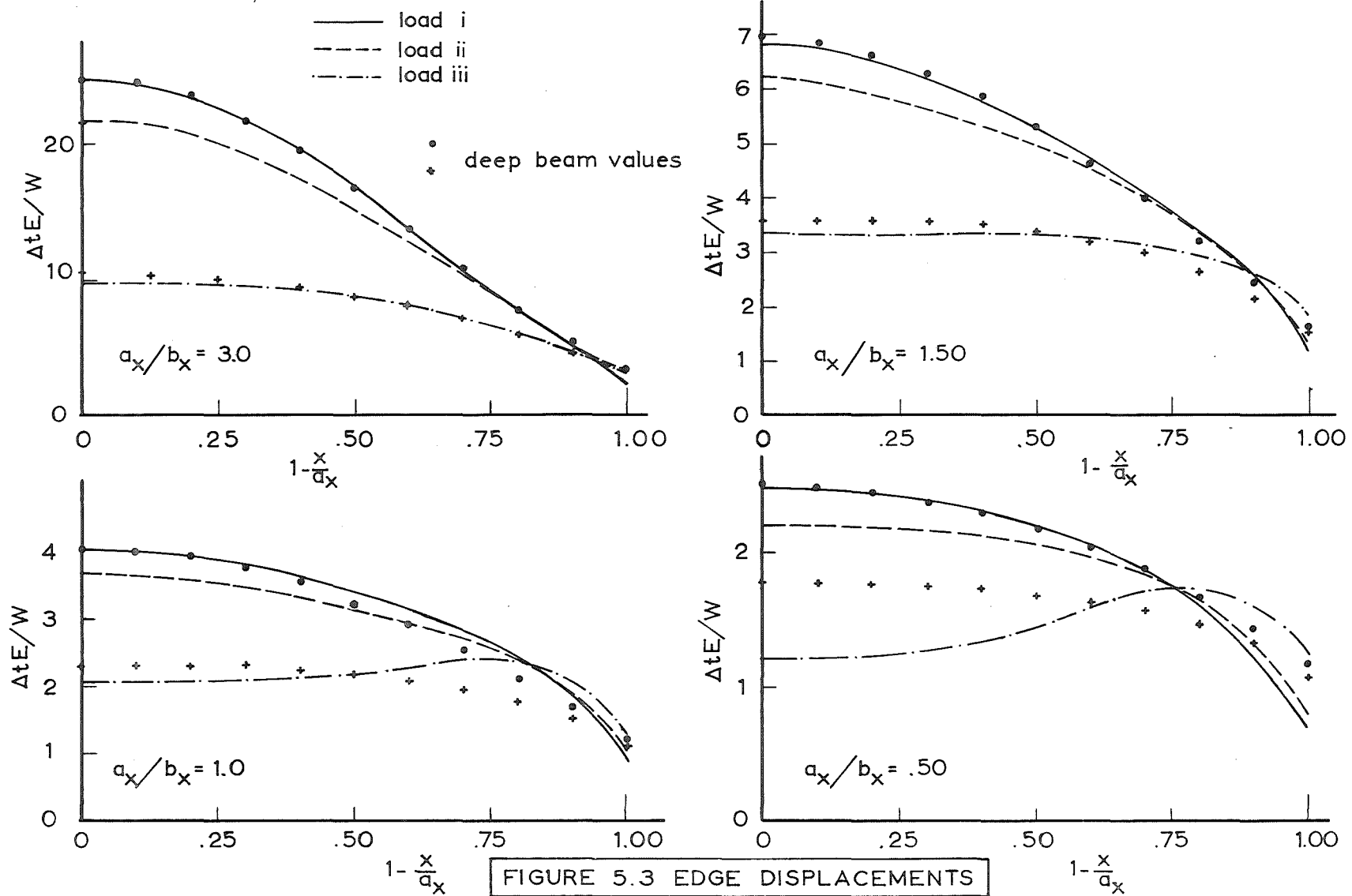


FIGURE 5.3 EDGE DISPLACEMENTS

is likely to reverse in cases of very wide surrounds where the contribution of the extension of the side CD is proportionately greater.

#### 5.4 STRESSES IN THE SURROUND

Because regions of high stress in reinforced concrete will crack, knowledge of the distribution of stress within the surround as computed for an elastic, homogeneous, isotropic material is of limited value. However, knowledge of the regions of high stress provides a means by which the surrounding panels may be adequately and efficiently reinforced to resist the stresses induced by membrane forces acting in the central panel.

In Figure 5.5(a), contours of the direct stress in the y direction are plotted for load case (i) on a surround of uniform thickness and with  $a_x/b_x = 1.0$ . The stress contour values relate to the intensity of the uniform pressure applied to BC and CD.

Figure 5.5(b) shows the contours of the shear stress along the face of a section taken parallel to either the x or y axis. Stress contours again refer to the intensity of applied pressure.

#### 5.5 DEEP BEAM APPROXIMATION

##### 5.5.1 Introduction

Detailed plane stress analysis is not straightforward



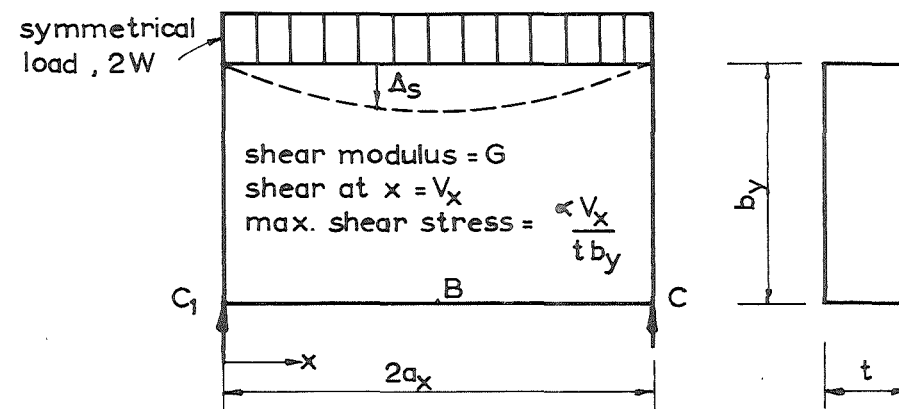
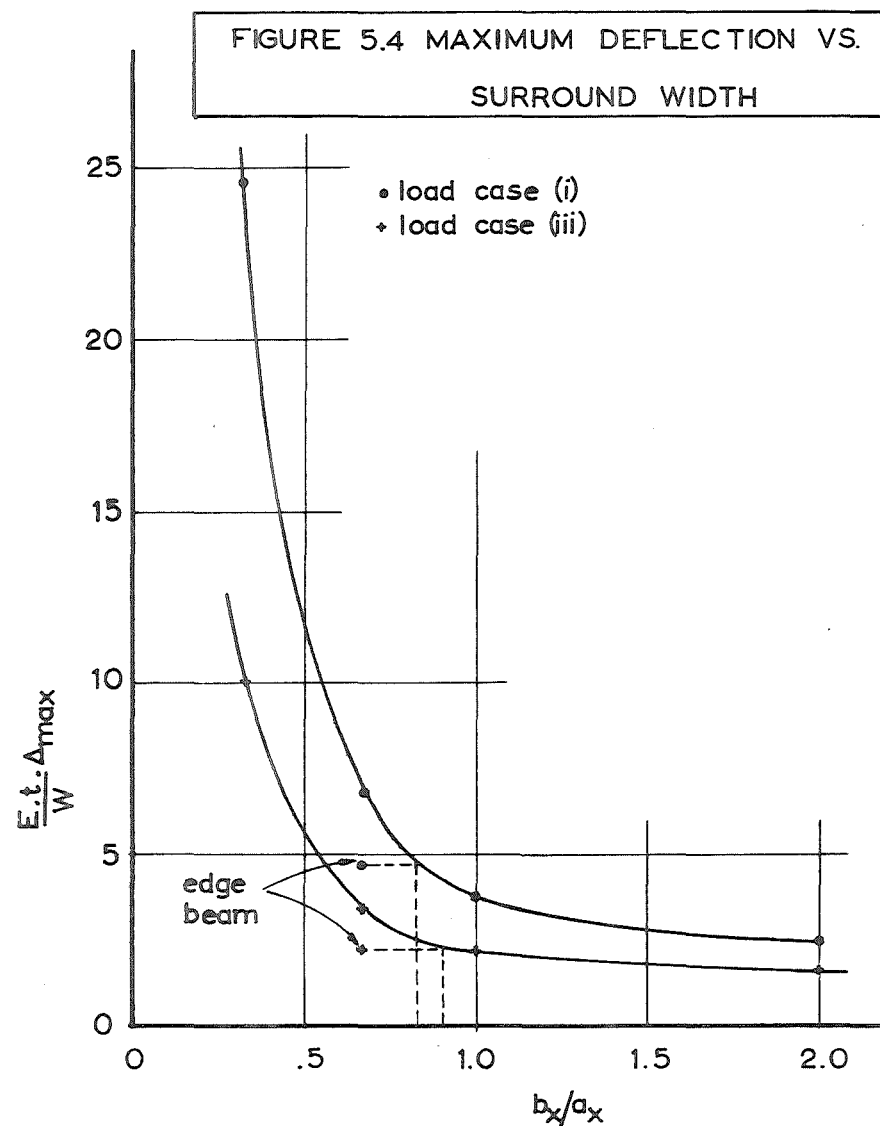


FIGURE 5.6 SHEAR DEFLECTION

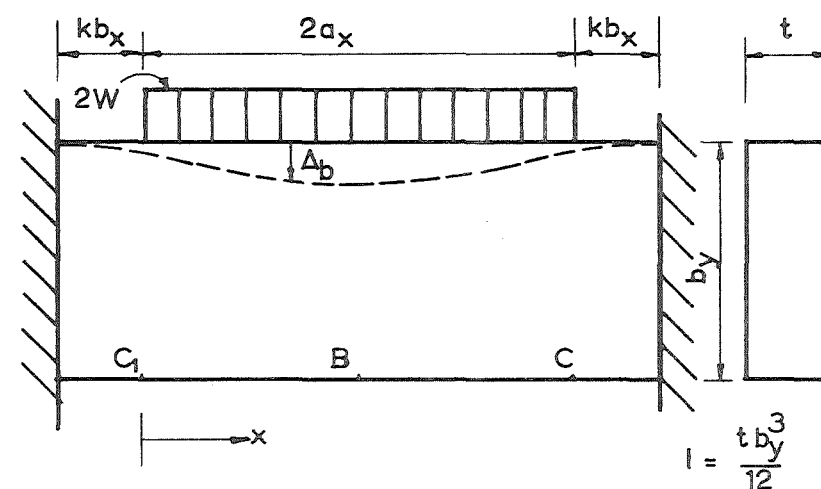
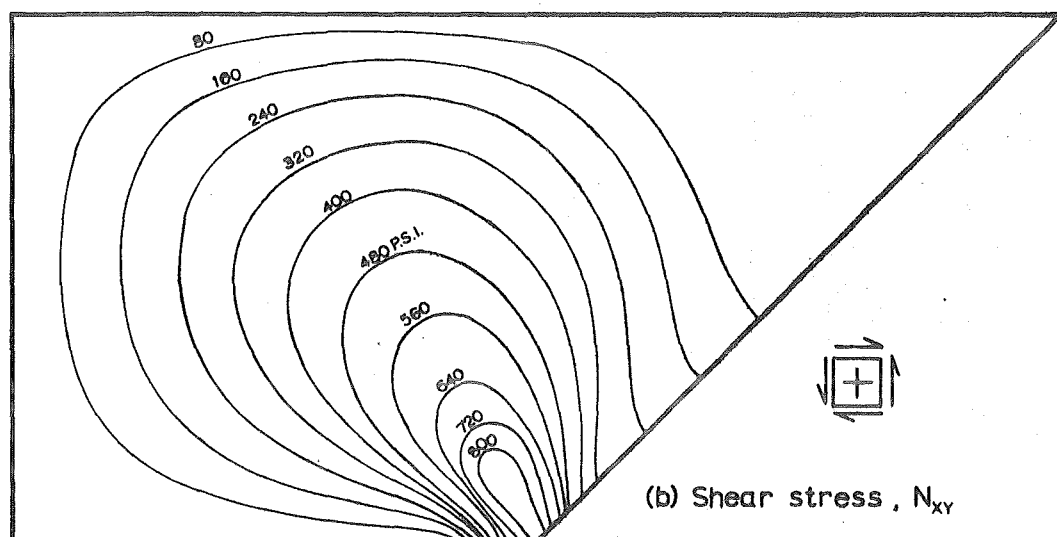
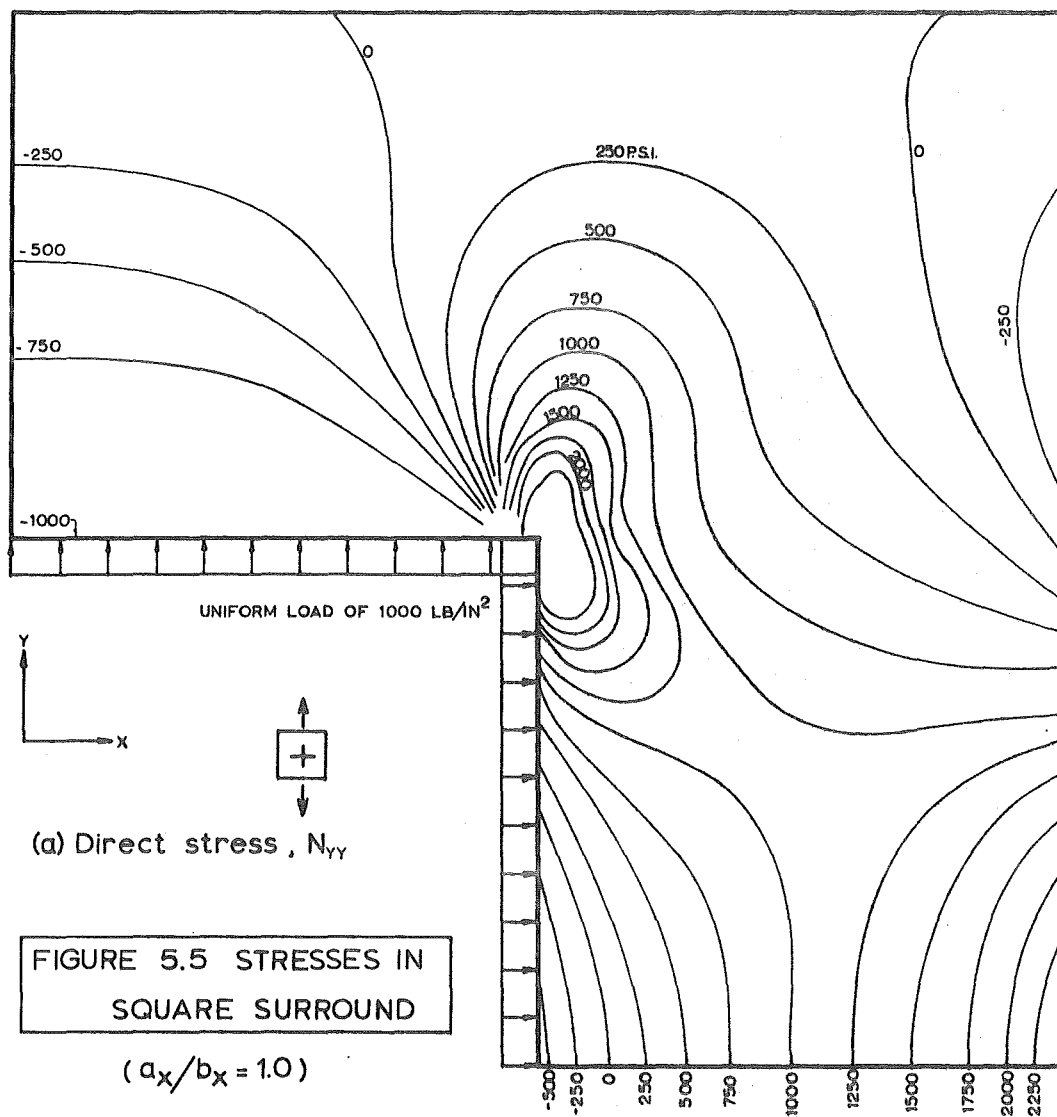


FIGURE 5.7 FLEXURAL DEFLECTION



and requires considerable computational effort. The interest in this problem in respect to membrane action in reinforced concrete slabs is chiefly in the deflection of the loaded edges. In membrane action theories such as that due to Park<sup>(11)</sup>, the edges of the slab are assumed to move out a uniform distance regardless of the variation of load intensity along the edge. A possible means of refining this would be to account for the interaction of load intensity and lateral deflection at the restraining edge of the slab. Such a method would require iteration of the load intensity until outward movements of the restraining surround were compatible with those of the slab edge.

A quick and reasonably accurate method of determining the surround deflection profile would therefore be extremely advantageous.

On the basis of the results of the plane stress analysis, an "equivalent" deep beam was found which gave the same maximum deflections and a similar deflected shape. This was done by considering deformation of the surround edge due to axial extension of the sides, shear deformations in the clear span, and flexural deformation of a beam of length slightly greater than the clear span.

#### 5.5.2 Deep Beam Model

The total deformation of the side  $C_1BC$  (Figures 5.1 and 5.6) of the surround was assumed to be made up of:

(i) axial extension of the portion  $CDEH$  (Figure 5.3),

(ii) shear deformation of the portion ABDG as if it were half of a simply supported beam of span  $2a_x$ , and (iii) flexural deformation of a fixed ended beam of span  $2(a_x + kb_x)$ . These are described in detail below.

(i) Axial Extension

This was computed assuming that CDEH was a tie rod. Force in tie rod =  $W$ , area of cross section =  $t b_x$ , length =  $a_y$

$$\therefore \text{Extension } \Delta_e = \frac{W \cdot a_y}{t b_x \cdot E} \quad \dots(5.2)$$

A useful non-dimensional form for the deflection is

$$\frac{\Delta_e \cdot Et}{W} = \frac{a_y}{b_x} \quad \dots(5.3)$$

This extension applied to the whole profile of BC, regardless of the distribution of the load,  $W$  along it.

(ii) Shear Deformation

For a simply supported beam as in Figure 5.6 the shear displacement,  $\Delta_s$  is given by

$$\frac{d\Delta_s}{dx} = \frac{\alpha V_x}{t b_y G}$$

Two cases of load were considered:

(a) uniform

(b) cubic - as in load case (iii) (Figure 5.1).

(i) Uniform load

This gives

$$\Delta_s \cdot Et/W = (\alpha E/2G)(a_x/b_y)(x/a_x)(2-x/a_x) \dots(5.4)$$

(ii) Cubic Variation as in Figure 5.1(c)

$$\frac{\Delta_s tE}{W} = \frac{\alpha E a_x}{G b_y} (X-2X^2 + 2X^3 - X^4 + X^5/5) \dots(5.5)$$

where  $X = x/a_x$

(iii) Bending Deflection

The model was as shown in Figure 5.7.

Deflections resulting were as follows:

(a) Uniform Load

$$\Delta_b \frac{tE}{W} = \left(\frac{a_x}{b_y}\right)^3 \left\{ \frac{\left[2 + 6\left(\frac{kb_x}{a_x}\right) + 3\left(\frac{kb_x}{a_x}\right)^2\right] \left[\frac{x}{a_x} + \frac{kb_x}{a_x}\right]^2}{\left(1 + \frac{kb_x}{a_x}\right)} - 2 \left[\left(\frac{x}{a_x}\right) + \left(\frac{kb_x}{a_x}\right)\right]^3 + \frac{1}{2} \left(\frac{x}{a_x}\right)^4 \right\} \dots(5.6)$$

(b) Cubic Distribution

$$\Delta_b \frac{tE}{W} = \left(\frac{a_x}{b_y}\right)^3 \left\{ \frac{\left[1 + 6\left(\frac{kb_x}{a_x}\right) + 3\left(\frac{kb_x}{a_x}\right)^2\right] \left[\frac{x}{a_x} + \frac{kb_x}{a_x}\right]^2}{\left(1 + \frac{kb_x}{a_x}\right)} - 2 \left(\frac{x}{a_x} + \frac{kb_x}{a_x}\right)^3 + \left(\frac{x}{a_x}\right)^4 \left[2 - \frac{6}{5} \left(\frac{x}{a_x}\right) + \frac{2}{5} \left(\frac{x}{a_x}\right)^2 - \frac{2}{35} \left(\frac{x}{a_x}\right)^3\right] \right\} \dots(5.7)$$

5.5.3 Determination of k and Deflected Shapes

For the uniform load case, the maximum deflection of the edge of the surround for each surround shape was

computed using plane stress analysis.

Comparison of the two maximum deflections using Equation 5.6 yielded a cubic equation in  $k$  which was solved for each surround shape. For a square hole in the centre of a square slab, the surround shape was defined by the value of  $b_x/a_x$ . For the four values of  $b_x/a_x$  the variation of  $k$  with  $b_x/a_x$  was close to parabolic and  $k$  was assumed to be given by

$$k = A(b_x/a_x)^2 + B(b_x/a_x) + C$$

Least squares analysis of the four values gave

$$k = .0795(b_x/a_x)^2 + .0795(b_x/a_x) + .126 \quad \dots(5.8)$$

This value of  $k$  was taken to apply for any symmetrical load distribution and was used in Equations 5.6 and 5.7 to obtain the deflected shapes of the equivalent deep beam. The shapes were calculated as the sum of deflections given by Equations 5.3, 5.4 or 5.5, and 5.6 or 5.7, and are plotted on Figure 5.3 for comparison with the plane stress analysis solutions.

## 5.6 CONCLUSIONS

In spite of the assumption that the material was elastic, isotropic and homogeneous, the results of the above analysis provide a valuable insight into the problem of determining the outward movement of the edges of a

reinforced concrete slab restrained laterally at its edges by a rectangular surrounding medium.

The following conclusions were drawn:

(i) Effect of Increase in Surround Width

Figure 5.4 shows clearly the effect of increase in  $b_x/a_x$  on the stiffness of the surround. For ratios of  $b_x/a_x$  greater than 1.0 very little gain will show up in the enhancement of the load capacity of the central panel. Increase of the ratio  $b_x/a_x$  above 2.0 may be assumed not to contribute to surround stiffness. This will be especially so when the effects of creep, shrinkage, cracking and vertical deflection of the central panel serve to reduce the effective surround stiffness

(ii) Deep Beam Approximation

The lateral deformations as computed for an equivalent deep beam agree well with the more rigorously derived values. The equivalent deep beam could be used with good effect in calculating outward movements of the surround in refining Park's theory<sup>(11)</sup> for the determination of the ultimate loads of laterally restrained reinforced concrete slabs. It is of interest to note that a steel surround of relatively low  $b_x/a_x$  and large thickness,  $t$ , would provide a stiff surround and would be well modelled by the deep beam approximation.

(iii) Stresses

The re-entrant corner caused a large increase in

stress and the region near it should be reinforced in both directions.

Large tensile stresses occur at the outside edge at the mid-span of the side of the surround and could well require special reinforcement.

An appreciable compressive stress normal to the "span" of the surround is developed, i.e., the panels adjacent to the central one are subject to in-plane compression in one direction which could enhance the transverse load capacity.



## CHAPTER 6

### DESIGN AND CONSTRUCTION OF MODEL SLAB AND BEAM FLOOR

#### 6.1 INTRODUCTION

This chapter describes the design and construction of a quarter scale, nine panel reinforced concrete slab and beam floor. Figure 6.1 is a structural drawing of the slab.

Both the slab itself and the testing programme were designed to investigate the effects of membrane action in a representative floor system. Compressive membrane action enhancement was allowed for in the centre and centre-edge panels. The appropriate beam spans were designed to accommodate the tension induced in them by the compressive forces in the plane of the panels. Particular note was taken of the following aspects of the behaviour of the floor under load:

- (a) The general effect of compressive membrane action on the behaviour of panels and beams and on the floor system as a whole.
- (b) The relative contributions of the surrounding



beams and panels in providing the lateral restraint necessary for load enhancement by compressive membrane action.

(c) The magnitude and distribution of in-plane forces in the slab panels, especially the centre panel.

(d) The magnitude of the tensions induced in the beams and the effect of this tension on the beam behaviour.

(e) The level of steel strains, especially in the beams, as a check on the adequacy of the steel provided in order that a more realistic steel volume comparison could be made between the design method used and design by conventional yield line theory.

Although the floor was to be a quarter scale model of a full size floor, no particular floor was modelled and dimensions used in design were those of the model floor. The design followed procedures as for a full size structure except for cover requirements which were scaled down from Code of Practice values.

For a model in which all dimensions of all components are scaled by the same factor, the behaviour is theoretically the same as that of the prototype and in the case of a floor, both model and prototype have the same load capacity per unit area. This prediction is based on the

assumption that the component materials of steel and concrete exhibit the same strength characteristics regardless of the absolute size of the model. That this assumption may not hold was shown by Little and Paparoni<sup>(28)</sup>, who reported greater strength with reduction in size. However, the order of the effect of reduction of absolute size was not significant in models for which the ratio of prototype to model lengths was not large. Alami and Ferguson<sup>(23)</sup> have reported satisfactory results for beams with scale factors up to 4.5 with the qualifications that cracking is only approximately modelled and that for beams failing primarily as a result of bond failure, reliable results cannot be expected. Tests on quarter scale model floors at the University of Illinois<sup>(24,25,26)</sup> revealed no significant small scale effects and small mortar beams tested at the Portland Cement Association Laboratories<sup>(38)</sup> further illustrated that modelling to quarter scale produced a satisfactory representation of prototype behaviour.

The modelling of crack behaviour is difficult, for in addition to the small scale influence reported by Alami and Ferguson, prediction of crack widths in full size structures is difficult in itself.

Investigations into the prediction of crack widths and the effects of scale factor<sup>(31,27,29,30,32)</sup> have resulted in the proposal of several different formulae to predict crack widths. Some of these imply that the crack

widths will vary according to the scale factor while others imply variation according to the square root of the scale factor. The results reported by Kaar<sup>(31)</sup> suggest that the actual variation lies between these limits.

## 6.2 GENERAL DESIGN BASIS AND SPECIFICATIONS

The overall size of the model floor was limited by the size of laboratory facilities and the proposed placement of strain gauges on the slab reinforcement imposed a lower limit on the diameter of the reinforcement rods used as panel reinforcement. These two factors permitted a rough assessment of the load carrying capacity of the floor to be made. With the slab dimensions as estimated, the effect of membrane action in enhancing the load carrying capacity was assessed using the theory due to Park<sup>(11, 12, 13)</sup>.

On the basis of preliminary investigations it was decided to design the floor to have an ultimate load of 800 psf. Even at this load it was found that, with the allowance for compressive membrane action, panel reinforcement contents were close to the minimum required by the British Code of Practice. This resulted in the placement of the minimum allowable reinforcement for bottom steel in both directions of all panels. The ratio of hogging to sagging moment reinforcement was to be constant for all panels. Enhancement of the centre panel was to be

sufficient to double its Johansen load. In the corner panels, no membrane action enhancement was to be allowed for. Thus the uniform panel thickness and the regularity of the panel reinforcement made it possible to determine the plan dimensions of the corner and centre panels. Plan dimensions and the required enhancement of the centre-edge panels were thus defined.

Limit design was used for the design of the beams. The presence of tensions in some spans required the provision of additional longitudinal steel and a re-assessment of the shear capacity.

All slab panels having one or two edges supported by an exterior beam were designed on the assumption that full hogging yield moments would be developed along these edges.

Accordingly, the exterior beams were to be designed to carry the torsional moments induced. Torsion induced in the interior beams during pattern loading was not designed for specifically.

Park's equations<sup>(11)</sup> were used to assess the membrane action enhancement of the panels, the Australian Code of Practice<sup>(33)</sup> was used for torsional design and the British Code of Practice for Reinforced Concrete - CP114<sup>(35)</sup> used for minimum panel reinforcement. The American Concrete Institute Building Code ACI 318-63 was used for all other aspects of design with the exception that a load factor of

2.0 was used for both dead and live load and the capacity reduction factor,  $\phi$ , was modified to 1.0 for bending and .945 for shear. This was equivalent to using ACI 318-63 with a load factor of 1.8, not 1.5 on dead load.

The following specifications as to loading and material properties resulted:

(a) Loading

Design Service Load = 400 psf consisting of 100 psf prototype dead load plus 300 psf live load.

Ultimate Load = 800 psf = 2.0 x Service Load.

Loading patterns with full live load on alternate panels were to be considered. Loading of the centre panel alone or the outer panels only to full live load was to be considered.

The capacity of the floor to resist "line" loads was to be checked but the floor was not designed to take full design live load in this configuration.

Figure 6.2(a) shows the notation used to describe the beams and panels of the floor and Figure 6.2(b) shows the loading patterns considered in design.

(b) Membrane Action Enhancement

The ratios of ultimate load to Johansen load for the panels were to be:

Centre panel	2.0
Corner panel	1.0
Centre-edge panel	About 1.3

(c) Concrete

Cylinder strength to be 4200 psi.

Cube strength to be 5300 psi.

(d) Steel

<u>Flexural:</u>	<u>Bar Diameter</u>	<u>Yield Force</u> (lb)	<u>Yield Stress</u> (psi)
	$\frac{1}{8}$ "	640	52,000
	$\frac{1}{4}$ "	2040	42,000
	$\frac{3}{8}$ "	4750	43,000
<u>Stirrups:</u>	$\frac{1}{8}$ "	530	

The design procedure followed that outlined above. A summary of the specific methods and results follows in the next two sections, 6.3 and 6.4. A more detailed description is given in Appendix A.

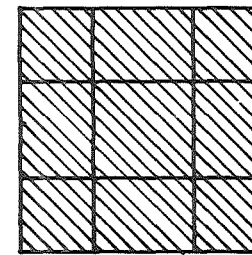
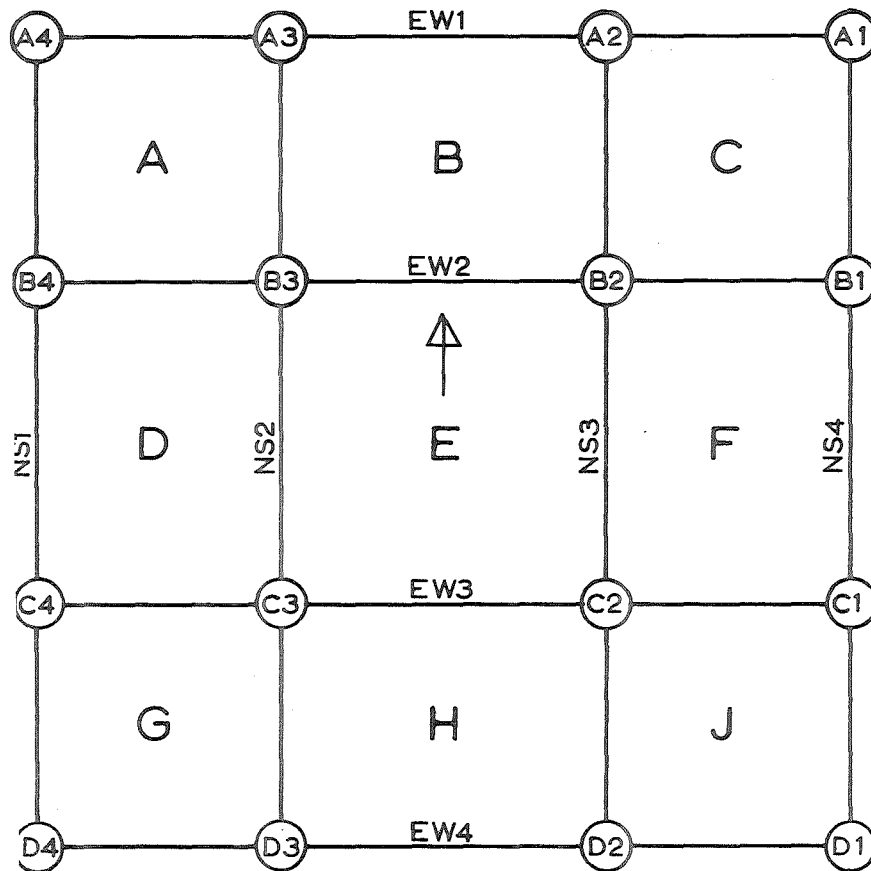
## 6.3 DESIGN OF FLOOR PANELS

6.3.1 Design Criteria

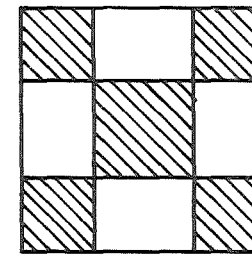
In order to keep the load capacity of the floor down to realistic proportions, the bottom reinforcement in the slab panels was designed so that the  $\frac{1}{8}$ " diameter bars available provided the minimum allowable reinforcement when placed at the maximum allowable spacing. British Code requirements for minimum steel were adopted in preference to the more stringent ACI requirements. The above combination enabled the determination of a suitable slab thickness.



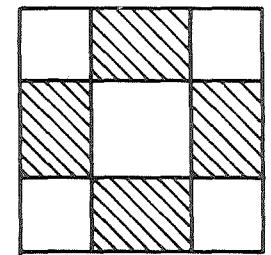
FIGURE 6.2(a) SLAB LAYOUT NOTATION



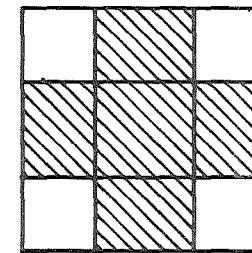
1



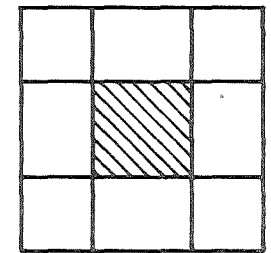
2



3




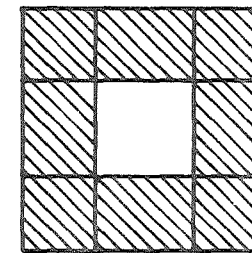
4



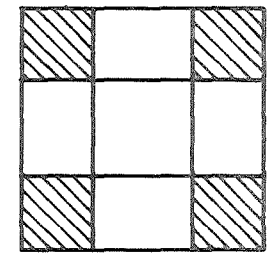
5

 DL + LL

 DL



6



7

FIGURE 6.2(b) LOAD PATTERNS CONSIDERED

The specification of an enhancement factor of 2.0 for the centre panel, set the Johansen load of the centre panel at 400 psf. The depth of slab and bottom reinforcement had been determined and the only unknowns for this panel were the clear span and the ratio of hogging to sagging yield moments,  $i$ . Ultimate load requirements thus defined a relationship between these two unknowns enabling the choice of both after several trials.

For the corner panels the same reinforcement and  $i$  value were used, and since no membrane action enhancement was to be allowed for, the Johansen load of these panels was to be 800 psf.

Only the short edges of the centre-edge panels were assumed to be laterally restrained. The plan dimensions were defined by the centre and corner panel dimensions and since the reinforcement was to be the same as in other panels the Johansen load of these panels could be determined directly. Checking of the lateral stiffness required to enhance this load to 800 psf revealed a reserve of strength. However, values of bottom reinforcement were already minimum and the value of  $i$  already well below 2.0 which was considered ideal (see Chapter 2). No modification was therefore made and the Johansen load of the centre edge panels remained at 594 psf.

### 6.3.2 Assessment of Membrane Action Enhancement of Panel Loads

The equations for ultimate loads of laterally restrained reinforced concrete panels derived by Park<sup>(11, 12, 13)</sup> were used in assessing the contribution of compressive membrane action towards the overall load carrying capacity of the slab panels.

The requirement of the panels to sustain specified loads enabled the solution of the equations for the maximum allowable lateral spread. This maximum value was used in calculating the magnitude of the membrane forces at ultimate load. These forces were then considered as outward, in-plane loads on the surrounding panels and beams and outward movement under these loads was estimated, allowance being made for elastic, creep and shrinkage strains. Modifications to slab parameters were made until the outward movement under the forces was less than the maximum allowed by an arbitrary safety margin.

An outline of Park's theory and details of the calculation of the maximum allowable lateral spread in the centre and centre-edge panels are given in Appendix A.

The loads acting on a part of the surround and the resulting deformed shape are shown in Figure 6.3(a).

Five principal effects were considered in obtaining the lateral stiffness in terms of a value equivalent to the  $\epsilon'_y$  value used by Park<sup>(11)</sup>:

- (a) Stretch of the supporting beams carrying the tensions  $T_1$  or  $T_2$  (Figure 6.3(a)).
- (b) Bending and shear deformations of the panels A and B under the loading system of Figure 6.3(a).
- (c) The axial shortening of a typical slab strip under the compressive membrane forces.
- (d) Shrinkage of the slab panel away from the supporting beams.
- (e) Creep deformations.

When panels B and C are all loaded and exhibit compressive membrane action, there can be no ring tension in the B panels to counter the forces C in the centre panel. However, before the centre-edge panels exhibit compressive membrane action it is possible for them to carry some of the tension induced in the surround by the membrane action in the centre panel. Compare the two force distributions of Figures 6.3(b) and 6.3(c).

In both cases the mean centre panel membrane force is C and this, in addition to inducing tension into the surround, sets up small bending stresses.

When no compressive membrane forces are present in the centre-edge panel (e.g. before it cracks) it is possible for this section to be in tension and for equilibrium of in-plane forces perpendicular to the section XX, the sum of  $T_3$ ,  $T_4$  and  $T_{CEP}$  must equal C. Hence  $T_{CEP}$

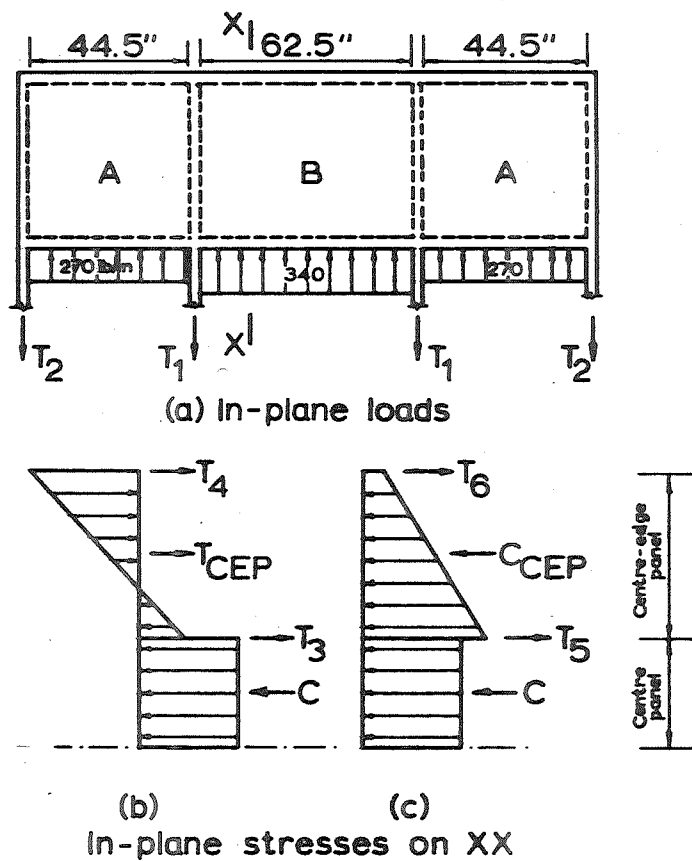


FIGURE 6.3 ACTIONS ON SURROUND

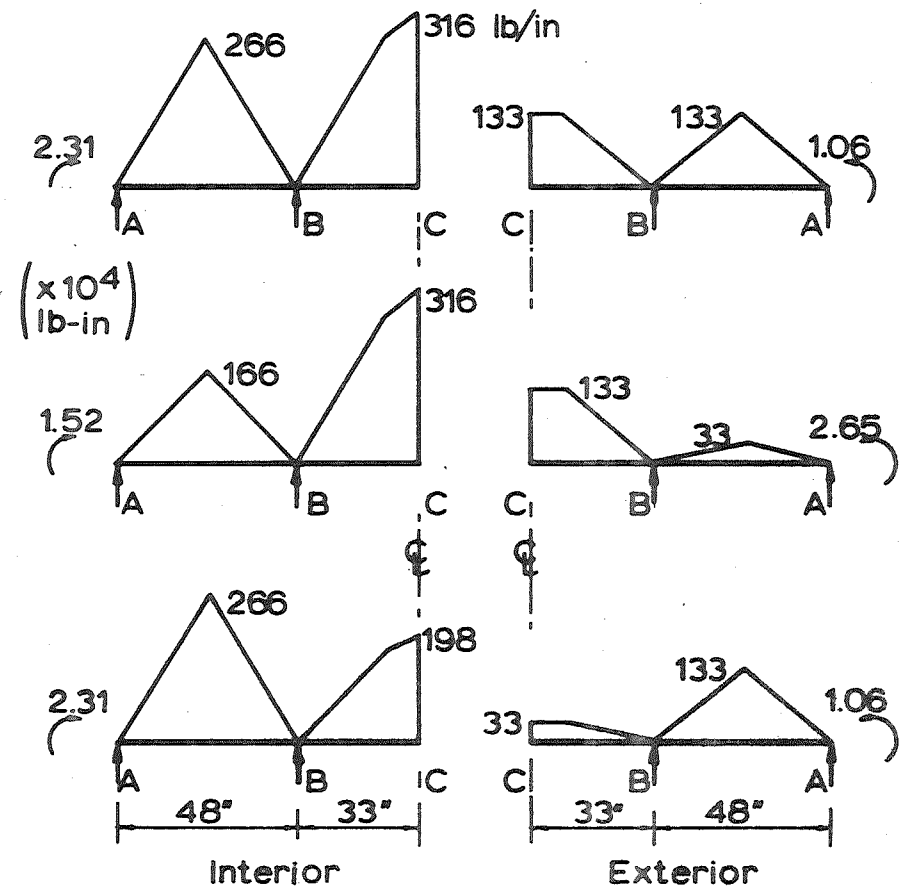


FIGURE 6.4 BEAM LOADING

assists in resisting the tension induced in the surround.

When the centre-edge panels exhibit compressive membrane action, the part of the section XX in the centre-edge panel will be in net compression and will no longer assist in resisting induced surround tension as is seen by the equilibrium equation for in-plane forces:

$$T_5 + T_6 = C + C_{CEP}. \quad \dots(6.1)$$

The beams must therefore take all the tension induced and act as ties. The B panels may, however, contribute to the bending stiffness of the span GH with respect to loads in the plane of the panel.

The span to depth ratio of this panel acting as a deep beam called for the consideration of both bending and shear deformations. These were calculated on the basis of an uncracked, elastic section and then increased in recognition of the loss of stiffness due to cracking and panel deflection under transverse load.

The shortening of the slab strips and extension of the beams were calculated on the assumption that these elements were uncracked, of elastic material and acted upon by axial force only.

Because the slab had lighter reinforcement and a greater specific area than the beams, there was clearly a possibility of the slab shrinking away from the supporting beams and the contribution of this phenomenon in

reducing the effective lateral stiffness was assessed.

Allowance was made for time-dependent deformations which were assumed equal to the short term values.

Design calculations, which are summarised in Appendix A, resulted in:

Clear span dimensions:	62.5" x 62.5"	Centre panel
	62.5" x 44.5"	Centre-edge panels
	44.5" x 44.5"	Corner panels
Panel depth:	1.94"	All panels
Span to depth ratios:	32.2	Centre panel
	22.9	Centre-edge and corner panels
Percentage bottom reinforcement:	.152 %	All panels
Percentage top reinforcement:	.162 %	All panels
Average sagging yield moment:	241 lb.in/in	All panels
Average hogging yield moment:	258 lb.in/in	All panels
Johansen load with 8% reduction: for corner effects	800 lb./ft <sup>2</sup>	Corner panel
	594 lb./ft <sup>2</sup>	Centre-edge panel
	400 lb./ft <sup>2</sup>	Centre panel
Enhancement factors required:	1.0	Corner panel
	1.35	Centre-edge panel
	2.0	Centre panel
Mean membrane force at ultimate:	340 lb/in	Centre panel
	270 lb/in	Centre-edge panel long direction

## 6.4 DESIGN OF BEAMS

### 6.4.1 General

#### (a) Loading Patterns Considered

The load patterns considered in design are shown in Figure 6.2(b). The worst case of full live load on loaded panels and dead load only on the unloaded panels was taken in all cases.

#### (b) Load Distribution and Computation of Moments and Shears

The triangular load distributions of Figure 6.4 were used in the calculation of both moments and shears. Span lengths were taken as the centre to centre distances and full support moments designed for, moments at the support face being considered to justify the reduction of steel area in cases where provision of the area of steel for the full support moment could not be achieved with a practical bar arrangement.

#### (c) Basis of Moment Diagram Determination

In order to limit the extension of the centre spans of beams, the degree of moment redistribution was kept to a minimum.

The fixed-end moments at an interior support were computed on the basis of a uniform section and redistributed according to the approximated relative stiffnesses, but in this case the ratio of the stiffness did



not greatly affect the final moments because of the small difference between the two fixed-end moments.

(d) Effect of Tension on Flexural Steel Requirements

The axial tensions induced in the centre spans of the beams called for a modified design method.

Equations 4.14 and 4.15 were used to determine the reinforcement content.

The provision of considerable extra steel to accommodate the tension posed problems at the supports, since according to the assumptions made, it was required on one side of the support and not on the other. Curtailment could not always be achieved and the section carrying no tension remained overdesigned.

(e) Curtailment of Flexural Steel

Required steel areas were calculated for four critical sections in each beam, viz., at the middle and ends of the centre span and the end and point of maximum positive moment in the outer spans. Curtailment followed the bending moment diagrams with due recognition of the tension to be carried. The small range of bar sizes available led to uneconomical arrangements in some cases.

(f) Torsion

Considerable torsional moments in the exterior beams resulted from the required development of full hogging

yield moments along the slab edges supported by these beams. The mid-point of each span was taken as a point of zero torque and no effort was made to redistribute the torsional moment imbalance at the beam junctions according to the flexural stiffnesses of the adjoining beams at right angles. Considerable positive bending moments were induced in the ends of these latter beams as a result of the edge beam torsion.

(g) Shear

Inclined stirrups were included in recognition of the steepening of shear cracks when axial tension is present. In spans subject to axial tension, the concrete was assumed to take no shear.

A summary of design results for the beams is given in Table 7.1.

## 6.5 CONSTRUCTION

### 6.5.1 General

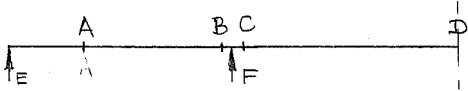
The floor was constructed in place on the strong floor of the Post Graduate Laboratory. Construction of formwork began in June 1967 and the concrete was placed in November 1967.

### 6.5.2 Formwork

The channels forming the beam soffit were placed on the supporting columns and levelled before the individual

Table 6.1. Summary of design results for beams.

Quantity	Units	Interior Beam					
		At A	At B	At C	At D	At E	At F
Tension	Kip	0	0	17.6	17.6	-	-
Moment	lb" x 10 <sup>4</sup>	+3.03	-7.00	-7.00	+5.50	-	-
Shear	lb" x 10 <sup>4</sup>	n.c.	.50	.58	0	-	-
Torque	lb" x 10 <sup>4</sup>	n.c.	n.c.	n.c.	n.c.		
Flexural steel )	in <sup>2</sup>	.11	.24	.57	.32		
Long. torsion steel )	in <sup>2</sup>	0	0	0	0		
Steel placed )	in <sup>2</sup>	.11	.22	.54	.32		
Reactions (800 psf in pattern 1) )	Kip	-	-	-	-	1.39	10.7

Quantity	Units	Exterior Beam					
		At A	At B	At C	At D	At E	At F
Tension	Kip	0	0	5.2	5.2	-	-
Moment	lb" x 10 <sup>4</sup>	+1.55	-3.29	-3.29	+2.66	-	-
Shear	lb" x 10 <sup>4</sup>	n.c.	.25	.28	0	-	-
Torque	lb" x 10 <sup>4</sup>	n.c.	.96	1.25	0		
Flexural steel )	in <sup>2</sup>	.07	.15	.25	.16		
Long. torsion steel )	in <sup>2</sup>	0	.086	.102	0		
Steel placed )	in <sup>2</sup>	.10	.32	.32	.15		
Reactions (800 psf in pattern 1) )	Kip	-	-	-	-	.75	5.4

n.c. - denotes not critical.

panel forms were placed and secured (Figure 6.5). Corrugated cardboard was used on the sides of the beam cavities to facilitate stripping. Adhesive tape was used to seal all cracks and a level check performed when all panels were positioned.

### 6.5.3 Steel Placement

Reinforcing cages for the exterior beams were made separately while the four interior beam cages were made up as a single unit. All beam steel was positioned before the slab steel was placed.

Mortar blocks tied to the reinforcing at strategic points were used to ensure correct cover to the steel at the sides and bottom. Ties through the beam soffit served to prevent the steel riding up and gave further rigidity. All beam steel was tied and no welds were used.

The bottom and top slab steel layers were then placed, tie wires again being used for all joints. All bottom steel was continuous for the whole width of the floor with some bars, top and bottom, being passed through the side beam moulds where they were anchored and tightened slightly to assist lining up and general rigidity. In the top reinforcement, in cases where tie wires proved insufficiently firm, a spot of Araldite glue was used to give a firm join. Mortar pads were again used to ensure correct cover.

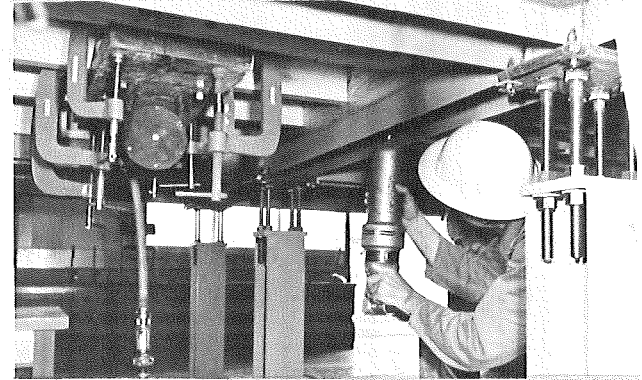
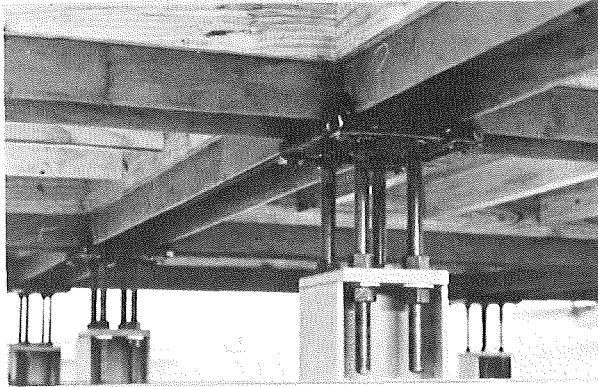
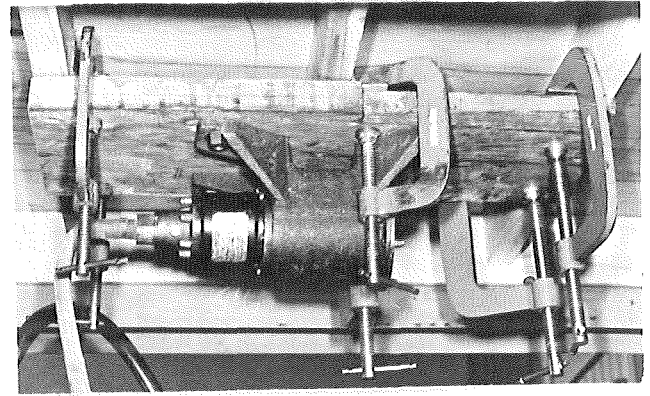
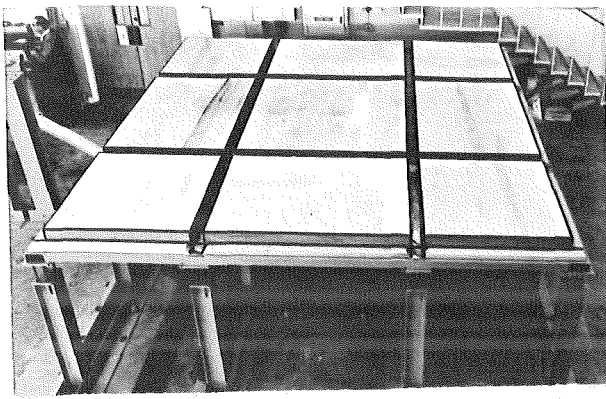


FIGURE 6.5 FORMWORK AND VIBRATION EQUIPMENT

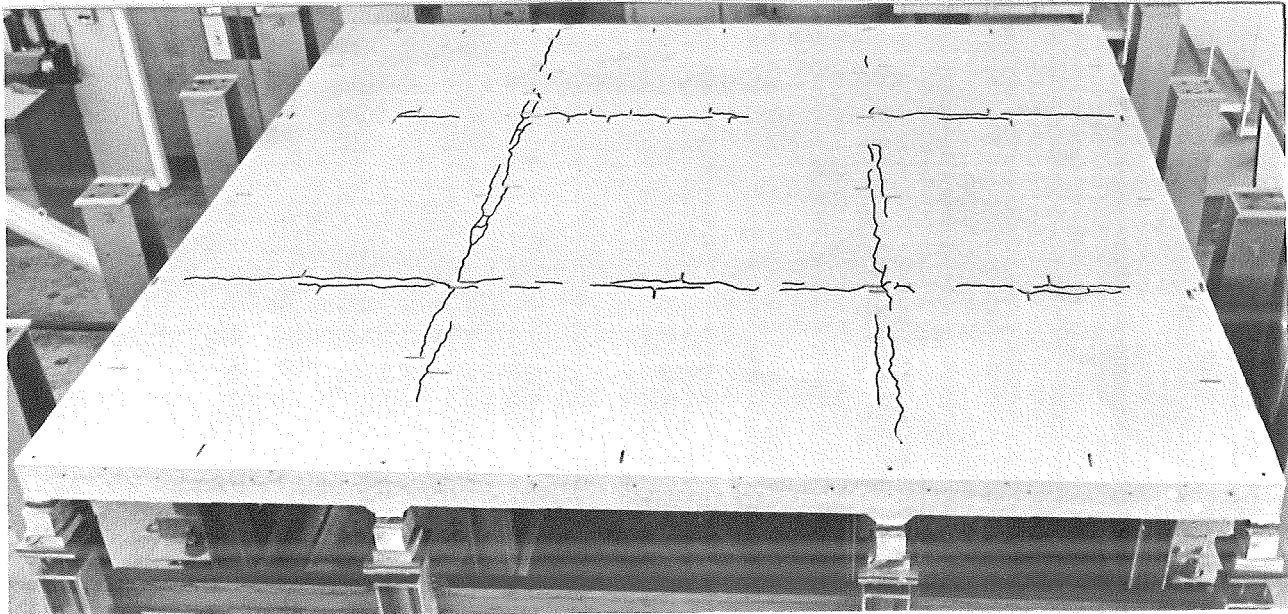


FIGURE 6.8 TOP SURFACE SHOWING SHRINKAGE CRACKS

Figure 6.6 shows the reinforcement as placed.

A thorough check of levels and cover was made after all steel was placed and secured.

#### 6.5.4 Concrete Placement

Concrete was first placed in all the beams up to the level of the panel forms and vibrated with kango hammers. Placement of the panel concrete then proceeded panel by panel, pneumatic form vibrators being used for compaction (see Figure 6.5).

The surface was screeded in two halves with a timber board using a 2" pipe as an intermediate support. After trowelling and initial set, the floor was covered with damp hessian and polythene.

#### 6.5.5 Curing and Stripping

The formwork could not be removed until sufficient concrete strength had been developed to ensure that cracking would not occur. The possibility of adverse effects due to drying shrinkage of the slab relative to the formwork meant that the concrete had to be kept moist until stripping of the formwork, 26 days after casting.

Stripping of the formwork was achieved by suspending the floor from 16 hangers supported by a frame erected over the slab. This enabled the panel forms and channels to be removed from underneath with little possibility of cracking. When stripping was complete, the slab was again

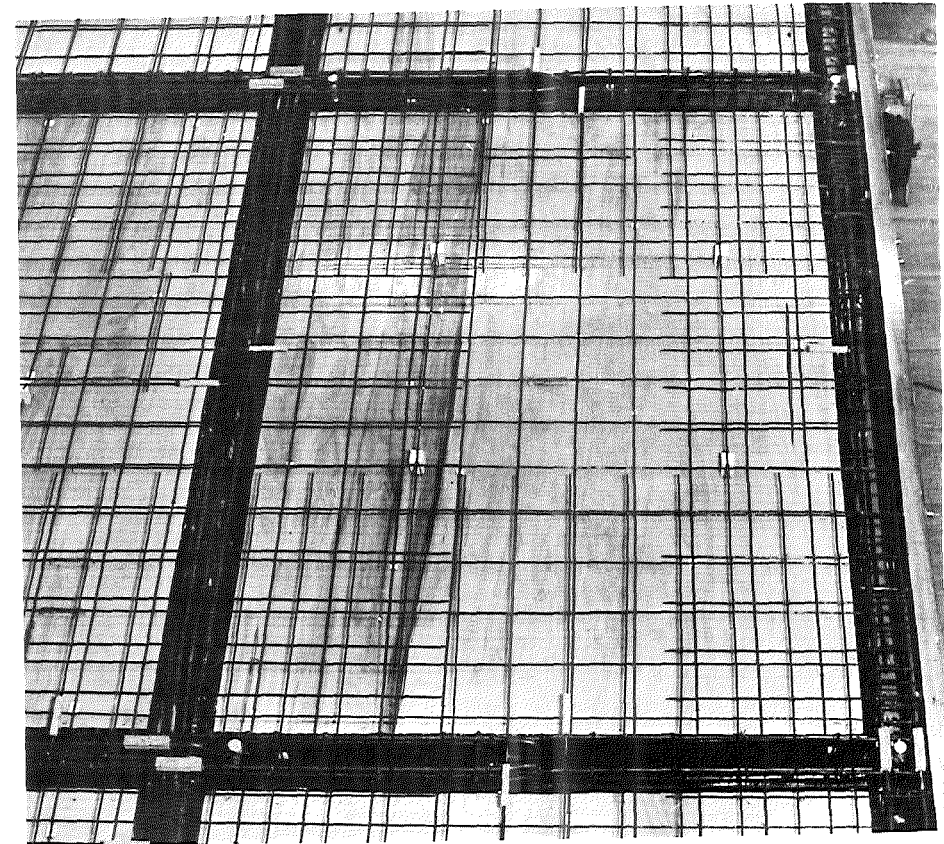
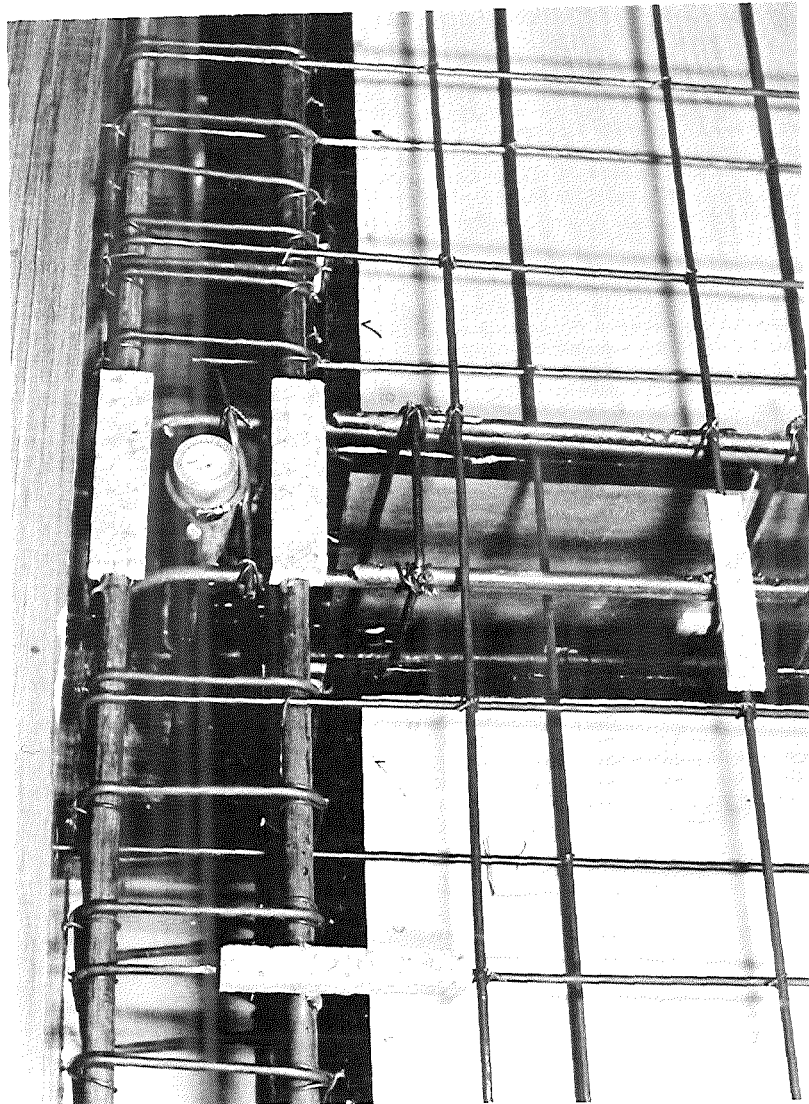


FIGURE 6.6  
REINFORCEMENT IN MODEL FLOOR

supported from underneath and the frame over it removed.

A check on the thickness and level was then made using a precise level with a foot rule as staff. The results of this check are given in Appendix B.

## 6.6 MATERIAL PROPERTIES AND FINAL SLAB DIMENSIONS

### 6.6.1 Material Properties

#### 6.6.1.1 Concrete

The concrete used was one batch of a specially mixed mortar supplied by a ready-mix concrete contractor. This had a maximum aggregate size of  $\frac{1}{4}$ " and a water-cement ratio of .69. Details of the mix are given in Appendix B.

The average strengths measured by tests on control specimens before and after the test were as follows:

Cylinder strength,	$f'_c = 4350$ psi
Cube strength,	$u = 5080$ psi
Modulus of Rupture,	$f_t = 690$ psi

Figure 6.7 shows the stress-strain curves of tests on two 12" x 6" diameter cylinders and two 18" x 6" x 6" prisms used to determine the modulus of elasticity, values of which are shown on the figure.

In addition to the normal control specimens, two 18" x  $7\frac{1}{2}$ " x  $3\frac{1}{2}$ " blocks, two 18" x 6" x  $3\frac{1}{2}$ " blocks and one strip 36" x 8" x 1.94" were cast without reinforcement. Demec gauges were used to take three readings of shrinkage strain on each block. The graphs of unrestrained shrink-



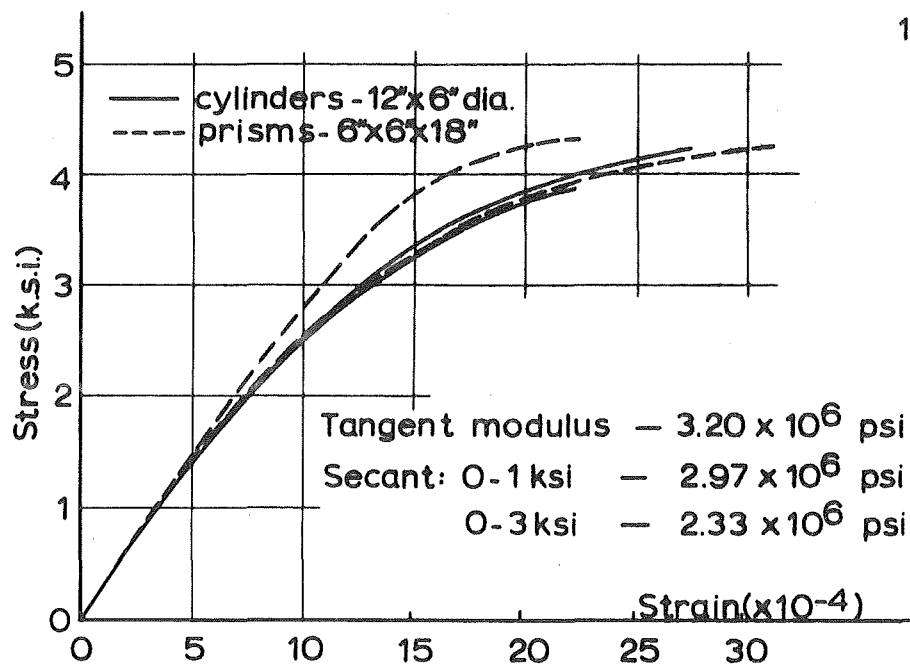


FIGURE 6.7  
STRESS — STRAIN CURVES FOR CONCRETE

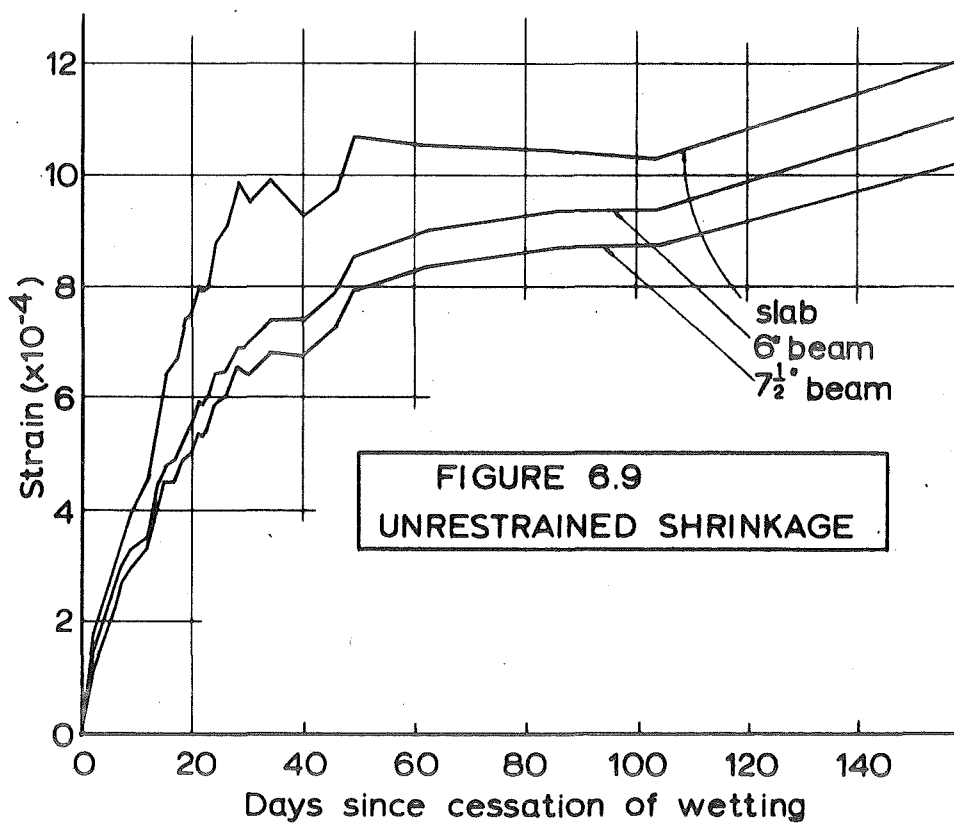


FIGURE 6.9  
UNRESTRAINED SHRINKAGE

age strain, corrected for temperature, against time indicate appreciable differential shrinkage between slab and beam elements. Twenty-eight days after the cessation of wetting, cracks appeared around the edges of most panels on the top surface only (Figure 6.8).

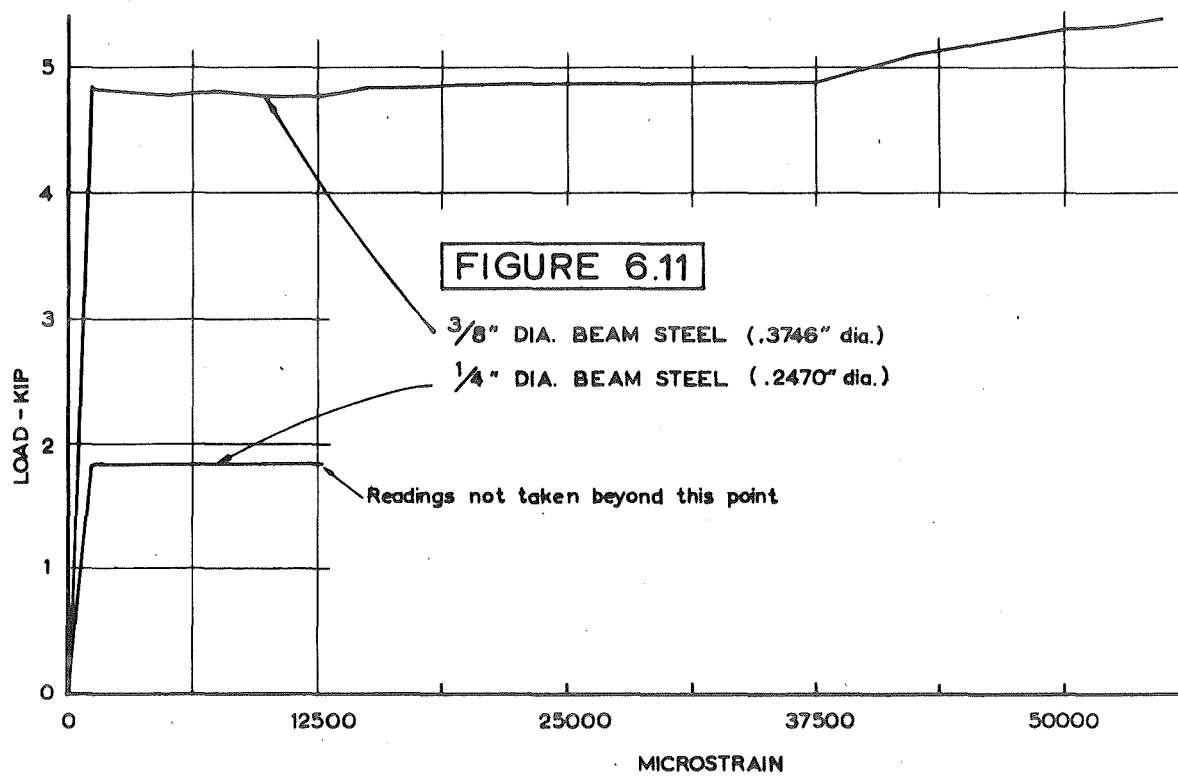
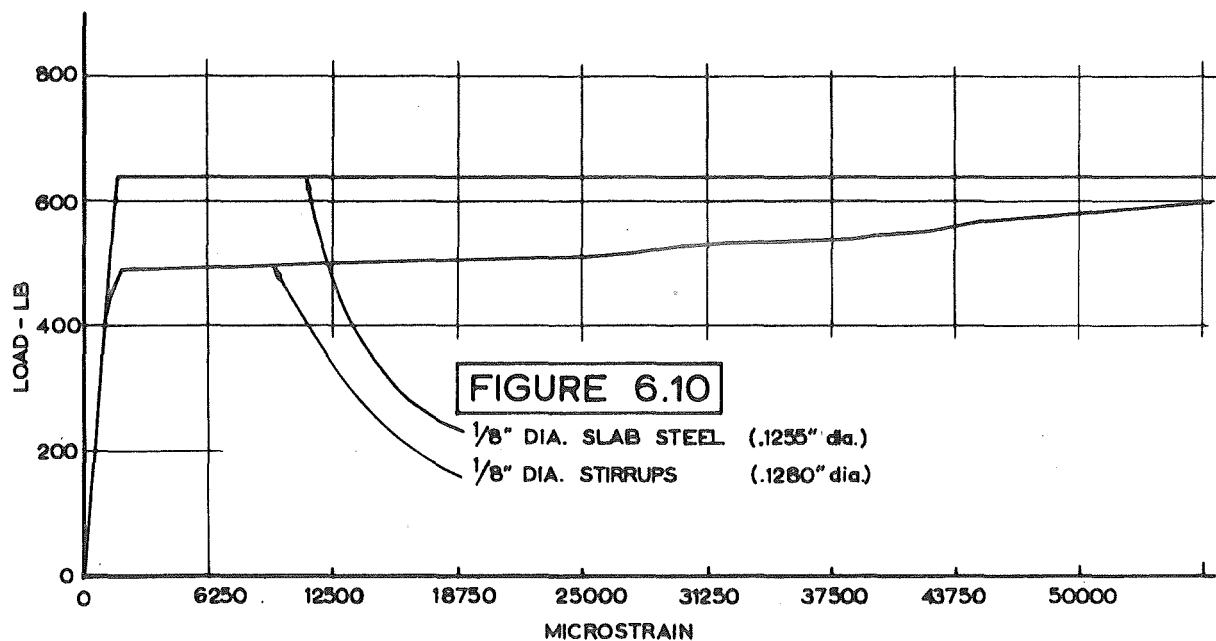
Figure 6.9 shows that the maximum differential shrinkage occurred at this time and it seems certain that the cracks of Figure 6.8, ranging up to .002 in width, were caused by this differential movement.

#### 6.6.1.2 Steel

Three different sizes of bar and two different types of steel were used in reinforcing the floor. Supplies of the  $\frac{1}{8}$ " diameter, lead bath annealed, British steel were limited and the New Zealand soft drawn wire was used for stirrups.

Figures 6.10 and 6.11 show typical stress-strain curves for the steel used. The lead bath annealed steel showed a distinctly bi-linear characteristic and since the yield plateau was extended and flat, the stress at the level of the yield plateau was taken as the yield stress. For the soft drawn wire, the yield stress was taken to be that at .2 per cent proof stress.

Results of the test on steel samples are given in Appendix B.



### 6.6.2 Final Slab Dimensions

(i) Level of Top Surfaces: Precise level readings on the top surface taken to  $\pm .005$ " varied from  $-.20$  to  $+.15$ " above the mean level. The standard deviation of the 169 readings was  $.073$ ". The planeness of the top surface was better than these figures indicate since readings revealed a small overall slope.

(ii) Panel Thickness: The overall average of nine readings per panel was  $1.976$ " with range of  $\pm .11$ " and a standard deviation of  $.048$ ". At the end of the test, thickness measurements were taken at the edges of the centre panel (E), and a centre-edge panel (H) and a corner panel (J). The average of all these readings was  $1.904$ ".

(iii) Beam Thickness: Beam depths were measured at the ends and quarter points of each span before the test. Results were:

6" beams: Average depth =  $5.965$ ", s.d. =  $.036$ "

$7\frac{1}{2}$ " beams: Average depth =  $7.490$ ", s.d. =  $.030$ "

(iv) Cover to Steel: A check was made after the test. Both panel and beam steel cover were generally within  $1/32$ " of the expected value.

Fuller details of the measurements of the slab are given in Appendix B.

## CHAPTER 7

### INSTRUMENTATION AND TEST PROGRAMME

#### 7.1 INSTRUMENTATION

##### 7.1.1 Reaction Measurements

Figure 7.1 shows details of a support B2. The 10-ton capacity Philips PR 9226 electrical resistance load cell is shown sitting between a two-way roller system and a  $1\frac{3}{4}$ " mild steel bearing pad. Adjustment of the nuts at the column head enabled the whole assembly to be levelled. All reaction points were of similar form. The roller supports for the outer ring of support points were  $\frac{1}{4}$ " ball bearings between hardened, ground plates. Two of the inner supports (B3 and C2) had one-way-rollers while support C3 was fixed against horizontal movement ensuring that, although the floor as a whole could not move, all reactions were vertical.

Each load cell was wired to a 16-way, four-channel switch connected to a Budd Strain Indicator, and readings on each cell recorded manually. Values of reactions were calculated using the load-strain calibration curves obtained for each cell as a result of tests performed before and after the testing of the floor.

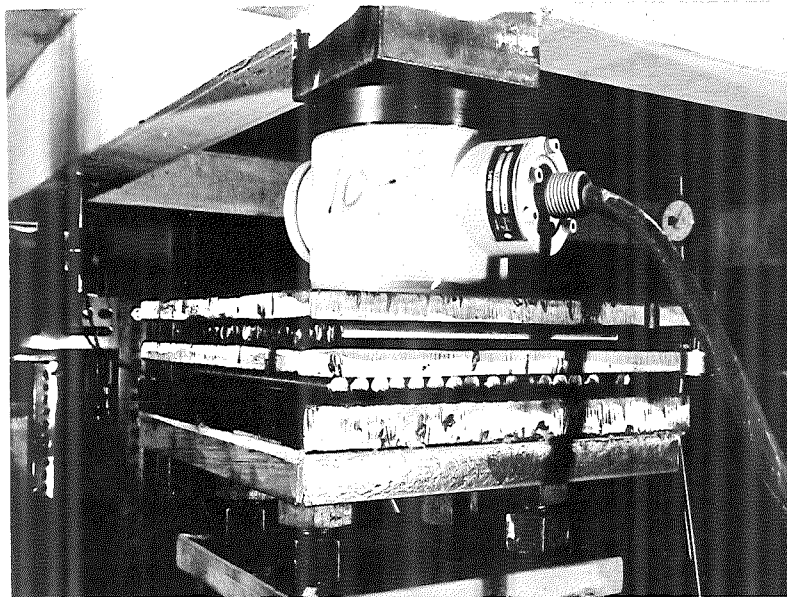


FIGURE 7.1 DETAIL OF SUPPORT B2

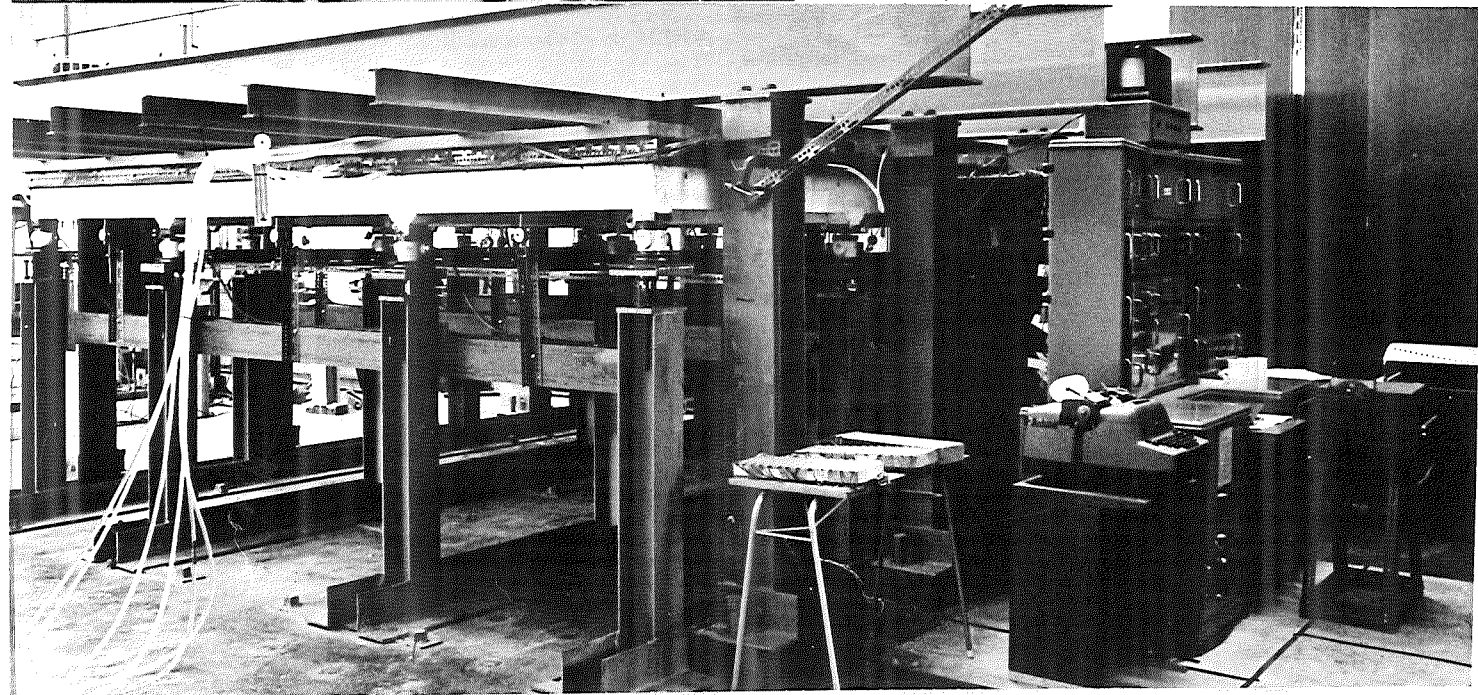


FIGURE 7.4 TEST SET-UP

### 7.1.2 Strain Measurement

Strain gauge positions are shown in Figures 7.2 and 7.3. All gauges were wired to a 140-channel strain data logger in a two-arm circuit. The data logger (right foreground of Figure 7.4) was accurate to  $\pm 5 \mu S$  and could read automatically each gauge in turn. A digital voltmeter incorporated in the logger provided output, in microstrain units, on a typewriter and tape punch.

The automatic switching facility required that each active gauge have its own dummy.

The active concrete gauges were Philips PR 9810 C/11 (600 ohms, flat grid, 1 inch gauge length,  $\frac{3}{4}$ " grid width) glued directly to the concrete with Philips cement kit PR 9244/04. Concrete dummy gauges were of the same type and glued in the same manner to the three concrete blocks to be seen in Figure 7.4.

Active steel gauges were BLH SR-4 A-12 paper backed gauges (flat grid, 1 inch gauge lengths, 120 ohms, gauge width,  $\frac{3}{32}$ "). The reinforcing steel was exposed by the removal of the cork blocks and considerable care was necessary in obtaining uniform adhesion onto the  $\frac{1}{8}$ " diameter bars. Grooved rubber pads were used to form the gauge around the bars. Nitrocellulose adhesive from the Duco Cement kit was used throughout. Dummies for these gauges were temperature-compensated, 120 ohm gauges mounted on Aluminium. Two unstressed SR-4 gauges mounted

in the same way as the active gauges and having dummies on the aluminium, were used to assess the effects of temperature on the strain readings.

Following initial placement, all gauges were checked for continuity and resistance to earth, the necessary replacements being made until all gauges were satisfactorily mounted. Gauges were then waterproofed with wax.

The 140 channels of the data logger were split into blocks of 20, the first channel of each block being wired to a Philips PR 9249A dummy strain gauge to check drift.

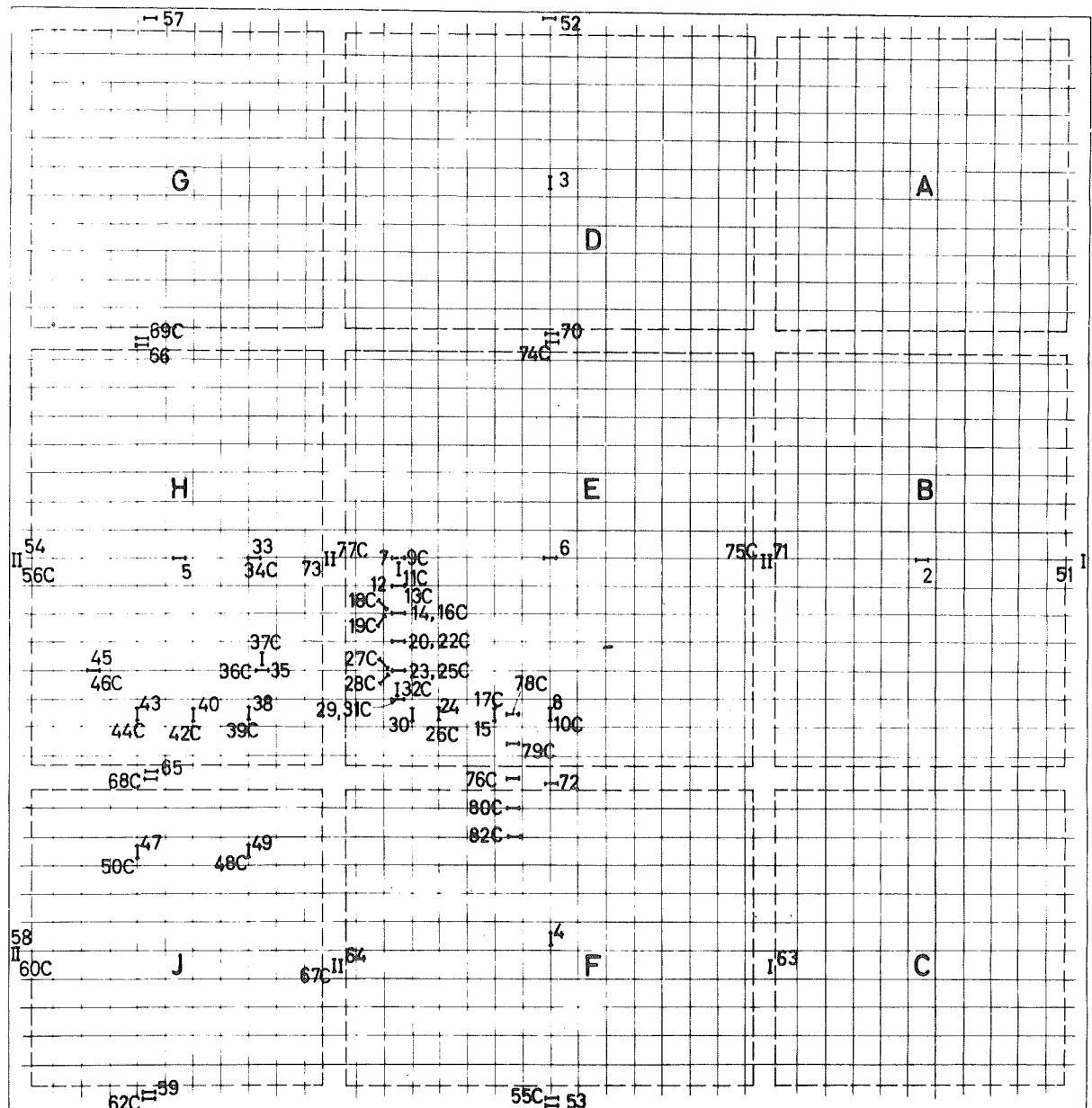
Gauges 7-32 were placed so as to afford measurement of membrane force in the centre panel in a region of low moment. Gauges 33-46 provided this facility in a centre-edge panel, 47-50 in a corner panel.

Gauges 78, 79, 76, 80, 82 were placed to give an indication of T-beam flange widths. Hair cracks normal to the line of the gauges in mid-span necessitated their placement slightly off centre.

Gauges 112-120 were placed for measurement of moment and membrane action force in a region of high moment. Gauges 94, 95, 105-108 served a similar purpose for a centre-edge panel.

All other gauges were placed to give an indication of stress levels at critical points and in some cases, means of calculating moments and forces at a section.





**FIGURE 7.2**  
**STRAIN GAUGE POSITIONS ON BOTTOM STEEL**

I - Denotes strain gauge position

C - Denotes concrete gauge on upper surface

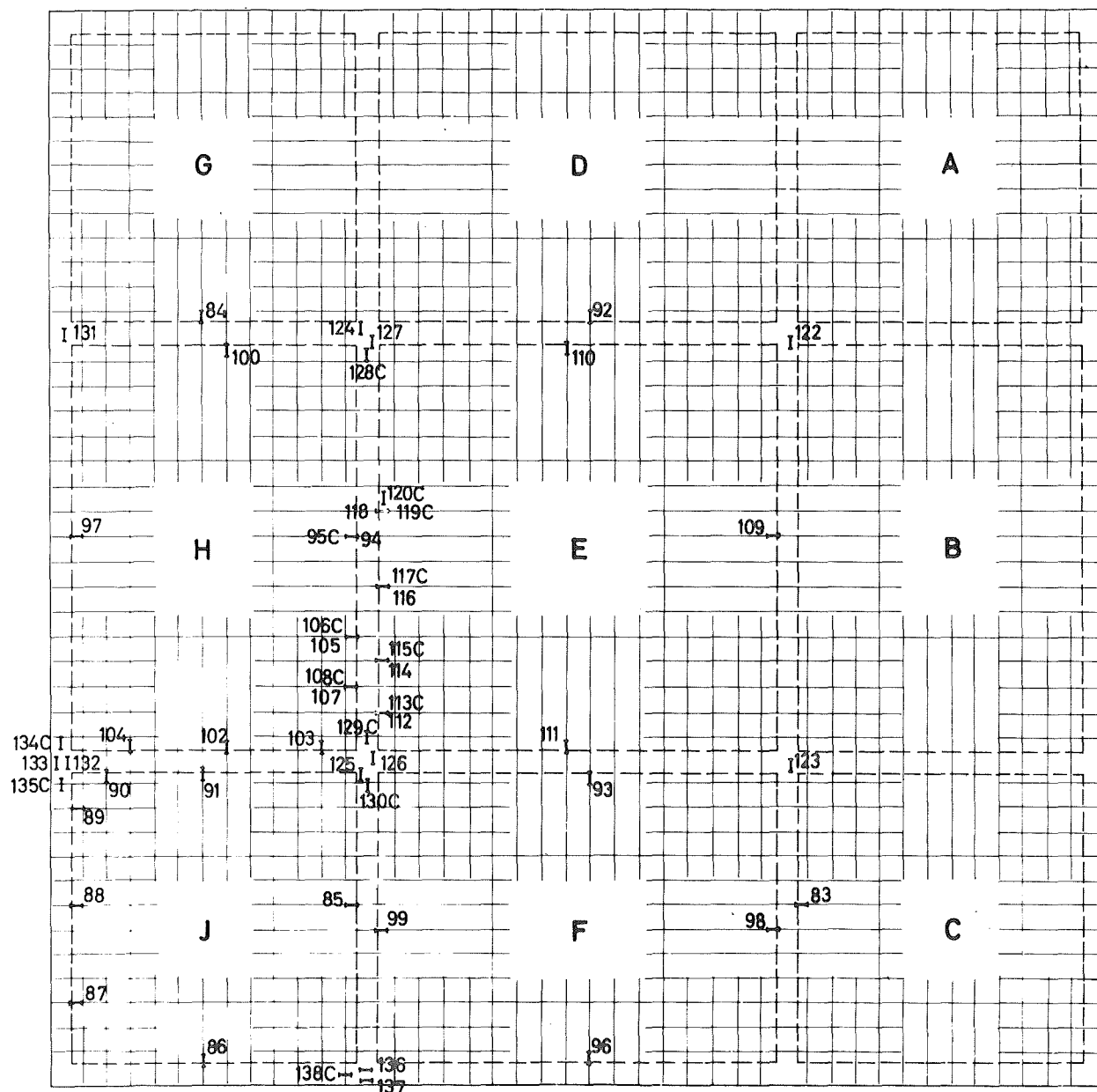


FIGURE 7.3

## STRAIN GAUGE POSITIONS ON TOP STEEL

I - Denotes gauge position

C - Denotes concrete gauge on underside

### 7.1.3 Deflection Measurement

Dial indicators mounted on a 'Dexion' frame attached near the top of the supporting columns were used to measure deflection at critical points.

One at the centre of each panel and one at the centre of each beam span provided vertical deflection data.

Gauges to measure horizontal movement at supports B3, B2, C2 were placed to measure movement in the direction of the rollers at the support points (North-South at B3, East-West at C2 and both North-South and East-West at B2).

### 7.1.4 Load Application and Measurement

Water-filled bags placed between a reaction platform (erected over the slab and tied down to the laboratory floor) and the top surface of the slab provided means of load application.

Nine bags (one over each panel) were made with a 3" high wall and covered the whole top surface of the slab when placed and filled with water.

Pressure was applied by forcing water into the bags. The four corner bags were inter-connected, there being no provision to have one corner panel at a higher load than the other three. The same was true of the centre-edge panel bags. The centre panel bag was a separate system.

Figure 7.5 is a diagrammatic representation of the

hydraulic loading system. Apart from the main feed hose which was 1" diameter, all hoses were  $\frac{1}{4}$ " diameter plastic tubing.

The main feed hose came from a constant head device which could be adjusted to any level to suit the load requirements, providing an effective means of maintaining the load at the set level.

Due to scaling down in the model, there was a difference of 75 psf between the self weights of prototype and model. Another constant head device fixed at the appropriate height above the level of the slab was used to apply this difference so that the self weight of the model plus the applied "dead load" was equal to the prototype dead load. This load was the starting point for all tests.

For pattern loads where two different load levels were required, panels not loaded with live load were switched to the "dead-load-only" constant head device leaving the variable device for setting of the live load on the others.

When the lower load of a pattern was greater than the prototype dead load, a mercury manometer was used to set the load and the dead load device was not used.

The mercury manometer served also as a means of checking the reading on the calibrated variable head device.

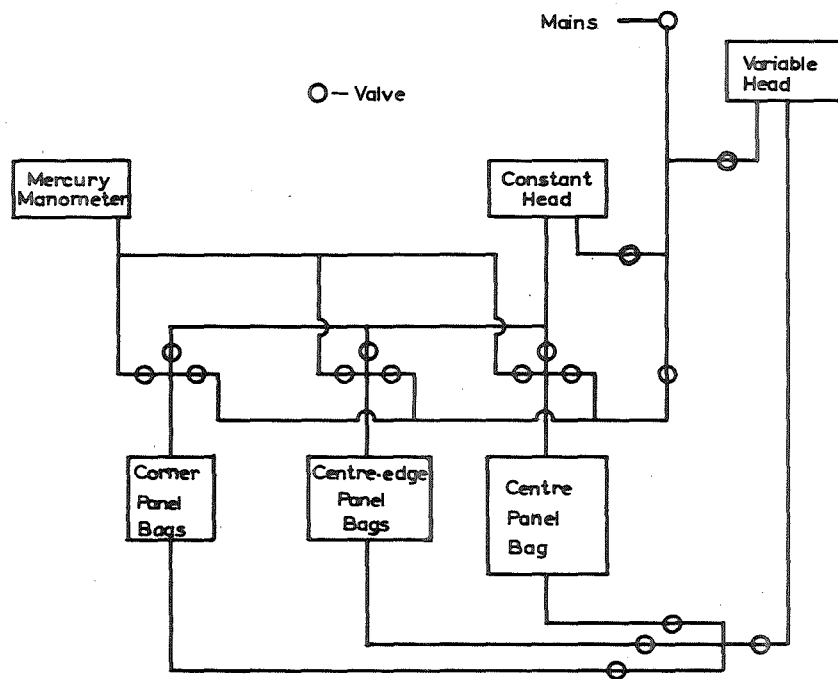


FIGURE 7.5 LOADING SYSTEM

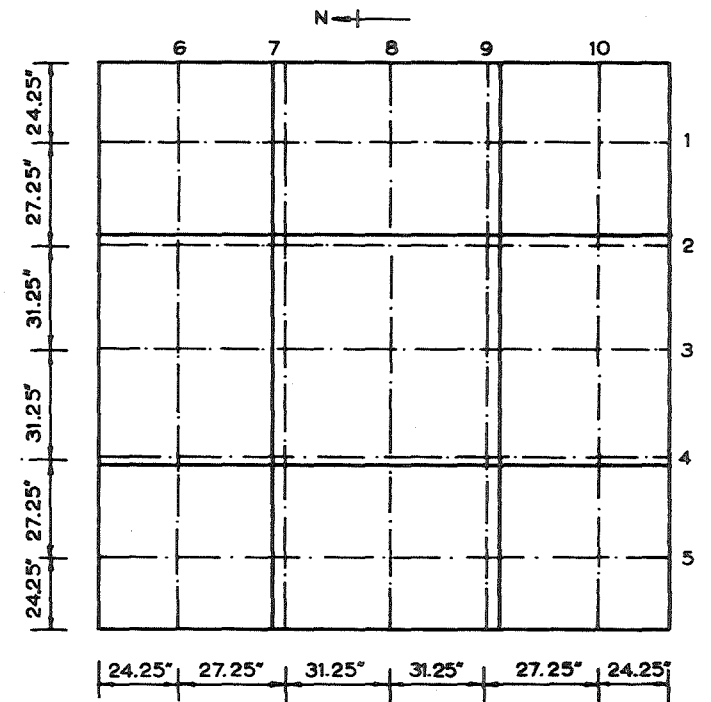


FIGURE 7.6 MOMENT LINES ACROSS SLAB

## 7.2 TEST PROGRAMME

### 7.2.1 Dead Load Reactions

The 75 psf difference between the prototype and model self weights was applied to the model throughout the programme. The application of this load provided a more stable arrangement in reducing the difficulty of setting and maintaining the dead load reactions at the required level. These reactions were set several times before the testing programme was started, for as long as the tendency for the corners to lift remained. When tolerable stability had been achieved, Tests 101 and 102 were performed.

In the design, moment redistribution was kept to a minimum and for this reason the dead load reaction for each support was taken equal to the reaction at ultimate load, scaled down linearly.

An initial setting of reactions was made for self weight only, before a more accurate setting was performed for prototype dead load. Successive trials were made until the required value at each point was obtained.

The corner reactions tended to reduce due to uplift and reactions were reset after Test 102 because this tendency was then less and small differential movement of reaction points had caused some redistribution. After this no further reaction adjustment was made.

### 7.2.2 Load Tests Performed

The overall test programme, carried out between 6th and 22nd May 1968 is summarised in Table 7.1.

Table 7.1. Summary of tests performed.

<u>Test No.</u>	<u>Load Stage Nos.</u>	<u>Maximum Panel Loads (psf)</u>			<u>No. of Increments</u>		<u>Remarks</u>
		<u>Centre</u>	<u>Centre -Edge</u>	<u>Corner</u>	<u>Up</u>	<u>Down</u>	
101	1-10	225	225	225	7	3	
102	13-23	225	225	225	7	5	
103	25-38	225	75	225	7	6	
104	51-63	75	225	75	7	6	
105	1A-13A	225	225	225	7	6	
106	76-94	375	375	375	12	10	
107	95-109	375	375	375	7	13	(Live load removed from outer panels with centre panel load at 375)
108	114-132	400	75	400	10	9	
109	133-151	200	375	200	10	12	(Corner and centre panel loads adjusted to give upward corner reactions)
110	152-167	450	450	450	11	10	
111	168-189	375	375	375	9	12	(Outer panels held at 225 while C.P. loaded to 375 and back. All then loaded to 375)
112	189-220	775	775	775	16		(66 hours at 375 then loaded to 775)
113	221-227	850	850	6			(To failure of C.P.)
114	228-239	600	966	1170	8		(To failure of centre-edge then corner panels)

Figures in psf are applied loads including the 75 psf difference between model and prototype self weights. Three hundred and seventy-five psf is dead load plus full live load. Seven hundred and seventy-five psf is twice dead load plus twice full live load.

Full details of all load increments are given in Appendix C.

### 7.2.3 Procedure at Each Load Increment

The load was set using the hydraulic system described in 7.1.4, a period of a few minutes being allowed for the system to settle. A check between mercury manometer readings and variable head device setting was used to ensure that a static state had been achieved.

Dial indicator readings were then taken, the load cell readings taken once and one cycle (140 channels) of strain readings performed. The whole floor was then checked for cracks, new cracks being marked with the corresponding load stage number. Load cell readings were taken again and if considerable cracking or reaction distribution had taken place since the start of the increment a further cycle of strain readings was taken.

On the completion of reading the load was set for the next increment and during the time taken for the load of the next increment to settle graphs of load versus deflection and load versus strain were drawn for some critical points.



## 7.3 REDUCTION AND PROCESSING OF RAW DATA

### 7.3.1 Deflections

Readings were taken in ten thousandths of an inch and punched into cards. The start of Test 104 was used as datum in the reduction of all readings.

### 7.3.2 Reactions

Bridge readings taken for each reaction point were punched into cards and the reactions at each point computed on the assumption of a linear relation between load and bridge reading. Calibration of each load cell provided the constant relating the two quantities.

As a check, the sum of the reactions was compared with the total applied load plus self weight, in which the total applied load was the sum of the products of the nominal bag pressure and full panel areas. In all cases the sum of the reactions was the smaller quantity since the bags could not be made to apply pressure over the whole area, due to curvature of the bag walls. The effective loaded area was 94 per cent of the total top surface area. The "clear span" area of slab panels was 81 per cent of the total top surface area so that the load applied represented some loading arrangement in between the total area and the clear span area of the panels. Placement of the bags was such that the unloaded area was directly above the beams and therefore each slab panel was subject to the full measured bag pressure over

its total clear span area. No reduction of this value was therefore necessary to obtain the pressure sustained by the panels.

Figure 7.6 shows the lines along which moments were calculated from the reaction values and applied loads, the latter being scaled down by the ratio of effective loaded area to total top surface area.

The moments so calculated were used in checking the results of moment computations from strain readings and in assessing moment redistribution.

### 7.3.3 Strain Readings

Readings of each gauge in microstrain were punched onto paper tape and processed by computer. The raw strain readings were reduced in the following manner.

#### (i) Datum correction

A particular load stage was chosen as datum, and for each gauge and the reading at the datum stage was subtracted from all other readings.

#### (ii) Drift correction

The first channel of each block of 20 gauges was a standard strain gauge of high stability. The variation of reading in these gauges was used to assess the electrical drift of the Strain Data Logger. Variation was not great (see Appendix D listing of gauges 1, 21, 41, 61, 81, 101, 121). The readings of gauge 81 were taken as representative and the datum-corrected reading

of this channel at any load stage was subtracted from the readings of all other channels at that stage.

(iii) Temperature correction

Dummy gauges for the active concrete gauges were of the same type and mounted on similar concrete blocks. Thus variations of length due to temperature were assumed to be compensatory and the concrete strain gauge readings assumed to require no correction for temperature.

The active steel gauges had dummies which were temperature compensated and mounted on aluminium. Temperature could therefore be expected to affect the readings of the steel gauges. To compensate, two steel gauges, (Nos. 139 and 140), mounted in the same fashion as the active gauges were used. These were of the same type and were mounted on steel reinforcement embedded in a block of concrete. The blocks remained unstressed by external forces and had identical dummies to the active gauges. The datum-corrected reading of channel 140 was subtracted from all steel gauge readings at each load stage to correct for temperature.

(iv) Special drift correction

At the beginning of each test, up to LS 151 (see Table 7.1), the corrected reading of each channel was compared with the corrected reading of that channel at the end of the previous test. If any difference occurred, the readings of the gauge in the test to follow were

corrected by this difference.

(v) Zero correction

Initial balancing of the gauges was performed when the total load on the slab was 100 psf. Allowance for this initial load was made by computing the difference in readings of each channel at LS1 (75 psf applied) and LS5 (175 psf applied) and adjusting all readings of that channel by this amount.

At sections at which measurement of normal force and moment were to be made one gauge was mounted on the main steel and one mounted on the opposite face of the concrete. This permitted the determination of the strain profile, assumed linear, across the section. This linear strain profile as given by the corrected strain readings was used, in conjunction with section properties, to determine the actions on the section. Computer sub-routines were written to compute the steel and concrete forces resulting. The stress-strain curve for the steel was assumed to be tri-linear and the stress-strain relationship for the concrete was assumed to be of the form proposed by Hognestad et al.<sup>(20)</sup>. The derivation of the subroutines is described more fully in Appendix E.

7.3.4 Computation of Section Actions from Strain Readings

7.3.4.1. General basis

The subroutines, CONACT and STEEL, described in

Appendix E were written to calculate the concrete and steel action in a section whose strain profile was linear. In the computation of section actions from the test readings, a linear profile was defined by a measured concrete strain and a measured steel strain.

The steps in the computation were as follows:

(i) Reduction of strain readings

This was done by the method outlined in Section 7.3.3.

(ii) Computation of strains for equivalent strain profile

(a) Equivalent steel strain: ( $e_s$ )

When two steel strain readings were taken at the section at the same level, the average value was taken. In cases where only one reading was taken, this was assumed to be the strain in the section at the level of the centroid of the steel.

(b) Equivalent concrete strain: ( $e_c$ )

When only one gauge was used it was placed parallel to the steel bar and the concrete gauge reading was taken as the section strain at the face of the concrete.

When two concrete gauges were used, one was at right angles and the other parallel to the reinforcement. Poisson effect was considered in reducing  $e_c$  according to the relation:

$$e_c = (e_1 + e_2)/(1 - \mu^2)$$

where  $e_1$  = concrete strain measured parallel to  
reinforcement

$e_2$  = concrete strain measured perpendicular to  
the reinforcement

$\mu$  = Poisson's ratio

For the two sections for which three concrete gauges were used these were in  $120^\circ$  "rosette" form and two-dimensional strain analysis was used to obtain the principal strains which were used to obtain the equivalent strain component parallel to the reinforcement.

The strain profile was then defined, and was as shown in Figure 7.7.

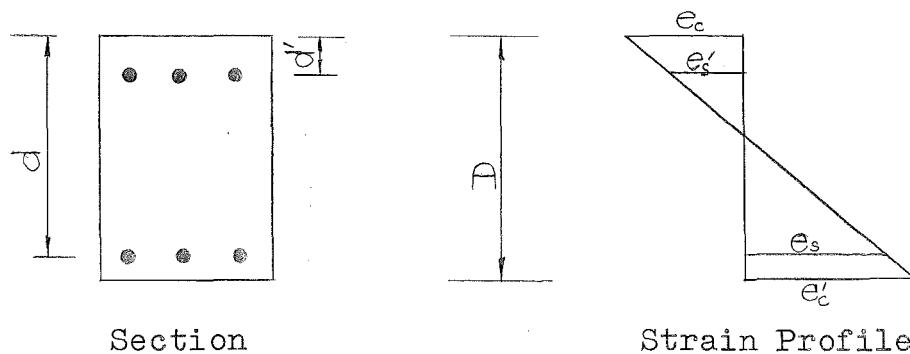


FIGURE 7.7. STRAIN PROFILE.

Values of equivalent top and bottom concrete strain,  $e_c$  and  $e'_c$  were computed directly and stored. Values of  $e_s$  and  $e'_s$  were likewise stored. For each load stage, the strains  $e_c$ ,  $e'_s$ ,  $e_s$  and  $e'_c$  corresponding to the strain profile defined by the values computed for  $e_c$  and  $e_s$  were

calculated and stored.

(iii) Computation of concrete actions

The values of  $e_c$  and  $e'_c$  were used in the subroutine CONACT as top and bottom concrete strains and the concrete forces determined.

(iv) Computation of steel actions

Arrays of top and bottom steel strains had been stored. The loading and unloading performed during the test necessitated the examination of the strain history to determine the plastic portion of the indicated strain. The method used to determine this is shown in Figure 7.8.

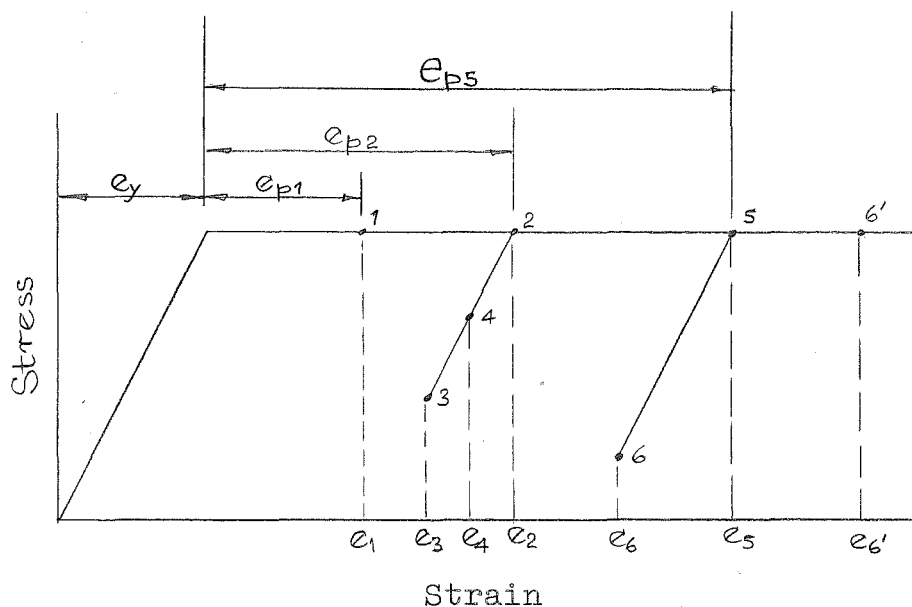


FIGURE 7.8. STEEL STRAIN DETERMINATION.

Consider the strain,  $e_1$  as known to be on the yield plateau. The elastic portion of  $e_1$  is  $e_1 - e_{p1} = e_y$ . If the next four strains are  $e_2$ ,  $e_3$ ,  $e_4$  and  $e_5$  as shown, then,

because  $e_1$  is on the yield plateau and  $e_2$  is greater than  $e_1$ ,  $e_2$  is also on the yield plateau and the plastic strain is then  $e_{p2}$ .  $e_3$  is less than  $e_2$  and unstressing is elastic and the plastic strain portion of  $e_3$  is still  $e_{p2}$ .  $e_4$  is greater than  $e_3$  but it is found that  $e_4 - e_{p2}$  is less than  $e_y$  so that the plastic strain portion of  $e_4$  is also  $e_{p2}$ .  $e_5 - e_{p2}$  is found to be greater than  $e_y$  and a new plastic portion  $e_{p5}$  must be defined to apply to consequent strains. Whether or not this applies to  $e_6$ , clearly depends on whether  $e_6 - e_{p5} > e_y$ .

Each array of top and bottom steel strains was searched in the manner outlined and only the elastic portion of the strain retained for input into subroutine STEEL for computation of steel forces.

(v) Calculation of section moments and forces

Output from the subroutines CONACT and STEEL were in non-dimensional form, giving the steel and concrete forces and moments, acting at and about the mid-depth. These non-dimensional values,  $M/f'_c b D^2$  and  $T/f'_c b D$ , were multiplied by the appropriate values of  $f'_c b D^2$  and  $f'_c b D$  respectively.

(vi) Cracked and uncracked sections

In tension the concrete stress-strain curve was assumed to be linearly elastic with a modulus of elasticity as given by the secant from 0 to 1000 psi on the compressive stress-strain curve.



For each load stage the concrete was assumed first to be uncracked in which case concrete tensile stress was assumed to be proportional to concrete tensile strain, no matter how large the strain. Actions were then computed and the section assumed to be cracked. In this case concrete was assumed to have no tensile strength and the actions were again computed.

(vii) Factoring of concrete strains

The reduced and corrected value of concrete strain parallel to the reinforcement,  $e_c$ , was factored by 1.0, 1.20 and 1.50 for each load stage for panel sections only. In regions of steep strain gradient, the gauge length of 1" would lead to an average strain value, when in fact the maximum strain was required.

Concrete gauges on the undersides of the panels were thought to suffer most from this effect but this factoring made little difference to the computed actions along panel edge sections and only in uncracked sections away from the edge where strain gradients were probably insufficient to warrant this factoring, was any appreciable difference evident. Special measures had to be taken to obtain more realistic values of panel edge section actions as described below.

(viii) Effect of T- and L-beam flange width

For all beam sections the procedure described above was used to determine the actions on the rectangular

portion of the section only. The effect of flange width was determined by assuming the flange to be of plain concrete and that the strains in the flange sections were the same as those in the rectangular portion at the same level.

Thus from the strain profile of Figure 7.7 the concrete strains at the top and bottom of the flange were calculated and used as input in the subroutine CONACT. For each load stage, total flange widths of 1.0, 2.0 and 3.0 times the web width were used in computing section actions.

#### 7.3.4.2 Modified method for calculation of panel edge section actions

The modified method to be described was necessary because the steel strain and concrete strain measured near a panel edge section did not apply to the same cross-section. This is illustrated in Figure 7.9(a). The steel strain measured corresponded to the cracked section at BB but the concrete strain to the uncracked section at AA. Further, at the end of the test the zone of crushing at Y was no wider than  $\frac{1}{8}$ ", and as the small values suggested, the concrete strain measured was not that existing at Y.

The key to the modified method is given by the forces on the section at BB shown in Figure 7.9(b). The values required were the action at mid-depth,  $m_E$  and  $C_E$ , resulting from the steel tension  $T_s$  and combined steel and concrete compression,  $c_c$ . Even for large variations of  $c_c$ ,

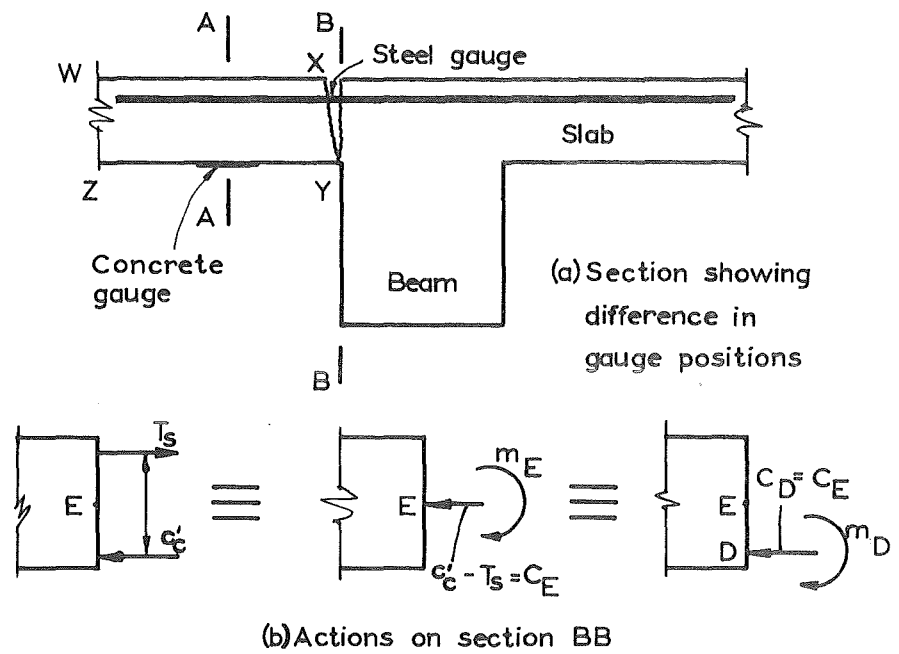


FIGURE 7.9 ACTIONS AT EDGE OF PANEL

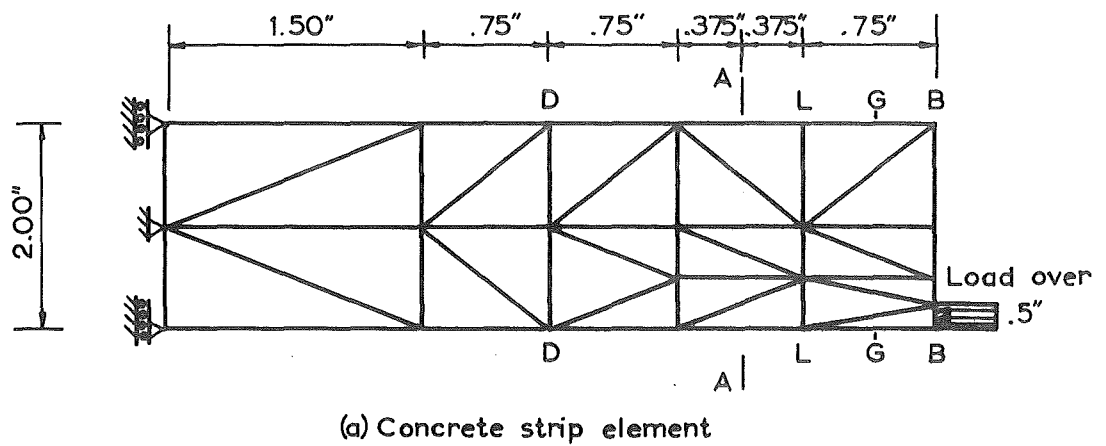
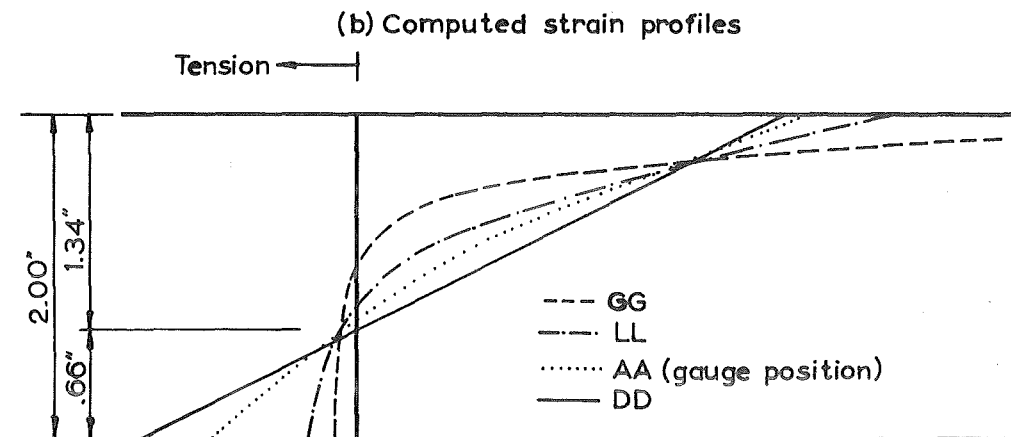


FIGURE 7.10



the level of its line of action will not alter significantly and may reasonably be assumed constant. The value of  $m_E$ , however, is dependent very largely on the magnitude of  $C_E = C_D$ , the shift in the line of action of  $c_c$  being of the second order. Thus, if moments are taken about the assumed line of action of  $c_c$ , the magnitude of  $C_E$  need not be known for an accurate assessment of  $m_D$  to be made.

It is reasonable to assume that the moment and force at Section AA will be equal to those at Section BB. If moments are taken about the level D at Section AA, these should sum to  $m_D$ .

On the basis that moments about D, at the level of the bottom steel, are equal at AA and BB it may be seen that

$$(m_D)_{AA} = (m_D)_{BB} = T_s l_a$$

Knowledge of the bottom concrete strain at AA was used to obtain  $m_E$  and  $C_E$  in two ways as follows.

(a) Assuming full bond transfer of steel force between BB and AA.

If full bond transfer occurs between BB and AA concrete and steel strains at the level of the top steel are equal at Section AA.  $m_D$  was calculated from the known steel force at BB. The section at AA was uncracked and the strain profile was found which satisfied the condition that  $(m_D)_{AA} = (m_D)_{BB}$  and having the bottom concrete strains

equal to that given by the reduced and corrected value of concrete gauge reading at AA. This was done by increasing the top strain from zero in steps of .000005 until  $(m_D)_{AA} = (m_D)_{BB}$ . The actions,  $m_E$  and  $C_E$  for this strain profile were then determined.

(b) Assuming no bond transfer between BB and AA

This assumption meant that at AA, the top steel force was equal to that at BB. A strain profile in the concrete, having the strain at the bottom surface equal to that given by the gauge at AA, may be found such that

$$(m_D)_{AA} = (m_D)_{BB}.$$

Since the contribution of the top steel force to  $m_D$  is the same at AA as at BB, the required strain profile would result in the moments of the concrete forces at BB, about the level D, being zero. For D at a level of .94 of the total depth the linear strain profile which gives zero moment of concrete forces about D has  $e'_c \approx -2.e_c$  (Figure 7.7) for a material linearly elastic in both tension and compression.

To check the linearity of strain profile, the strip of concrete WXYZ, assumed to be of elastic material, was analysed for a load at Y and the relationship between top and bottom concrete strain at AA was found.

Figure 7.10(a) shows the unit width concrete strip analysed, and the load assumed to be acting upon it. Analysis of this element was done using a library finite

element computer programme, with elements as drawn.

It was found that the strain in the concrete at the top surface was approximately equal to  $-.5$  times the concrete strain on the bottom surface when the strain profile was linear. At AA the strain profile was not precisely linear but very nearly so as may be seen in Figure 7.10(b) which shows the computed strain profiles.

In this case, therefore, the concrete strain profile was calculated directly from  $e_c = -\frac{1}{2} e'_c$  where  $e'_c$  was known, and the section actions computed.

The difference between methods (a) and (b) above was not large and in the analysis of results, values of method (a) were used.

## CHAPTER 8

### TESTS ON THE PERFORMANCE OF THE METHOD USED TO CALCULATE SECTION ACTIONS

#### 8.1 SUMMARY

In this chapter two types of test on the method used to compute the moment and normal force on a section are described. The first was on a series of three specially cast slab strips with identical strain gauges to those on the model floor. Known actions were applied to the gauged section and these were compared with the values computed from the strain readings.

The second test was on the sensitivity of the actions on a section to change in strain reading in order that the likely effect of electrical drift and other unwanted components of the strain reading could be assessed.

#### 8.2 TESTS ON SPECIAL CONTROL SPECIMENS

##### 8.2.1 Introduction

In order to check the suitability of the method used to compute axial force and moment in slab sections, a series of three slab strips of the same mortar mix used for the model floor was tested. The strips had the same

depth and bottom reinforcement as the model panels. Strain gauges on the steel and concrete were of the same type and mounted in the same way. A range of moments and axial forces was applied to the gauged section. Gauge readings were processed by the method described in Section 7.3 and the computed and applied axial forces and moments compared.

#### 8.2.2 Strip Dimensions and Test Set-Up

Each strip was 36" x 8½" x 1.98" with two ⅜" diameter lead bath annealed bars as reinforcement. The bars were 4¼" apart, symmetrically placed in plan with 3/16" cover at the bottom. Each strip was loaded at the third points of the 33" span.

Vertical load was applied with a screw jack through a proving ring and spreader beam.

At each end of the strip a steel end block was attached, covering both the ends and the end portions of the underside in order to transfer both the vertical reaction and the applied axial compression.

Axial compression was applied by tightening each of the two tie rods. Two diametrically opposite strain gauges on each rod placed parallel to the longitudinal axis provided the means of force measurement, each rod being thoroughly checked and calibrated before and after the tests.

Force in the rods was transferred to the slab strip through beams across the ends. These beams consisted of



two steel flats with a gap for the rods. Force from these onto the end blocks was transmitted through two half-round mild steel pieces for which the end blocks were shaped. This arrangement ensured that the tie rods remained horizontal throughout the test. Figure 8.1 shows the test set up at the end of a test and Figure 8.2 shows strips 1 and 2 after testing.

### 8.2.3 Instrumentation

The mid-span section of each strip was strain gauged with a gauge on each steel reinforcement bar and a gauge on the top concrete surface above each bar.

Each tie rod had two electrical resistance strain gauges cemented to it which were used to measure axial force. Dial gauges were used to measure the vertical displacement at mid-span and the horizontal movement at the roller support. Proving ring readings provided a measure of the applied vertical load.

### 8.2.4 Tests Performed

Each load increment represented a combination of moment and axial force at the mid-span section. Increments of proving ring force were 50 lbs giving moment increments of 275 lb-in. Axial force increments were approximately 1000 lb or 118 lb/in width.

Table 8.1 gives a summary of tests performed on the three strips.

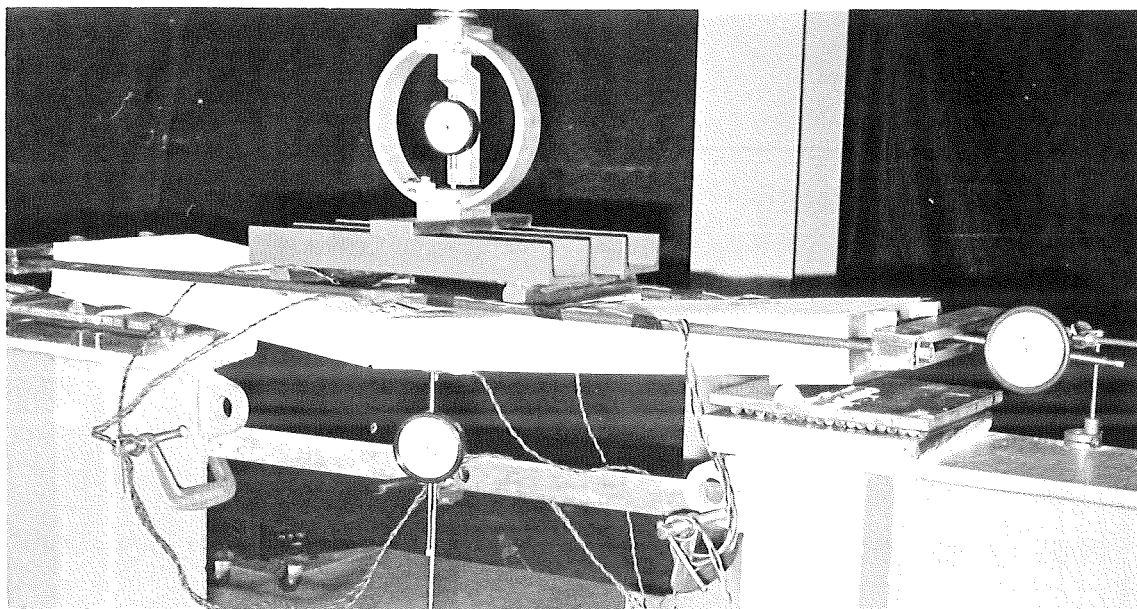


FIGURE 8.1 TEST SET-UP FOR STRIPS

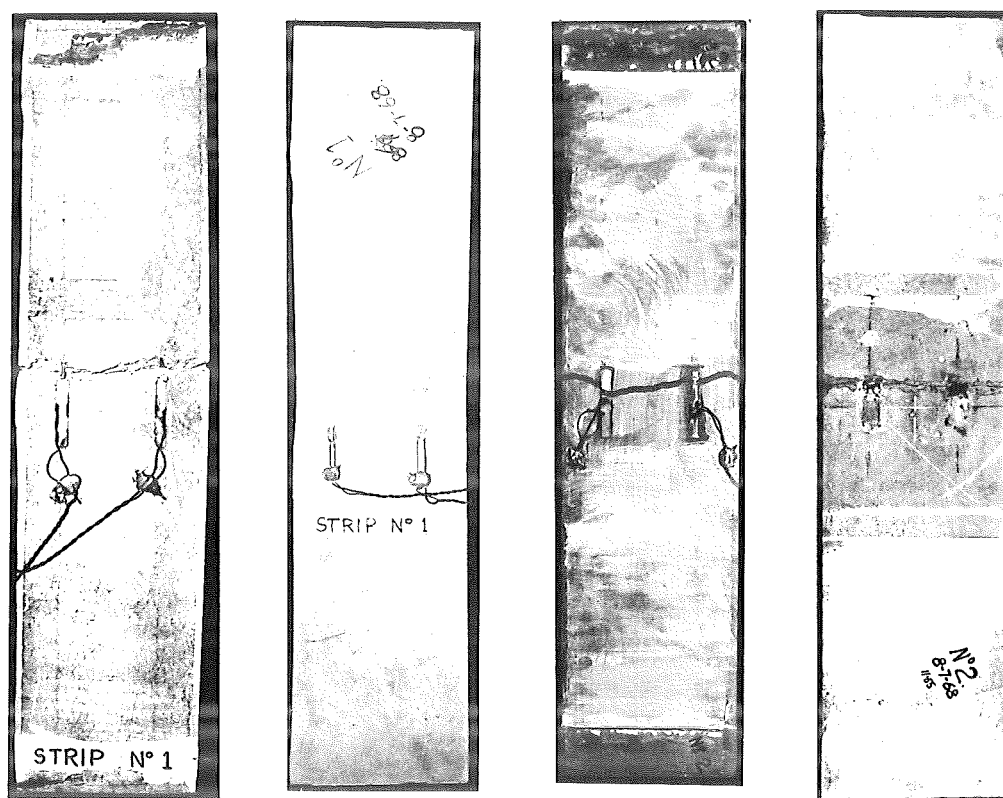


FIGURE 8.2 STRIPS 1 AND 2 AFTER TESTING

Table 8.1. Strip Test Summary.

<u>Strip</u> <u>No.</u>	<u>Load</u> <u>Range</u> <u>lb.</u>	<u>Axial</u> <u>Force</u> <u>Range</u> <u>lb.</u>	<u>Strip</u> <u>No.</u>	<u>Load</u> <u>Range</u> <u>lb.</u>	<u>Axial</u> <u>Force</u> <u>Range</u> <u>lb.</u>	<u>Strip</u> <u>No.</u>	<u>Load</u> <u>Range</u> <u>lb.</u>	<u>Axial</u> <u>Force</u> <u>Range</u> <u>lb.</u>
1	0-450	0-5000	2	0-800	3500-4000	3*	0-700	5000
1*	0	0-5000	2*	0-700	3000	3*	0-600	4000
1*	0-450	5000	2*	0-550	2000	3*	0-500	3000
1*	100-450	0-5000	2*	0-400	1000	3*	0-400	2000
1*	0-400	1000	2*	0-200	0	3*	0-400	1000
2	0-400	0-5000	2*	0-700	2000-4000	3*	0-350	0
2	400-950	5000	3	0-550	0	3*	350-450	0-2000

\* Denotes cracked section.

### 8.2.5 Behaviour During Tests

All strips developed a single crack near mid-span which led to high steel strains. The cracks in strips 1 and 2 did not form directly beneath the centre of the concrete gauges on the top surface and these readings were low as a result. For strip 3 a groove was made in the underside exactly at mid-span. This ensured that the cracking took place at mid-span and that the region of highest concrete strain was near the middle of the gauges.

The very small percentage of reinforcement made the ultimate moment less than the cracking moment and cracking was accompanied by large increases in steel strain, especially when the applied axial force was low.

When the vertical load was increased for a set value of axial force, the outward spread of the ends caused an increase in axial force, but only in cases where variation became large was any adjustment made.

#### 8.2.6 Results

Only the comparison of calculated and applied values of moment and normal force is presented in this Section. The full results are given in Appendix F.

##### (a) Determination of Applied Actions:

Moment at the mid-span section about its mid-depth was computed from the three components: (i) Dead load moments, including allowance for the weight of the proving ring and spreader beam; (ii) Moment induced by the vertical applied load and (iii) Moments induced by the eccentricity of horizontal force applied at the ends of the strip.

##### (b) Determination of Section Actions from Strain Readings:

The method of Section 7.3 was used. Section strain values were taken as the average of the two taken on the steel and on the concrete. Both the normal method and the second modified method (Section 7.3.4) were used in this analysis. For strip 3, the normal method was used since the crack formed exactly at mid-span but for strips 1 and 2, cracking was not exactly at mid-span and a situation

similar to that described in Section 7.3.4.2 arose whereby concrete strain readings greatly underestimated the maximum concrete strain. The second modified method, in which no bond transfer was assumed, was used.

(c) Comparison of Applied and Calculated Section Actions:

Figures 8.3 and 8.4 show graphically the results of this comparison. In Figure 8.3(a), the ratio of calculated moment to applied moment is plotted against applied moment for the uncracked sections.

Results from each strip are recorded, and for strips 1 and 2, values of the ratio for applied axial compression,  $N_{app} = 0$  and  $N_{app} = 5000$  lb are given for each level of  $M_{app}$ .

Figure 8.3(b) is a similar plot for the ratio of calculated and applied normal forces,  $N_{calc}/N_{app}$  for an uncracked section. For each value of  $N_{app}$ , the ratio is plotted for  $M_{app} = 330$  lb-in and  $M_{app} = 2550$  lb-in.

Figure 8.4 shows similar plots for a cracked section. The range of normal force and moment was not as great as that applied before cracking and less points are shown.

Because the cracks were close to the gauge, the results of strips 1 and 2 after cracking were calculated with a linear strain profile approximating that given for Section GG of Figure 7.10. For this the strain at the level of the bottom surface was taken as -1.8 times the top surface

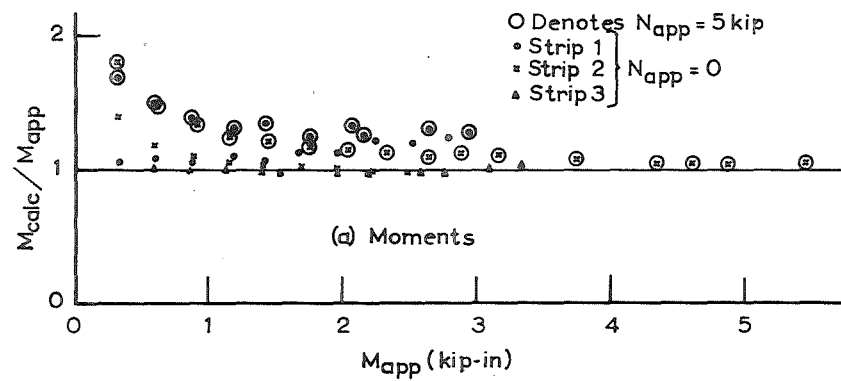


FIGURE 8.3 ACTION COMPARISON BEFORE CRACKING

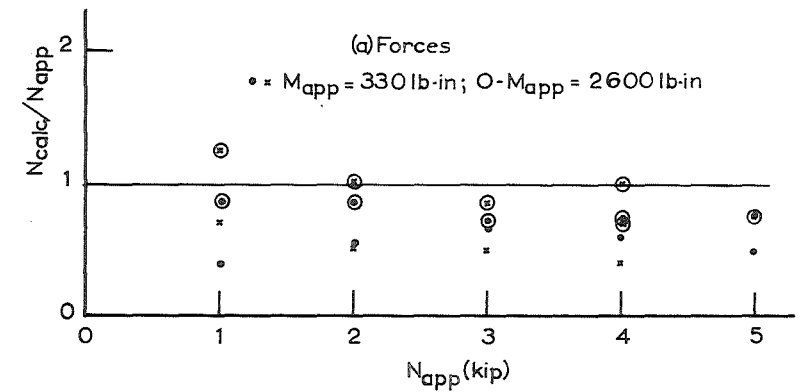
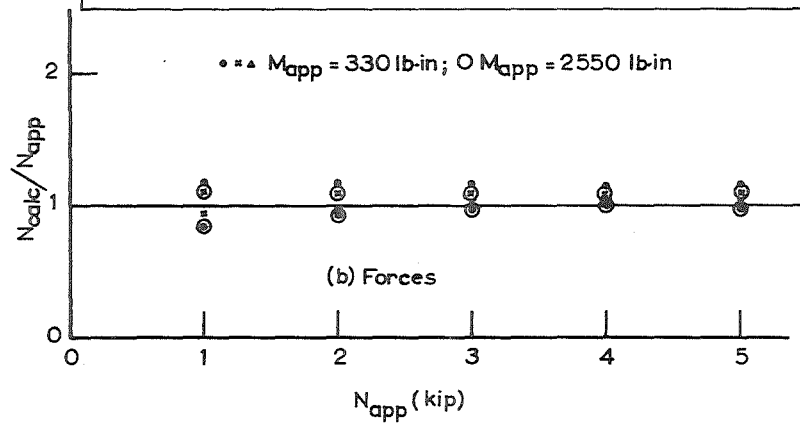
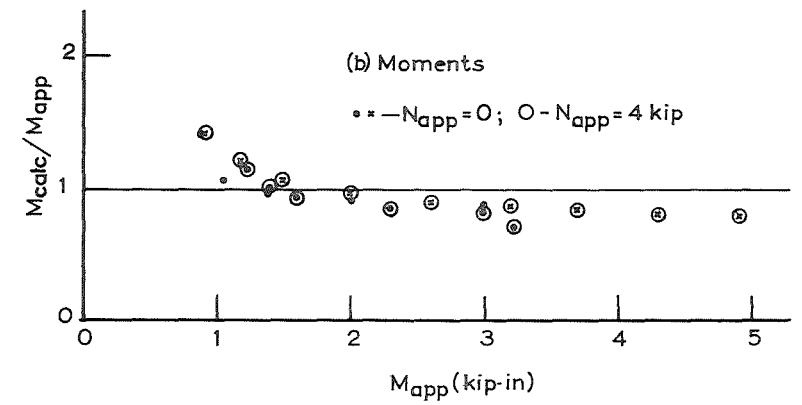


FIGURE 8.4 ACTION COMPARISON AFTER CRACKING



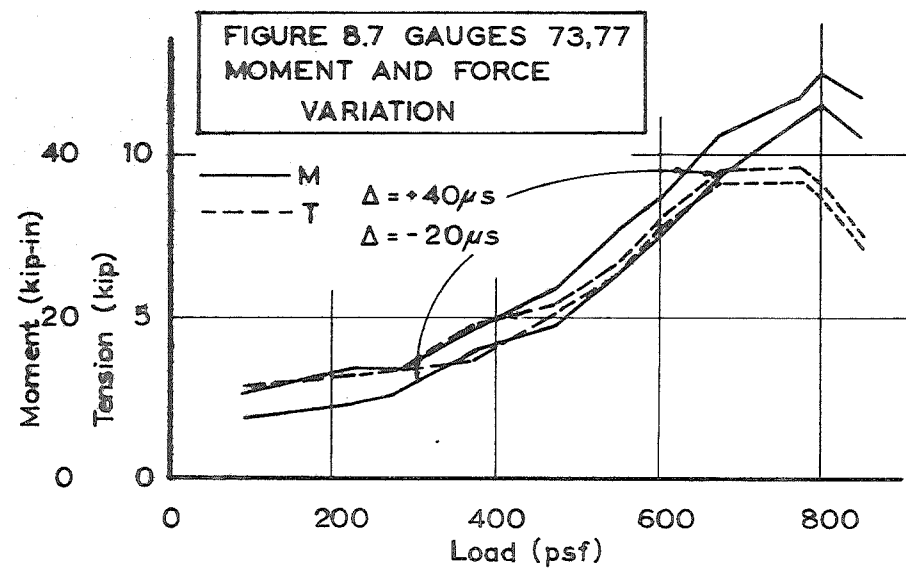
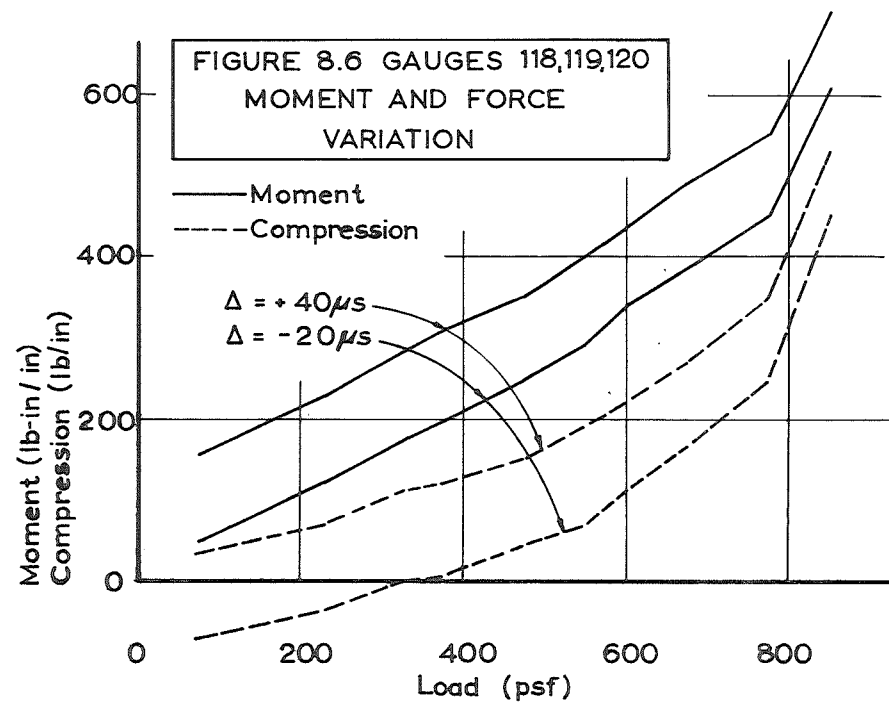
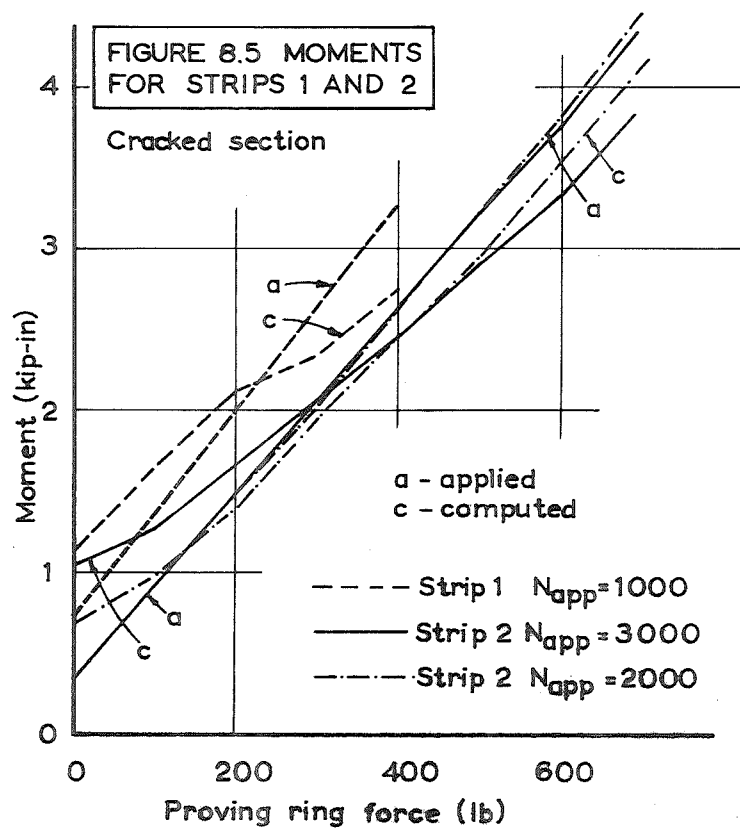
strain reading.

Further evidence of good correlation of results for strips 1 and 2 is given in Figure 8.5. This shows plots of moment, both calculated and applied, versus proving ring force. The results cover tests on strip 2 in which the proving ring force was increased with the applied compression set at 2000 lb and later 3000 lb, and a similar test for strip 1 for  $N_{app} = 1000$  lb.

#### 8.2.7 Discussion

Results from all strips before cracking showed agreement within  $\pm 20$  per cent for most cases, many of which corresponded to within 10 per cent. Before cracking, strain was easier to measure in that the effect of finite gauge length was not as great as after cracking. This led to more accurate calculation of section moments and forces but the low values of strain at this stage made the effects of electrical drift and other strain reading errors relatively greater.

The position of the crack in relation to the concrete gauges was obviously significant. For strips 1 and 2 where the cracks did not form at the gauge points, it was possible to obtain good correlation of applied and calculated values of section actions. These were still dependent on the position of the crack since it was shown that the strain profile across a section near the crack was not linear. By taking account of this factor, satisfactory





correlation of results was achieved, especially for strip 2 where the crack corresponded almost exactly to the end of the concrete gauges.

The results of strip 3 did not compare as favourably. The measurement of concrete strain directly above the crack was not simple because of its rapid variation along the gauge length.

This method of calculation of panel section action could be expected to give results within approximately 30 per cent of actual values.

In assuming the applicability of this conclusion to results of the model floor, the following points must be borne in mind:

- (i) For the uncracked sections of the model the variation of strain reading due to electrical drift and other time effects may have had a significant effect.
- (ii) For sections at the panel edge the concrete gauges were at a considerable distance from the cracked section and therefore the assumption of a linear strain profile for the concrete afforded a closer approximation to actual behaviour than a similar assumption used for these strip tests.
- (iii) Each strip was tested over a period of several hours. Strain reading errors introduced by time-dependent effects in the slab model test may therefore have been greater than in the strip tests.

### 8.3 THE EFFECT OF VARIATION IN STRAIN READINGS

Of importance in the interpretation of results is the sensitivity of the values calculated to change in strain reading.

Considerable variation in strain readings between the end of one test and the beginning of the next test on the following day was detected and although this was accounted for in reducing readings, it pointed to the possibility of appreciable discrepancies between strain readings and the true strain due to stress alone. In order to examine the effects of strain reading variation on the section actions, four typical sections were chosen and the raw readings of steel and concrete gauges varied from the actual values. The resulting moments and forces were compared.

The four sections taken were as follows:

<u>Gauge Numbers</u>	<u>Description of Section</u>
118, 119, 120	Centre panel edge, modified method used on cracked section.
8, 10	Centre panel span, normal method used. Section uncracked almost throughout test.
73, 77	Interior beam, centre span, at mid-span, normal method used.
126, 129	Interior beam, centre span, at support, normal method used.

Four runs were performed for each section using different values of strain deviation,  $\Delta$ . In each run the value,  $\Delta$ , was subtracted from datum-corrected readings of concrete

strain gauges and added to datum-corrected readings of steel strain gauges. The four values of  $\Delta$  used were: -20, 0, +20, +40 microstrains.

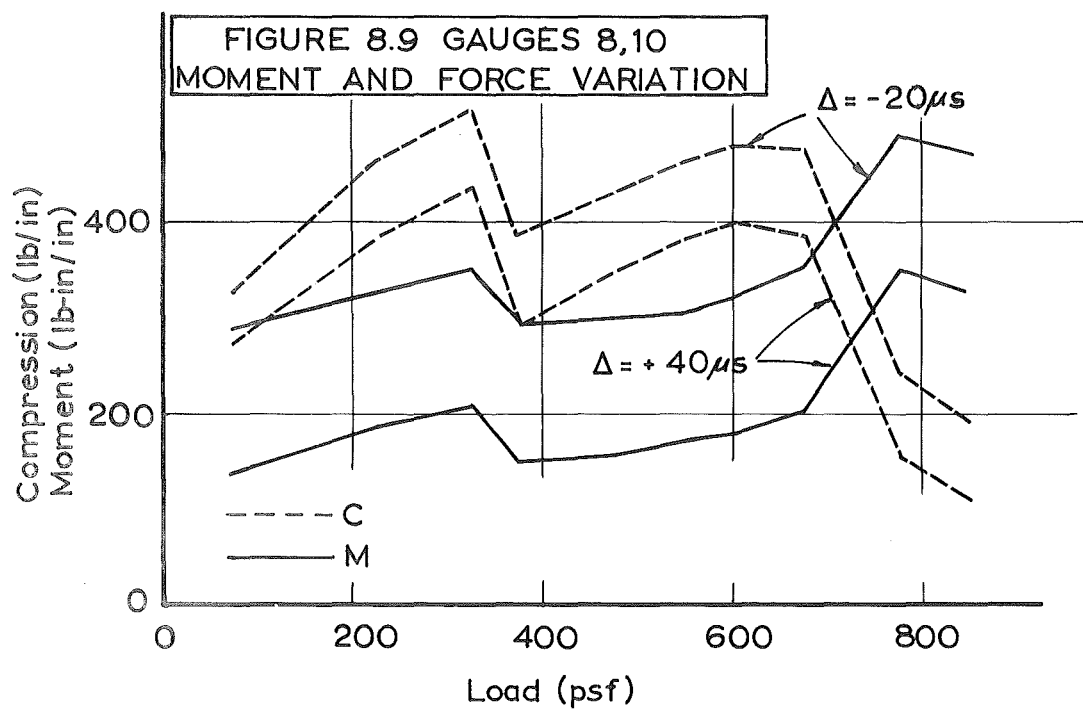
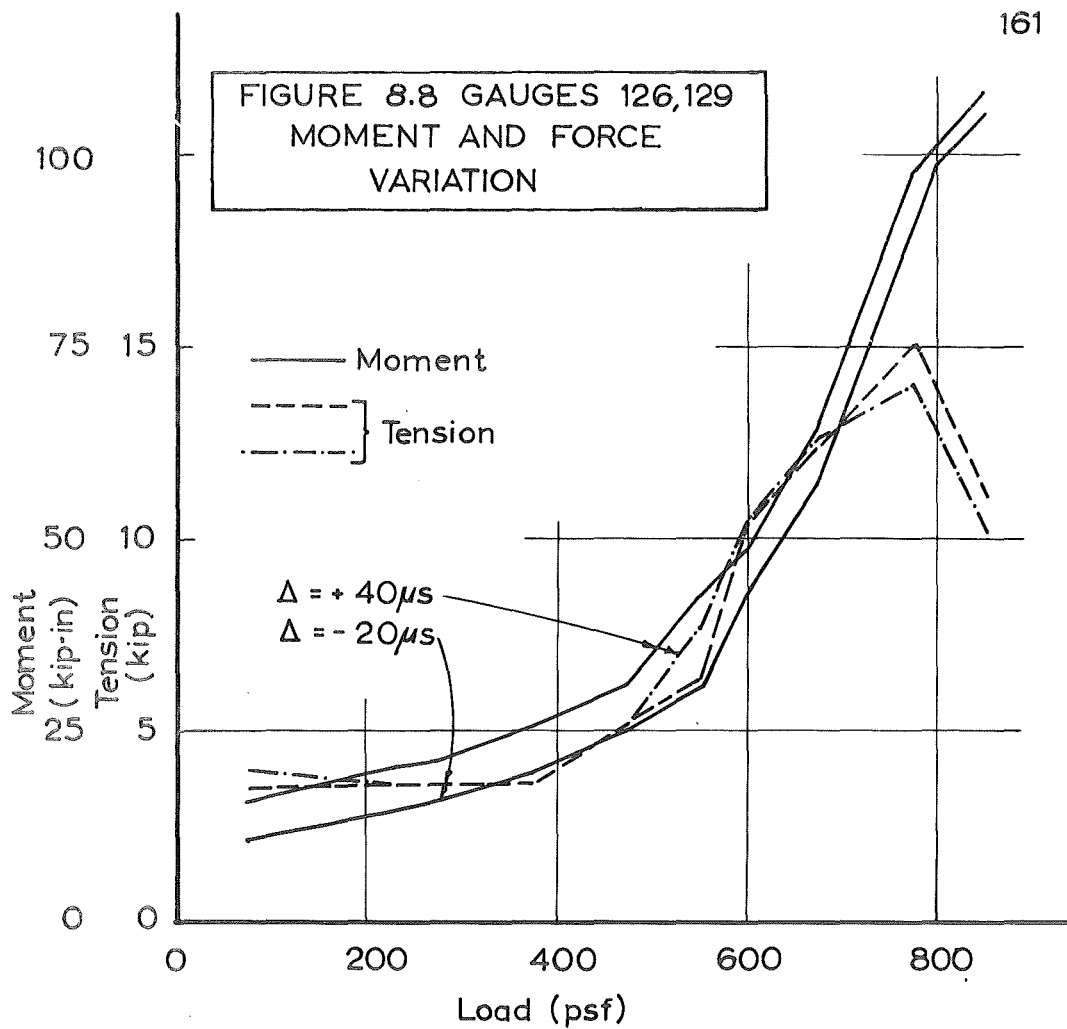
Results are compared graphically in Figures 8.6 to 8.9 inclusive. These show the increase of section actions with increasing load after load stage 168.

At 775 psf the ratio of moment or normal force for  $\Delta = +40$  to the moment or normal force at  $\Delta = -20$  had the following values:

<u>Section</u>	<u>Ratio</u> $M_{\max}/M_{\min}$	<u>Ratio</u> $N_{\max}/N_{\min}$
118, 119, 120	1.23	1.40
8, 10	1.40	1.60
73, 77	1.05	1.04
126, 129	1.08	1.07

The curves shown represent a variation of 60 micro-strain in both concrete and steel strain. The fact that steel strain was increased and concrete strain decreased could be expected to produce a greater effect on the moments than on the axial forces.

Variation in the panel sections was greater than in the beams. Gauges 118, 119 and 120 were at a centre panel edge section where the modified method of computation was used. The 60 microstrain variation in this case is a large proportion of the measured concrete strain. The same is true of the section at gauges 8, 10 which did not crack



until late in the test. The variation of moment (23 per cent and 40 per cent) and of normal force (40 per cent and 60 per cent) for the 60 microstrain variation indicates the appreciable sensitivity of the computed actions to strain reading variations. For this same strain variation, the beam actions show markedly less change. The variation of less than 10 per cent in these actions due to the 60 microstrain variation is clear evidence of their insensitivity to such change.

The magnitude of likely strain variation in the slab test is difficult to determine exactly but variations in the temperature and zero gauges during the test suggested that 30 microstrain would be an upper limit. Most of the actions computed from strain readings during the test would therefore vary by less than one half of the above values.

## CHAPTER 9

### BEHAVIOUR OF THE NINE - PANEL MODEL FLOOR DURING THE TEST PROGRAMME

#### 9.1 SUMMARY

This chapter describes the behaviour of the floor during the test programme in terms of the strains, deflections, loads and reactions measured at each load stage, and the examination, during and after the test, of physical effects such as cracking. The floor had been designed for an ultimate load of 800 psf including membrane action. This load was twice the Johansen ultimate load of the centre panel, 1.35 times the Johansen load of the centre-edge panels and equal to the Johansen load of the corner panels. Pattern loads were applied in early test runs but beyond 400 psf all panels were loaded equally until the centre panel failed at almost 850 psf, a failure brought about by the transition of the panel from a state of predominantly compressive membrane action to one of predominantly tensile membrane action. The outer panels were intact at this stage. Following the failure of the centre panel the load fell to 540 psf. Load on all panels was then increased to 710 psf at which time the centre

panel loading bag was in danger of bursting through the full depth cracks which had formed at the centre of the panel. Load on the centre panel was then reduced to 600 psf and the load on all outer panels increased to 960 psf when the centre-edge panels failed in a combined panel and beam mechanism. The centre-edge panels were held at 960 psf while the loading on the corner panels was increased. The end spans of the interior beams developed plastic hinges at 1170 psf\* and the test was stopped at this load with panel failure mechanisms in the corner panels incompletely developed.

Symmetry of behaviour was excellent throughout the test programme until after the centre panel failure. During the loading to failure of the outer panels the plastic hinges in the end spans of the interior beams did not develop simultaneously and the symmetry was upset noticeably.

Reactions were not affected greatly by moment redistribution and values remained close to those expected. Summation of reaction values indicated that the loading bags applied load over only 90 - 95 per cent of the total top floor area due to rounding of the bag edges.

---

\* Figures quoted indicate the intensity of load applied to the panels of the model floor. This includes the 75 psf difference between prototype and model self weights but does not include the self weight of the model (= 25 psf).

Compressive membrane action enhancement was exhibited by all panels. Measured compressions at the edge of the centre panel were of the order used in design and beam tensions in the centre spans of the interior beams were accordingly large. Tension in the exterior beam centre spans indicated the presence of compressive membrane forces in the long direction of these panels as expected. Forces measured along the interior long edge, parallel to the short side, were large enough to suggest considerable membrane action in this direction. Beam tensions in the centre spans of both interior and exterior beams were large and may have been larger if all panels had failed simultaneously. Values were higher at the support than at mid-span.

Initial cracking of the undersides of the outer panels produced a marked effect on the centre panel. The loss of lateral restraint caused an increase in deflection and strain values in the centre panel. Stability during 66 hours of sustained loading at 375 psf was good but instability was evident at 550 psf when the undersides of the corner panels cracked for the first time and cracking of the centre-edge panels extended.

The effect of membrane action on the torsion in the edge beams was evident in the slow increase in strain in the panel reinforcement at the sections adjoining the beams. Torsional deformation in the beams was not large



until after the centre panel had failed and the end spans of the interior beams had developed large cracks prior to the full development of plastic hinges there.

Moments along lines traversing the whole floor were calculated from reactions and applied loads. The rise with load of the 'free' moment so calculated was linear and agreed well with the expected value throughout the test. Initially, moments along mid-span sections were relatively high in comparison with the support values but as load increased, the rate of increase of mid-span moment fell and a corresponding rise in the rate of increase of support moment took place.

Moments at beam sections computed from the strain readings showed a similar trend. The line moments, calculated from the sum of beam section moments, showed satisfactory agreement with those calculated from the reactions and applied loads. The effect on line moment calculations of the net beam tension and net slab compression was large since each force was taken to act at a different depth below the top surface of the slab. The two forces thus formed a couple which had to be taken into account.

The rate of increase of compression at the edges of the centre panel was similar to that of the increase in supporting beam tension, being small at low load levels and increasing with load.

Although strain readings afforded some measure of panel and beam section forces and moments which in many cases compared satisfactorily with values determined by other means, the accuracy of the results was not sufficient to distinguish any difference in centre panel behaviour with varying load pattern. Only the variation of steel strain at the middle of the centre panel showed signs of the surround being slightly stiffer laterally when the outer panels were not loaded fully.

Deflections at  $DL + LL^*$  were small for all components with the centre panel showing greatest deflection to span ratio. This ratio first exceeded  $L/360$  at 450 psf when considerable surround stiffness loss occurred with the initial cracking of the underside of the centre-edge panels. This loss and the extended cracking of the centre panel caused appreciable unrecoverable deflections.

Strain levels were also low at  $DL + LL$ . At this load, after the floor had been loaded to a maximum of 450 psf, strains at the panel edges ranged up to two-thirds of yield values. Steel strains in the beams were approximately one half yield values. The application of 450 psf had yielded the steel at the middle of the centre panel.

At the stage of failure of the centre panel most of the beam steel had yielded or was near to yield, and steel

---

\*The abbreviation DL denotes the prototype dead load = 100 psf  
 " " LL " " " live " = 300 psf

at the edge of the panel was well beyond yield. Panel edge steel along the exterior beams, however, showed very small values of strain.

Panel deflections at this stage were large in both centre-edge and centre panels though rapid increase had not commenced until 600 psf. The deflections of the centre spans of all beams were less than  $1/360$  of the span and other beams deflected little in excess of this.

The applied load of almost 850 psf at the stage of failure of the centre panel was 10 per cent in excess of the design ultimate load.

Details of slab behaviour follow in the next two sections. In Section 9.2 the behaviour of the floor during each of the 14 tests performed is described. Although chronological order of testing is not strictly adhered to, this section is intended to give a clear impression of the floor behaviour as the test progressed and to indicate the effect of different load patterns.

A more detailed analysis of particular aspects of the floor behaviour is given in Section 9.3 which deals mainly with all-over load. Deflections, strain readings, cracking, reactions, moments and membrane action effects are dealt with in turn.

## 9.2 TEST BY TEST DESCRIPTION OF FLOOR BEHAVIOUR

### 9.2.1 Tests 101, 102, 105 and 106

In these tests the slab was loaded over its whole

surface to a maximum of dead load plus full live load (375 psf applied).

#### 9.2.1.1 General

Tests 101 and 102 (to DL +  $\frac{1}{2}$ LL) were preliminary tests only, serving to test the loading system, data recording devices and the symmetry of response. Embedment of the load cell ball bearings into the mild steel bearing plates caused differential settlement of the reaction points and redistribution of reactions. This, and the tendency for the corners to lift made resetting of the reactions necessary after Tests 101 and 102. No further adjustment was made.

Test 105 was a repeat of Tests 101 and 102, performed after the pattern load tests (103 and 104) had been performed.

In Test 106 the load was increased to DL + LL before being released in stages.

#### 9.2.1.2 Deflections

Load-deflection relations were linear for all vertical deflection gauge points. In Tests 101 and 102 full recovery was not achieved due to the embedment of the load cell bearings into the mild steel bearing plates. Deflection levels in Tests 101, 102 and 105 were very low.

The maximum deflections occurred in Test 106 when DL + LL was applied. Values of the largest deflection

occurring within each of the element type groups are given below (Table 9.1).

Table 9.1. Deflection at Load Stage 85 (375 psf).

<u>Element Type</u>	<u>Reference Mark</u> <u>(Figure 6.2(a))</u>	<u>Maximum</u> <u>Deflection</u> <u>(inches)</u>	<u>Deflection:</u> <u>Span (ratio)</u>
Interior Beam	Beam NS3	.0285	1:2190
Exterior Beam	Beam NS1	.0154	1:4050
Corner Panel	Panel C	.0210	1:2120
Centre-edge Panel	Panel H	.0403	1:1100
Centre Panel	Panel G	.0616	1:1012

#### 9.2.1.3 Membrane Action Effects

There was no cracking of the underside of the centre panel during these tests but the cracking at the edges could be expected to cause the development of compressive membrane forces normal to the edge. Tension in the beams was not high but compressive membrane forces were appreciable. Figure 9.1 shows the increase of this edge compression during Test 106.

#### 9.2.2 Tests 103 and 108

##### 9.2.2.1 General

In both these tests the load on the centre-edge panels was held at 75 psf while the centre and corner panels were loaded to 225 psf (DL + .5LL) in Test 103 and

to 400 psf (DL + 1.08LL) in Test 108.

#### 9.2.2.2 Deflections

With one exception the deflections of beams and panels were smaller than those occurring at LS85 (see Table 9.1). The cracking of the underside of the centre panel which took place during Test 107 produced non-recoverable deflections and the maximum deflection to span ratio rose to 1:678.

#### 9.2.3 Tests 104 and 109

In Test 104 the centre-edge panels only were loaded to 225 psf, while the load on the other panels was maintained at 75 psf.

In Test 109 the load was taken up to 375 psf on the centre-edge panels. The load on the other panels was kept at 75 psf until, at a load of 250 psf on the centre-edge panels, when the corner reactions were about to become zero, the load on the other panels was increased to 200 psf to ensure that the corner points of the floor did not lift off their supports. When 375 psf was reached on the centre-edge panels the load on the other panels was reduced from 200 to 150 psf at which stage the corner reactions were again nearly zero. This latter condition represented the most severe loading applied during Test 109. Test 104 brought no further cracking but in Test 109 cracks appeared near the centre of the middle spans of the exterior beams

NS4 and EW1. Deflections during both tests were not large.

#### 9.2.4 Tests 107, 110 and 111

##### 9.2.4.1 General

The loading sequence in these tests was designed specifically to examine the behaviour of the centre panel in the presence of reduced load on the surrounding panels, the effect of reduced edge moment restraint and modified surround stiffness being of particular interest. Time dependent effects were examined during two periods in the course of these tests.

The whole floor was loaded to a maximum of 375 psf in Test 107. This was followed by reduction of the load on all but the centre panel to 75 psf, the original condition of 75 psf all over then being achieved by reduction of the centre panel load in stages.

All panels were loaded equally in Test 110. The applied load was first increased to 450 psf, reduced then to 375 and held for 22 hours and then reduced to 75 psf.

In Test 111 the load on all panels was taken up to 225 psf, the centre panel load then being raised to 375 psf and reduced again to 225 psf. All panels were then loaded to 375 psf and held at this load for 66 hours while time-dependent effects were examined.

##### 9.2.4.2 Deflections

Cracking produced by the higher load levels caused

larger deflections than in previous tests. Much of the deformation in the centre panel was not recovered on release of load. The effect of cracking is clear from the examination of the maximum element deflections for each test (see Table 9.2) but the different load conditions must be taken into account in making any comparison.

Table 9.2. Maximum Deflections of Elements for Tests 107, 110 and 111.

<u>Element Type</u>	<u>Reference Mark (Figure 6.2(a))</u>	<u>Test No.</u>	<u>Maximum Deflec- tion (inches)</u>	<u>Span: Deflec- tion (ratio)</u>
Interior Beam	NS3	107*	.0305	2040
	EW3	110**	.0550	1140
	EW3	111***	.0470	1330
Exterior Beam	NS1	107	.0169	3700
	NS1	110	.0399	1570
	NS1	111	.0309	2020
Corner Panel	J	107	.0219	2030
	J	110	.0305	1460
	J	111	.0197	2260
Centre-edge Panel	F	107	.0380	1170
	F	110	.0732	610
	D	111	.0546	810
Centre Panel	G	107	.0871	720
	G	110	.2166	289
	G	111	.2137	294

- 
- \* 375 psf on centre panel; 75 psf on all others.  
 \*\* 450 psf on all panels.  
 \*\*\* 375 psf on centre panel; 225 psf on all others.

The effect of the application of 450 psf (75 psf in excess of the design service load) on the centre panel



deflections was very marked. The maximum deflection of the centre panel before design service load was exceeded was only  $1/600$  of the span.

#### 9.2.4.3 Cracking

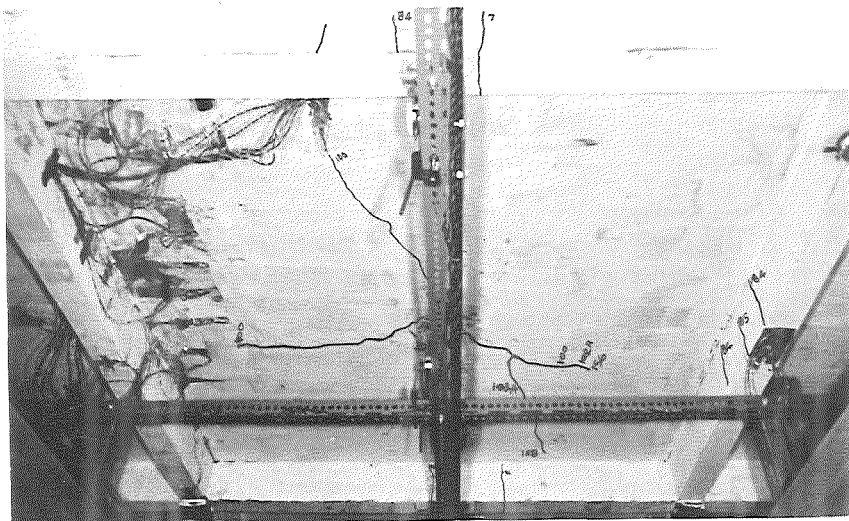
Cracking in the centre spans of beams and in both the centre and centre-edge panels took place during these tests.

First cracking of the underside of the centre panel occurred when the load on the outer panels was reduced to 275 psf and left for one hour (LS100). Three cracks radiated from the centre and extended well towards the edges of the panel (see Figure 9.2 (a)). On further reduction of outer panel load, considerable extension of one of these cracks took place. The maximum crack width in the centre panel, measured when the load on the outer panels was 75 psf, was .002".

The maximum load of 450 psf ( $DL + 1.25LL$ ), applied in Test 110, produced further cracking in the centre panel, in the centre spans of all beams and caused the initial cracking of the underside of the centre-edge panels.

At 400 psf and 425 psf (LS156 and 157) small extensions in the centre panel cracks were noticed and the maximum crack width was .003". Some new cracks appeared in the centre spans of interior beams.

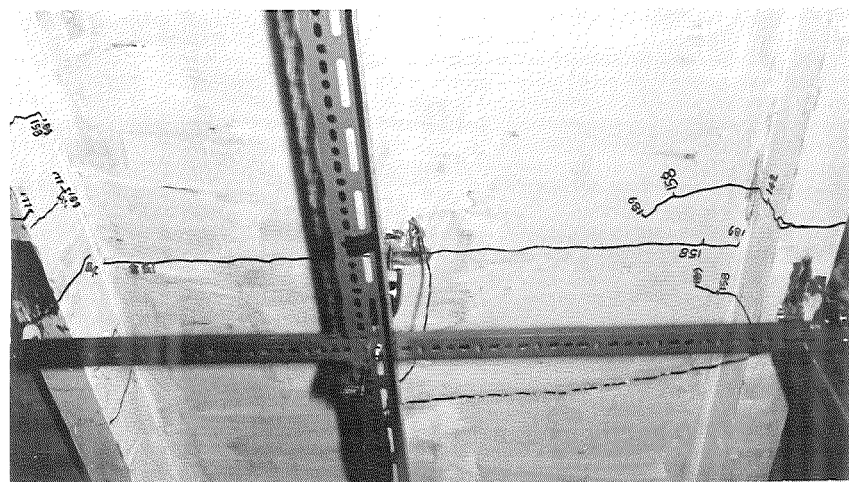
At 450 psf (LS158) cracks formed in all elements except the corner panels and their supporting spans. In the middle of each centre-edge panel a crack ran the full



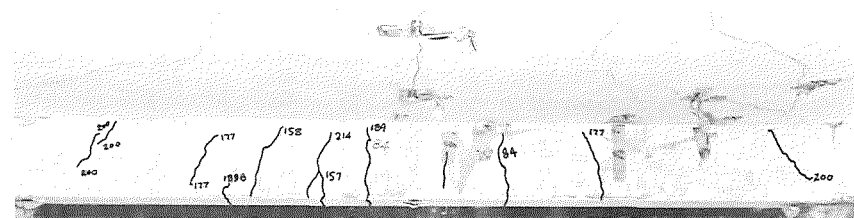
(a) Centre Panel - Test 107 - 375 psf



(c) Centre panel - Test 110 - 450 psf



(b) Centre-edge panel - Test 110 - 450 psf



(d) Interior beam, centre span - 550 psf

FIGURE 9.2 CRACKING DURING TESTS

107, 110 AND 111

width, parallel to the short sides, and in one panel two smaller cracks formed in the L-beam flange, either side of mid-span (Figure 9.2(b)).

Cracking at the supports of the centre spans of the NS interior beams was noticed for the first time and several new cracks appeared at the middle of these spans.

Each centre-edge panel crack caused increased cracking in the centre panel and since an appreciable time elapsed before all four centre-edge panels had cracked, a similar time passed before cracking of the centre panel ceased. Comparison of Figures 9.2(a) and 9.2(c) reveals the extent of cracking in the centre panel produced by this load increment. Figure 9.3 shows the crack pattern for the whole slab at this stage.

New cracks appeared in Test 111 at load stage 177 in some beams supporting the centre panel. In beam EW3 two steeply inclined cracks (marked "177" in Figure 9.2) appeared at the third points of the centre span. One of these did not extend to the bottom of the beam.

Further, smaller cracks of a similar nature appeared after the load of 375 psf on all panels had been maintained for nine hours. After 21 hours very few new cracks had formed and after 29 hours the extension of existing cracks was negligible.

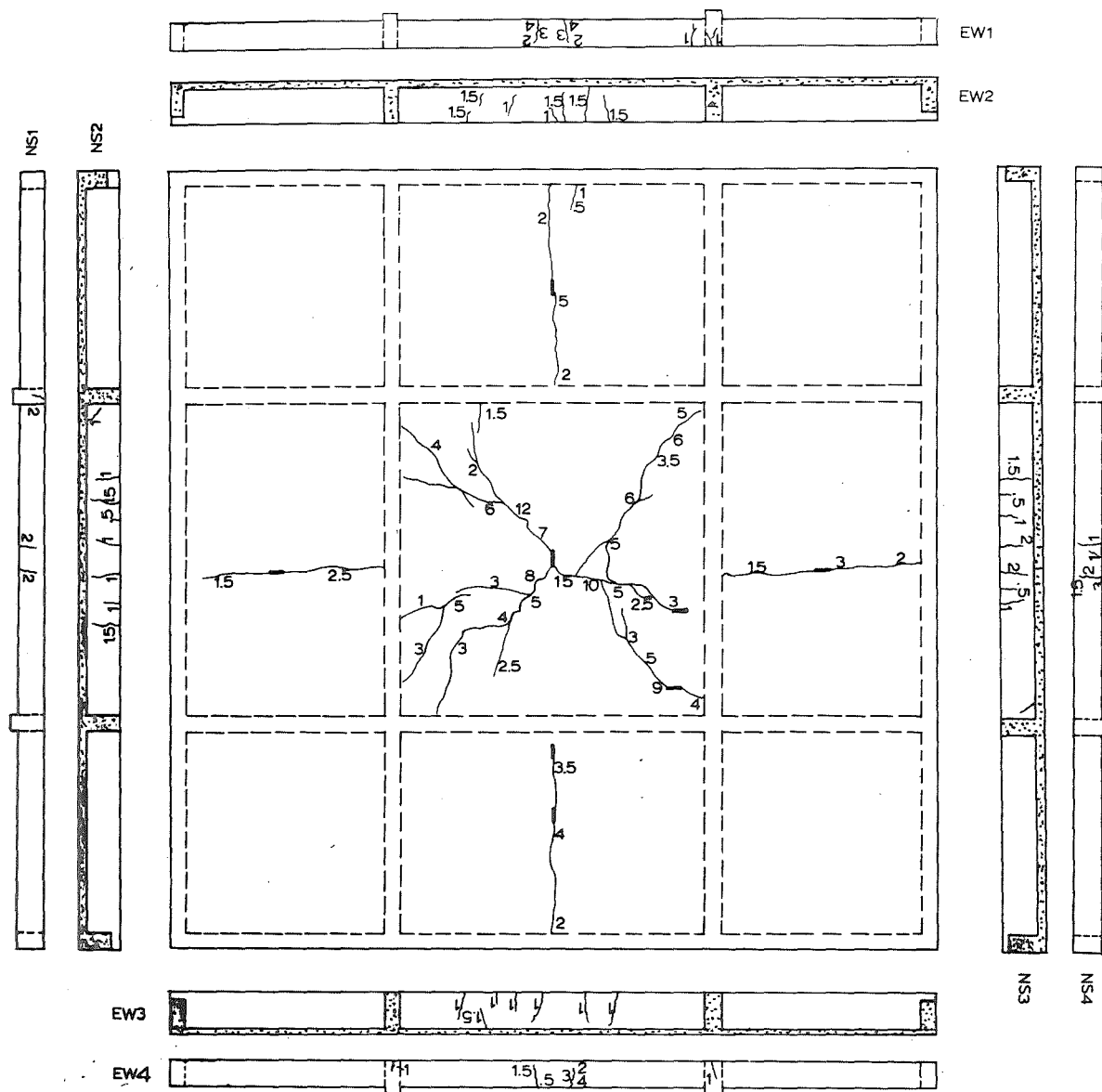


FIGURE 9.3  
CRACK PATTERN AS AT  
450 PSF APPLIED LOAD

Maximum crack widths shown  
in .001" units for load at 375 psf.

#### 9.2.4.4 Strain, Moment and Normal Force Levels at Maximum Load

Table 9.3 shows the values of strains and computed moments and normal forces for four critical load stages.

Load stage 98 preceded the first cracking of the underside of the centre panel and much of the beam cracking. Strains are low as a result. The effect of the application of 450 psf at LS158 was to increase steel strains sharply, particularly in the centre panel. At both panel and beam sections, sharp increases were evident in the values of moments and membrane forces.

Loads applied in Tests 111 produced relatively little change.

#### 9.2.4.5 Membrane Action Effects

Small changes in beam tensions and panel membrane forces resulted from the removal of load from the outer panels in Test 107.

The difference in behaviour between the load configuration in Test 111 and that in which load was applied equally to all panels was not large enough to be detected.

The most vivid expression of membrane action came in Test 110 with the application of 450 psf when the loss of surround stiffness resulting from the cracking of the centre-edge panels caused a marked change in the behaviour of the centre panel. The cracks in the centre-edge panels (Figure 9.2(b)) ran along radial lines from the centre of

TABLE 9.3 - STRAINS, MOMENTS AND NORMAL FORCES AT LOAD STAGES 98, 158, 176 and 189

ELEMENT		GAUGE	POSITION	GAUGE NO'S	MAXIMUM CONC. STRAIN				MAXIMUM STEEL STRAIN				MOMENT (Kip-in and lb-in/in)				FORCE (Kips and lb/in)			
					LSN	98	158	176	189	98	158	176	189	98	158	176	189	98	158	176
Ext.	Beam	C.Span	Support	133,134	-143	-246	-182	-225	89	303	231	297	-3.6	-13.0	-10.5	-13.1	-2.9	-2.4	-1.7	-2.3
Ext.	Beam	C.Span	Mid-Span	53,55	-70	-76	-20	-45	94	534	486	508	6.4	7.5	4.5	5.8	-1.9	1.4	1.9	1.6
Ext.	Beam	E.Span	Mid-Span	59,62	-45	-63	-31	-51	40	53	21	50	4.6	+3.2	-.3	1.7	-2.6	-4.9	-4.5	-5.1
Int.	Beam	C.Span	Support	126,129	-97	-163	-75	-124	106	409	371	423	-13.6	-23.6	-17.0	-21.7	-.5	2.7	3.9	3.5
Int.	Beam	C.Span	Mid-Span	73,77	-68	-92	-31	-50	339	596	504	549	12.4	18.6	13.8	15.2	1.9	4.0	4.0	3.9
Int	Beam	E.Span	Mid-Span	64,67	-44	-63	-38	-59	102	109	164	101	7.4	5.5	1.9	4.5	.5	-1.8	-2.6	-2.7
Centre Panel	Centre	Bottom	6						279	1650	1575	1638								
Centre Panel	Edge		114,115	-54	-52	-14	-18	306	1441	1305	1422	-114	-141	-88	-97	-76	73	115	117	
Centre Panel	Edge		118,119	-117	-161	-115	-128	338	1431	1261	-1390	-206	-300	-226	-257	-178	-109	-106	-63	
Centre Panel	9" from Edge		20,22	40	62	61	73	-38	-91	-98	-110	-74	-171	-169	-189	-74	-207	-213	-220	
Edge	Panel H Centre	Bottom	5						39	-3	-42	-13								
Edge	Panel H Edge	Int.Long	94,95	-108	-182	-107	-133	172	719	681	776	-188	-302	-197	-239	-181	-232	-121	-158	
Edge	Panel H Edge	Ext.Long	97					8	16	-29	-13									
Edge	Panel H Edge	Short	102					195	390	328	404									
Corner Panel	Edge	Int.	91					246	870	780	919									
Corner Panel	Edge	Ext.	86					14	12	-21	-1									

All Strains Corrected for Drift (Gauge 81) and 100 PSF Initial Load.

Steel Strains Corrected for Temperature (Gauge 140).

Moments and Forces Calculated From Strains Shown.

Refer to Figures 7.2 and 7.3 For Gauge Positions.

the floor. This, and the presence of more cracks towards the outside edge indicated that these panels were acting as deep beams and ties against the compressive membrane forces in the centre panel. Each of these long cracks was seen to produce immediate and sharp deterioration of centre panel behaviour.

#### 9.2.4.6 Effects of Sustained Loading

At two stages during these tests, design service load was maintained on all panels for an appreciable time. The application of 375 psf for 22 hours at LS161 revealed negligible time effects, but the 66 hours at this load (LS189) produced detectable changes.

Figure 9.4 shows deflection in the centre panel, steel strain at its edge and steel strain at the mid-span section of an interior beam plotted against time for LS189. The effect at zero time has been set to zero for each curve and steel strains have been corrected for temperature variation. The total increases over the 66 hours are small and a general trend towards stability with time is apparent. The values of the centre panel parameters continued to rise at the end of 66 hours but at a decreasing rate.

Changes in compressive membrane forces in the centre panel and changes in beam tensions were slight.

### 9.2.5 Test to Failure of Floor as a Whole

#### 9.2.5.1 General

This test was performed in two parts: the slab was first loaded to the predicted ultimate load of 775 psf applied after which the load was reduced to 400 psf. The load was then taken up again until failure of the centre panel at almost 850 psf. Failure of the centre panel was deemed to be the failure of the floor as a whole. At this stage the deflection of the centre panel increased markedly as tensile membrane action took over from compressive membrane action as the principal load carrying mechanism. Centre-edge panels were showing only moderate signs of distress at this stage and the corner panels even less.

#### 9.2.5.2 Deflections

Maximum levels of deflection for the floor elements at the predicted ultimate load are shown in Table 9.4.

Most elements showed a sharp increase in deflection at 550 psf when the first cracking of the underside of the corner panels occurred, and a general loss of stiffness was evident after this stage.

The deflection of the centre panel increased steadily with load and was approximately equal to the depth of the slab when failure occurred and tensile membrane behaviour became predominant. The centre spans of all interior beams and the EW exterior beams tended to stiffen in the latter stages of the test, immediately prior to the failure of the



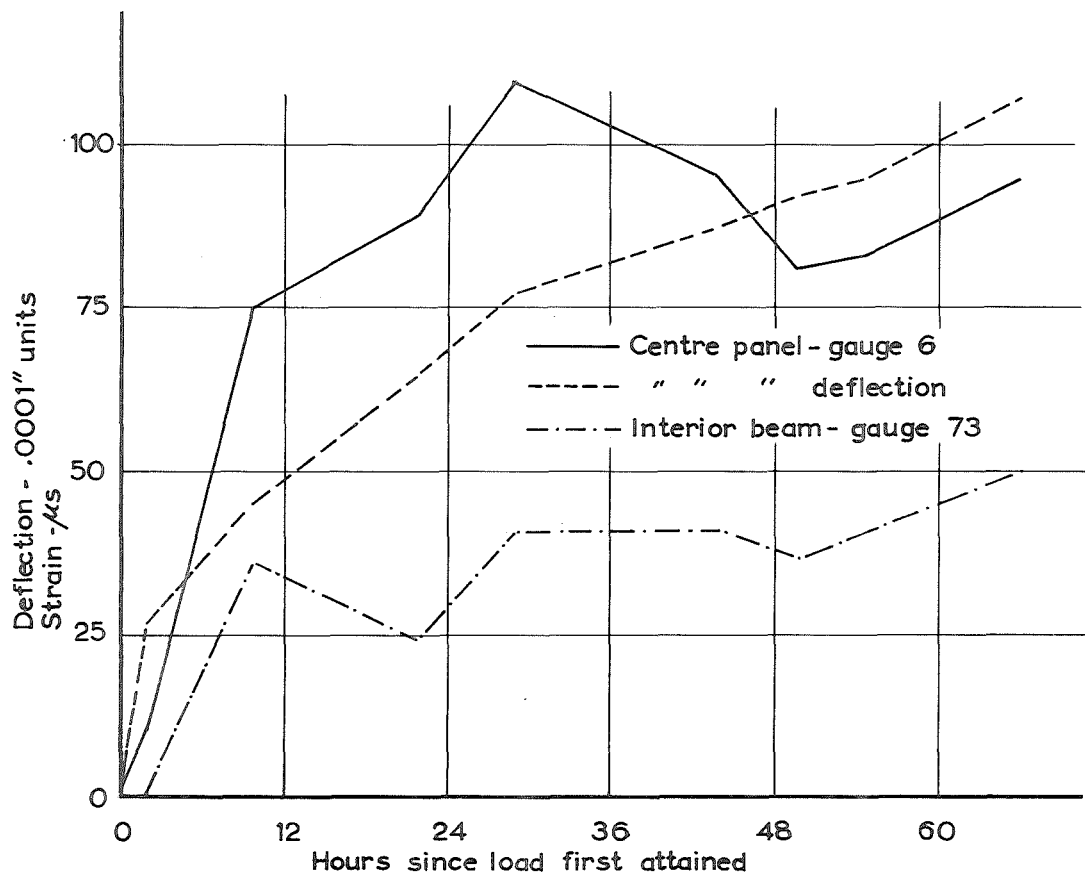


FIGURE 9.4 TIME EFFECT - LS189

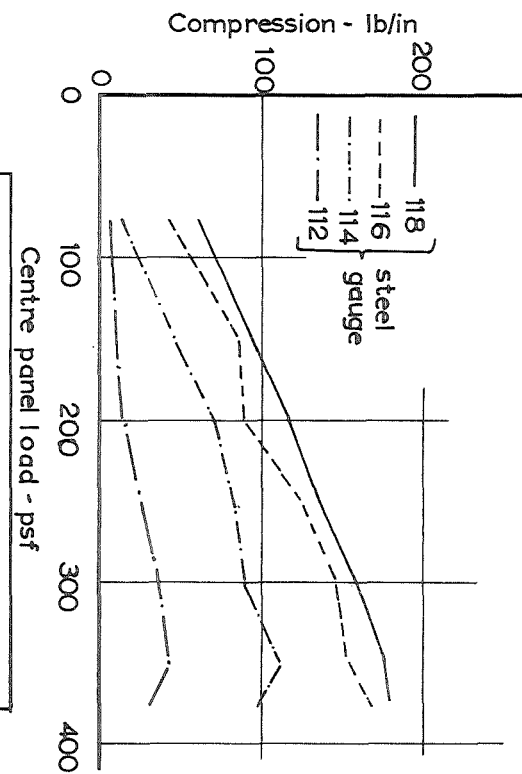


FIGURE 9.1 CENTRE PANEL EDGE  
COMPRESSION - TEST 110

centre panel.

Table 9.4. Deflections at LS220 (775 psf).

<u>Element Type</u>	<u>Reference Mark (Figure 6.2(a))</u>	<u>Maximum Deflection (inches)</u>	<u>Deflection: Span (ratio)</u>
Interior Beam	NS2	.143	438
Exterior Beam	NS4	.123	510
Corner Panel	A	.523	85
Centre-edge Panel	F	.649	68
Centre Panel	E	1.32	47
Interior Beam) East Span )	EW2	.430	104
Exterior Beam) East Span )	EW1	.135	330

### 9.2.5.3 Cracking

No fresh cracks appeared until a load of 500 psf was applied when a small number of cracks appeared in the beams. At 525 psf one further crack in the centre span of beam NS4 appeared.

The application of 550 psf (LS200, 200A, 200B) produced cracks in almost all elements with dramatic effect.

Further cracks appeared in the centre panel (Figure 9.5) and some centre-edge panels. Cracks appeared in all beam spans and first cracking of the undersurface of the corner panels occurred (Figure 9.7).

Again each new crack in any of the panels surrounding

the centre panel brought further cracking in the under-surface of the centre panel. The cracks in the corner panels were limited to one per panel running along the diagonal passing through the middle point of the centre panel giving the floor panel crack pattern an even more radial nature and further indicating the effect of compressive membrane action in the centre panel. The low reinforcement content of the panels meant that the cracking and ultimate loads of the corner panels were almost equal, and cracks formed rapidly and extended almost the whole distance from one corner to the other. In some cases the crack formation caused dull thuds.

Cracking in the beams at this stage was also significant. In the exterior beams cracks appeared over some interior supports and at the middle of some centre spans. In the end spans, cracks appeared very near the corner, (lower right of Figure 9.7) indicating the considerable bending moment induced by the twisting moment in the adjacent exterior beam at right angles. Similarly induced cracking took place in the end spans of interior beams (Figure 9.6 left middle; Figure 9.7). Cracks also appeared over the interior supports of these beams.

Although the crack widths in the panels and end spans of the beams shown in Figures 9.9, 9.10, 9.11 and 9.12 (taken at the end of the test programme) are very much greater than they were at failure of the centre panel,

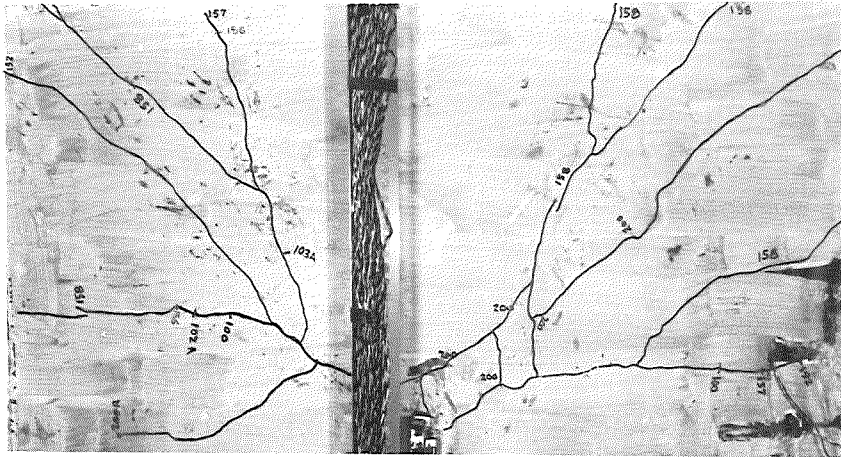


FIGURE 9.5 CENTRE PANEL

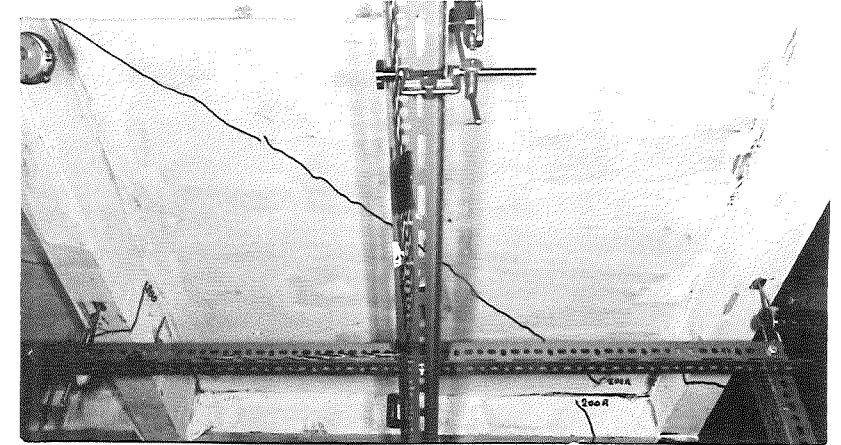
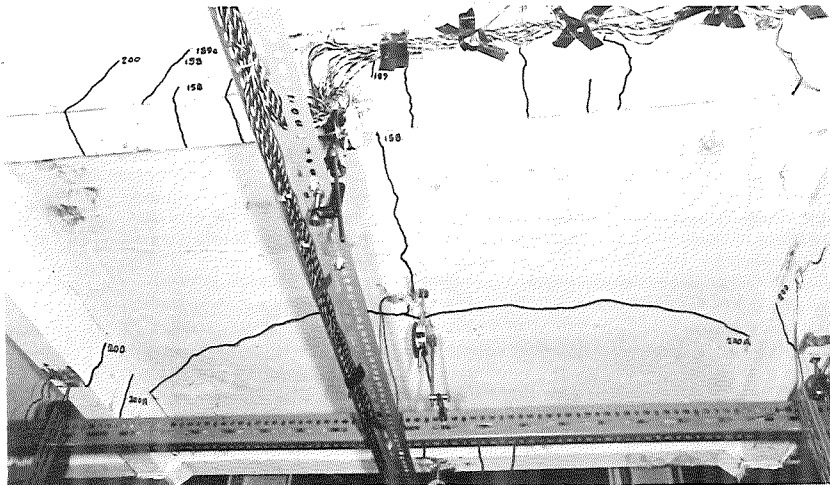


FIGURE 9.7 CORNER PANEL



the figures do show that much of the new cracking after LS200 (550 psf) was confined to the outer panels and end spans of beams (numbers lower than 228 indicate the extent of cracks formed before centre panel failure). The centre spans of interior beams showed few further cracks but the centre panel cracking extended considerably on the application of loads greater than 550 psf.

Load increase beyond 550 psf brought more cracks in the centre panel, radiating from the centre, extending further towards the edges of the panel as the tensile membrane region extended. These cracks became wider near the centre of the panel, becoming full depth before loading of the panel was stopped. The state of cracking in the centre panel after loading of it had been stopped may be seen in Figures 9.11 and 9.12. The zones of crushing on the top along the diagonals show the effects of the large "circumferential" compression. Full depth cracks extended further towards the edges of the panel in regions away from the diagonals.

#### 9.2.5.4 Moment, Strain, and Normal Force Levels at Maximum Load

The wide load range of this test caused great changes in the levels of the above quantities and only a brief description of the changes occurring is given here. A detailed description follows in later sections (9.3.2, 9.3.5, 9.3.6).

Table 9.5 shows the values of strains, moments and normal forces for LS220 (775 psf) affording comparison with Table 9.3.

Almost all steel strains tabulated are either past yield or very close to it and the values of these at mid-span and support of the centre spans of both interior and exterior beams are nearly equal indicating little post-yield moment redistribution. Formation of cracks in the end spans did not coincide with the steel gauge position and some erratic strain values resulted.

In the centre panel, the strain in the steel at the centre increased to beyond the limit of the data logger. Steel strains at the edge were well in excess of yield as was the case for most points along the edges that were continuous over the beam supporting them. Values of steel strain at the panel edges supported by the exterior beams were remarkably low, especially in the corner panels.

Values of beam moments compared favourably with design moments at the supports but were lower than design values at mid-span. Tensions at the supports of the centre spans of both interior and exterior beams were larger than those at mid-span. The average magnitude compared well with design values but exterior beams carried a greater portion of the total than was expected.

#### 9.2.5.5 Evidence of Membrane Action

The application of 550 psf at load stage 200 provided

Table 9.5. Strains, Moments, and Normal Forces at Load Stage 220.

		<u>Gauge</u> <u>Position</u>	<u>Gauge</u> <u>Numbers</u>	<u>Max.</u> <u>Conc.St.</u>	<u>Max.</u> <u>Steel</u> <u>Strain</u>	<u>Moment</u> <u>K" or</u>	<u>Force</u> <u>K or</u>
				$\mu S$	$\mu S$	lb"/"	lb/"
<u>Ext. Beam:</u>							
	C. Span	Support	133,134	-212	1256	30.2	10.6
	C. Span	Mid-span	53,55	19	1584	13.1	7.3
	E. Span	Mid-span	59,62	-11	1978	-3.4	1.7
<u>Int. Beam:</u>							
	C. Span	Support	126,129	-572	1447	-92.0	15.3
	C. Span	Mid-span	73,77	-209	1270	43.5	9.6
	E. Span	Mid-span	64,67	-*	-*	9.3	3.6
<u>Centre Panel:</u>							
	Centre	Bottom	6	-	*6979		
	Edge		114,115	-187	8158*	-352	-149
	Edge		118,119	-295	2428*	-509	-308
	9" from edge		20,22	48	-71	-113	-197
<u>Edge Panel H:</u>							
	Centre	Bottom	5	-	2306		
	Edge	Int. Long	94,95	-222	2136	-405	-195
	Edge	Ext. Long	97	-	193		
	Edge	Short	102	-	4137		
<u>Corner Panel:</u>							
	Edge	Int.	91	-	2723		
	Edge	Ext.	86	-	103		

All strains corrected for drift (gauge 81) and 100 psf initial load.

Steel strains corrected for temperature (gauge 140).

Moments and forces calculated from strains shown.

\* Values off scale or gauge broken.

clear evidence of the reliance of the centre panel on compressive membrane action. Later in the test, as failure of the centre panel approached, the level of beam tension and slab compression rose steadily but finally fell away rapidly with the push-through of the centre panel.

At LS200 cracking in the outer panels was radial in nature indicating the effect of membrane action in the centre panel. Again the effect of outer panel cracking was observed - the thuds produced by the cracking of the corner panels were coincident with sharp increases in centre panel deflection.

The three-quarters of an hour taken to settle at LS200 was a measure of the instability of the centre panel and a static situation prevailed only when all outer panels had ceased to crack.

Steeply inclined shear cracks in the interior beam centre span were indicative of the presence of considerable tension.

#### 9.2.5.6 Failure Mechanism

The centre panel "failed" with the progression of the tensile membrane region towards the slab edges and panel edge compression decreased with consequent loss of beam tension. Centre spans of interior beams accordingly stiffened. Towards the outside edges of the centre panel a wide region of slab at high ("circumferential") compression developed to support the tensile membrane area at the centre.



As the panel was pushed on into a more complete tensile membrane stage this region became narrower until crushing occurred.

The centre-edge panels at this stage were in a fairly advanced stage of forming a composite panel and beam mechanism as can be seen in Figures 9.10, 9.11, 9.12. (The predominance of the beam mechanism evident in this illustration developed as a result of later loading.) Corner panels had cracked across both diagonals and were forming a panel mechanism, but again, later loading brought about the predominance of the beam failure mechanism.

Beams showed little sign of distress at this point. Centre spans of interior beams became increasingly stiff with the reduction in tension carried and the cracks in their end spans, which were later to develop into wide cracks at plastic hinges, were still narrow (see Figure 9.10).

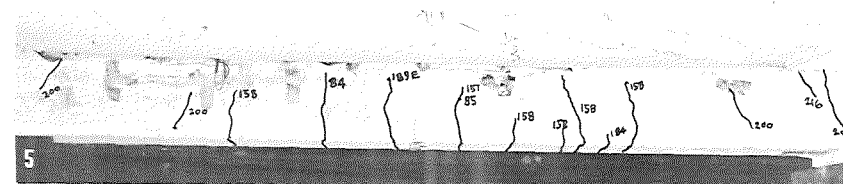
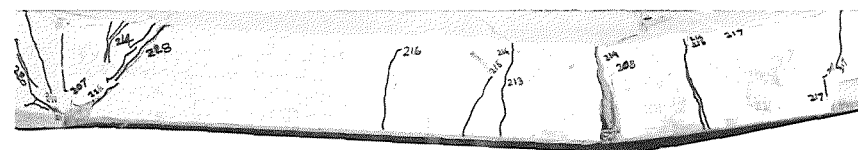
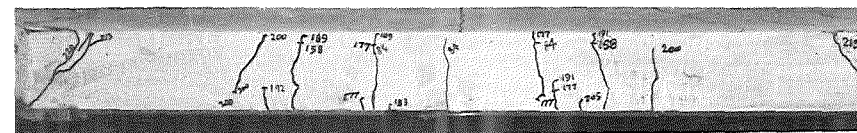
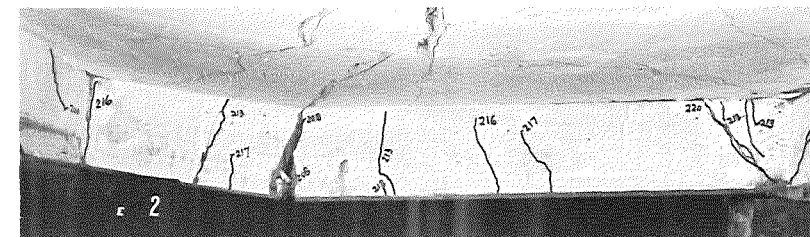
#### 9.2.6 Test to Failure of Outer Panels

In this test the centre panel load was kept constant at 600 psf while the outer panel load was increased until the centre-edge panels "failed" at 966 psf. Corner panel load was then increased with centre panel load still 600 psf and centre-edge panel load 950 psf. Failure of the corner panels occurred at 1170 psf.

Only a general description of the floor behaviour and failure modes is given. Many steel gauges had gone off the



Exterior beam EW1



Interior beam EW2

FIGURE 9.10 BEAMS AT END OF TEST

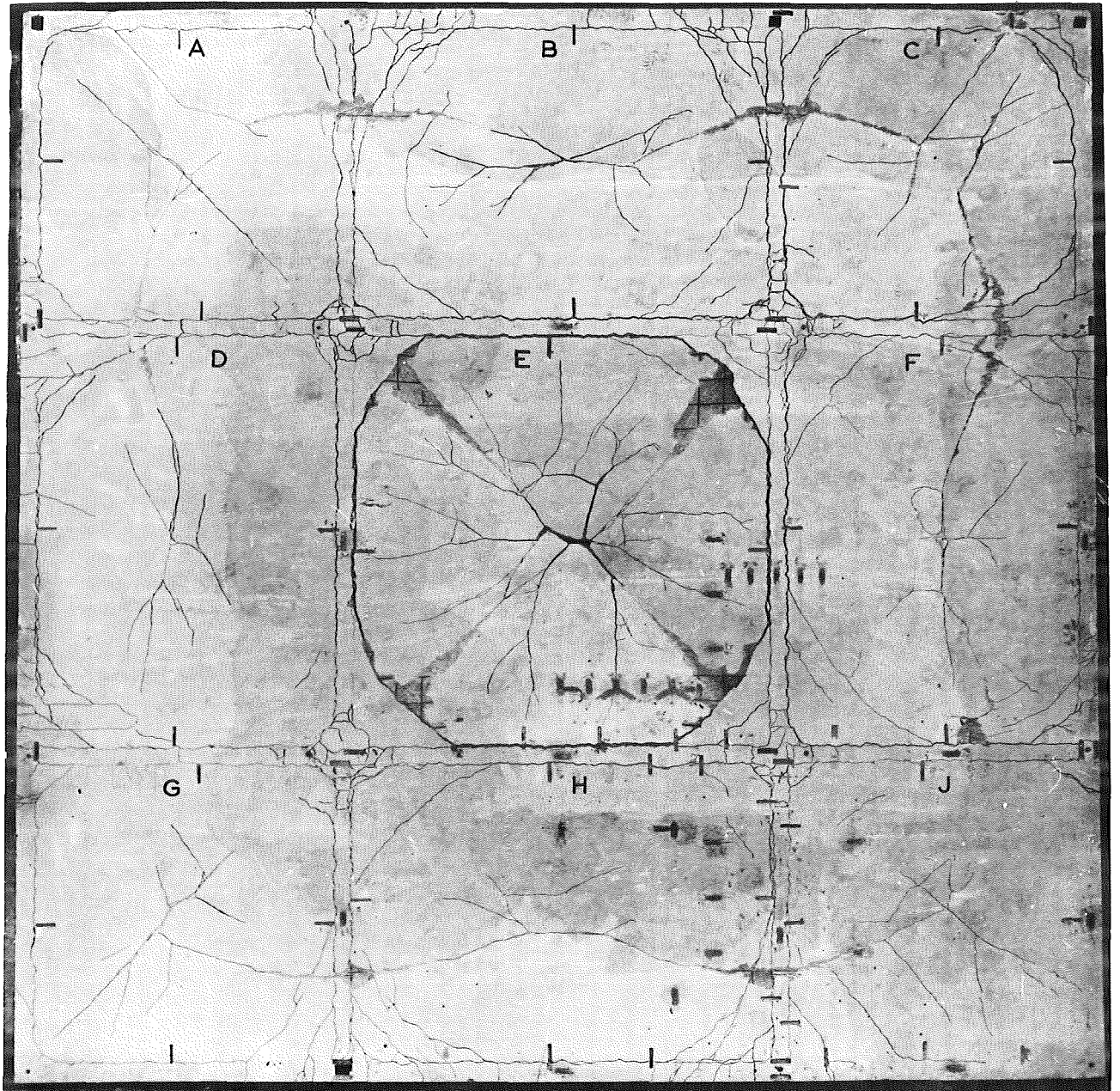


FIGURE 9.11 LOADED SURFACE AT END OF TEST

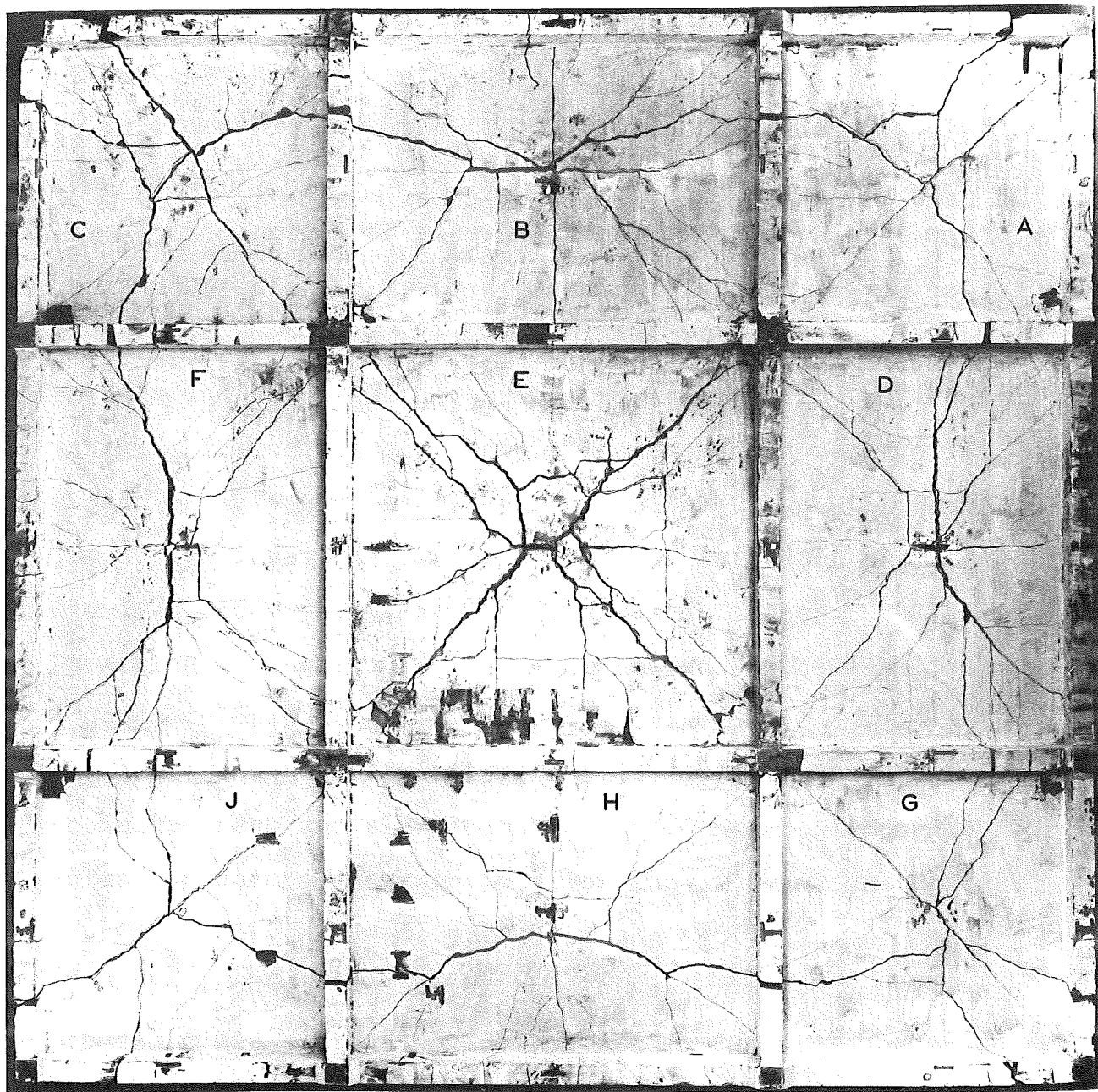


FIGURE 9.12 UNLOADED SURFACE AT END OF TEST

data logger scale and cracks had rendered many concrete gauges useless.

Figures 9.10, 9.11, and 9.12 show the final state of the floor.

The formation of plastic hinges in the positive moment regions of the end spans of the interior beams brought about a pronounced folding mechanism in the centre-edge panels and affected the corner panels similarly at a later stage. The centre edge panels showed no sudden drop in load capacity but at 966 psf on all outer panels, the rate of deflection under constant load was so great that the load on these panels was not increased further. Full depth cracking at the middle of the centre-edge panels had only just developed at this stage, the principal cause of the loss of load capacity being the full development of the combined beam and slab mechanism, evident when concrete crushing occurred at the interior supports and on the top surface above the wide cracks in the end spans.

The load on the corner panels was taken up until these panels could sustain no further load. Again, beam mechanisms were responsible for this inability to sustain further load. Concrete crushing at the supports of the interior beams continued and large rotation of plastic hinges in the end spans caused considerable twisting of the exterior beams and the development of the combined torsional and flexural hinges near the corners resulted (see Figures 9.10, 9.11

and 9.12).

The test was stopped at 1170 psf when the deformation rate was excessive.

An interesting feature of this test was the lack of development of yield moments along the slab edges supported by the exterior beams.

The following steel strains indicate the degree to which yield moments were developed along these edges. Readings were taken at LS239.

<u>Position</u>	<u>Gauge No.</u>	<u>Microstrain</u>
<u>Corner panel:</u>		
Interior edge	83	1870
	91	4440
	84	2130
	90	2000
	85	2300
Exterior edge	86	240
	88	2200
	87	220
	89	970
<u>Centre edge panels:</u>		
Interior edge (short)	98	2970
	99	3100
	100	2040
	102	8000+
Exterior edge	96	1860
	97	2220

At the end of the test the principal crack in each centre-edge panel was that along an arc between cracks in

the end spans of the interior beams supporting the panel (see Figure 9.12). This crack was full depth for the middle 24" but T-beam flange effects caused closure at the top of this crack in the region of the beams (see Figure 9.11).

Cracks along the exterior edges of the corner panels were measured at .002" at the end of the test programme.

Development of flexural hinges in the end spans of interior beams allowed large torsional rotation of the exterior beams and torsional resistance was provided only by the end spans of the exterior beams. Each such span showed the effect of this with the development of a torsional and flexural hinge, to a greater degree in some beams than others. Figure 9.10 shows the most fully developed of these at the end of the test programme.

### 9.3 EXAMINATION OF ASPECTS OF FLOOR BEHAVIOUR DURING TESTING

#### 9.3.1 Deflections

Figures 9.13 and 9.14 show load-deflection plots for the full range of load applied over the whole top surface. Each curve is typical of its group and the values plotted include residual deflections. The difference between NS and EW exterior beams is apparent when the curves for the east and south exterior beams are compared.

The curves for the centre, corner, and centre-edge panels all show the effects of cracking at 550 psf but at



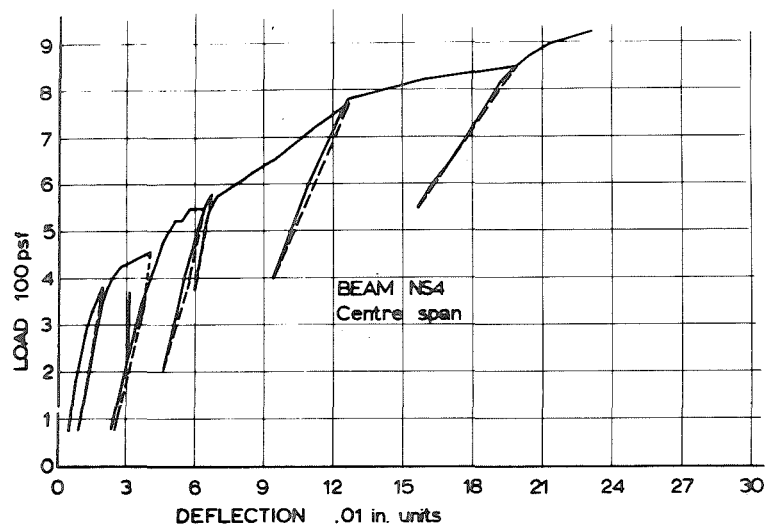
450 psf, only the centre-edge and centre panel deflections show a marked increase.

Loss of stiffness of all panels after 550 psf is clearly seen and the similarity of shape of the corner and centre-edge curves after this stage show the effects of supporting beam deflection. The centre panel load-deflection curve indicates the push-through failure that occurred at a deflection of nearly 2". Because 850 psf was not fully attained the path of the load-deflection curve for the centre panel was not accurately determined. The load-deflection plot for the tensile membrane stage is close to a straight line through the origin.

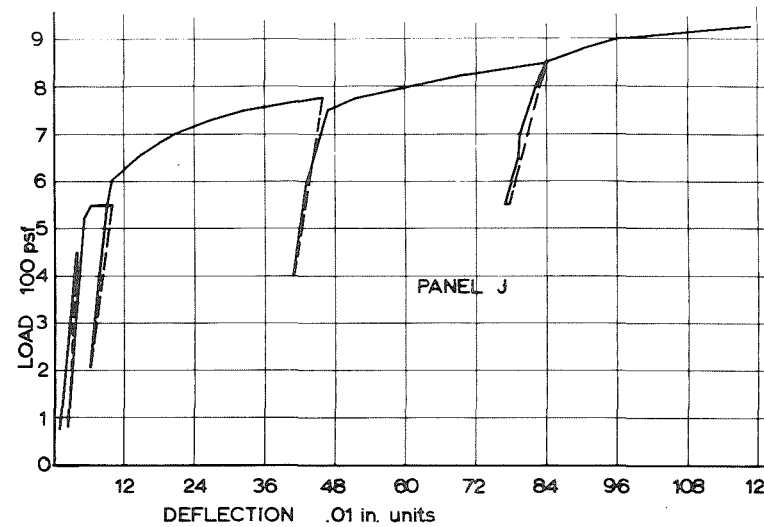
The curious shape of the curves for the centre spans of interior and exterior beams is due to the effect of tension in these spans. The loss of tension in the beams towards the end of the test is evident in the steepening of these curves, especially in the interior beams in which deflection decreased with increase in load near the end of the test. However, this was due in part to the formation of plastic hinges in the end spans of these beams.

The varying scale used in Figures 9.13 and 9.14 makes comparison of stiffnesses difficult. Figures 9.15 and 9.16 show load-deflection plots for Tests 106 and 110 in which deflection at the start of Test 110 has been set equal to that at the end of Test 106 and the constant horizontal scale makes direct comparison of relative stiffnesses

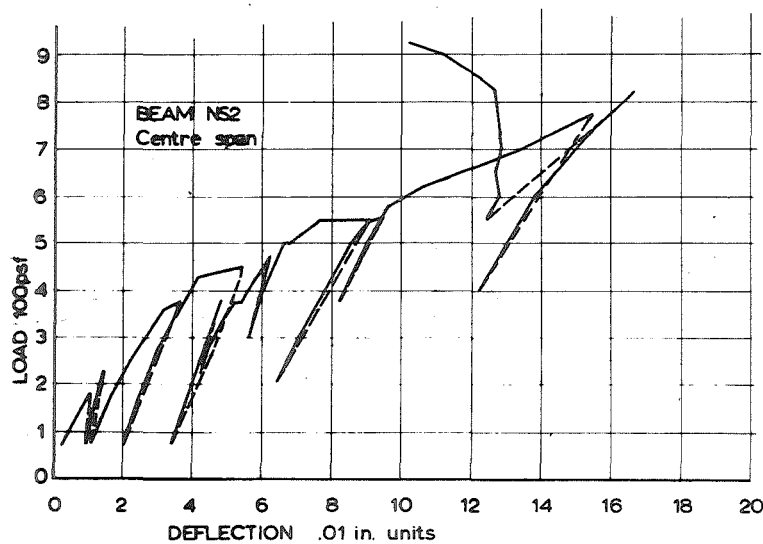




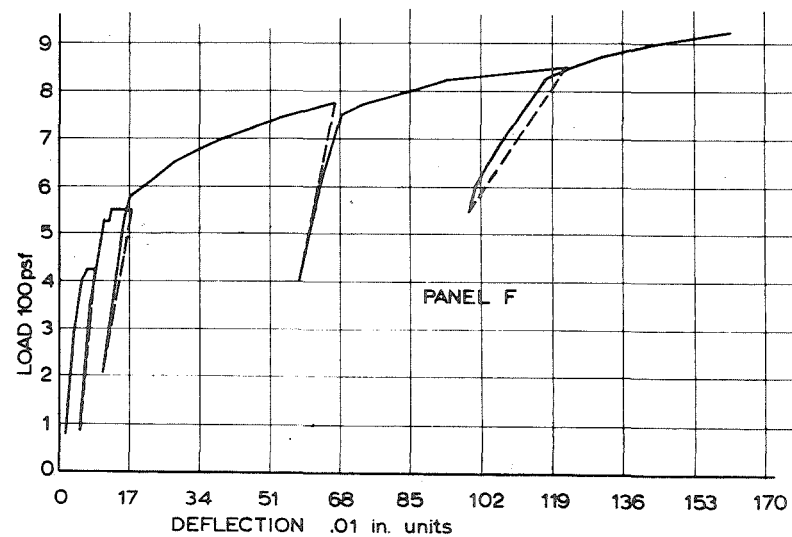
(a)



(b)

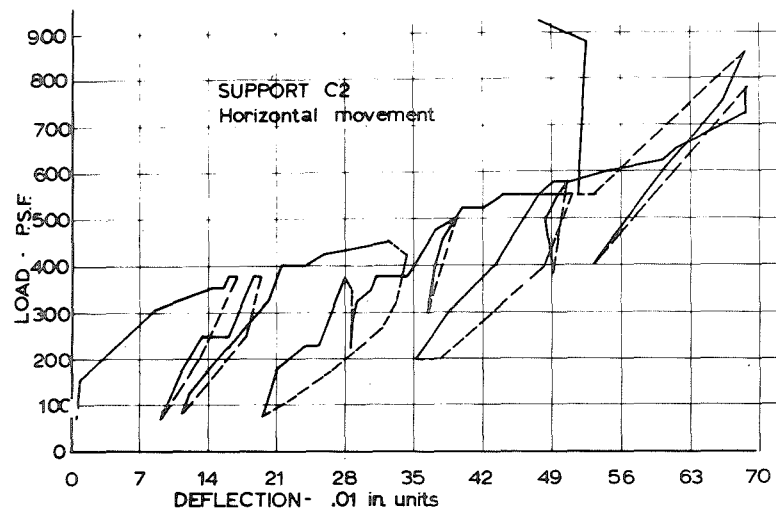


(c)

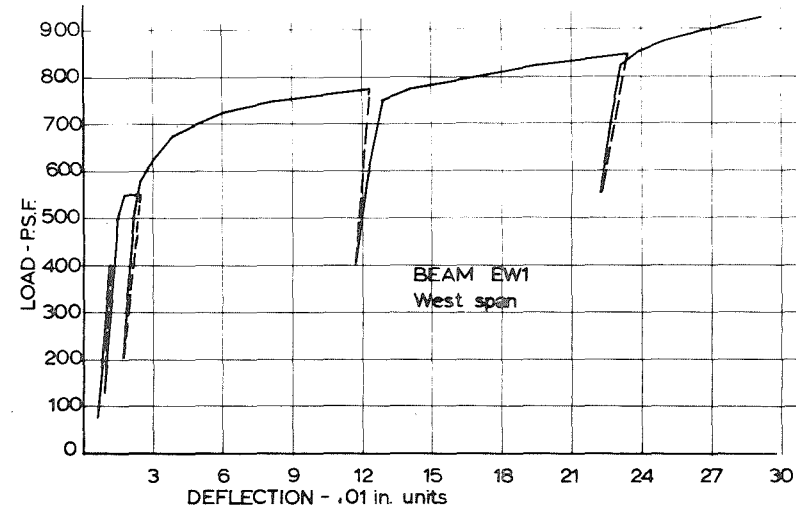


(d)

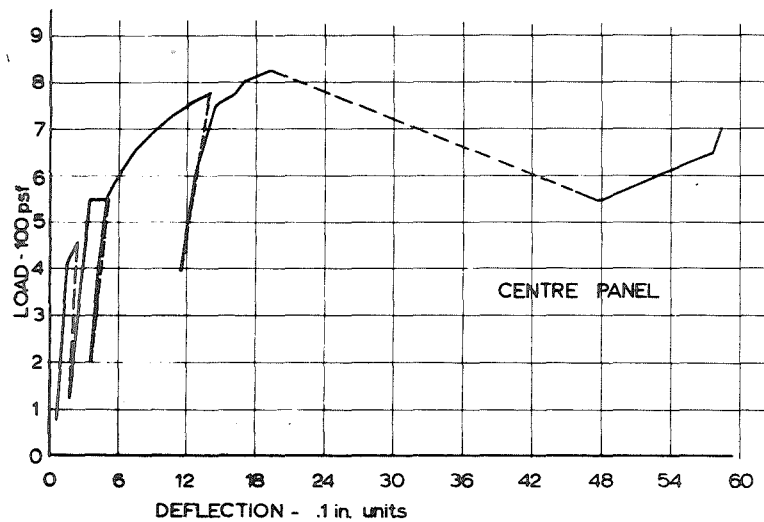
FIGURE 9.13



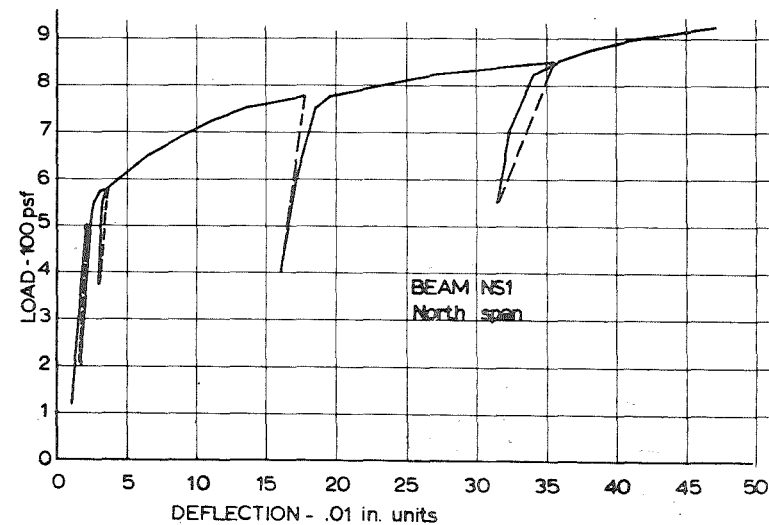
(a)



(b)



(c)



(d)

FIGURE 9.14

possible.

Table 9.6 gives the deflection readings for all gauge points. In some cases, pattern loading caused upward deflections (negative values) and the sharp increases in deflection at LS158 and LS200 are noticeable, especially in panels and centre spans of beams.

It is of interest to compare the deflections in the table with ACI code requirements for deflections. ACI-318-63 Clause 209 specifies  $1/360$  of the span as the maximum allowable for floors carrying plaster ceilings,  $1/180$  of the clear span otherwise. The most stringent requirement for long term loading is the allowance of an additional deflection of twice the short-term deflection.

The first values which exceed the  $L/360$  requirement are marked with an asterisk in Table 9.6. When the first values of deflections at design service load are factored by 3.0 to allow for long term deflections, the centre panel just exceeds the  $L/360$  requirement.

However, the dependence of the centre panel on compressive membrane action makes the assessment of long term deflections a special case in which the deflection is unusually sensitive to outward creep of surrounding elements which provide the necessary lateral restraint. At service load, however, the magnitude of the membrane forces may not be high and it is reasonable to conclude that the deflections of the floor at service load would not be

TABLE 9.6 DEFLECTIONS AT SELECTED LOAD STAGES FOR ALL GAUGE POINTS (.0001 INCH UNITS)

LOAD STAGE	32	57	7A	85	104	123A	142	142C	155	158	177	189	194	213	217	220	226
MAX LOAD	225	225	225	375	375	400	375	375	375	450	375	375	500	600	700	775	825
PATTERN	2	3	1	1	5	2	3	3	1	1	5	1	1	1	1	1	1
GAUGE NO.																	
1	39	-16	23	64	25	107	25	15	64	85	46	73	99	234	512	900	1435*
2	48	-19	25	57	7	97	20	0	68	81	43	85	110	268	450	1000	1560*
3	37	-8	28	58	18	107	21	9	59	77	52	69	90	134	212	527	877
4	41	-6	33	76	15	116	26	8	71	90	57	86	109	345	623	1346*	2136
5	42	-12	30	69	20	110	25	10	51	80	56	80	98	212	410	1160	1900*
6	41	-9	24	55	21	101	21	6	53	71	56	72	91	141	436	591	881
7	42	-18	30	79	30	102	36	25	77	98	65	90	110	195	425	950	1630*
8	34	-17	29	59	2	94	-6	-21	39	49	22	46	70	129	391	559	1029
9	29	21	40	136	61	101	112	111	124	175	123	155	213	362	719	1591*	2397
10	27	28	53	144	47	104	119	115	143	190	130	176	231	475	1188	2302*	2943
11	17	21	39	118	37	87	103	97	106	147	103	147	191	492	1642*	4307	6447
12	20	21	40	121	55	93	111	108	116	161	150	221	256	478	801	1811*	2731
13	22	26	41	111	43	90	99	93	71	68	54	131	163	391	881	1701*	2661
14	24	24	45	120	32	84	95	93	115	155	106	152	198	495	944	1795*	2645
15	25	25	43	122	37	87	101	95	122	154	106	151	194	379	757	1462*	2232
16	11	21	32	111	31	86	87	80	103	141	93	141	191	318	691	1571*	2461
17	32	40	75	262	230	220	250	240	310	550	470	510	650	963	1234	1342	1452
18	40	45	85	285	266	273	285	257	315	409	465	445	555	861	1135	1186	1245
19	25	30	60	261	227	210	240	231	290	540	445	490	612	902	1090	1147	1220
20	40	35	80	253	210	205	225	225	274	435	365	405	555	901	1235	1425	1555
21	-35	70	40	110	15	-37	141	162	121	320	240	300	371	491	580	562	425
22	-30	73	50	140	30	-18	170	200	165	340	260	345	435	738	1007	1228	1540
23	-33	65	40	110	34	-22	164	223	184	367	293	176	464	587	685	590	440
24	-21	84	61	154	39	-1	189	218	179	399	309	384	479	761	969	1139	1204
25	100	-5	85	205	40	250	115	85	215	305	197	293	400	886	1975*	4500	6880
26	100	-5	90	210	48	268	120	89	210	291	193	296	400	1230	2405*	4342	8130
27	100	5	82	185	42	239	101	75	190	282	195	282	383	1242*	2770	5230	7650
28	92	-1	79	184	31	229	94	69	189	279	179	269	372	785	2074*	4279	6579
29	20	122	122	365	105	90	400	417	430	732	535	700	920	2050*	3855	6490	9230
30	-10	133	122	335	121	96	402	415	330	672	440	648	840	1924*	3390	6330	8882
31	5	145	138	345	97	75	367	390	385	727	546	705	924	1802*	3385	5428	7537
32	75	135	135	403	114	95	378	385	391	725	543	694	907	1287*	3054	5655	7775
33	211	-6	214	616	871	921	596	524	976	2166*	2137	2139	2746	5586	8931	13167	18739

\* First value in excess of L/360  
L/360 = 1240 units for short spans  
L/360 = 1730 units for long spans.

FIGURE 9.15 DEFLECTIONS — TESTS 106, 110

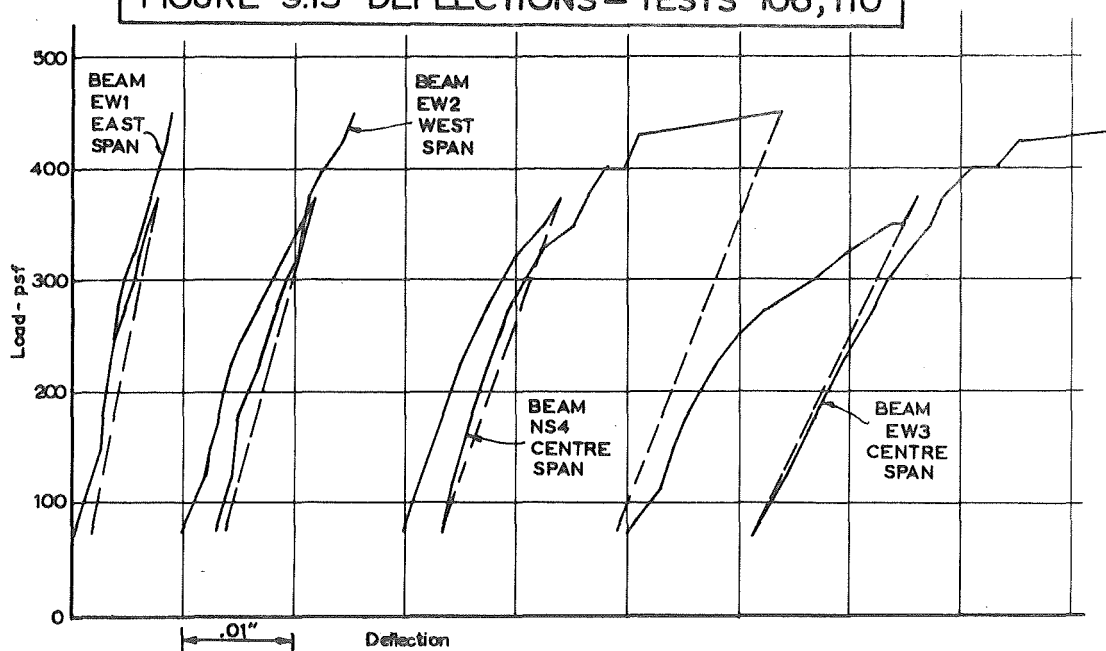
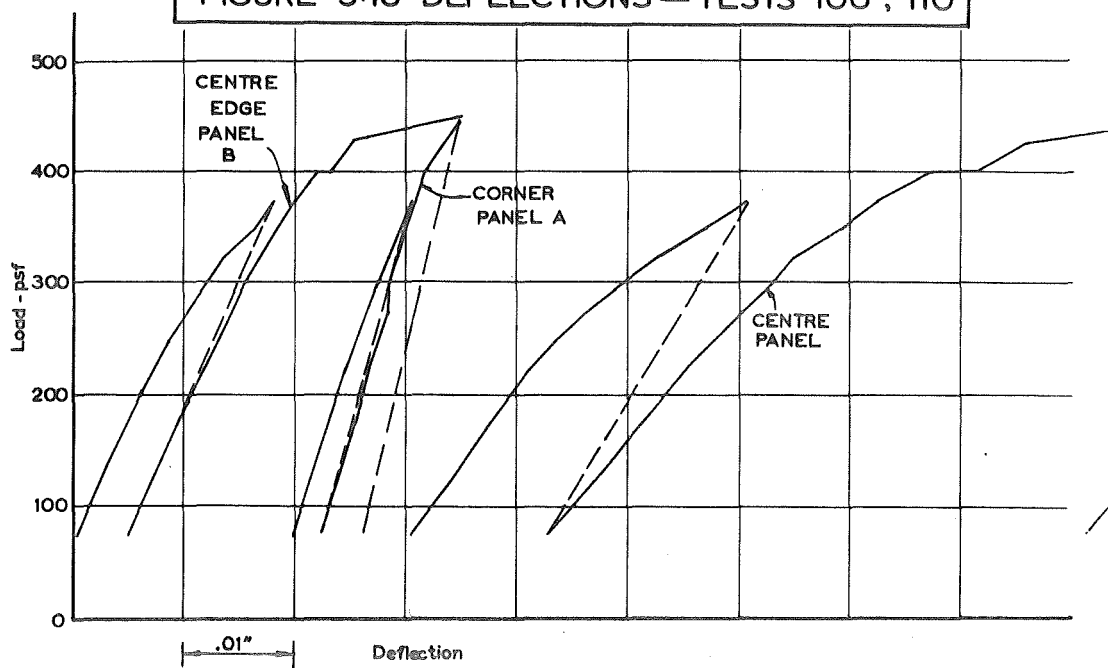


FIGURE 9.16 DEFLECTIONS — TESTS 106, 110



excessive in the long term.

### 9.3.2 Strains

#### 9.3.2.1 General

Readings in microstrain at selected gauge positions are presented in Table 9.7. Load-strain curves for the latter part of the test programme appear in Figures 9.17 to 9.21. Appendix C contains readings for all channels at all load stages.

#### 9.3.2.2 Strain Levels

Table 9.7 shows the generally low level of strain at 375 psf applied at LS85, no underside panel cracking having taken place at this stage, but the shrinkage cracks present before testing commenced, show up in the higher strain values at the panel edge sections. Cracking of the underside of the centre panel at LS100 (as the outer panel load was reduced) brought a sharp increase in strain in the centre panel bottom steel (e.g. gauge 6) with little effect on the strains at the edge of the panel.

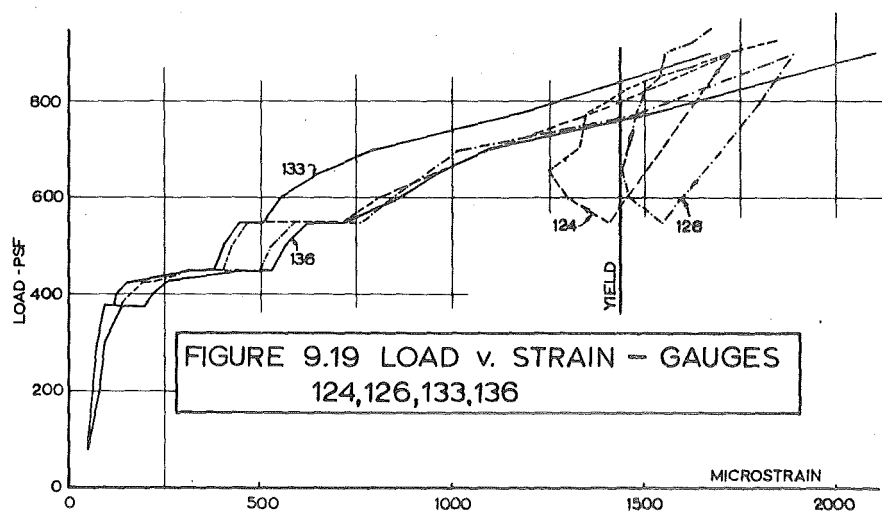
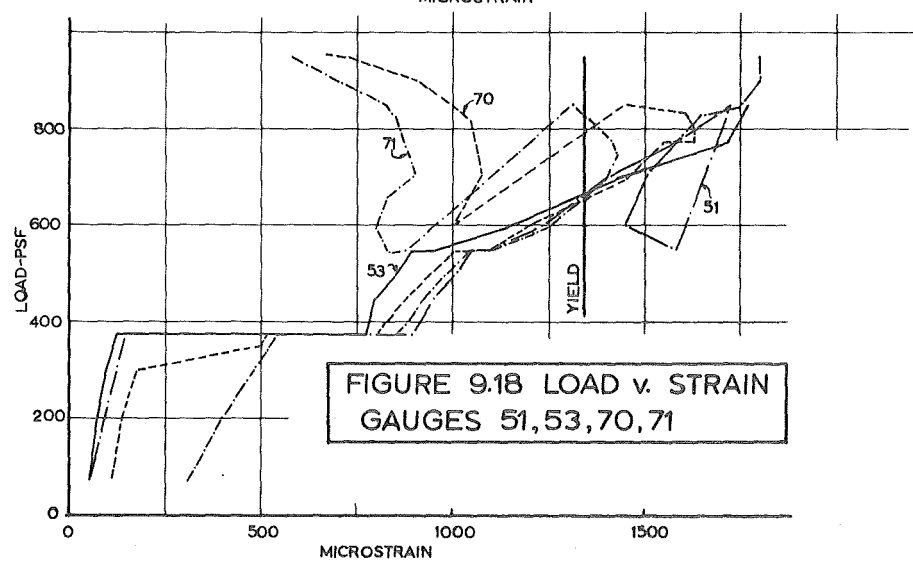
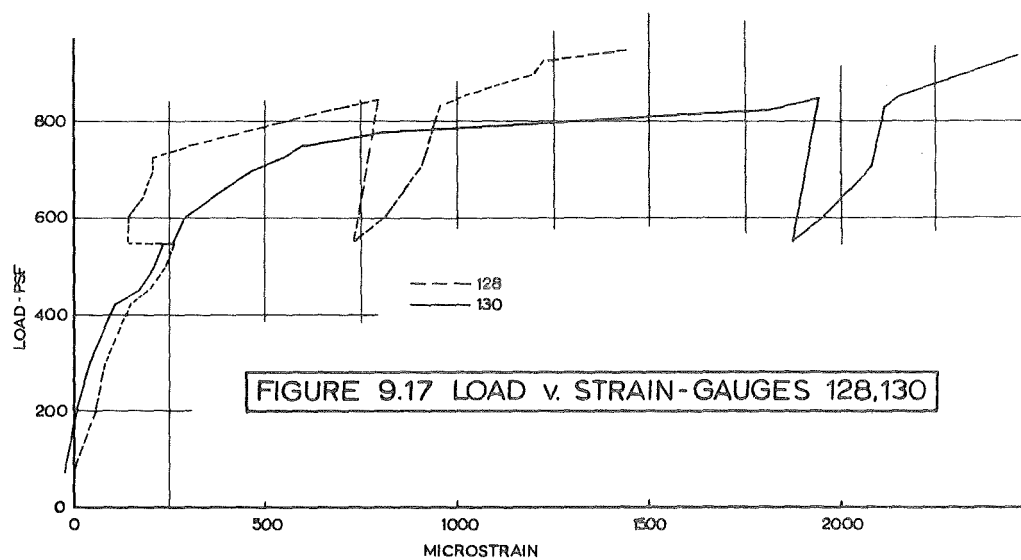
Strain values were still comparatively low at LS155, gauge 5 recording the highest level at less than half the yield strain. The effect on the strain levels of the application of 450 psf is seen most clearly in Figures 9.18 to 9.21 inclusive. Centre-edge and centre panel strains showed a particularly large rise with the occurrence of underside cracking in these panels, yield being reached in

TABLE 9.7 STRAINS 4T SELECTED POINTS

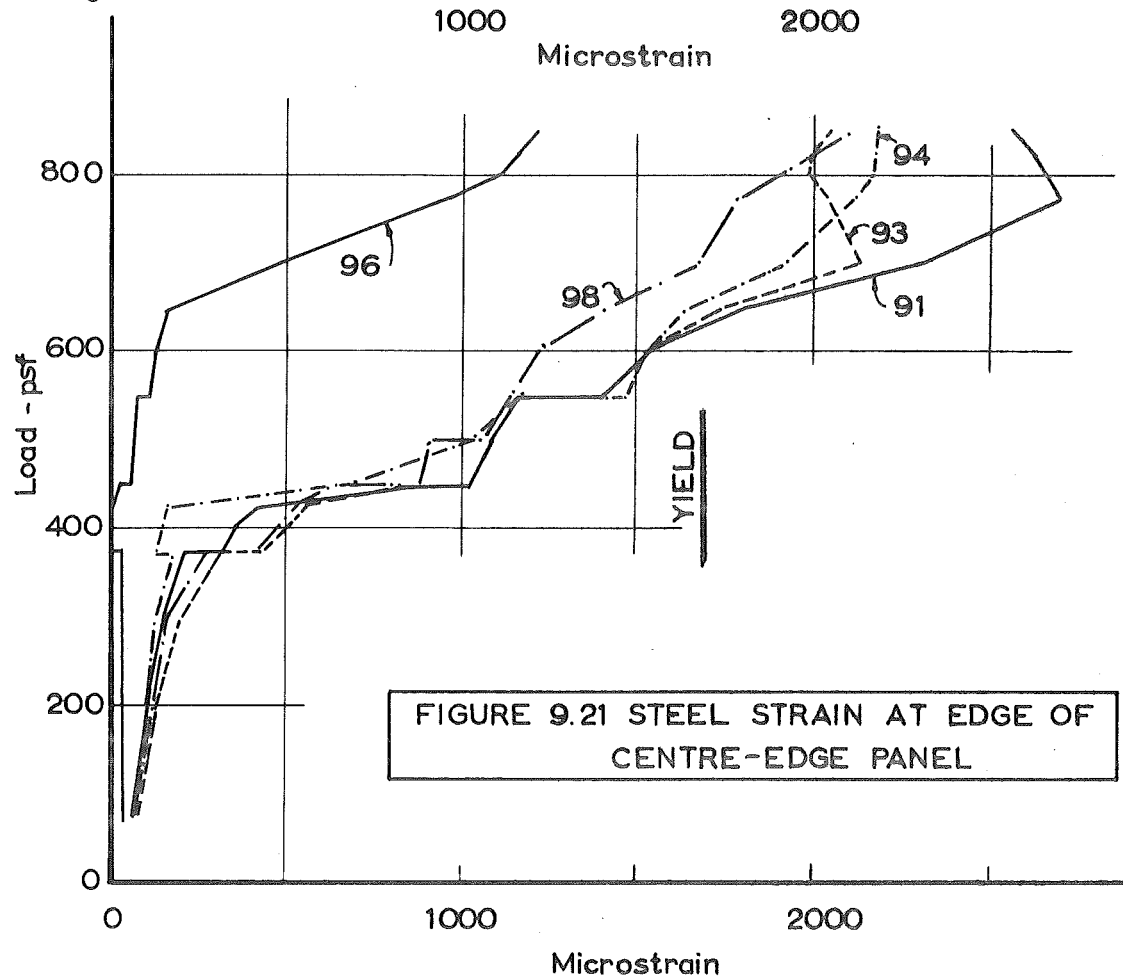
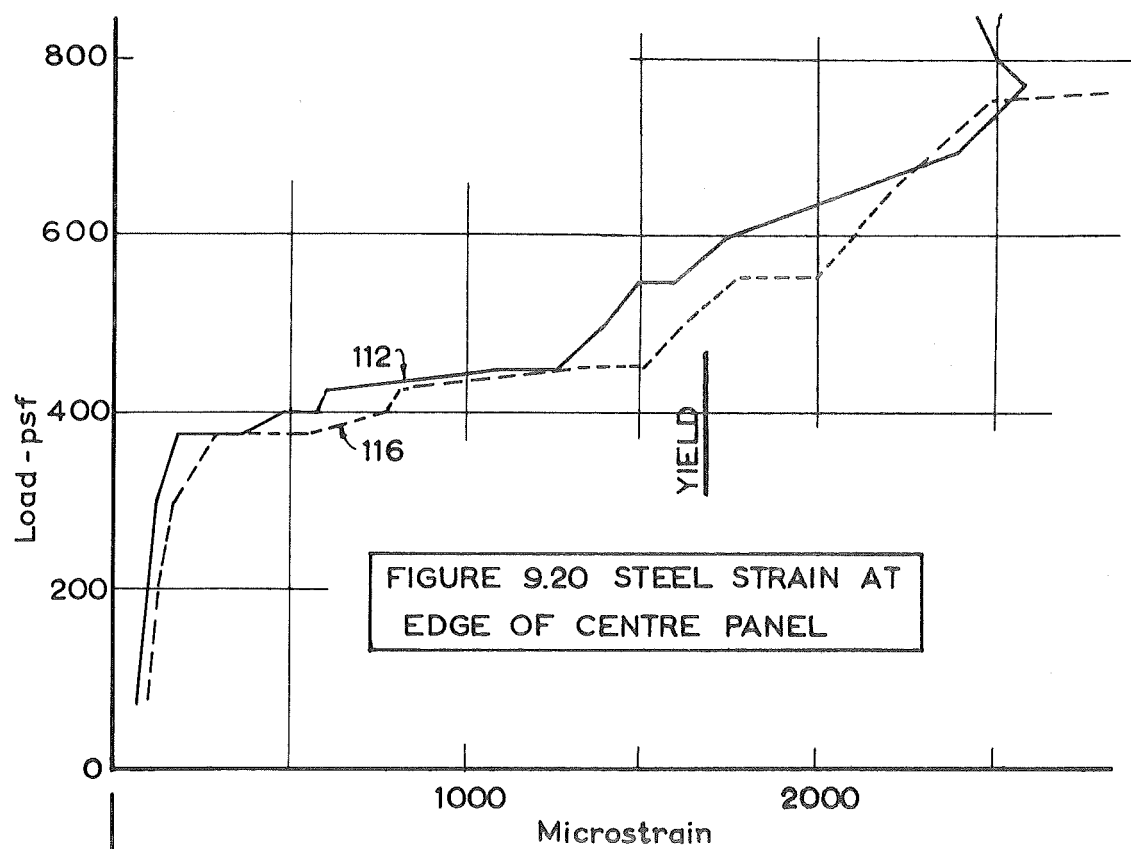
GAUGE No.	YIELD STRAIN	LSN LOAD	32 225/2	57 225/3	7A 225/1	85 375/1	104 375/5	123A 400/2	142B 375/3	155 375/1	158 450/1	175 350/5	189 375/1	193 475/1	200 550/1	213 600/1	218 725/1	220 775/1	226 825/1
57	1340		49	-9	23	45	-5	84	-19	33	47	7	38	77	83	134	1566	2135	2159
52	1340		11	95	71	112	18	-27	117	107	548	478	529	641	996	1145	1362	1478	1685
63	1340		73	65	83	125	26	97	97	132	161	96	136	193	985	1636	2098	4713	6629
73	1340		125	101	160	323	299	279	265	331	596	497	549	680	794	982	1271	1270	1297
124	1430		44	49	63	111	87	110	135	168	373	330	377	443	496	804	1206	1358	1630
136	1430		43	54	65	135	87	104	175	216	439	379	452	543	618	846	1206	1462	1916
96	1690		-6	9	-3	9	-39	-64	-52	-54	-35	-83	-71	-27	-27	20	599	840	1046
98	1690		55	88	97	260	126	165	306	390	633	542	659	813	890	1133	1786	1922	2000
88	1690		13	6	7	18	-12	2	-17	-6	2	-35	-19	13	11	21	35	91	128
91	1690		89	83	118	233	128	216	242	383	870	779	919	1079	1196	1513	2623	2723	2655
111	1690		113	85	139	221	246	278	237	361	1272	1063	1223	1528	1764	1921	1945	1976	1600
6	1690		68	29	56	177	625	683	494	671	1650	1540	1638	1909	2264	-	-	-	-

All values corrected for temperature and drift.

Refer to figures 7.2 and 7.3 for gauge positions.







the bottom steel at the middle of the centre panel.

Levels of strain continued to rise with load but not always at the expected rate, a feature particularly noticeable at the edges of the centre panel. The slower increase at the edges of the panels (see Figure 9.20) coupled with the steady increase in beam steel strain indicate quite clearly the effect of membrane action.

A slow rate of steel strain development in the edges of the centre-edge and corner panels was also evident. In the centre-edge panel, steel strain development along the short edges lagged that along the interior long edge but yield was reached before 775 psf was applied to the whole floor. At this stage, however, gauge 96, on the exterior long edge showed only  $990 \mu\text{S}$  and it was only during the test to failure of this panel that the steel along this edge yielded.

Along the outer edges of the corner panels steel strains were small throughout and even in the later test to failure of these panels these strains never became large.

The reason for this low value of strain at the edges was clearly a result of the smaller edge restraint afforded by the edge beams, retarding the development of moment. Although the edge beams were sufficiently strong to carry the torsion induced by the full yield moment, the rotation required to achieve this was too great and compressive

membrane action developed in the panels to compensate for the slow development of the full yield value. In the corner panels the beam mechanism formed completely before the panel mechanism was fully developed and so the yield value was never reached at the edge.

Figure 9.19 shows the strains at the supports of the centre spans of both interior and exterior beams while Figure 9.18 shows the steel strains at mid-span of both beams. The similarity between exterior and interior beams is good, and after cracking, the separate curves of load versus strain have nearly identical shape for both mid-span and support.

Beam steel strains at 775 psf are seen to be in the vicinity of yield. This has two important implications. The closeness of both mid-span and support values to yield indicates that little moment redistribution was required and secondly, the fact that yield of this steel was accomplished is indicative of large beam tensions of the order expected.

Steel strains in the interior beams show a tendency to reduce with increasing load beyond about 750 psf, a clear indication that the maximum tension had been reached and was reducing. This effect was more marked at mid-span than at the support where steel was required to take the moment due to the load on the end spans.

Generally the concrete strains were of little value as

a means of determining the maximum strains in the concrete. This was particularly noticeable for the panel edge sections where the region of high concrete strain was confined to about one eighth of an inch width at the beam-slab junction. The gauge was not therefore in the correct position to measure the maximum strain. Even if the gauges had been correctly positioned the small area over which high strains took place would have led to reduced readings since the gauge reading would be an average over the 1 inch gauge length. These factors did not render the readings useless for the purposes of computing membrane forces as is discussed in Section 7.3.4.

Beam concrete strains were less sensitive to this effect and Figure 9.17 shows the strains as measured by gauges 130 and 128 followed through increasing load. The curve for gauge 130 has a continuous form and the two curves are almost identical up to 550 psf, the small increase at 450 psf showing up in both curves. At 550 psf when the corner panel cracked on the underside for the first time and the centre-edge panels cracked further, the curves part, the strain in gauge 128 dropping significantly in magnitude. This drop, with the slower increase that followed it give a clear indication of the presence of tension in the beams.

### 9.3.3 Cracking

#### 9.3.3.1 General

Development of crack patterns in the elements of the

floor during testing has been described fully in the preceding sections on test by test behaviour of the floor (see Sections 9.2.4.3, 9.2.5.3, 9.2.6). This section is devoted to the examination of the serviceability of the floor at design service load with respect to crack widths.

#### 9.3.3.2 Crack Width Serviceability

Only at Load Stage 161 were widths measured in detail. These are shown in Figure 9.3 (p. 185). Although the measurements were taken at an applied load of 375 psf (DL + LL), the maximum load sustained up to that stage was 450 psf. This overload had little effect on the beams and centre-edge panels, but the cracking in the centre panel that took place at 450 psf was considerable and crack widths were substantially larger than the first DL + LL values.

The values shown in Figure 9.3 are maximum values and as such may not be compared directly with the quoted limits of ACI 318-63 Clause 1508 which gives .015" as the maximum mean crack width for interior members, .010" for exterior members.

In this comparison, the effect of scale and of the relation between maximum mean crack widths and maximum crack widths was accounted for by adjusting the code values. Average crack widths are generally taken as two-thirds of the maximum values and the ACI code values were therefore increased by 50 per cent for comparison with maximum

prototype crack widths.

Allowance for scale was made in two ways: (i) on the assumption that crack width varies as the square root of the scale factor and (ii) on the assumption that crack width varies directly with the scale factor.

The maximum allowable model crack widths resulting from the above adjustments are summarised in Table 9.8.

Table 9.8. Maximum Allowable Crack Widths For the  $\frac{1}{4}$  Scale Model Floor.

<u>Exposure Condition</u>	<u>Maximum Allowable Crack Widths (inches)</u>						<u>Max. Observed Crack Width Figure 9.3</u>
	1	2	3	3A	4	4A	
Interior	.015	.022	.005	.013	.011	.028	.015
Exterior	.010	.015	.004	.010	.007	.018	.015

The numbers 1-4 in the table refer to the difference adjustments, as follows:

1. Normal ACI 318-63 Code values for maximum allowable mean crack width.
2. Values in 1. increased by 50 per cent for comparison with absolute maximum crack widths on prototype.
3. Values of 2. adjusted for scale variation directly proportional to the scale factor.
4. Values of 2. adjusted for scale variation proportional to the square root of the scale.

Columns 3A and 4A require further explanation. The crack widths in Figure 9.3 were measured at the design service load but only after the overload to 450 psf had produced a marked effect on the centre panel cracking. Values of columns 3 and 4 were factored by the ratio of steel strain in the bottom steel of the centre panel for design service load, before and after the application of overload. This was found to be approximately 1:2.5. Since crack width is proportional to steel stress, the relationship between the values of columns 3A or 4A and those of Figure 9.3 may be assumed to be the same as the relationship between centre panel crack widths before overload, and the actual maximum allowable crack widths for the model.

Comparison of values of Table 9.8 with those of Figure 9.3 reveals that for an assumed variation proportional to the square root of the scale factor, all beams and outer panels satisfy the more stringent limit of .007". Centre panel crack widths do not satisfy either exposure condition but when adjustment is made according to the ratio of steel stresses, all centre panel crack widths are seen to be less than the more stringent exterior exposure condition for maximum allowable crack widths.

It was concluded that if crack widths were assumed to vary as the square root of the scale factor, the serviceability of the model floor with respect to crack widths was

more than adequate for loads not in excess of the design service load. Two qualifications must accompany this conclusion, viz:

(i) Exposure to exterior conditions would result in marginal serviceability if crack widths varied directly as the scale factor.

(ii) The dependence of the centre panel on compressive membrane action to improve its load carrying capacity and serviceability.

#### 9.3.4 Reactions

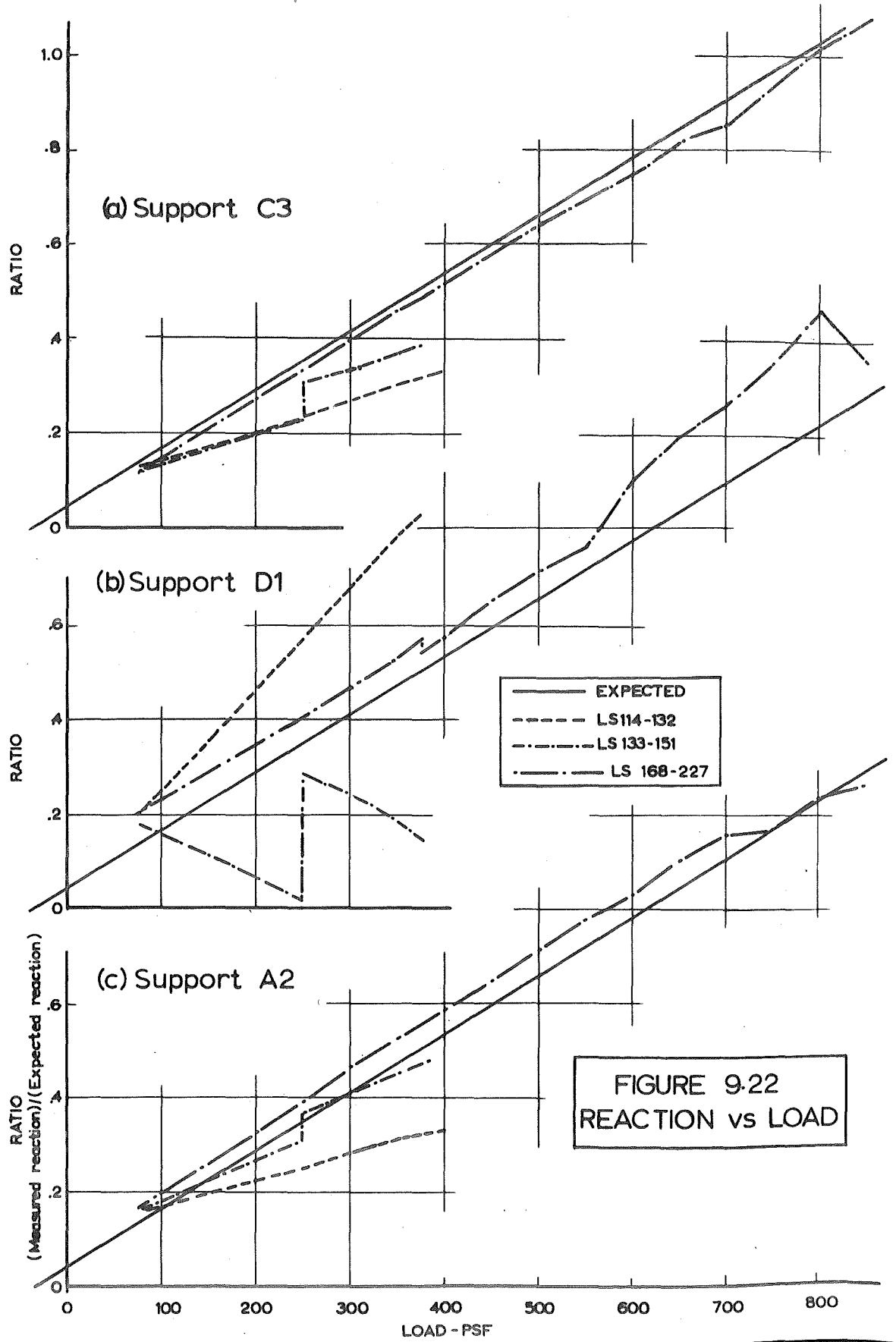
##### 9.3.4.1 General

Measured reactions came close to expected values throughout most of the test programme. The prime use for these was in the calculation of moments across full width sections of the floor (see next section). In this section, the variation of reaction with load is discussed briefly and a comparison with expected values is made.

##### 9.3.4.2 Variation of Reaction with Applied Load

Figure 9.22 shows plots of reaction value against load for support points C3, A2, and D1 respectively. The scale for reaction value was chosen to make direct comparison of the three figures possible. The reaction ratio plotted is the value of the reaction measured, divided by the expected value of reaction at the point for a load of 775 psf applied over the effective loaded area of the floor surface. The true origin for the graph is at -33 psf (= dead weight/





effective loaded area) and the straight line joining the origin with the point (775, 1.0) provides a useful reference.

For equal load on all panels, the corner support reaction,  $D_1$ , was uniformly higher than expected up to 550 psf, thus when the initial discrepancy was allowed for, the variation with load almost exactly corresponded to that of the expected reference line. After 550 psf the rate of increase of this reaction became greater at the expense of the other reactions. The degree to which this affected the other reaction was exaggerated by the scaling effect used to plot the reaction variation.

A detailed study of the variation of the reactions provided no reliable information as to the distribution of loading along the beams.

#### 9.3.4.3 Method of Calculation of Line Moments from Reactions and Applied Loads

The moments,  $M_1 \dots M_{10}$ , about lines 1....10 of Figure 7.5 (p.130) were calculated using the measured values of reactions and the known values of the loading pressures on the panels. Nominal values of applied load could not be used because the sum of all 16 reactions was always less than the sum of the products (nominal applied load x corresponding total available area), indicating that the bags did not exert pressure over the full area, rather 92-96 per cent of it. It was most likely that the unloaded area was in the region of the beams (at the edges of the

bags) but in calculating the line moments, load was assumed to act over the full area with reduced intensity. Calculation of the line moments was therefore both accurate and straightforward.

### 9.3.5 Moments

#### 9.3.5.1 General

Two sources were available for the determination of moments in the slab. Strain readings were used (see Section 7.3.4.3) to compute the moment and normal force at sections of the slab and beams. The other source was the reaction values and applied load, which provided a means of determining the moment along a full width section of the floor.

Moment computation from the strain readings gave the values at particular sections whereas those computed from the reactions afforded only the total moment along the section line. The results of the latter method were inherently more accurate than those of the former. Comparisons between the two methods were made by summing the section moments across the floor and plotting the load-moment curves for both methods.

#### 9.3.5.2 Basis of Calculation of Line Moments from the Sum of Section Moments

Consider the element of floor cut out by lines 2 and 3 of Figure 7.5. Each line cuts through four beams and exposes three lengths of panel edge. The total moment

acting along each of these lines, as given by the strain readings, was calculated by summing the individual beam and slab moments across the line.

Let Figure 9.23 represent one of the beams and enough slab section on either side of it to make the sum of the slab compression equal to the tension in the beam, with the following notation:

$M'_b$  = moment in the beam at the support about the mid-depth, as calculated from the strain readings.

$T'_b$  = tension in the beam at the support acting at mid-depth as calculated from the strain readings.

$C'_{sum}$  = sum of slab compression over the length of slab considered such that  $C'_{sum} = T'_b$ .

$m'_{sum}$  = sum of slab moments acting about the mid-depth of the slab, summed over the length of slab as defined by  $C'_{sum} = T'_b$ .

$M_b$ ,  $T_b$ ,  $C_{sum}$ ,  $m_{sum}$  are similar values at mid-span.

The moment of the exposed actions in the beam,  $M'_{total}$  is therefore given by

$$M'_{total} = M'_b + m'_{sum} - T'_b(D-D_s)/2 \quad \dots(9.1)$$

and so across the full line 2, the moment is the sum of the computed beam moments plus the sum of the computed slab moments across the full width minus the sum of the products

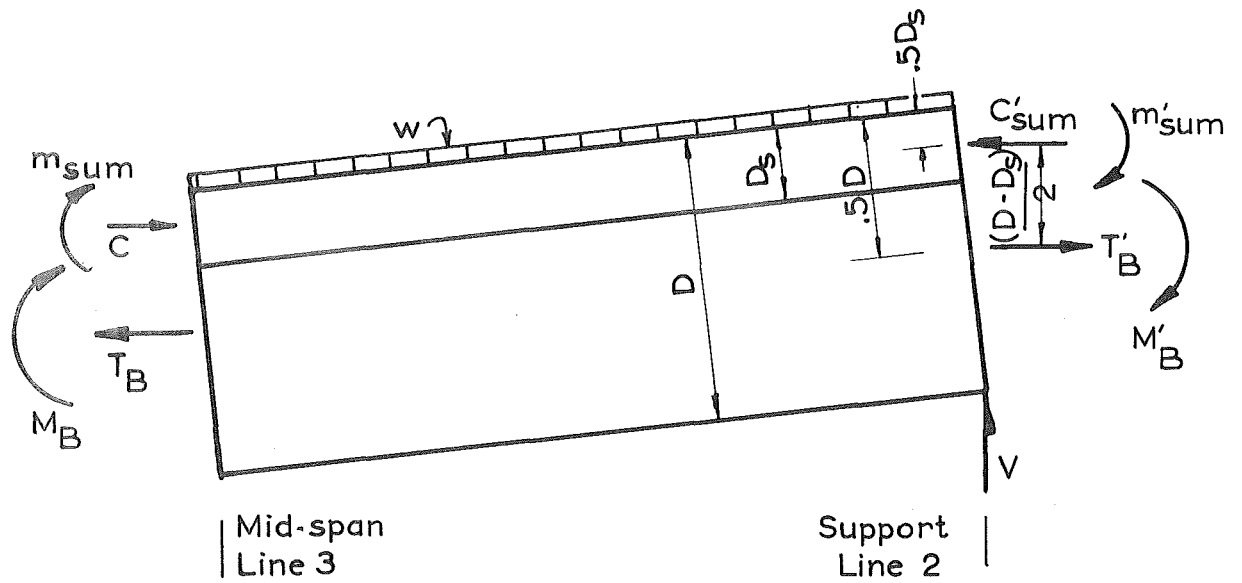


FIGURE 9.23 COMPUTED ACTIONS ON A TYPICAL SLAB AND BEAM ELEMENT

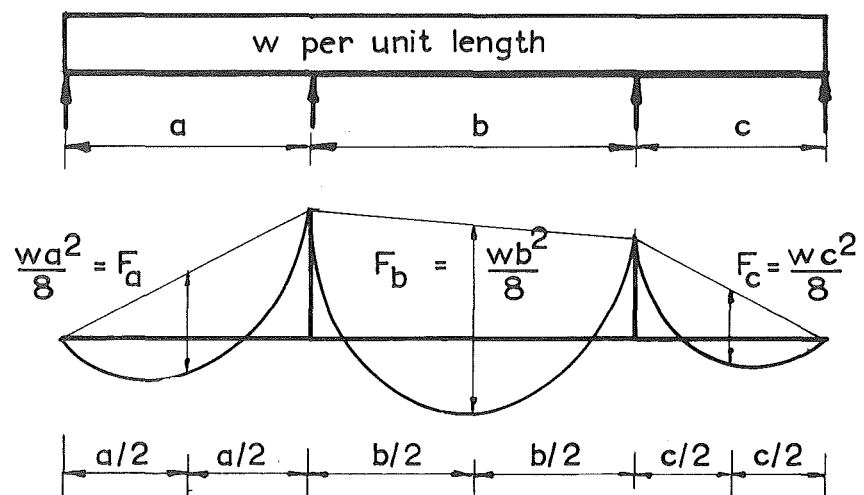


FIGURE 9.24 FREE MOMENTS

of  $T'_b(D-D_s)/2$  for each beam, bearing in mind that  $D$  may vary from beam to beam.

At mid-span the total moment,  $M_{total}$ , of the actions exposed in the beam of 9.23 is

$$M_{total} = M_b + m_{sum} + T_b(D-D_s)/2 \quad \dots(9.2)$$

and a similar summation of these quantities, beam by beam yields the total moment along a line such as line 3.

For checking purposes, a most useful quantity is the "free" moment, which for any symmetrically loaded span is the average of the two support moments plus the moment at mid-span. This moment should equal the moment induced at mid-span by the same load on a simply supported span of the same length. The case of a uniformly distributed load is illustrated in Figure 9.24.

Referring to this figure and denoting the total moment at the opposite support (not shown) as  $M''_{total}$ :

$$\begin{aligned} \text{Free moment, } M_f &= \frac{1}{2}(M'_{total} + M''_{total}) + M_{total} \\ &= \frac{1}{2}(M'_b + M''_b) + \frac{1}{2}(M'_{sum} + M''_{sum}) \\ &\quad - \frac{1}{2}(T'_b + T''_b)(D-D_s)/2 \\ &\quad + M_b + m_{sum} + T_b(D-D_s)/2 \quad \dots(9.3) \end{aligned}$$

#### 9.3.5.3 Comparison of Line Moments

Each line cut through four beams, ~~not all of which~~

were strain-gauged sufficiently to determine moments at the sections cut. The sum of moments in the beams cut by any line was computed by assuming complete symmetry of floor behaviour, e.g., when only two beams (one exterior and one interior) were suitably gauged, the sum of the two known moments was doubled. Unknown tension couples were similarly treated.

The slab moments,  $m_{\text{sum}}$ , were not known at all and for  $m'_{\text{sum}}$  only one edge of the centre panel was suitably gauged. Thus assessment of the contribution of slab moment was not at all accurate and in most cases the difference between the full moment as calculated from the reactions and the sum of beam moments only was examined to ensure that it was of reasonable magnitude.

Figures 9.25 to 9.28 show moment-load curves for lines 2, 3, and 4 calculated from reactions and applied loads and from strain readings. All curves are for increasing load from LS168 upward to LS227. Each figure is more fully described and discussed below.

Figure 9.25:

All curves in this figure are calculated from the reactions and applied load by the method described above (9.3.4). Line 1, line 2 and line 3 moments are shown individually, together with the free moment in the end span ( $\frac{1}{2}$  line 2 + line 1) and that in the centre span ( $\frac{1}{2}(\text{line 2} + \text{line 4}) + \text{line 3}$ ). The latter may be seen to compare

favourably with the  $wl^2/8$  values.

Line 3 moment increased linearly from the outset but curled over to reach a maximum value at approximately 800 psf. Line 2 accordingly showed the reverse tendency, increasing more sharply after 650 psf.

The larger value of mid-span moment initially suggested a relatively large EI value in this region, probably due to the contribution of flanges in the T- and L-beams, and the subsequent reduction in the rate of increase of moment was probably due to the decreasing role played by the flanges, and to the increased cracking at mid-span.

Figure 9.26:

Comparison of line 2 moments is made in this figure, the curve for moments calculated from the reactions and applied loads being the basis for comparison (curve 3).

Along line 2, only two beams were gauged to give values of beam tension and moment (gauges 133,134 in the exterior beam; 126,129 in the interior beam). Curve 1 is the sum of moments only in these two beams, calculated from the strain readings and doubled to allow for the other two beams. For curve 2, curve 1 values were reduced by the total value of the tension couples as given by Equation 9.1. The difference between curve 3 and curve 2 represents the sum of slab moments along line 2.

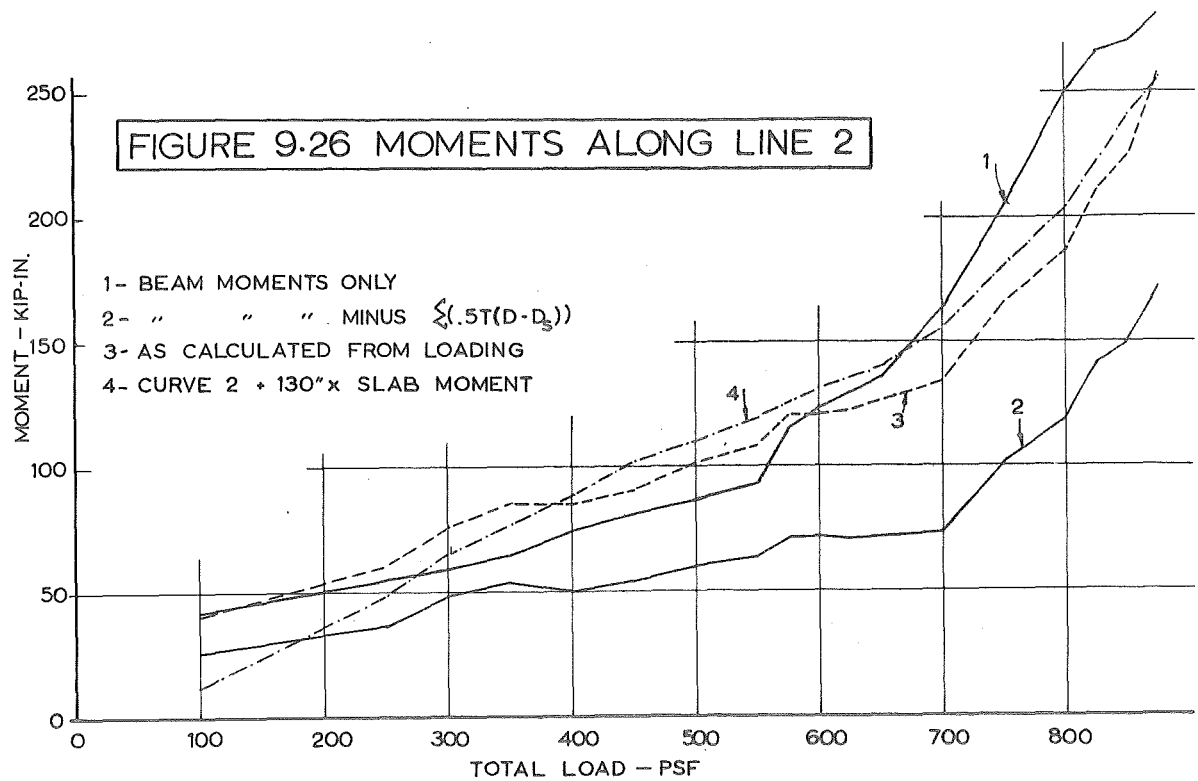
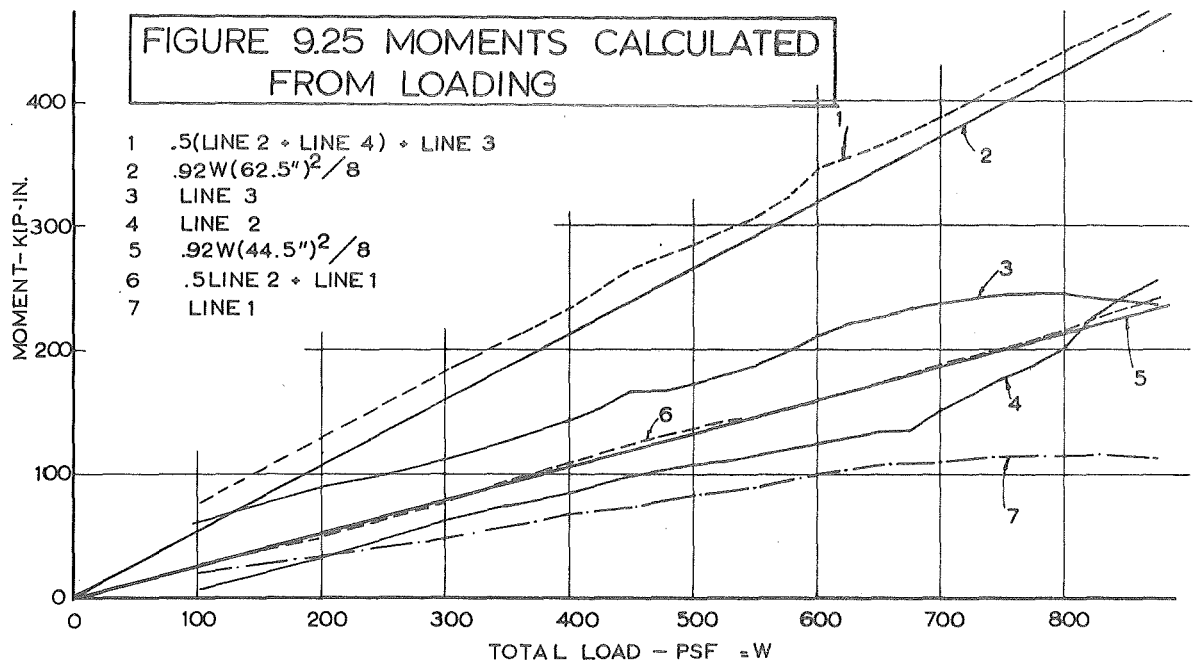
No slab edge moments were measured along line 2 but it is reasonable to assume that the centre panel edge moments will be approximately equal to those along the centre panel



edge at right angles to line 2. Gauges 118,119,120; 114,115; 116,117; showed nearly equal values of slab edge moment at LS227 and it is reasonable to take this value as acting along the whole length of the centre panel edge. Further, since no moment values were obtained for the edges of the centre-edge panel, the values of moment per unit length of edge obtained for the edge of the centre panel were taken as representative of the centre-edge panel values. The total length of edge over which this moment could act was thus  $62.5 + 2(44.5) = 151.5$  inches.

At load stage 227 the slab edge moment per inch given by gauges 118,119 etc., (650 lb/in) required multiplication by 130 inches to make values of curve 2 + slab moments equal to curve 3. This same factor was applied to the slab moment at the other load stages, resulting in curve 4 which compares favourably with curve 2.

The factor of 130 inches implies a high value of moment (500 lb/in) along the short edge of the centre-edge panels. Some estimate of the feasibility of this value may be gained by comparison of the expected normal forces along these edges (340 lb/in. in the centre panel; 270 lb/in. in the centre-edge panels (see Figure 6.3)). The centre panel edge forces given at these sections from which the moments were taken are all of greater magnitude than expected at LS227. If it is assumed that the expected and actual membrane force values compare as well in the centre-edge



panels, an enhanced moment of 500 lb/in along the short edges is reasonable.

Figure 9.27:

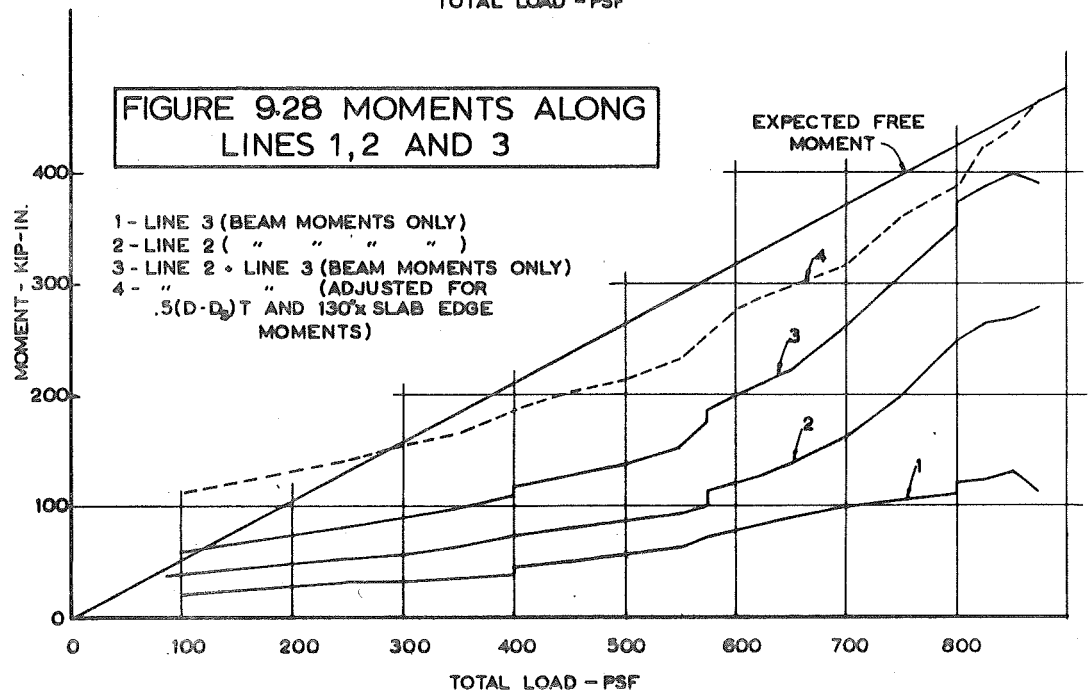
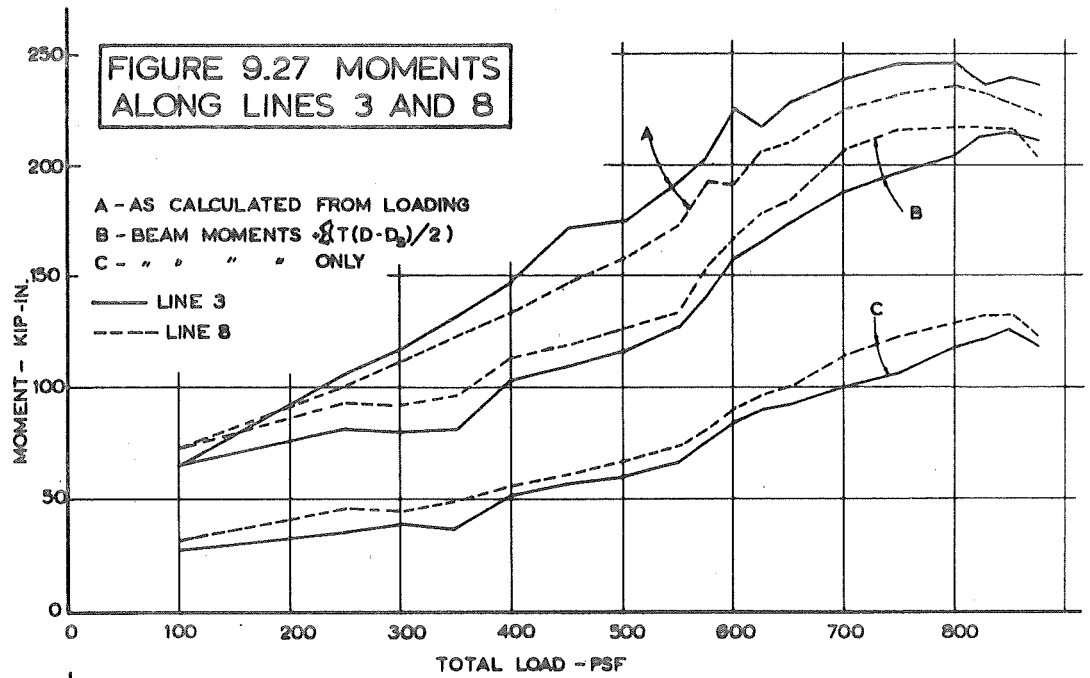
This figure shows line moment values for the middle sections of the floor in both directions (lines 3 and 8). The lower two curves are plots of the sum of beam moments only, in each case this sum comprising the two separate interior beam values and twice the one exterior beam value obtained. Both these curves fell well short of the curves calculated from the reactions (upper two curves).

The two middle curves compare far more favourably with the top pair, since for these the necessary addition of tension couples has been made, according to Equation 9.2. The difference remaining represents  $m_{\text{sum}}$  and is well within the capacity of the slab portion.

Figure 9.28:

The lowest curve (1) in this figure is the graph of the sum of beam moments only along line 3, again being twice the exterior beam value + the two separate interior beam values. No tension couple adjustment was made for this or for curve 2 which is a plot of line 2 moments. Curve 3 shows the sum of these. If it is assumed in Equation 9.3 that  $M'_{\text{total}} = M''_{\text{total}}$ ,  $T_B = T'_B = T''_B$  then this curve represents the total free moment, less the portion of moment taken by the slab sections ( $m_{\text{sum}} + \frac{1}{2}(m'_{\text{sum}} + m''_{\text{sum}})$ ).

When 130" times the centre panel edge moment per unit



width is added to this curve, values are significantly in excess of the theoretical free moment (solid line). However, when each beam moment was adjusted separately for the  $T_b(D-D_s)/2$  terms and the same slab edge moment term added, curve 4 resulted.

#### 9.3.5.4 Variation of Section Moments with Load

Values of section moments as calculated from the strain readings are shown for several critical sections in Table 9.9, for increasing load in pattern 1 after LS168 and for critical load stages before LS168. Some of the former values are plotted in Figures 9.29 to 9.31 inclusive.

Figure 9.29 shows the beam moments plotted against load. For the exterior beam centre spans, the support moment rose far more sharply than the mid-span values. In the interior beam centre spans, values at support and mid-span showed marked equality up to 550 psf after which a sharp rise in support moment occurred and the rate of increase in mid-span moment fell. The values of design moment are marked in the figure and may be seen to compare favourably at the interior beam centre span and the exterior beam support. Values at the exterior beam mid-span were less than the design moment, while those at the interior beam support were greater.

In Figure 9.30, the moments at sections along the edge of the centre panel are plotted. The curves for gauge positions 118,119,120 and 114,115 (near the middle of the edge) are

TABLE 9.9 - MOMENTS AT SELECTED LOAD STAGES (CRACKED SECTIONS BF=1.0 FOR BEAMS)

\* Assuming complete bond transfer.

\*\*Concrete gauge not at mid-span.

		BEAM MOMENTS - KIP-IN										SLAB MOMENTS lb.in/in.						
		71	73	70	72**	127	126	132	136	54	53	118*	116*	114*	112*	107*	105*	94*
STEEL GAUGE																		
LSN	LOAD																	
32	225/2/75	9.1	12.9	11.6	12.1	-6.9	-5.0	-3.5	-3.8	+1.3	1.6	-124	-116	-82	-49	-67	-82	-86
57	225/3/75	7.4	10.3	11.0	10.0	-6.9	-5.0	-4.2	-6.4	6.4	6.1	-79	-82	-49	-25	-97	-103	-99
7A	225/1	9.6	15.4	13.0	13.0	-9.2	-7.1	-4.9	-6.7	4.6	4.3	-131	-129	-82	-40	-100	-114	-128
79	225/1	8.8	15.2	12.7	13.2	-9.2	-7.0	-5.0	-6.3	3.9	3.9	-141	-124	-83	-37	-103	-115	-130
84	350/1	15.4	10.8	17.2	14.3	-15.5	-12.5	-7.9	-10.1	6.5	6.3	-190	-179	-127	-51	-131	-165	-178
85	375/1	16.9	12.2	18.4	16.3	-16.9	-13.2	-8.9	-11.4	7.2	7.0	-205	-193	-135	-58	-142	-171	-188
96A	225/1	12.3	8.7	13.1	12.1	-11.6	-7.8	-6.4	-7.6	3.2	3.7	-128	-109	-71	-21	-87	-113	-119
98	375/1	16.8	12.4	17.8	17.4	-17.9	-13.6	-9.4	-11.6	6.2	6.4	-206	-192	-114	-43	-128	-169	-188
104	375/5/75	13.8	9.9	14.9	15.5	-9.4	-5.4	-3.7	-4.5	-1.0	.1	-194	-172	-86	-26	-71	-114	-130
123A	400/2/75	11.3	8.2	12.2	14.1	-11.9	-6.9	-4.7	-4.0	-5.3	-3.8	-213	-184	-81	-23	-62	-107	-134
142B	375/3/150	10.1	7.3	11.3	13.2	-13.4	-6.4	-6.3	-10.5	3.9	4.9	-175	-132	-36	19	-114	-151	-176
153A	225/1	8.6	6.2	9.7	11.8	-11.2	-4.0	-4.8	-7.2	-1.6	.4	-162	-123	-30	19	-83	-113	-135
155	375/1	13.9	10.4	18.9	17.5	-18.9	-11.7	-8.6	-12.5	2.3	3.7	-208	-176	-57	18	-112	-166	-190
158	450/1	23.0	18.6	23.5	23.8	-30.0	-23.9	-9.5	-15.0	3.4	6.4	-293	-241	-141	-94	-167	-229	-302
168	75	9.8	8.5	10.6	10.3	16.0	12.2	8.4	7.9	1.0	3.5	-114	-80	-7	-53	-48	-77	-109
171A	225	15.1	12.1	15.5	15.2	21.4	16.2	10.3	10.6	1.9	4.6	-187	-145	-47	-73	-82	-128	-170
183A	225	13.7	11.0	14.9	14.2	21.5	16.4	10.8	10.7	1.6	4.3	-184	-143	-44	-72	-79	-129	-170
185	275	15.4	12.0	16.6	15.7	23.4	17.6	11.5	11.7	1.9	4.7	-212	-165	-63	-83	-102	-148	-195
187	325	17.1	13.7	18.4	17.4	25.3	19.5	12.4	12.8	2.3	5.3	-237	-192	-78	-90	-118	-170	-213
189H	375	18.9	15.2	20.2	19.0	27.6	21.7	13.1	13.9	2.6	5.3	-270	-213	-97	-93	-132	-188	-239
		22.7	17.3	22.6	19.4	30.6	23.4	13.5	14.7	3.3	6.4	-270	-217	-97	-103	-146	-196	-232
191	425	24.3	18.6	24.5	20.6	32.9	25.2	14.1	16.0	3.8	6.9	-293	-234	-104	-113	-170	-217	-257
193	475	26.6	20.5	26.8	22.8	35.2	27.4	15.3	17.3	4.0	7.5	-310	-256	-124	-142	-182	-242	-283
199	525	29.4	23.6	30.1	25.9	38.5	30.2	16.4	19.4	4.6	8.2	-341	-285	-145	-246	-200	-265	-302
200	550	38.2	24.9	31.9	27.4	40.3	32.0	17.2	20.0	5.0	8.4	-370	-305	-159	-286	-213	-277	-326
		32.7	27.2	35.7	30.1	37.3	39.2	18.5	23.3	5.6	8.5	-370	-305	-165	-424	-208	-302	-323
208	575	35.6	29.0	38.5	32.8	38.1	41.4	20.0	24.4	6.6	9.3	-384	-340	-180	-472	-221	-322	-313
213	600	38.1	31.5	40.3	36.0	40.6	44.0	20.5	25.9	7.0	9.6	-405	-362	-195	-494	-236	-335	-297
214	625	40.3	35.4	42.0	38.4	45.2	50.6	16.8	28.5	6.9	9.5	-388	-369	-205	-519	-270	-385	-241
216	675	44.3	38.9	49.5	44.5	51.6	60.5	20.8	29.7	7.4	10.9	-451	-447	-263	-586	-358	-443	-316
218	725	47.6	42.1	57.0	46.5	59.9	75.0	26.9	30.0	7.8	12.9	-494	-492	-281	-726	-375	-428	-374
220	775	48.7	43.5	63.2	47.6	74.8	91.9	29.5	37.5	9.4	13.0	-515	-494	-352	-869	-356	-434	-405
224	775	51.0	45.7	66.6	47.5	80.3	96.1	31.4	38.4	11.5	13.2	-512	-506	-418	-923	-370	-476	-420
225	800	52.4	47.5	68.2	47.2	-	99.2	33.3	40.5	11.6	12.8	-537	-554	-511	-1024	-401	-514	-445
226	825	54.8	50.3	71.3	46.9	98.6	102.5	33.7	42.2	12.0	13.0	-560	-555	-575	-1175	-418	-459	-474
227	850	50.8	40.4	67.0	39.1	108.8	106.5	34.0	43.8	12.2	13.1	-650	-659	-1953	-1866	-542	-541	-509

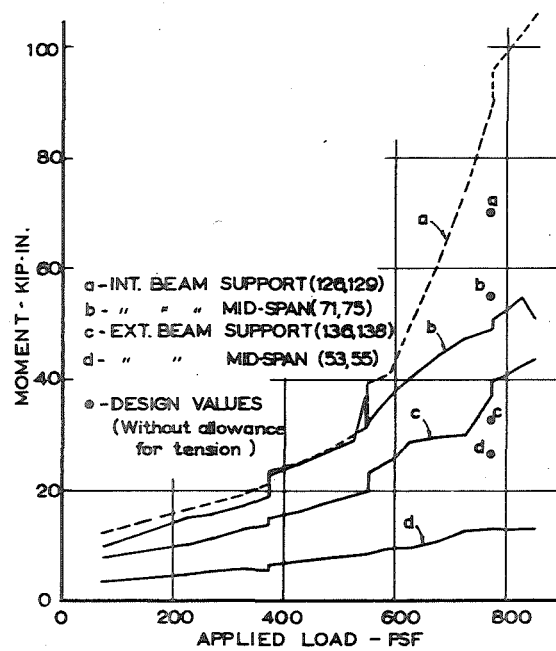


FIGURE 9.29 MOMENTS  
AT BEAM SECTIONS

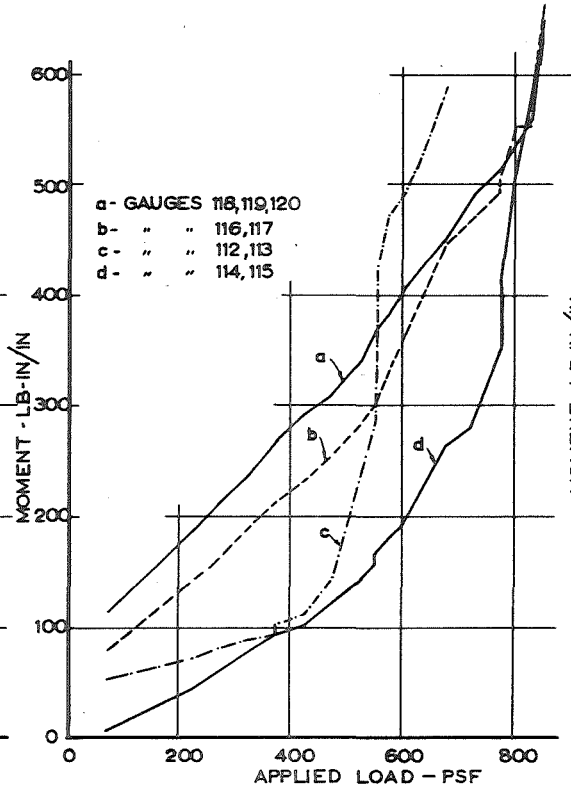


FIGURE 9.30 MOMENTS  
AT EDGE OF CENTRE PANEL

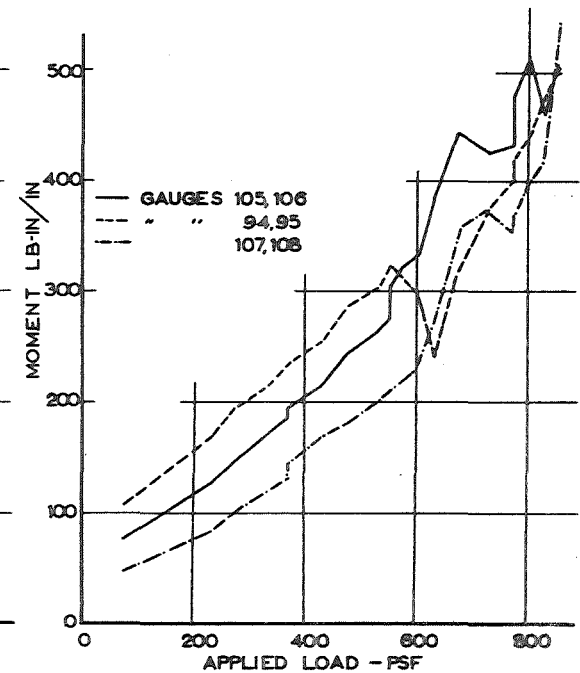


FIGURE 9.31 MOMENTS AT  
EDGE OF CENTRE-EDGE  
PANEL

similar but towards the corners the initial rate of increase of moment was lower. Membrane compression became enormous near the corners towards the end of the test, a fact which explains the steep rise in moments in this region.

Moment values at sections along the interior long edge of the centre-edge panel showed good grouping as Figure 9.31 shows. The effect of the crack along the centre of each of these panels was evident in the discontinuity in the curve for gauges 94,95 which were located on the line of this crack. The moment values of 400 lb"/" at 775 psf indicate considerable compressive membrane action in this direction.

#### 9.3.5.5 Discussion

Line moments calculated from the measured reactions and applied loads were expected to be reliable and accurate and were shown to be so. Values of line moments computed from the strain readings showed similar trends to the reaction-load line moments and the values compared well.

The effect of beam tension and slab compression on the line moments was shown to be large and the conclusion that the strain moments compared well with the reaction-load moments was based on values of strain moments in beam sections only, corrected for the couple induced by the beam tension and slab compression.

The assumption that concrete in a cracked section



carried no tension in regions of tensile strain once the extreme fibre strain exceeded the nominal cracking strain could have been the cause of the general tendency for values computed from the strains to rise slowly until relatively high loads were reached. Cracks did not form exactly at the gauge positions and bond transfer from steel to concrete between the crack and the gauge position would have reduced the tension in the steel, while at the same time inducing some tension in the concrete. The loss of steel tension was accounted for inherently in the strain reading but the "no tension" assumption ignored the corresponding tension in the concrete and therefore the section moment and tension would have been underestimated in the most likely case of this tension having its centre of action near the tension steel. At higher loads, further cracking would result in reduction of the force transferred by bond and better values from the computation would result.

Residual strains at LS168 have clearly led to high initial values, though not in all cases is this fully applicable. Cracking of the floor in previous tests caused redistribution of moments which remained effective when load was removed, causing significant alteration in the initial conditions of subsequent tests.

The effect of variation of flange width on the computed moments at the mid-span sections was small. For a

section at the mid-span of an interior beam section, the maximum change in moment due to an increase in flange width from 1.0 to 3.0 times the web width was 14 per cent. All values plotted are for a flange width equal to the web width.

#### 9.3.5.6 Conclusion

Line moments calculated from reaction values and applied loads showed good agreement with expected values. Lack of slab moment data made direct comparison of line moments difficult. Nevertheless, favourable results were obtained from comparisons of line moments calculated from the two independent methods.

Beam section moments followed the same trend as the line moments and compared well, overall, with the design values.

Mid-span moments for both lines and sections tended to be large initially showing a slower rate of increase at higher load while support moments showed the reverse tendency.

Slab moments were well in excess of Johansen values due to enhancement by compressive membrane action. Variation of these moments with load was approximately linear for sections near the middle of the edges but values nearer the corners showed slow development initially followed by a sharp rise at higher load values.

All moment values calculated from strain readings

contained inherent inaccuracies of sufficient size to make it difficult to draw firm conclusions from their variation with load, but good results were obtained in the comparisons of these values with the moments calculated from the reactions and applied loads. The slow rise in moment in some beam sections was attributable to the transfer of steel force to concrete, a factor not accounted for in the method of moment computation from the strain readings.

### 9.3.6 Membrane Action Effects

#### 9.3.6.1 General

The effects of membrane action were the subject of particular study in this experiment. Analysis of strain readings, deflections, beam and slab section moments and axial forces provided quantitative data on the membrane action in the floor while effects observed both during and after the test provided qualitative information on the action of membrane forces.

Values of forces computed for the slab and beam sections compared well with those expected but no useful information was obtained from these as to the effect of varying load pattern on the distribution of membrane forces. However, study of the centre panel deflection and the strain in the bottom steel at the middle of the centre panel did reveal some differences.

Effects of sustained loading were negligible, except for the centre panel where deflection and strains increased

by detectable amounts and redistribution of compressive forces took place.

In Section 9.3.6.2 the effects of membrane action on each of the floor elements is examined in detail, Section 9.3.6.3 deals with the comparison of membrane forces, and some aspects of particular interest are discussed in Section 9.3.6.4. Table 9.10 shows values of net force on critical sections at selected load stages.

#### 9.3.6.2 Effect of Membrane Action on Floor Elements

Compressive membrane action caused enhancement of the load carrying capacities of all three panel types. At what was deemed to be failure of each panel type, the following values of the ratio of actual load to Johansen load were obtained:

Centre panel:	2.18	cf	2.0	required	in	design.
Centre-edge panel:	1.55	cf	1.35	"	"	"
Corner panel:	1.46	cf	1.00	"	"	"

Although values for the centre-edge and corner panels were affected by large beam deflections, it is clear that for these panels, the enhancement due to membrane action was significantly in excess of that required.

Compressive forces in the panels gave rise to considerable tensions in the beams, thereby reducing their flexural capacity.

The fact that the panel types had unequal ultimate loads eased the burden of tension carried by the beams,

TABLE 9.10 - SECTION FORCES AT SELECTED LOAD STAGES

		BEAM FORCES KIPS										SLAB FORCES - lb/in.						
STEEL GAUGE	→	71	73	70	72	127	126	132	136	54	53	118	116	114	112	107	105	94
LSN	LOAD																	
32	225/2/75	1.6	4.0	2.7	2.6	-.2	1.1	-1.1	-.5	-1.1	-.7	-106	-112	-68	-30	-52	-68	-80
57	225/3/75	1.1	2.6	2.6	2.2	-.2	.8	-1.1	-1.6	.1	.1	-59	-68	-30	-17	-84	-102	-90
7A	225/1	1.2	4.8	2.9	3.0	-1.2	.5	-2.3	-1.9	-1.0	-.6	-128	-122	-68	-33	-93	-106	-118
79	225/1	1.0	4.8	2.9	2.6	-1.8	.1	-2.7	-2.3	-1.4	-1.0	-128	-106	-71	-23	-102	-109	-125
84	350/1	2.7	1.5	3.5	1.5	-2.4	-.2	-2.4	-1.8	-.6	-.7	-181	-154	-115	-36	-128	-141	-181
85	375/1	3.0	1.8	3.6	2.0	-2.5	-.3	-2.0	-1.4	-.6	-.3	-175	-166	-110	-27	-131	-159	-181
96A	225/1	2.3	1.6	3.0	1.9	-2.4	-.4	-2.7	-1.4	-1.5	-1.4	-118	-90	-37	-4	-83	-103	-121
98	375/1	3.0	1.9	3.8	2.4	-2.8	-.5	-2.6	-1.3	-.9	-.9	-178	-163	-76	-12	-118	-153	-181
104	375/5/75	2.6	1.7	3.5	2.5	-3.7	-1.0	-4.4	-1.9	-3.2	-2.9	-169	-132	-53	11	-64	-106	-125
123A	400/2/75	1.9	1.5	3.1	2.0	-4.9	-2.2	-7.2	-2.5	-5.5	-4.7	-170	-142	-38	20	-40	-84	-137
142B	375/3/150	1.6	.9	2.8	1.6	-6.4	-3.0	-8.1	-4.5	-3.5	-3.0	-141	-100	10	58	-106	-128	-175
153A	225/1	1.3	.8	2.6	1.5	-6.9	-2.9	-8.8	-4.2	-4.9	-4.1	-132	-76	25	58	-71	-103	-140
155	375/1	2.2	1.2	3.5	2.2	-6.0	-1.4	-6.8	-2.6	-3.6	-3.0	-124	-87	33	84	-100	-144	-187
158	450/1	4.4	4.0	5.0	3.8	-1.9	2.9	-2.4	-1.0	.8	1.4	-118	-51	73	67	-120	-131	-232
168	75	2.4	3.0	3.2	3.0	.6	3.7	-1.2	.8	1.0	1.7	+9	+52	+125	75	3	5	-33
171A	225	3.4	3.7	4.1	3.5	.2	4.0	-1.3	.5	1.2	1.9	-78	4	119	71	-41	-31	-99
183A	225	3.0	3.3	3.9	3.2	-.4	3.7	-2.3	.0	1.0	1.7	-25	10	128	74	-32	-34	-99
185	275	3.2	3.4	4.1	3.3	-.7	3.5	-2.3	-.1	1.0	1.7	-50	3	130	70	-42	-62	-115
187	325	3.5	3.7	4.4	3.5	-.9	3.5	-2.4	-.3	1.0	1.7	-66	-19	115	79	-61	-69	-140
189H	375	3.8	3.9	4.6	3.7	-1.0	5.0	-.7	-.4	1.1	1.6	-69	-26	117	70	-73	-94	-158
		4.6	4.8	5.1	5.1	-.1	5.0	-.7	+6	1.6	2.3	-79	-8	117	69	-86	-94	-140
191	425	4.8	5.0	5.3	5.3	-.3	5.0	-.6	.5	1.5	2.4	-88	-30	123	69	-99	-95	-156
193	475	5.2	5.3	5.6	5.6	-.2	5.2	-.6	.4	1.7	2.6	-113	-36	122	40	-105	-111	-175
199	525	5.5	5.8	8.9	6.1	.2	5.8	-.5	.5	2.0	3.0	-116	-37	118	-66	-100	-120	-175
200	550	5.7	6.1	6.1	6.2	.4	7.8	.3	.6	2.3	3.8	-135	-68	105	-97	-110	-130	-188
		6.0	6.1	6.7	6.9	5.4	7.8	.3	1.2	2.6	3.3	-159	-69	87	-222	-11	-89	-152
208	575	6.9	7.2	7.3	7.9	6.6	8.9	.8	1.0	3.2	4.4	-159	-113	74	-201	-20	-89	-122
213	600	7.8	7.9	7.4	8.3	7.2	10.5	.4	3.0	3.5	5.2	-195	-123	59	-290	-6	-98	-100
214	625	8.0	8.9	7.5	8.6	8.0	11.3	3.2	3.1	3.7	5.3	-171	-144	28	-308	-22	-162	-21
216	675	8.5	9.4	8.4	9.2	9.9	12.4	5.1	4.9	4.3	6.2	-246	-234	58	-398	-141	-222	-71
218	725	8.1	10.0	7.9	9.7	12.8	13.6	6.9	8.5	4.8	7.2	-290	-314	-82	-569	-162	-234	-159
220	775	7.7	9.6	7.2	9.9	13.0	15.3	10.2	10.4	5.5	7.3	-308	-320	-149	-722	-161	-254	-195
224	775	7.4	9.4	6.0	10.5	14.7	14.6	11.9	10.7	6.1	7.3	-317	-328	-234	-812	-177	-293	-210
225	800	7.2	9.0	5.5	10.7	-	15.5	12.7	9.8	6.4	7.2	-334	-416	-255	-933	-213	-352	-228
226	825	6.7	8.5	4.4	11.1	13.6	12.4	12.6	9.2	6.5	7.2	-370	-390	-422	-1099	-234	-272	-258
227	850	4.9	7.3	3.3	10.6	9.8	10.7	12.4	8.5	6.5	7.1	-467	-507	-2017	-1899	-378	-375	-308

particularly the centre spans of the interior beams, because the degree of development of compressive forces in each panel type was different, i.e., by the time the centre-edge and corner panels were in greatest need of compressive membrane action enhancement, the centre panel had failed and formed a tensile net which tended to reduce the tension in the beam spans supporting it.

The interaction of elements was important in assessing the effects of membrane action in the floor, a fact revealed in the following element by element analysis of the effects of membrane action on the floor behaviour.

(i) Centre Panel

The development of membrane forces in this panel was slow at low load levels but increased very rapidly after the Johansen load was exceeded. As the collapse load was approached, evidence of a significant reduction in membrane compression near the centre of the panel was detected. Edge forces continued to rise during this stage and strains which indicated the level of "circumferential" compression near the edges increased sharply.

The variation of edge force with increasing load beyond LS168 is shown in Figure 9.32, from which it may be seen that the delay in rise of compressive force is more marked near the corners of the panel.

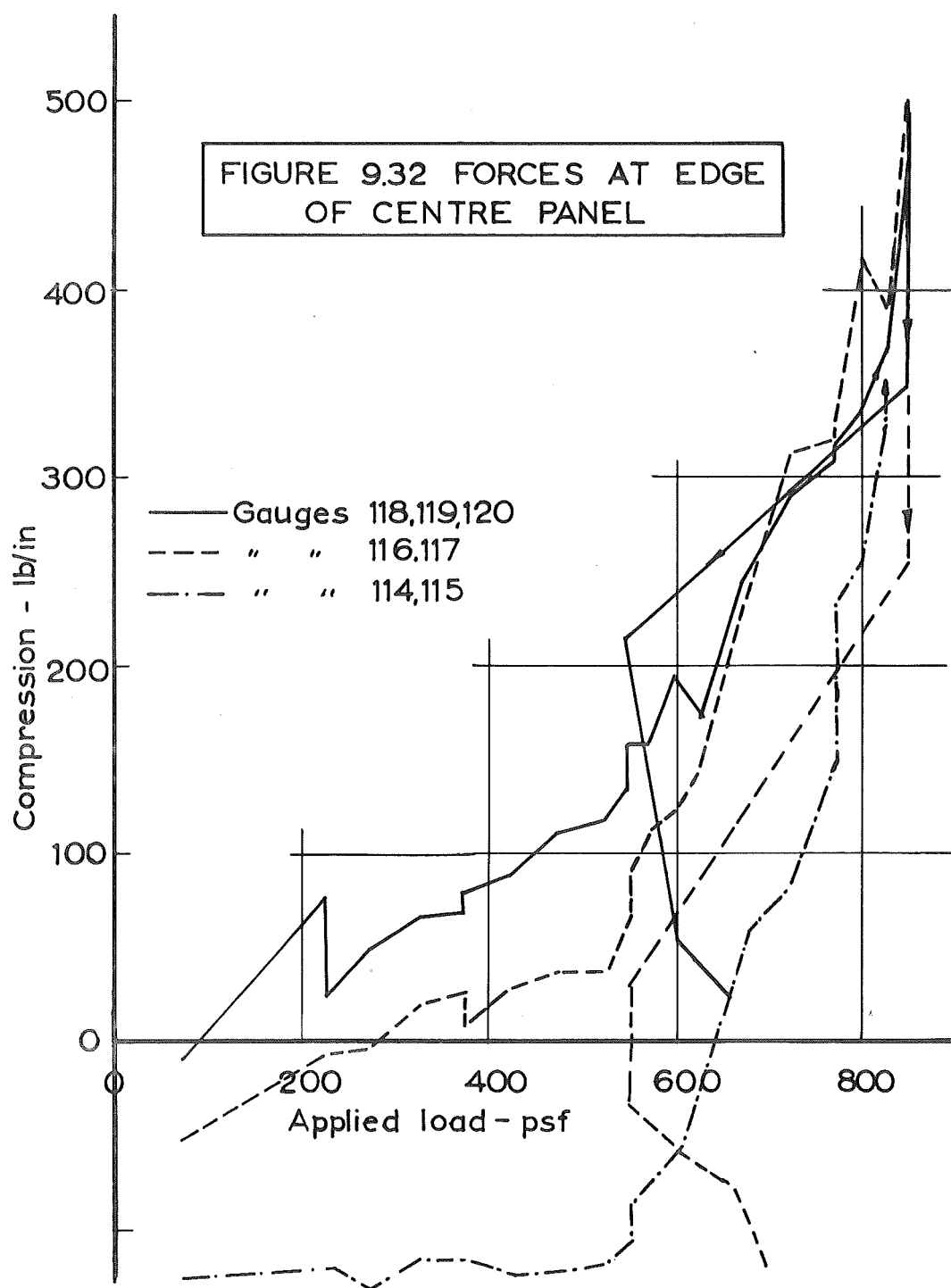
Values at 775 psf compare reasonably with the predicted average force of 340 lb/in. The rate of increase

in this edge force showed no sign of reduction while the load was increasing, but the level of compression did drop with the push-through failure of the centre panel.

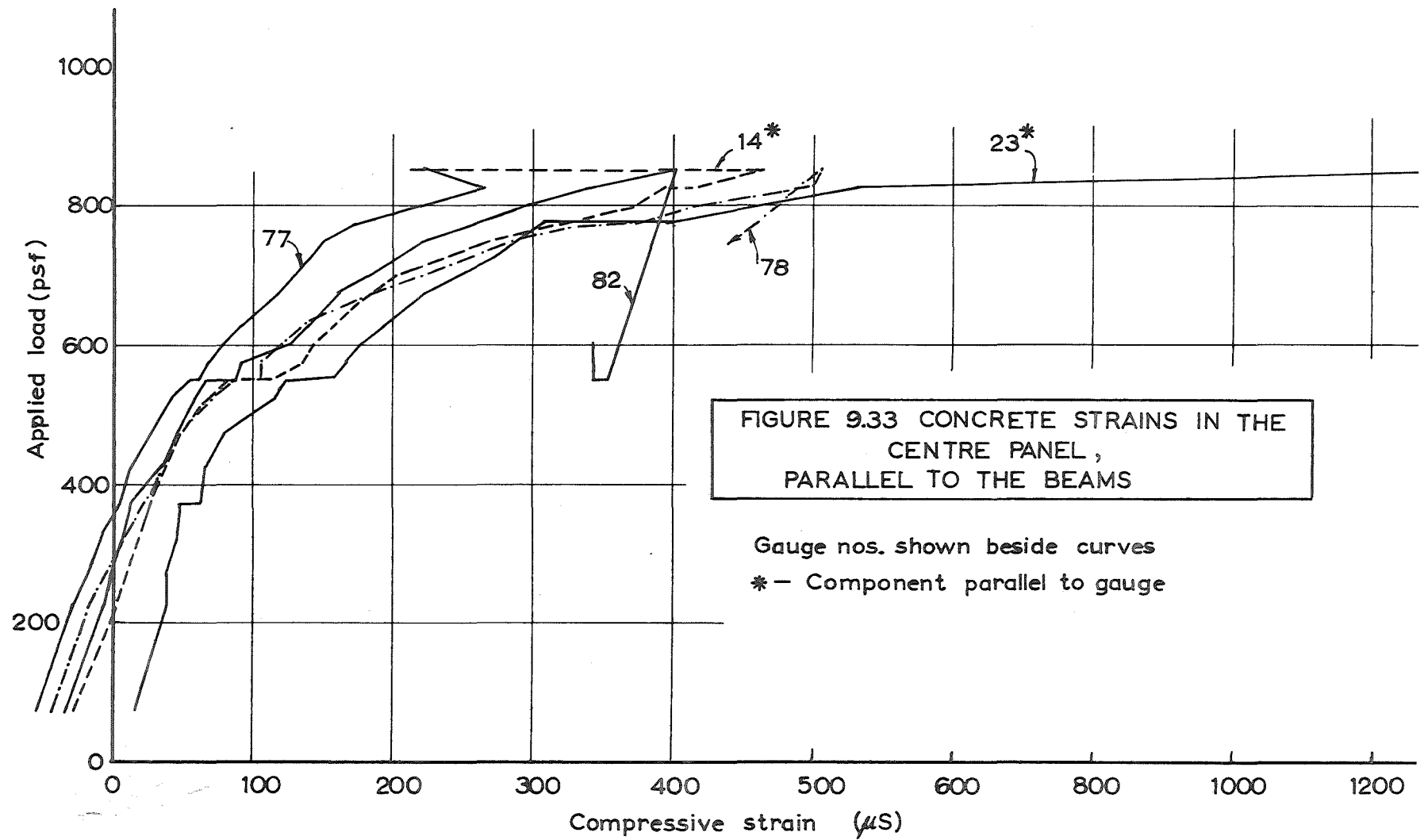
Figures 9.11 and 9.12 (pp. 192-3) illustrate clearly the transfer of compressive force from the middle region to the edge. Zones of crushing on the diagonals reach only half way along, decreasing almost linearly in width. An increase in crack width is then evident. These photographs were taken after this panel was loaded well into the tensile membrane range but they only exaggerate an effect which was evident at initial failure.

Strains parallel to the edge provided clear evidence of the increasing compression and subsequent decrease. Readings of gauges placed in this direction were examined and the readings of the two rosette stations were resolved into components parallel to and perpendicular to the edge. The variation of some of these with load is shown in Figure 9.33. This figure shows the variation for channel 78 and the components perpendicular to gauge 14 and gauge 25, the latter showing larger values by virtue of its closeness to the diagonal, where compression was higher.

For comparison, values for gauges 82 and 76 are plotted. Gauge 76 represents the strain in the top of the beam, directly above the web, and values are very much less than those for gauge 78, indicating that the strain in gauge 78







was due principally to centre panel action and not to compression in the T-beam flange. Gauge 82 shows a little of this effect of "circumferential" compression. Whereas the strain in gauge 78 became tensile as the centre panel failed, gauge 82 strain remained compressive.

Study of Figure 9.11 reveals that the spread of the tensile membrane is greater away from the diagonals, revealing an important difference between circular and square slabs in this respect. Comparison of the curves for strain in gauge 78 and the strain perpendicular to gauge 25 illustrates that this effect was present at the time of initial failure, and again this effect is merely exaggerated in the photograph.

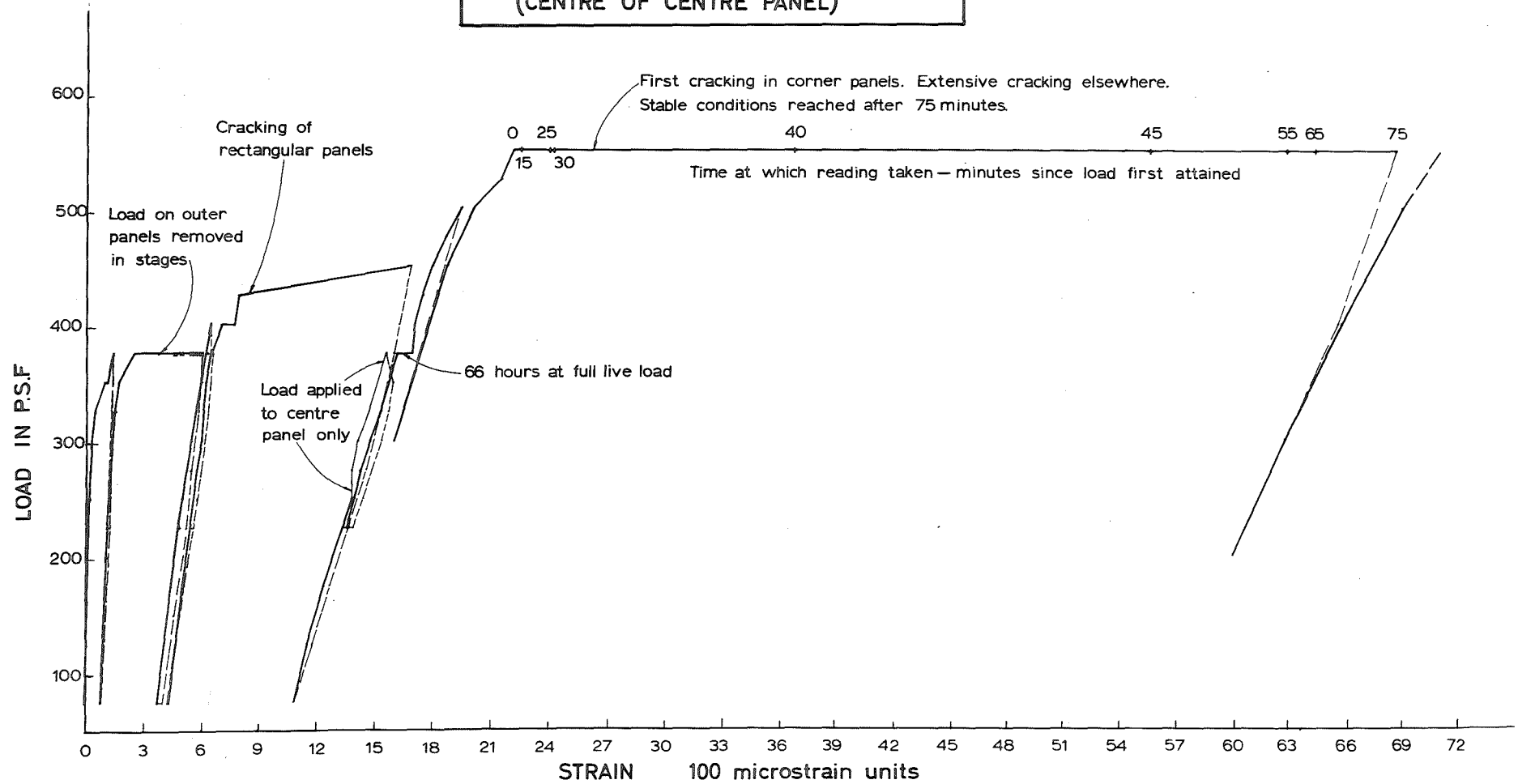
The effect of surround stiffness on the centre panel behaviour was particularly marked at three stages during the test programme as described earlier.

The effect of loss of surround stiffness on steel strain at the middle of the centre panel is shown in Figure 9.34. Causes of the large increases are shown on the figure.

At 550 psf readings of strains were taken several times and the variation of strain with time during this unstable period was quite erratic; i.e., there was no suggestion that the cause of the increase in deflection was due to creep deformation of the surround.

This graph shows clearly the effect of having a lower

FIGURE 9.34  
LOAD v. STRAIN — GAUGE 6  
(CENTRE OF CENTRE PANEL)



load on the outer panels. In spite of reduced moment restraint at the edge of the centre panel, the increased surround stiffness resulting from the lower load on the outer panels caused a slower rise in strain with load.

The effect of the application of 375 psf for 66 hours is shown to be small and a recovery to the original path on application of further load is evident. The increasing stability with time during this test was illustrated previously (see Section 9.2.4.6).

The membrane forces perpendicular to the diagonals appeared to vary approximately linearly. Some assessment of these forces was made by measuring the depth of crushing along the diagonals at the end of the test. Results of this investigation are given in Figure 9.35. Measurements were taken along each of the four diagonals. The average force per unit width was determined and plotted against the distance from the centre. Variation is almost linear and very large values are reached near the edge of the panel.

(ii) Centre-edge Panels

These panels sustained loads well in excess of their Johansen loads due to enhancement by compressive membrane action but evidence of this was not as clear as in the centre panel.

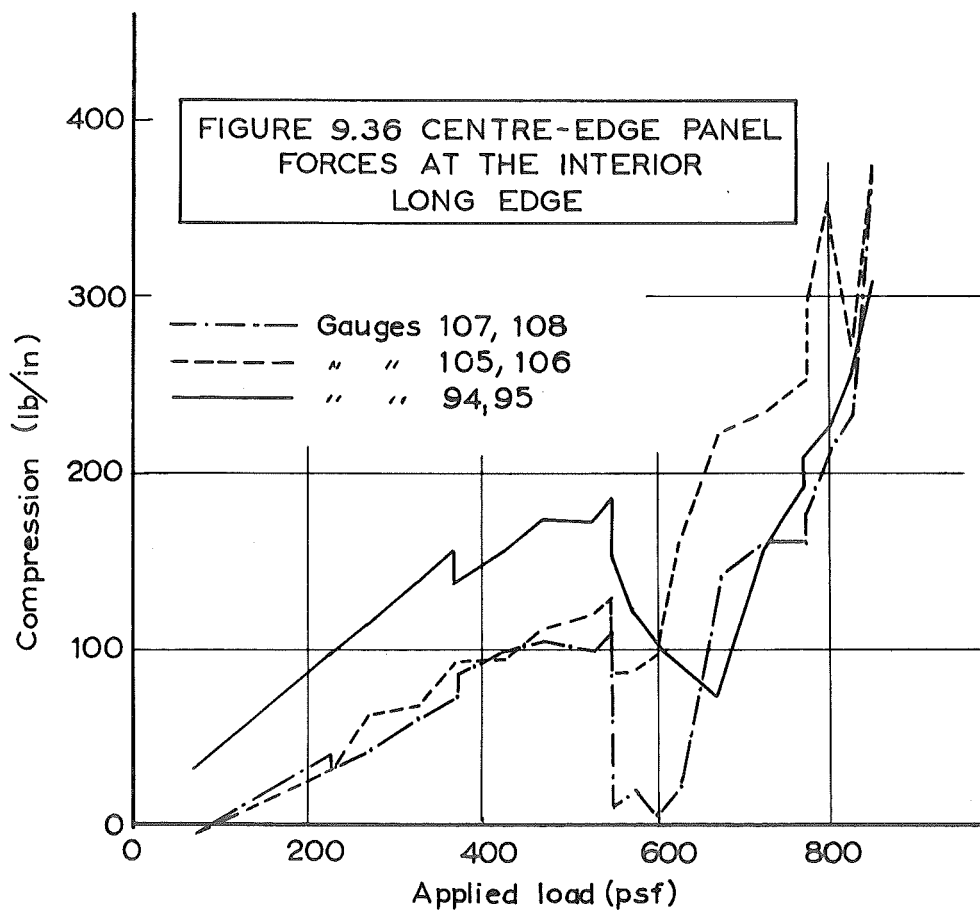
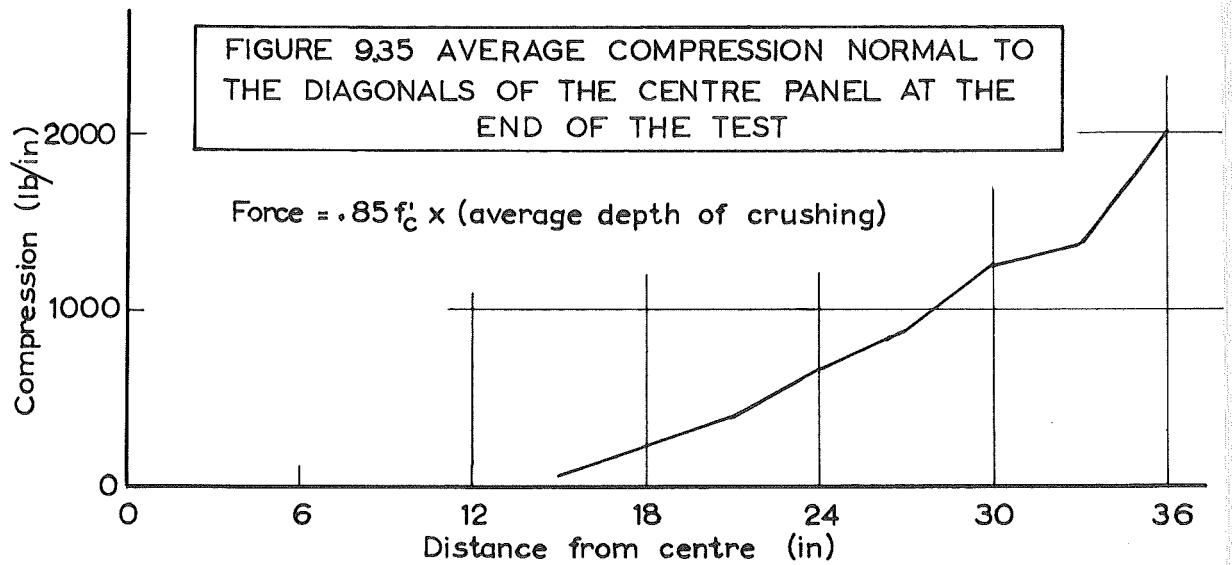
Compressive forces were expected parallel to the long side and although no provision for measurement of these

forces was made, the presence of tension in the centre spans of the exterior beams indicated that panel compression in this direction was considerable. Figure 9.36 shows the values of measured compression along the interior long edge of one of these panels, plotted against load. The rate of rise was steadier than for similar sections in the centre panel but there was still the evidence of a steeper rise for loads greater than 600 psf.

Values are considerably less than those in the centre panel but indicate substantial compressive membrane action in this direction, although much of this force was a reaction to the centre panel forces. At the end of the test programme the panel mechanism was considerably developed as Figures 9.11 and 9.12 show. These Figures show clearly the zones of concrete crushing in the end spans of the interior beams and a study of the panel crack joining two of these zones revealed the presence of membrane action of a different nature. Near the beams, this crack was present on the underside of the panel only, while the concrete at the upper surface above this crack had crushed. At its middle, the crack penetrated the full slab depth so that the panel sections along the crack were subject to high compression near the beams and tension in the middle.

### (iii) Corner Panels

The assumption that membrane action would not enhance the load capacity of these panels was clearly conservative.



The lower span to depth ratio partially compensated for the more flexible surround of these panels. The T-beam flange effect described for the centre-edge panels was also evident in these panels and the panel mechanism was not as fully developed even at the end of the test programme, suggesting that more membrane action enhancement may have been available if the beams had not failed.

The low steel strains at the exterior edges of the panels indicate the degree of development of the full yield moment along these edges. Extra membrane compression would account for this, the moment required being taken by the moment of concrete compression force about the mid-depth rather than by steel force moment. High concrete compression along these edges affects the torque induced in the exterior beams for the reasons discussed in Section 4.3.

#### (iv) Interior Beams

In the absence of any net axial tension, the centre spans of these beams were capable of carrying a far greater load than 800 psf but in fact steel strain readings reached yield values at this load, indicating the presence of large tensions in the spans.

Analysis of section strains showed larger values at the support than at mid-span as may be seen from Table 9.10 and Figure 9.37(a). The rate of rise in beam tensions followed a similar pattern to that followed by the panel

edge compressions, tensions being small at low load levels and rising steeply in regions of higher load.

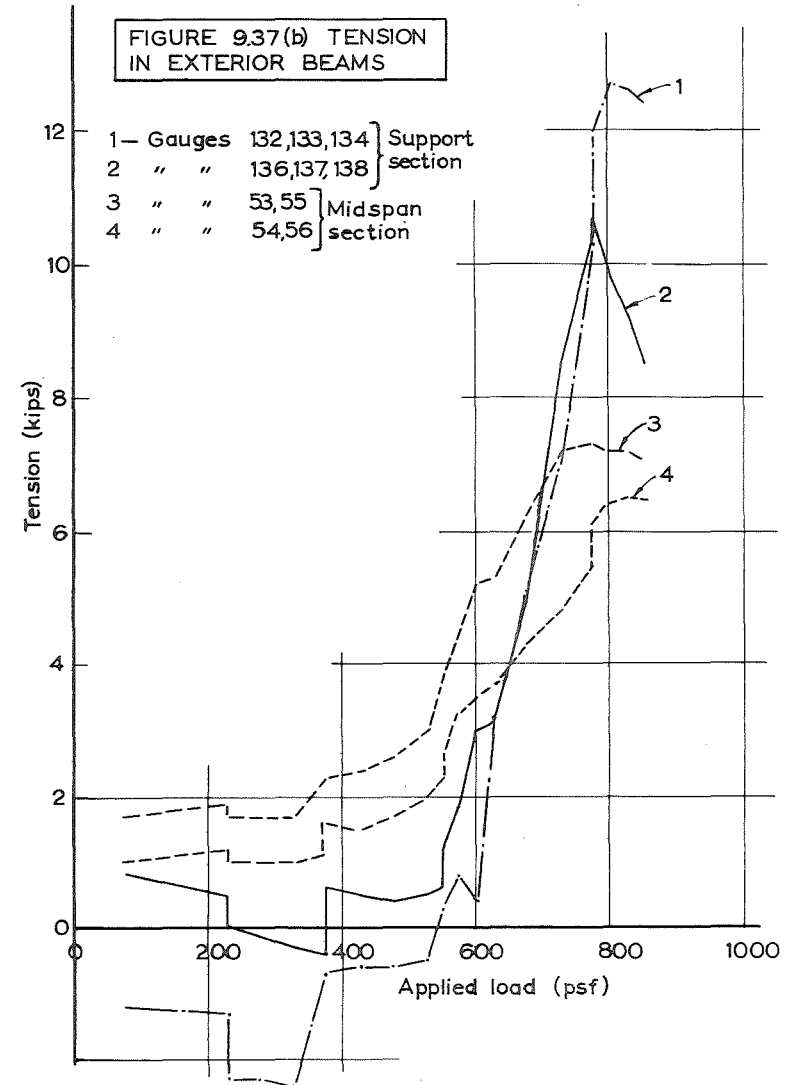
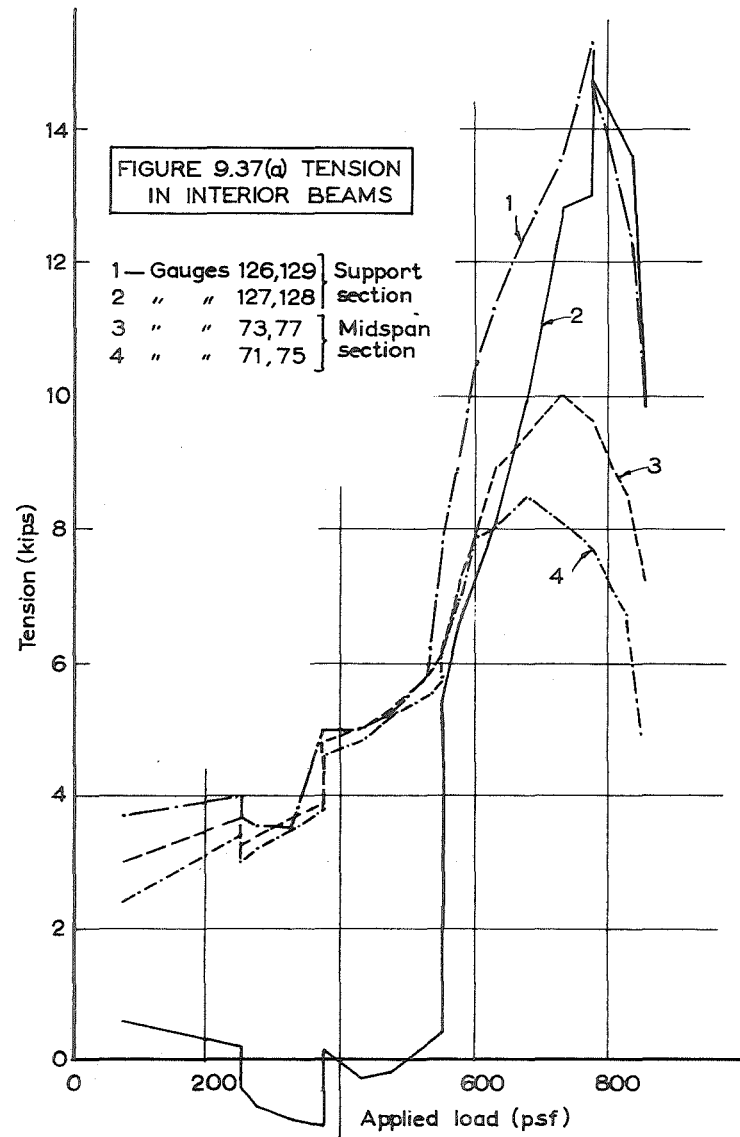
During the test, the tension gave evidence of its presence with the formation of steeply inclined shear cracks (see Figure 9.10). . . Values of tension measured in the end spans were not reliable and the behaviour of these spans during the test showed no conclusive signs of the tension implied by the presence of compressive forces along the interior long edge of the centre-edge panels.

After the centre panel pushed through to form a well developed tensile membrane, the effect of reduction of induced tension was clear. Deflections and mid-span steel strains reduced considerably, but this was not wholly due to the effects of reduced tension because at this time, the end spans were showing signs of development of plastic hinges in the positive moment regions and the resulting increase in support moment tended to produce the same effect as the reduced tensions. As loading progressed this effect became more marked and the tensions continued to reduce.

(v) Exterior Beams

Visually detectable effects of membrane action on these beams were few and confined to the centre spans. The forces measured at the sections showed a similar trend to the interior beams in their variation with load, as may be seen in Figure 9.37(b). Values were appreciably less





than interior beam values and again the mid-span tensions were less than those measured at the support. In spite of this, even the lowest mid-span value was larger than the design tension.

The presence of membrane forces in the centre-edge and corner panels reduced the torque which would normally have been induced in the exterior beams and slowed the development of steel strains at these edge sections. It was only after the formation of plastic hinges in the end spans of the interior beams that the torsion in the end spans of the exterior beams showed up clearly. The reduction in torque to be carried would cause the beams to have greater flexural strength but the presence of axial tension would offset this advantage.

#### 9.3.6.3 Comparison of Measured Membrane Forces

Membrane forces were compared in two ways: Panel and beam forces were compared with the design values, and the beam tensions compared with the sum of slab compressions along a line traversing the full width of the floor.

##### (i) Comparison of Membrane Forces with Those Expected

In designing the beams, the mean membrane forces were taken as 340 lb/in for the centre panel; 270 lb/in in the long direction of the centre-edge panels; zero in the short direction of the centre-edge panels and in the corner panels.

Figure 9.32 shows that, at 775 psf, centre panel forces

were close to 340 lb/in. No measurement of forces was made in the long direction of the centre-edge panels but Figure 9.36 shows clearly that the membrane action force in the short directions was underestimated and had a value of approximately 200 lb/in at 775 psf, set up principally as a reaction against the compressive forces in the centre panel.

Expected and actual beam tensions did not show particularly good agreement at 775 psf as may be seen from Table 9.11:

Table 9.11. Beam Tensions at Predicted Ultimate Load (775 psf).

	<u>Expected Value</u>	<u>Measured (Mid-span)</u>	<u>Measured (Support)</u>
Interior Beam Centre Span	17.6 <sup>K</sup>	8.7 <sup>K</sup>	14.9 <sup>K</sup>
Exterior Beam Centre Span	5.2 <sup>K</sup>	6.6 <sup>K</sup>	11.4 <sup>K</sup>
Total	22.8	15.2	26.3

(ii) Comparison of Tensions with Compressions

Line 2 was the only line along which sufficient data existed to allow such a comparison to be made. Figure 9.38 shows the variation of the sum of support section tensions in the exterior and interior beam sections cut by line 2. As in the summing of moments along this line, the figure of 130" was used to factor the panel edge forces per unit

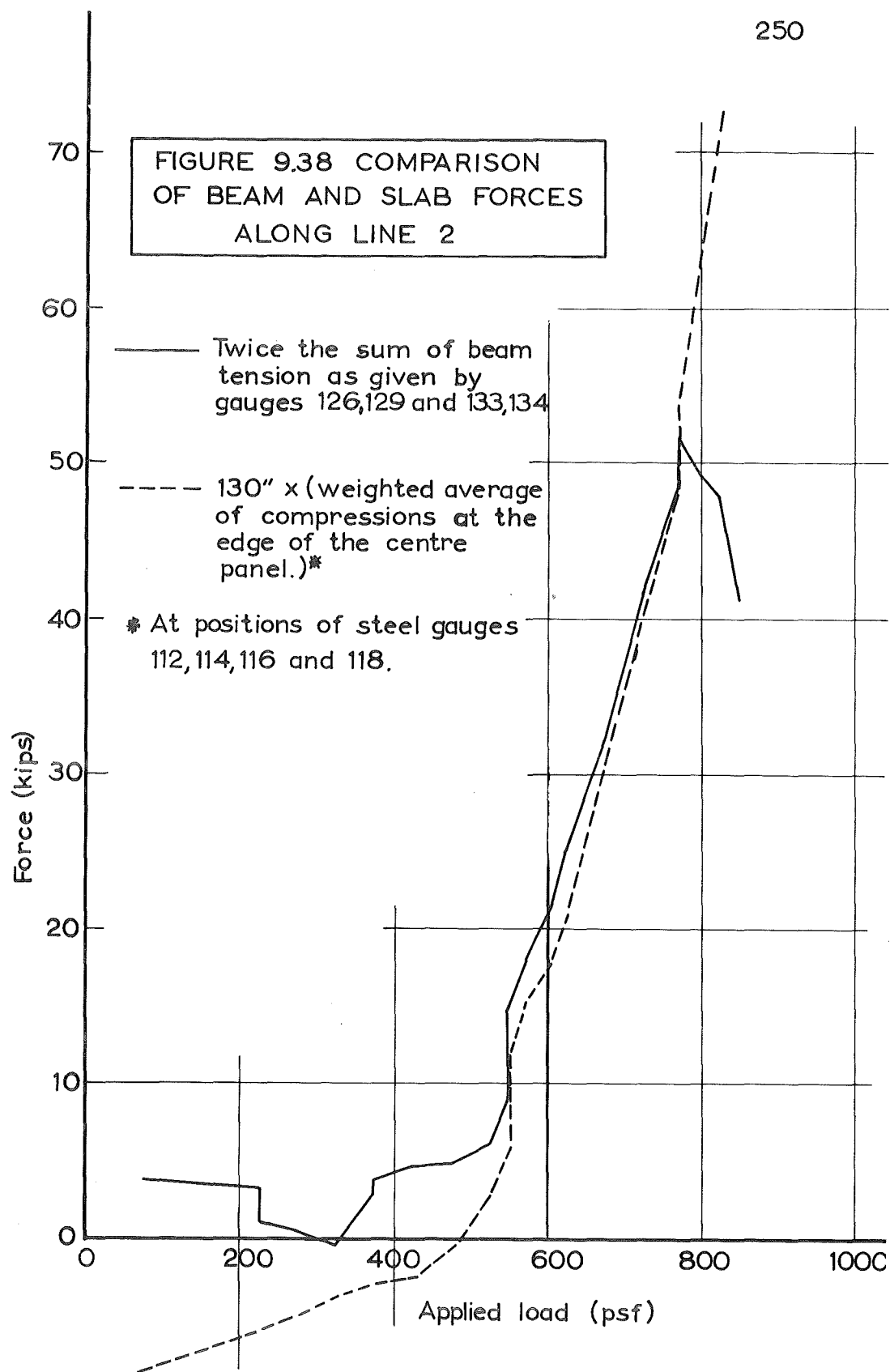
width. The force at each of the panel edge sections was weighted according to the length of centre panel edge it covered (half the distance to the next gauged section on either side).

Between 550 psf and 775 psf, the values compared well but after 775 psf, panel compression continued to rise while the tension in the beams fell. In this comparison it was assumed that the centre-edge panel forces were of a similar order to that expected, which leaves room for considerable variation. However, unreliable strain readings in the panel edge sections seem to be the only possible source of this divergence of values. Values of compression at the panel edge did fall sharply as the push-through failure took place and continued to fall as the tensile membrane was forced to spread from the centre. The curves show good correlation of rates of increase for the greater part of the load range.

#### 9.3.6.4 Conclusions and Discussion

In spite of some inconsistent results, the measured tensions and compressions and the variation of strain readings with load served to illustrate how enhancement of panel strength by membrane action was achieved and the effect it had on the supporting structure.

The mechanism by which panel compression was resisted by beam tensions was clearly active. The presence of compressive membrane action in the corner panels and the short



direction of the centre-edge panels produced a more complex distribution of membrane forces than would have resulted from the simple mechanism assumed in the design of the floor.

Beams would have shown greater distress if all panels had reached failure simultaneously since all panels would then have exhibited maximum compressive membrane action.

Cracking, especially initial cracking, of the panels surrounding the centre panel had a marked effect on the centre panel behaviour: The centre panel deflection increased with the loss of surround stiffness.

As centre panel deflection increased, membrane compressive forces normal to the diagonals increased near the corners but decreased towards the centre of the panel.

The deflection at failure of the centre panel was almost equal to the panel depth, as compared with  $.5D$  used in Park's equations. The deflections of the beams had little to do with this high value. The more flexible surround clearly allowed greater deflection, while the development of high compression near the edges of the slab provided sufficient enhancement for the panel to sustain the required load in spite of a small central tensile membrane region. The low reinforcement content meant that a relatively low compressive force was needed to produce the required enhancement and the high span to depth ratio and low surround stiffness combined to affect the geometry

of the mechanism in a way that allowed the development of the tensile membrane before concrete crushing occurred. These factors also led to the higher stability in the centre panel, though at the expense of load enhancement. The instability brought by a stiffer surround was seen at LS200 when the deflection of the centre panel increased in jumps and it was clear that had the surround not cracked and become less stiff the ultimate load of the centre panel would have been greater than 850 psf.

The large difference between measured tensions at the mid-span and support sections of the beams could be due, in part, to the effect of horizontal shear along the junction of beam and panel. Further difference could have resulted in the different accuracies of the "no-tension" assumption in the computation of moments due to the different flexural bond requirements at these points.

## CHAPTER 10

### DISCUSSION OF TEST RESULTS

#### 10.1 SUMMARY

The effect of membrane action on the behaviour of the model floor was the subject of particular interest. The preceding three chapters have dealt with the design, construction, instrumentation and behaviour under load, of the nine-panel model floor. In this chapter the principal findings of the test are discussed. Particular reference is made to the adequacy of the design method. General conclusions as to the behaviour of the floor and the suitability of the design method are drawn.

#### 10.2 DISCUSSION OF TEST RESULTS

##### 10.2.1 Beam Behaviour

Without question, the behaviour of all spans of all beams was satisfactory at service load. Flexural steel in the end spans was known to be excessive and it was the behaviour of the centre spans of both interior and exterior beams which was of chief interest. That all the additional longitudinal steel placed in these spans was required to resist the induced tensions was evidenced by the high



tensions measured and the high level of steel strains recorded simultaneously at mid-span and at the support, immediately prior to the failure of the centre panel.

The behaviour of these centre spans showed that the assumption that the concrete would take no shear was conservative for the interior beams at least. This was probably true for the exterior beams but the incomplete development of yield moments along the edges of panels adjoining these spans reduced the torsional load on the exterior beams and the situation was not as clear.

The proportion of the total tension taken by the exterior beams at 775 psf was larger than calculated in design. Design values, computed assuming the two corner and one centre-edge panel to be a continuous beam of constant flexural rigidity, were  $17.6^K$  and  $5.2^K$  for the interior and exterior beam respectively, a ratio of 3.4 to 1. Had the deep surrounding beam, formed by the outer panels, been assumed rigid and the tensions distributed according to the concrete section areas of the beams, values of  $12.8^K$  and  $10^K$  would have resulted giving a ratio of 1.28 to 1. Ratios of measured values were 1.32 at mid-span and 1.30 at the support. Both methods of calculation are simplifications but the measured values suggest that the latter method is a closer approximation to the actual relative distribution of tension.

### 10.2.2 Lateral Restraint of the Edges of the Centre Panel

Outward movements of the elements surrounding the centre panel had a marked effect on the centre panel behaviour. The outer panels clearly contributed to the lateral surround stiffness by flexural and shear action. The fact that cracking of the undersides of the outer panels produced large increases in centre panel deflections, strains and cracking, was a vivid illustration of this. The reduction in lateral stiffness produced by this cracking was not measured but the sharp change in centre panel behaviour after cracking suggested that the uncracked surround would have had sufficient lateral stiffness to enhance the load well beyond that finally attained.

### 10.2.3 Centre Panel Behaviour

The behaviour of this panel at service load was very satisfactory but an illustration of the possible effects of surround stiffness loss which could occur with time was obtained when the load was raised 75 psf above the total service load of 400 psf. Cracking of the panels surrounding the centre panel caused large increases in strains, deflections and cracking in the centre panel. The possibility that this could have resulted from sustained service loading can not be overlooked, but the centre panel did show adequate stability during the application of service load for 66 hours.

The increase in membrane compression normal to the edges was sharper at higher loads, most probably as a result of the high cracking load and the greater tendency for the edges to spread outward after underside cracking.

With the loss of lateral stiffness of the surround, edge compression reduced and the deflection increased, but the sensitivity of the panel to further loss of surround stiffness was reduced. There was an increased tendency for the panel to form a tensile net at the centre, supported by an outer region of high compression. With very stiff surrounds, much greater enhancement factors than 2.0 may be achieved for lightly reinforced panels and the failure is far more unstable. The failure of the centre panel in this case was not sudden, due to the gradual spread of the tensile membrane region and large deflection which took place before very high compressive forces normal to the diagonals crushed the concrete in these regions and brought about failure. It was because this region of high compression did not extend the full length of the diagonal and because the deflection at the middle was already high that "failure" was comparatively gentle.

The ability of the centre panel to sustain more than twice its Johansen load in this practical situation was encouraging, especially in view of the near equality of experimental and predicted ultimate loads.

#### 10.2.4 Centre-edge and Corner Panel Behaviour

These panels sustained well in excess of 800 psf due to enhancement by compressive membrane action. Values of measured membrane forces suggested that membrane action enhancement was active in both directions. The low level of hogging moment along the exterior long edge indicated that enhancement due to membrane action was larger than expected. Two possible causes account for the low moments along this line.

Membrane forces perpendicular to this edge would have reduced the torsion in the exterior beam and at the same time enhanced the moment at the edge beyond that indicated by the low level of steel strains.

If no compressive membrane forces had existed perpendicular to the beam at the edge of the slab, the edge moments would have been very low and the load carried by membrane action in the long direction would have had to be greater. Hogging moments would not develop because of the reduced torsional stiffness of the exterior beams after cracking.

Which of these situations applied was not clear. Large membrane forces were measured perpendicular to the interior long edge and for equilibrium it appears that forces perpendicular to the exterior long edge must be of similar magnitude. However, it is unlikely that the exterior beams alone could withstand a lateral force of

200 lb/in without deflecting sideways.

It seems more likely that only small compressive membrane forces acted normal to the exterior long edge and that the large forces in this direction at the interior long edge were distributed to the beams in the manner shown in Figure 10.1, leaving very little compressive membrane force reaction against the laterally flexible edge beam.

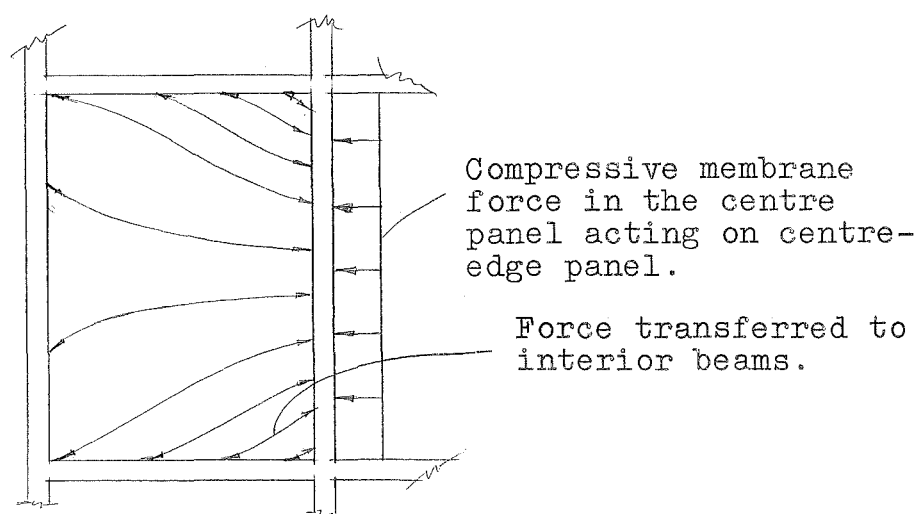


FIGURE 10.1. MEMBRANE FORCE DISTRIBUTION IN SHORT DIRECTION OF CENTRE-EDGE PANEL.

Compressive membrane action accounts for the high load capacity of the corner panels, although in this case membrane action was not allowed for in either direction. The low span to depth ratio and the relatively higher lateral stiffness of the edge beams (due to their shorter spans and to the effect of the extra steel placed in sections where cutoff could not be achieved) favoured the

development of compressive membrane action. Again, forces perpendicular to the exterior edges of the slab could not develop to any large degree and the reaction due to the centre-edge panel membrane action could enhance the load in the manner shown in Figure 10.2.

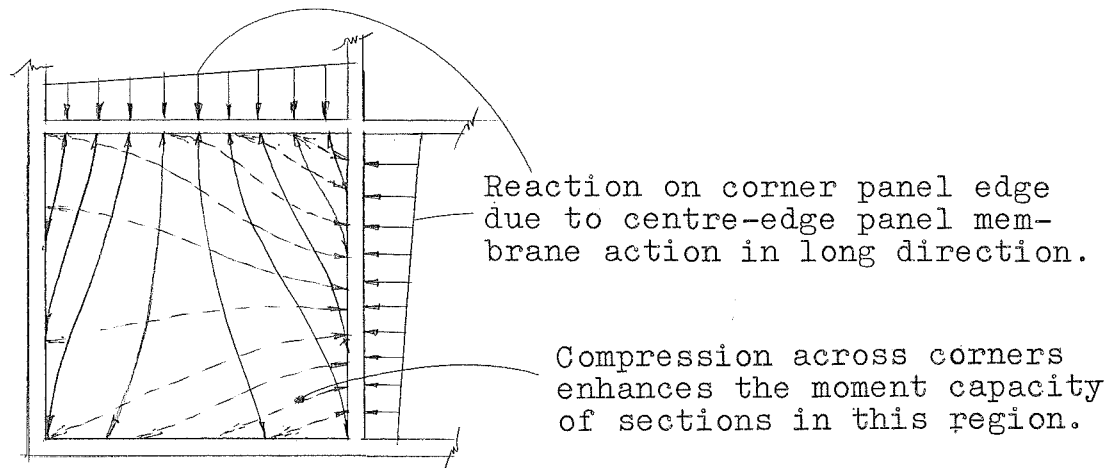


FIGURE 10.2. CORNER PANEL MEMBRANE FORCES.

#### 10.2.5 General Behaviour of Floor

The method of design for the centre panel and beams proved adequate in that the expected loads were sustained and the extra steel placed in the beams was required. The interaction of elements was seen to be of critical importance when membrane action is to be relied upon to enhance the load carrying capacity of slab panels. Had the enhanced capacities of the outer panels all been 850 psf, the centre panel may not have carried this load. Increased deflection of the outer panels would have reduced the

lateral stiffness of the surround restraining the centre panel edges. Such a situation could have been achieved by increasing the size of the outer panels but this would have meant designing the corner panels with an enhancement factor substantially greater than 1.0. The effects of an increase in outer panel size would be beneficial to the centre panel initially but after the outer panels cracked and their deflection increased, the advantage of greater breadth of surround would be lost. Had all panels shown approximately the same load capacity, beam tension would have been higher as a result of the simultaneous action of high membrane forces.

Extrapolation of the results of this test is therefore difficult in view of the unknown effect that transverse loading of the outer panels has on their lateral stiffness. However, the results indicated that it would be possible to assess the contribution of membrane action provided due allowance was made for the sensitivity of the panels to loss of surround stiffness.

#### 10.2.6 Measurement of Moments and Forces at Slab and Beam Sections

The methods used to measure forces and moments at sections by means of strain readings proved satisfactory. The performance of the method in this test pointed to several ways in which the method could be improved.

Measurement of concrete strain must be made over a

length sufficient to average the effects of aggregate size. In lightly reinforced slab sections the length over which very high concrete strains occur is much smaller than the desirable length for gauges. Furthermore, in any section, measurement of concrete strain at the point where crushing will occur, must be subject to doubt when high strains are reached because of the steep strain gradient likely to occur along the length of the gauge. It appears more reliable to place the concrete gauge in a position of low strain gradient and relatively low maximum concrete strain.

In the centre panel, the compression perpendicular to the diagonals reached a very high value and increased with distance from the centre. Measurements of this compression during the test would have been valuable, especially when the initial failure of the centre panel was imminent.

In tests carried out over a period of days, electrical drift and time effects in the concrete are likely to introduce errors into strain readings. Reduced sensitivity to such errors may be achieved by placing gauges in regions of relatively high strain.

In cases, such as in the centre panel of this floor, when membrane forces will be only moderately high, tests of short duration would probably yield more reliable results.

#### 10.2.7 Technical Aspects

The methods used for recording and measuring reactions,



strains and deflections were entirely satisfactory.

The use of water in the loading bags presented problems in the manufacture of absolutely water-tight bags but this did not outweigh the advantage of safety arising from the use of water instead of air in the pressure bags. The simplicity of setting and maintaining the load with water-filled bags proved a great advantage. The flexibility of the reaction frame did reduce considerably the sensitivity of the loading system to rapid fall-off in load and although this meant that the falling branch of the load-deflection curve of the centre panel could not be followed exactly, the use of water permitted satisfactory control of load during failure.

### 10.3 CONCLUSIONS

On the basis of the behaviour of the model floor under load and the above discussion, the following conclusions as to the behaviour of the floor and design method were drawn.

(i) The design method for the panels proved satisfactory but left no margin for deterioration of behaviour of the centre panel under the action of service load for an indefinite period.

(ii) Compressive membrane action enhanced the load carrying capacities of all panels. The corner and centre-edge panels carried well in excess of the required 800 psf.

In the centre panel, compressive membrane action more than doubled the load capacity and enabled it to perform satisfactorily at a total service load of 400 psf.

(iii) Membrane forces measured at the edge of the centre panel were of the same order as those predicted by the theory due to Park.

(iv) The deflection of the centre panel at failure was approximately equal to the slab depth and occurred after tensile membrane forces had developed at the centre.

(v) Only moderate lateral restraint was provided by the panels surrounding the centre panel, resulting in large deflection at failure and the formation of a partially self-equilibrating system of a central tensile region supported by an outer region of compression.

(vi) Cracking of the panels surrounding the centre panel caused a significant loss of lateral stiffness.

(vii) Compressive membrane forces in the floor panels were carried almost entirely by tension in the beams. Outer panels provided stiffness against outward bowing of the surround but carried little or no tension after they had cracked.

(viii) The tension induced in the beams was of the same order as designed for.

(ix) It is conservative to neglect shear taken by the concrete in beams carrying axial tension but some account must be taken of the reduced shear capacity due

to the effect of axial tension.

(x) Membrane action in the outer panels suppressed the formation of hogging yield moments along those edges supported by exterior beams: the panel deflection required to develop sufficient membrane action was less than that required to develop full hogging yield moments against the torsionally flexible edge beams.

(xi) Stability of the centre panel under 66 hours of sustained service load was more than satisfactory but extrapolation of this result to predict behaviour under loading sustained indefinitely is difficult in view of the sensitivity of the centre panel behaviour to very small increases in outward movement of the panels surrounding it.

(xii) Had the outer panels been larger, their increased deflection and cracking at any given load would have reduced the surround stiffness even further, and the simultaneous demand of all panels for high membrane action enhancement would have increased the tension induced in the beams.

(xiii) Measurement of compressive membrane forces perpendicular to the diagonals would have provided interesting information as to the extent of the tensile membrane at the time of initial failure. The large values that these attained would have made their measurement easier.

(xiv) The interaction of the different elements of

the floor was particularly noticeable in this case - an example of the value of testing structural systems rather than separate elements.

## CHAPTER 11

### A COMPARISON OF THE REINFORCING STEEL REQUIREMENTS OF THE MODEL FLOOR, DESIGNED WITH AND WITHOUT ALLOWANCE FOR MEMBRANE ACTION

#### 11.1 INTRODUCTION AND SUMMARY

When compared with normal design procedure, the method of design used for the model floor resulted in a saving of panel reinforcement but an increased amount of steel in the beams. In view of the satisfactory behaviour of the model floor it is of interest to compare the actual amounts of steel involved and to determine whether a net loss or gain results. Such an analysis was performed using straightforward procedures to calculate the steel volumes required. The analysis showed that for the model floor, approximately 7 per cent extra steel was required for membrane action design.

However, in cases where the beam steel for earthquake moments ( $EQ + DL + \text{Seismic LL}$ ) exceeded that required for full service load moments ( $DL + LL$ ) plus tension induced by membrane action, a saving of total steel could be made by allowing for membrane action in the design of the panels. It was concluded that when earthquake moments governed the

strength of the beams, design of the panels for a service load of  $DL + \frac{2}{3}LL$  (without allowance for membrane action) could be considered.

## 11.2 GENERAL BASIS OF COMPARISON

In calculating the volume of longitudinal steel in the beams, the area of steel at any section of the beam was found by linear interpolation between the critical points (see Figure 11.1). No allowance was made for anchorage length or for standard bar sizes.

One quarter of the positive steel was continued to the support unless a greater amount was required for torsion. One third of the negative steel was extended a distance of one tenth of the span past the point of inflexion. The additional steel required for beam tension was calculated from the difference between steel areas at the critical sections with and without tension. The extra volume is represented by the shaded areas on Figure 11.1.

The volume of shear and torsion steel stirrups was calculated according to the actual area of the shear force and torsion diagrams. No extra torsion steel was required for membrane action design but extra shear steel was required because, when the beams were required to carry tension, the shear force carried by the concrete was assumed to be zero.

Panel steel was calculated from the lengths actually

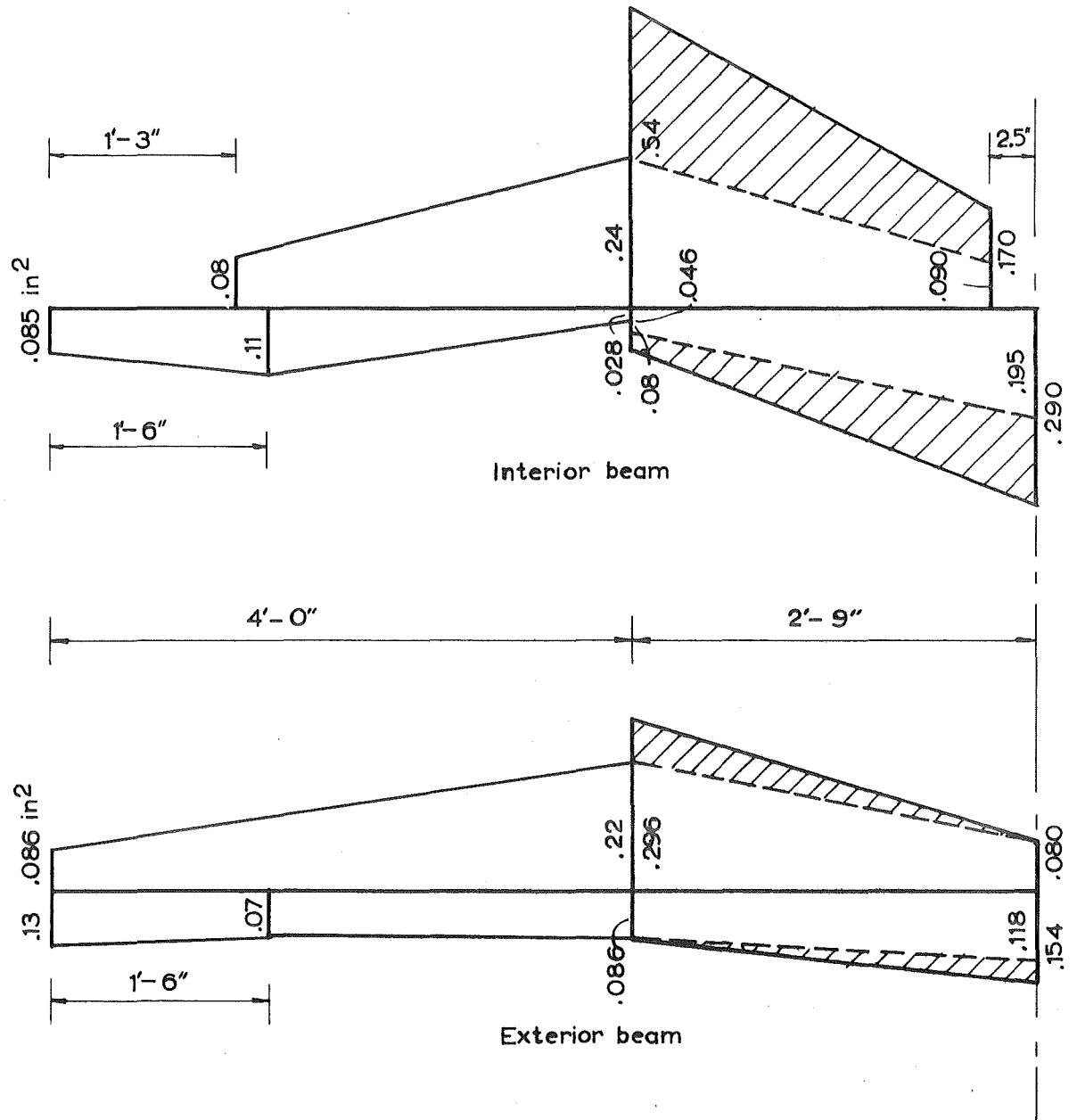


FIGURE 11.1 LONGITUDINAL STEEL IN BEAMS

used. For design with no membrane action the volume of steel in the slab was taken as the volume allocated for the membrane action design multiplied by the enhancement factor appropriate to the panel.

### 11.3 COMPARISON OF STEEL VOLUMES

#### 11.3.1 Panel Steel

(a) Bottom steel as placed:

35 lengths of  $\frac{1}{8}$ " diameter each way, 13.79 ft.  
long

$$\text{Volume} = 142.2 \text{ in}^3$$

(b) Top steel as placed: (5" off each end for anchorage)

80 lengths of  $\frac{1}{8}$ " diameter each way x 19.5"

80 " " " " " " x 11.0"

$$\text{Volume} = 57.8 \text{ in}^3$$

Distribution between the panels was the same for top and bottom steel as follows:

Centre panel	.165	times	total	area
4 Rectangular panels	.485	"	"	"
4 Corner panels	.350	"	"	"
	<hr/>			
	1.000			

Without membrane action, panel steel volumes were increased according to the enhancement factors, viz., 1.00 for the corner panels, 1.35 for the rectangular panels and 1.97 for the centre panel.



Table 11.1 summarises the results of the panel steel comparison.

Table 11.1. Panel Steel Volume Comparison.

<u>Membrane Action</u> <u>Design:</u>	<u>Panel(s)</u>			
	<u>Centre</u>	<u>Rectangular (4)</u>	<u>Corner (4)</u>	<u>All</u>
Top	9.5	28.1	20.2	57.8
Bottom	23.5	69.0	49.7	142.2
Total	33.0	97.1	69.9	200.0
<u>Conventional Yield</u> <u>Line Theory Design:</u>				
Top	18.7	38.0	20.2	76.9
Bottom	46.3	93.0	49.7	189.0
Total	65.0	131.0	69.9	265.9
<u>Difference:</u>				
Top	9.2	9.9	-	19.1
Bottom	22.8	24.0	-	46.8
Total	32.0	33.9	-	65.9

---

All volumes in cubic inches.

### 11.3.2 Overall Comparison

The volumes of longitudinal beam steel were calculated from the areas shown in Figure 11.1.

The total volume of shear steel in the beams was assumed to be proportional to the total area of the shear force diagram, less the area represented by the shear taken by the concrete. Similarly the total volume of torsion stirrups was assumed to be proportional to the net area of the torsion diagram.

The results of calculations of beam and slab steel volumes are given in Table 11.2.

Table 11.2. Steel Volume Comparison - All Elements.

<u>Element</u>	<u>Steel Volume (in<sup>3</sup>)</u>			<u>Per Cent</u>
	<u>Membrane</u>	<u>Y.L.T.</u>	<u>Differ-</u>	<u>Saving</u>
	<u>Action</u>	<u>Design</u>	<u>ence</u>	
	<u>Design</u>			
SLAB				
Centre Panel	33.0	65.0	32.0	49.3
4 Rect. Panels	97.1	131.0	33.9	25.9
4 Corner Panels	69.9	69.9	0.0	0.0
All Panels	200.0	265.9	65.9	24.8
EXTERIOR BEAMS				
Long. Steel	171.8	153.9	-17.9	-11.3
Shear Steel	24.8	16.8	-8.0	-47.7
Torsion Steel	56.0	56.0	0.0	0.0
EXT. BEAM TOTAL	252.6	226.7	-25.9	-11.3
INT. BEAMS				
Long. Steel	213.6	146.6	-67.0	-45.8
Shear Steel	40.6	20.4	-20.2	-99.1
Torsion Steel	0.0	0.0	0.0	0.0
INT. BEAM TOTAL	245.2	167.0	-87.2	-52.2
BEAM TOTAL	506.8	393.7	-113.1	-28.8
FLOOR TOTAL	706.8	659.6	47.2	-7.2

#### 11.4 DISCUSSION

The figures of Table 11.2 show that for the membrane action design the volume of the additional steel required in the beams exceeded the volume of steel saved in the

panels and that the net difference was 7.2 per cent of the total steel volume which would have been required for normal yield line theory design. Before conclusions can be drawn from these figures several aspects require discussion.

(a) Method of Steel Volume Calculation

The method of longitudinal steel volume calculation represents a compromise between the exact following of bending moment, tension, and torsion variation, and the restraints imposed by practical considerations. The method used for shear and torsional stirrup requirements, in following exactly the variation of shear force and torsion, took no account of minimum steel requirements of codes of practice. There was therefore a tendency to underestimate the total stirrup steel volume and to overestimate the additional steel required when tension was present.

(b) Adequacy of Design Assumptions

The volume of steel required for membrane action design was computed on the basis of the steel used in the model floor. High steel strains in both interior and exterior beams confirmed that the longitudinal steel placed was not excessive. However the beams did not show signs of failure at any stage and a small percentage of this steel could have been unnecessary. The same may be said of the stirrups. No strain measurements were taken

on this steel and the degree of excess was difficult to determine.

It is reasonable to conclude that a small amount of the steel placed in the beams was unnecessary and that the net loss would be no greater than the 7.2 per cent quoted in Table 11.2.

(c) Dual Use of Beam Steel Required for Earthquake Actions

The model floor was typical of a floor in a multi-storey reinforced concrete frame building but the beams were designed for vertical loads only. In earthquake-prone areas, beams supporting a typical floor of a multi-storey frame building would be required to resist considerable earthquake moments. The steel placed to counter these moments could well be more than is required to resist the moments and tensions due to vertical loads alone. Two principal reasons exist for this. Firstly, the earthquake moments in the beams may act in either direction requiring additional steel at the bottom of the support sections. The second factor is the allowable reduction in live load when earthquake forces are considered. NZSS 1900 Chapter 8<sup>(36)</sup> allows design for the combination of earthquake forces and the vertical loads to be for a load of

Dead load +  $\frac{1}{3}$  live load + earthquake

(DL +  $\frac{1}{3}$  LL + EQ)

for buildings with relatively low live loads and

$$DL + \frac{2}{3} LL + EQ$$

for high live loads.

Thus, when earthquake beam moments are relatively high, it may be possible to design some interior floor panels by ordinary yield line theory for a load of  $DL + \frac{1}{3} LL$  or  $DL + \frac{2}{3} LL$  having ensured that when vertical load only is considered:

(i) Membrane action in the panels will provide sufficient assistance to carry the balance of live load.

(ii) The beam steel required for the full live load condition does not exceed that required for  $DL + \text{part } LL + EQ$ .

Condition (i) will be satisfied if the surrounding panels provide sufficient lateral stiffness, and if the beam steel is sufficient to carry the tension induced by the membrane action. Satisfaction of condition (ii) will depend upon the relative magnitudes of earthquake and full live load moments.

For the steel areas involved in the model slab, the ratio ( $M_{EQ}/M_{DL+LL}$ ) was determined for which, at the support section of the beams:

$$(\text{Steel for } DL + \text{part } LL + EQ) = (\text{Steel for } DL + LL)$$

The method by which comparison was made is described below.

Let  $A$  = total area of steel at section for moment and

tension at DL + LL.

$A_m$  = that part of A required for moment only.

$A_t = A - A_m$  = extra steel required for tension

F = ratio of panel ultimate load to Johansen load.

v = the proportion of live load considered to act concurrently with horizontal earthquake loads.

The moment acting on the section is directly proportional to the load and the following assumptions were made in determining the steel areas:

(a)  $A_m$  was directly proportional to moment. This is true to a first approximation since the distance between the lines of action of the steel and concrete forces in the section is relatively insensitive to change in moment. In fact, an increase in moment will cause a reduction in this distance and the actual amount of steel will be slightly more than assumed here.

(b)  $A_t$  was directly proportional to tension (c.f. Figure 4.3 (b)).

(c) Tension was directly proportional to the amount by which the applied vertical loading exceeded the Johansen load. This implies that compressive membrane action in the panels commences when the Johansen load is reached, which, although open to question is reasonable in this context.

(d) The tension induced in the centre spans of beams at the ultimate load was  $5.2^K$  for the exterior beams and  $17.6^K$  for the interior beams. It was assumed that  $5.2^K$  of

the  $17.6^K$  was due to the compression in the centre-edge panel.

Calculation of  $M_{EQ}/M_{DL+LL}$  (=Z) for the Interior Beam for

$$v = \frac{2}{3}$$

At the support:  $A = .54 \text{ in}^2$ ;  $A_m = .24 \text{ in}^2$ ;  $A_t = .30 \text{ in}^2$   
 $= 1.25 A_m$ . In this case  $DL = 100 \text{ psf}$ ,  $LL = 300 \text{ psf}$ ,  
 ultimate load =  $800 \text{ psf}$ . Johansen load of centre-edge  
 panel =  $800 \div 1.35 = 594 \text{ psf}$ . Johansen load of centre  
 panel =  $800 \div 2.0 = 400 \text{ psf}$ .  $DL + \frac{2}{3}LL = 300 \text{ psf}$  which  
 requires design for an ultimate load of  $300 \times 2.0 = 600$   
 psf.

By assumption (c) there is no membrane action in the  
 centre-edge panel at this load and from assumption (d)  
 the tension in the interior beam will be reduced by  $5.2^K$ .

Membrane action in the centre panel will be reduced  
 to  $(600-400)/(800-400) = \frac{1}{2}$  of its full load value. The  
 contribution of the centre panel to the interior beam  
 tension at full load is, by assumption (d),  $= 17.6^K - 5.2^K =$   
 $12.4^K$ . Therefore the tension must be reduced by half of  
 this  $= 6.2^K$ . Thus the tension in the beam at  $600 \text{ psf}$  is  
 assumed to be

$$T = 17.6^K - 5.2^K - 6.2^K = \underline{\underline{6.2^K}}.$$

Using assumption (b) it is found that the area of steel  
 required for this tension is  $(6.2/17.6)A_t = .35A_t = .44A_m$ .  
 The steel required for moment will be  $(600/800) A_m = .75A_m$

and the steel required for earthquake moment only is equal to

$$A_m (M_{EQ}/M_{DL+LL}) = A_m \cdot Z$$

The total steel required for  $DL + \frac{2}{3}LL + EQ$  will thus be

$$A_m (.44 + .75 + Z)$$

whereas for  $DL + LL$  the total required is  $A_m (1+1.25) = 2.25A_m$ .

Hence for earthquake conditions to govern:

$$1.19 + Z > 2.25 \text{ or } Z > 1.06.$$

Conditions for this case and the others were:

$$\underline{DL + \frac{2}{3}LL} \quad \text{Interior Beam:} \quad Z > 1.06$$

$$\text{Exterior Beam:} \quad Z > .72$$

$$\underline{DL + \frac{1}{3}LL} \quad \text{Interior Beam:} \quad Z > 1.75$$

$$\text{Exterior Beam:} \quad Z > .97$$

It is important to note that whereas the  $DL + \frac{2}{3}LL$  condition required extra tension steel, the  $DL + \frac{1}{3}LL$  condition did not.

However, any disadvantage in the former case is offset by the presence of earthquake steel required for the reversal of loading which was not included in the above analysis. Since the values of  $Z$  shown above are frequently exceeded in practice, it would be possible in many cases to design the panels by normal yield line theory to sustain substantially less than the full live load.

Such a design procedure would require careful



consideration of the conditions of lateral restraint at the edges of the panels which would make the method less attractive. But the above analysis indicates that existing floors satisfying the necessary conditions for membrane action would have a considerable reserve of strength.

#### 11.5 CONCLUSIONS

The preceding analysis has shown that membrane action design requires more steel to be placed in the supporting beams than could normally be saved in the panels.

In situations in which beam steel is required for other loads such as earthquake loading, a net saving of steel could be achieved.

Floors in which this saving could be made would have to:

- (i) Be required to sustain live loads high enough for minimum steel requirements not to govern the determination of panel steel.
- (ii) Be part of relatively tall frame buildings in which earthquake moments are high.
- (iii) Contain panels whose edges meet a high degree of restraint against lateral movement.

An important corollary to the conclusions above refers to panels of multi-panel slab and beam floors in which the beams have been designed to resist earthquake moments, viz., many of these panels, even when designed by yield

line theory, will be capable of carrying loads which are very much greater than those for which they have been designed. Furthermore, this will apply to cases in which adjacent panels of the floor are loaded simultaneously, provided the supporting columns are not overloaded.

## CHAPTER 12

### GENERAL CONCLUSIONS

#### 12.1 CONCLUSIONS FROM WORK PERFORMED

Conclusions have been drawn at the end of each section, some of which are included in the following general conclusions.

(a) Concrete slabs reinforced with the minimum of steel required by Codes of Practice can sustain high loads without assistance from compressive membrane action. The benefits of enhancement of load due to membrane action will therefore be of greatest significance for slabs which are required to carry high loads.

(b) For a rectangular, orthotropically reinforced slab with equal hogging moments along opposite edges, a ratio of hogging to sagging moment in each direction equal to 2.0 gives the least volume of slab steel. Negative moment steel should extend into the slab for a fraction,  $\lambda$ , of the span from each edge such that  $2\lambda = 1 - \frac{1}{\sqrt{1+i}}$ , where  $i$  is the ratio of hogging yield moment to sagging yield moment in that direction. This length of top steel results in identical collapse loads for all four symmetrical yield line patterns for the panel.

(c) The assumption of rigid-plastic materials in the analysis of a clamped circular slab with its edges restrained elastically against outward movement is not accurate when the edge restraint is small. For very stiff surrounds the assumption is sufficiently accurate to compare well with experimental results.

(d) The absence of top steel at the edges of laterally restrained slabs has little effect on the ultimate load. The complete omission of top steel may not be wise but its length could be reduced in slabs subject to compressive membrane forces.

(e) Assessment of the effective surround movement should include the effects of slab shortening, creep and shrinkage. As the flexibility of the surround increases, it becomes increasingly important to account for vertical slab deformations occurring prior to the full development of yield lines.

(f) When compressive membrane action is exhibited in two adjacent panels of a slab and beam floor system, the common supporting beam must be designed to accommodate the tension induced. Design of the critical sections of such a beam may be performed using the ultimate strength method and limit analysis. It is recommended that in these cases moment redistribution should be kept to a minimum to guard against the adverse effects of beam deformation on the development of compressive membrane action in the panels.

(g) Extra longitudinal beam steel is required in beams which are designed for tension as well as flexure. However, the extra steel required is less than would be required for a pure tie of the same length as the beam.

(h) Membrane forces in slab panels can have an appreciable effect on the torsional moments induced in the beams supporting them.

(i) The outward deformations of the sides of a square surround of elastic material subject to in-plane loads can be closely approximated to those of an equivalent deep beam. Such a simplification would greatly assist in the development of a theory for membrane action which takes into account the interaction between membrane forces and surround movement.

(j) The theory due to Park proved satisfactory in designing a nine-panel model floor. High margins of safety were required when the outward movements of the surrounding panels were calculated on the basis of an elastic, uncracked surround.

(k) Failure of the centre panel of the model floor took place at a higher deflection than the  $0.5D$  used in Park's theory and although membrane forces at the edge were of the same order as predicted by the theory, the tensile membrane stage had commenced before failure occurred.

(l) The extra steel added to the beams of the model floor to take the tension induced was no more than sufficient,

indicating that the beams must be designed to resist the tension induced and that the magnitude of the tensions was satisfactorily predicted and designed for in this case.

(m) Strain gauge measurements on the steel and concrete afforded a successful means of measuring compressive membrane forces in the panels and the tensile forces in the beam sections.

(n) The serviceability of the model floor designed by membrane action theory met code requirements as to deflections and crack widths at service load. The stability of the central panel under sustained service loading was encouraging, especially in view of the high span to depth ratio of 32. More knowledge of the effect of long term loading on restrained slabs in practical situations is required before confident predictions of the long term behaviour of such slabs can be made.

(o) Consideration of membrane action in the design of the nine-panel model floor resulted in a considerable saving of slab steel but the extra beam steel required for tension exceeded that saved in the panels. In favourable circumstances, however, a net saving of steel could be achieved by using the beam steel provided for earthquake moments to carry the tension induced.

(p) When design for earthquake allows a reduction in live load, the steel required for earthquake moments in the beams can be used to carry the tension induced by panel

membrane action. The panels could be designed for reduced live load by yield line theory provided the capacity of membrane action to take the balance is ensured.

## 12.2 SUGGESTIONS FOR FURTHER RESEARCH

An additional margin for safety exists in panels, designed by yield line theory, but having boundary conditions conducive to the development of membrane action. This additional capacity may be utilised by permitting floors to be loaded in excess of the design live load in favourable circumstances.

However, the design of such panels to allow for membrane action is another matter, requiring a reliable and accurate means of assessing the enhancement that membrane action will produce. Although the ultimate load of the central panel of the nine-panel model floor described in Chapter 9 was accurately predicted by an existing theory for membrane action, more research would be required before a reliable design method could be derived. Existing theories and methods of analysis which have been developed principally for slabs with high lateral restraint allow quite accurate prediction of the behaviour of such slabs. But in floor slabs where only moderate lateral restraint exists, these methods cannot be regarded as reliable.

In the case of floor panels in buildings, extremely high design loads would be required before the benefits of

membrane action could be fully exploited. In floors where the enhancement by membrane action could be used, it appears that the overall economic advantages would not be great. The development of a reliable design procedure for slab and beam floors would require:

(i) The development of a theory which accounts for the interaction of membrane forces along the boundary of the slab and the outward movement of the restraining medium. This in itself would not be sufficient because the increasing deflection at ultimate load with decrease in surround stiffness would have to be recognised. In particular, future theories should recognise the tendency for a tensile membrane region to form at the middle of the slab before the ultimate load is reached.

Extension of Park's theory<sup>(11)</sup> using a more refined strip approximation, possibly using the results of Gurfinkel<sup>(16)</sup>, could provide a solution, but the assumption that the membrane force is constant along each strip would require close examination.

(ii) Further investigation of the effects of tension on the behaviour of beams, particularly as to the flexural and shear reinforcement requirements. In cases where the beams provide much of the lateral restraint, knowledge of the effect of tension on the axial stretch would be valuable.

(iii) Experimental studies of the effects of long



term loading of slabs with surrounds of reinforced concrete. These would do much to remove the uncertainty inherent in the sensitivity of membrane action to loss in lateral stiffness.

This work would probably not be warranted in the case of floors where lateral restraint at the edges is usually low and the design loads insufficiently high. For structures such as pressure vessels and blast resistant structures, where the surround stiffness is high, the rigid-plastic theories incorporating an allowance for edge movement (e.g., the theory due to Park) will give satisfactory results, but research on (i) and (ii) above could provide useful improvements for this situation.

The study of the effects of panel membrane action on other parts of the structure is important whether or not the enhancement of the panel is allowed for in design. Further research, particularly experimental, on the effects of membrane action on the torsion induced in the supporting beams could lead to less stringent design requirements for torsion in edge beams in some cases.

This points to the need for further studies of whole structural systems. Tests on separate structural elements have the advantage that the actions applied to the element may be accurately determined because forces due to the interaction of elements may be eliminated. Membrane action is a very good example of a case in which these

interaction effects are beneficial to a degree which is worth considering in design, even if very high safety margins must be imposed.

In studies of whole structural systems it is not sufficient to rely on the equality of steel tension and concrete compression in a beam or slab section and greater importance must therefore be placed on the role of the concrete strain gauges. Further research into the measurement of actions on a reinforced concrete section would be valuable in providing a reliable means of interpreting the experimental data obtained.

# APPENDIX A - DESIGN CALCULATIONS

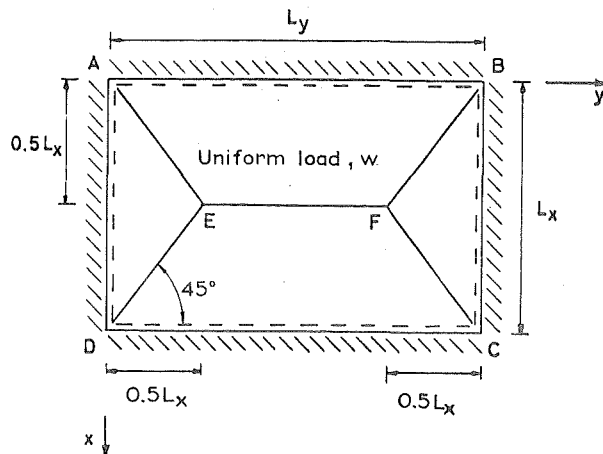
## A.1 PARK'S EQUATIONS FOR THE ULTIMATE LOADS OF PANELS

For the design of the centre and centre-edge panels of the nine-panel model floor, the equations derived by Park<sup>(11)</sup> were used to estimate the contribution of compressive membrane action to their load carrying capacities.

The equations were derived using the approximate yield line pattern of Figure A.1(a). The slab was envisaged as a series of strips in each direction and the sum of axial, creep and shrinkage strains,  $\epsilon$ , and the outward boundary movement,  $t$ , was the same for all strips in the same direction. Conditions of geometrical compatibility and equilibrium of horizontal forces were used to obtain the actions at the critical sections of each strip (see Figures A.1(b), (c), (d)).

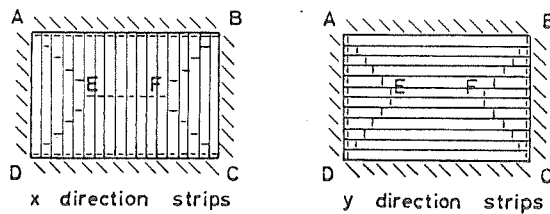
Analysis by virtual work for a slab with all edges restrained and with an empirical value of  $0.5D$  for the central deflection at the ultimate load gave

$$\begin{aligned}
 \frac{wL_x^2}{24} \left( \frac{3L_y}{L_x} - 1 \right) &= k_1 k_3 u D^2 \left\{ \frac{L_y}{L_x} (0.188 - 0.281 k_2) + (0.479 - 0.490 k_2) \right. \\
 &+ \frac{\epsilon'_x (L_x/D)^2}{16} \left[ 2 \frac{L_y}{L_x} (3k_2 - 1) + k_2 - 1 \right] + \frac{\epsilon'_y (L_x/D)^2}{16} \frac{L_y}{L_x} (7k_2 - 3) - \frac{k_2}{8} \frac{L_y (L_x/D)^4}{L_x} \left[ \epsilon_x'^2 + \frac{L_y}{L_x} \epsilon_y'^2 \right] \Big\} \\
 &- \frac{k_2}{2k_1 k_3 u} \left\{ \frac{L_y}{L_x} (T'_x - T_x - C'_{sx} + C_{sx})^2 + (T'_y - T_y - C'_{sy} + C_{sy})^2 \right\} \\
 &+ C_{sx} \left\{ \frac{L_y}{L_x} \left( \frac{D}{4} - d_{2x} \right) + \frac{D}{8} \right\} + C'_{sx} \left\{ \frac{L_y}{L_x} \left( \frac{D}{4} - d'_{2x} \right) + \frac{D}{8} \right\} + T_x \left\{ \frac{L_y}{L_x} \left( d_{1x} - \frac{D}{4} \right) - \frac{D}{8} \right\} \\
 &+ T'_x \left\{ \frac{L_y}{L_x} \left( d'_{1x} - \frac{D}{4} \right) - \frac{D}{8} \right\} + C_{sy} \left( \frac{3D}{8} - d_{2y} \right) + C'_{sy} \left( \frac{3D}{8} - d'_{2y} \right) \\
 &+ T_y \left( d_{1y} - \frac{3D}{8} \right) + T'_y \left( d'_{1y} - \frac{3D}{8} \right) \dots (A.1)
 \end{aligned}$$



— — Hogging moment yield line  
 — — Sagging moment yield line  
 // Fully fixed edge

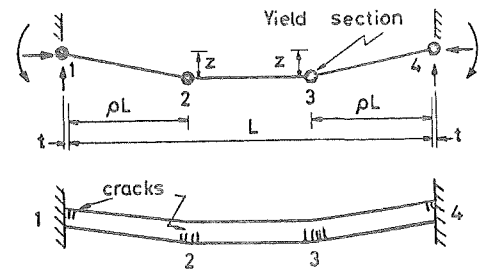
ASSUMED YIELD LINE PATTERN



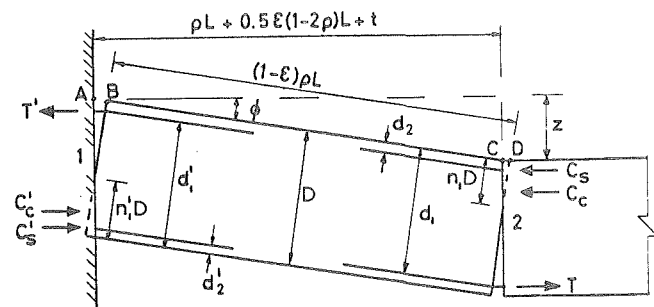
or - Yield sections

STRIPS OF EQUIVALENT SLAB

(a) UNIFORMLY LOADED TWO-WAY SLAB  
 WITH ALL EDGES FULLY FIXED

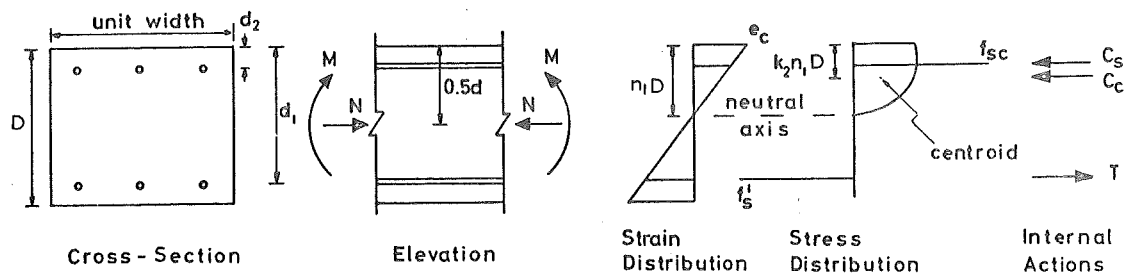


(b) COLLAPSE MECHANISM OF A STRIP.



(c) INTERNAL ACTIONS AT YIELD SECTIONS OF  
 END PORTION OF STRIP.

FIG. 2



(d) CONDITIONS AT A SECTION ON A YIELD LINE WITH SAGGING MOMENT.

FIGURE A.1 STRIP APPROXIMATION IN THEORY  
 DUE TO PARK

In which subscripts x and y denote values in the x and y directions and  $\epsilon'_x = \epsilon_x + \frac{2t_x}{L_x}$ ,  $\epsilon'_y = \epsilon_y + \frac{2t_y}{L_y}$ .

At this load, w, the mean values of the membrane forces in each direction were given by:

$$\begin{aligned} \text{Mean } N_y = k_1 k_3 u D \left[ \frac{7}{16} - \frac{\epsilon'_y}{4} \frac{L_y}{L_x} \left( \frac{L_x}{D} \right)^2 \right] \\ + \frac{1}{2} (C'_{sy} + C_{sy} - T'_y - T_y) \end{aligned} \quad \dots (A.2)$$

$$\begin{aligned} \text{Mean } N_x = k_1 k_3 u D \left[ \frac{3}{8} + \frac{1}{16} \frac{L_x}{L_y} - \frac{\epsilon'_x}{4} \left( \frac{L_x}{D} \right)^2 \right] \\ + \frac{1}{2} (C'_{sx} + C_{sx} - T'_x - T_x) \end{aligned} \quad \dots (A.3)$$

When only three edges were restrained, membrane action was considered to act only in the strips between opposite restrained edges. For a long edge ( $L_y$  direction) unrestrained laterally but restrained against rotation, the ultimate load, w, was given by

$$\begin{aligned} \frac{w L_x^2}{24} \left( 3 \frac{L_y}{L_x} - 1 \right) = k_1 k_3 u D^2 \left\{ .363 - .406 k_2 + \epsilon'_y \left( \frac{L_x}{D} \right)^2 \frac{L_y}{L_x} (.562 k_2 - .25) \right. \\ - .195 \epsilon_y'^2 k_2 \left( \frac{L_y}{L_x} \right)^2 \left( \frac{L_x}{D} \right)^4 + C'_{sy} (.4D - d'_{2y}) + C_{sy} (.4D - d_{2y}) + T'_y (d'_{1y} - .4D) \\ + T_y (d_{1y} - .4D) - \frac{k_2}{2k_1 k_3 u} (T'_y - T_y - C'_{sy} + C_{sy})^2 \\ \left. + \frac{L_y}{L_x} \left\{ T'_x \left( d'_{1x} - \frac{k_2 T'_x}{k_1 k_3 u} \right) + T_x \left( d_{1x} - \frac{k_2 T_x}{k_1 k_3 u} \right) \right\} \right\} \end{aligned} \quad \dots (A.4)$$

and the mean membrane force was given by:

$$\text{Mean } N_y = k_1 k_3 u D \left\{ .4 + .05 \frac{L_x}{L_y} - .312 \epsilon'_x \left( \frac{L_x}{D} \right)^2 \right\} \\ + \frac{1}{2} (C'_{sx} + C_{sx} - T'_x - T_x) \quad \dots (A.5)$$

## A.2 DESIGN OF PANELS

### A.2.1 Slab Thickness

Placement of minimum reinforcement at maximum spacing imposed the following conditions when the British Code<sup>(35)</sup> was used:

$$A_s \geq .0015 s D \quad \dots (A.6)$$

and

$$s \leq 3d \quad \dots (A.7)$$

With two layers of steel of  $\frac{1}{8}$ " diameter and minimum cover =  $\frac{3}{16}$ ", the mean effective depth of the centroid of the two layers of steel was

$$d = D - \frac{5}{16} \quad \dots (A.8)$$

Since  $A_s$  was known, Equations A.6, A.7, A.8 could be solved for  $s$ ,  $D$  and  $d$ . Solution gave  $D = 1.81$  in. but a value of  $1.94$ " was finally set to give a smaller span to depth ratio to assist in the development of compressive membrane action. This gave  $d$  from Equation A.8 as  $1.62$ " which led to a

spacing of 4.25" when Equation A.6 was applied.

### A.2.2 Determination of Panel Size and Negative Reinforcement

#### (a) Centre Panel

The Johansen load,  $w_J$ , of the panel was to be  $w \div 2 = 400$  psf.

The panel was to be square and symmetrical and hence  $m_x = m_y$ ,  $m'_x = m'_y$ ,  $i_x = i_y$ ,  $L_x = L_y$ . When a reduction of 8 per cent for corner effects (see Wood<sup>(7)</sup>, p. 66) is applied, yield line theory gives

$$w_J = \frac{22.1 m_x (1 + i_x)}{L_x^2} \quad \dots(A.9)$$

With  $\frac{1}{8}$ " bars of yield force 640 lb. at 4.25 inch spacing the sagging yield moment is given by ACI 318, Equation 16.1:

$$m_x = \phi A_s f_y (d - a/2) \quad \dots(A.10)$$

where  $\phi = 1.0$  in this case,  $A_s f_y = \frac{640 \text{ lb.}}{.85 f'_c b}$  ( $b = 4.25$ " )

Therefore  $m_x = 241$  lb.in/in

Substituting  $m_x = 241$  lb.in/in,  $w_J = 400/144$  in Equation A.9 gives

$$L_x^2 = 1915 (1 + i_x) \quad \dots(A.11)$$

Several trials were made before values of  $L_x = 62.5$ ",  $i_x = 1.07$  were chosen.

(b) Corner Panels

Since hogging yield moments were to be fully developed along all four edges of these square panels, yield line analysis was identical to that of the centre panel. In this case membrane action was assumed to provide no enhancement of load-carrying capacity and  $w_J = w = 800$  psf.

Both top and bottom reinforcing were to be the same as in the centre panels so that from Equation A.9,  $L_x = 44.5$ ".

(c) Centre-edge Panels

For these panels, then,  $L_x = 44.5$  in.  $L_y = 62.5$  in. The same reinforcement as in the other panels was to be placed. The quantities  $m_x = m_y$ ,  $i_x = i_y$  etc., had the same average values as in the square panels. Equation 2.3, for the collapse load of a rectangular slab, restrained at its edges with allowance for an eight per cent reduction for corner effects and with  $L_y/L_x = 2$  then gave  $w_J = 594$  psf indicating a required enhancement factor of 1.35.

A.2.3 Computation of Maximum Allowable Lateral Spread(a) Centre Panel

The values of  $\epsilon'_x (= \epsilon'_y)$  which gave an ultimate load of 800 psf were determined directly from Equation A.1 in which  $D = 1.94$  in.,  $L_x = 62.5$  in.,  $L_y/L_x = 1.0$ ,  $w = 6.05$  psi (increased by eight per cent for corner effects),  $u = 5250$  psi,  $L_x/D = 32.2$ , mean  $d' = 1.62$  in.,  $T_x = 154$  lb/in



$$T'_x = 164 \text{ lb/in.}$$

For  $u = 5250$ ,  $k_2 = .445$ ,  $k_1 k_3 = .575$ . Substitution of the above quantities in Equation A.1, neglecting the effects of compression steel, gave

$$\epsilon'_x = \epsilon'_y = 13.6 \times 10^{-4}$$

The minimum value of  $\epsilon'_x$  to make the neutral axis depth zero as given by Park<sup>(11)</sup> is

$$\epsilon'_x = 1.5 \left( \frac{D}{L_x} \right)^2 = 14.5 \times 10^{-4}$$

indicating that the neutral axis depth would not reduce to zero at failure.

Substitution of  $\epsilon'_x = 13.6 \times 10^{-4}$  into Equation A.2 gave

$$\text{Mean } N_y = 340 \text{ lb/in.}$$

(b) Centre-edge Panel

In this case:  $L_x = 44.5 \text{ in.}$ ,  $L_y = 62.5 \text{ in.}$ ,  $L_y/L_x = 1.41$ ,  $w = 6.05 \text{ psi.}$ ,  $u = 5250 \text{ psi.}$ ,  $k_2 = .445$ ,  $k_1 k_3 = .575$ ,  $L_x/D = 22.9$ .  $T'_x = 164 \text{ lb/in.}$ ,  $T_x = 154 \text{ lb/in.}$ ,  $T'_y = 172 \text{ lb/in.}$ ,  $T_y = 144 \text{ lb/in.}$

Again ignoring the effects of compression reinforcement forces, substitution in Equation A.4 gave

$$\epsilon' = 16.3 \times 10^{-4}$$

The limiting value for the use of Equation A.4 given by Park is

$$\epsilon'_y = 1.75 \frac{D}{L_x}^2 L_x/L_y = 23.6 \times 10^{-4}$$

Substitution of  $\epsilon'_y = 16.3 \times 10^{-4}$  in Equation A.5 gave  
Mean  $N_y = 270$  lb/in.

#### A.2.4 Beam Tensions

Only the centre spans of the beams had tension induced in them as may be seen in Figure 6.3(a). The outer line of panels was considered as a deep beam of uniform flexural stiffness to give tensions of  $5.2^K$  in the exterior beams and  $17.6^K$  in the interior beams.

#### A.2.5 Outward Movement of Surround

(a) Axial strain in beams was calculated assuming an uncracked concrete section of area,  $A$ , and modulus of elasticity,  $E$ . The contribution of this axial stretch to  $\epsilon'_x$  in Equations A.1 to A.5 was:

$$\epsilon'_{at} = T/EA \quad \dots(A.12)$$

(b) Bending and shear deformation of the surrounding panels was calculated assuming that each panel was a simply supported beam of uncracked concrete with properties as shown in Figure A.2.

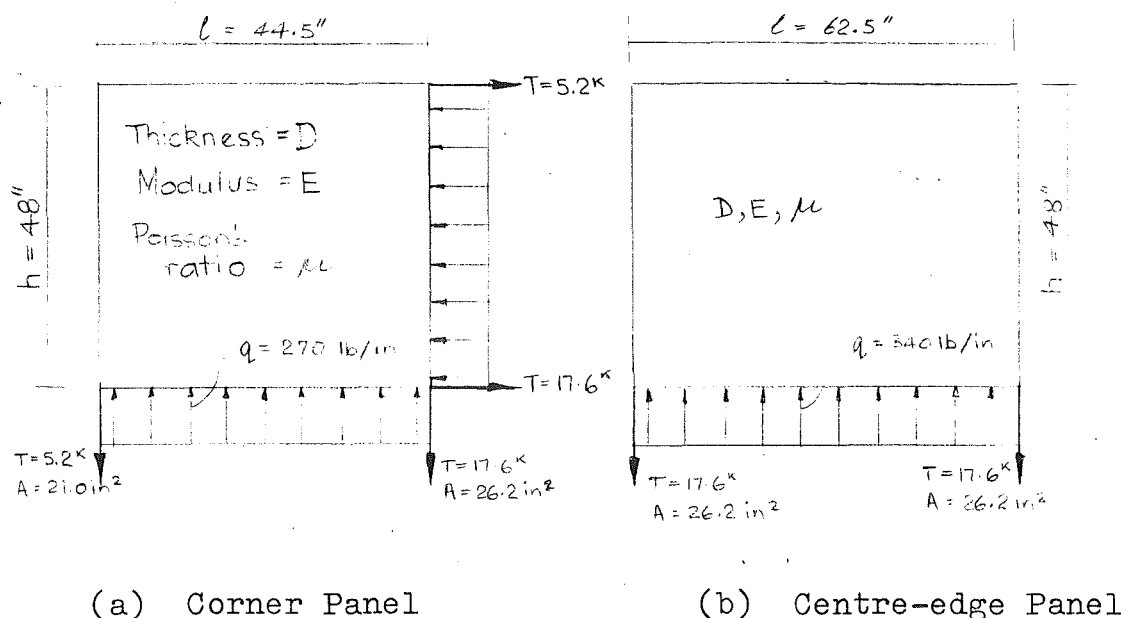


FIGURE A.2. SURROUNDING PANELS AS DEEP BEAMS

Deflection due to bending was negligible compared with shear deformation which may be shown to have a maximum value of

$$\frac{5}{384} \frac{q l^4}{EI} \left( \frac{h}{l} \right)^2 (1 + \mu)(2.4) \quad \dots(A.13)$$

The contribution to surround movement was assumed to be .75 of this and for  $\mu = .15$ ,  $E = 3 \times 10^6$  psi, the contribution to  $\epsilon'_x$  was:

$$\epsilon'_s = 2.16 \times 10^{-8} \frac{q}{D} \frac{1}{h} \quad \dots(A.14)$$

(c) The contribution of axial shortening of a typical slab strip to  $\epsilon'_x$  was

$$\epsilon'_{ss} = (\text{Mean } N_y) / (D \cdot E) \quad \dots(A.15)$$

(d) The contribution of differential shrinkage to  $\epsilon'_x$

was assessed as follows: for a strip of concrete reinforced with a ratio,  $p$ , of reinforcement which has a modulus of elasticity equal to  $n$  times that of the concrete the restrained shrinkage strain,  $\epsilon_r$  may be shown to be given by:

$$\epsilon_r = \epsilon_u / (1 + np) \quad \dots (A.16)$$

in which  $\epsilon_u$  is the shrinkage of an unrestrained strip which was assumed to be .001 (c.f. Figure 6.9). For  $n = 10$ , slab steel ratio = .0025, beam steel ratio = .02, the differential shrinkage strain from Equation A.16 was:  $\epsilon'_{sh} = 1.5 \times 10^{-4}$ .

The total surround movement,  $\epsilon'_x$ , was assumed to be

$$\epsilon'_x = (\epsilon'_s + \epsilon'_{at} + \epsilon'_{ss}) K_s K_c + \epsilon'_{sh} \quad \dots (A.17)$$

in which  $K_s$  was a constant expressing the effect of loss of surround stiffness due to cracking and flexural action of the beams and slabs and  $K_c$  was a factor expressing the effect of creep deformations.

#### A.2.6 Determination of $K_s K_c$

If the maximum allowable outward spread strain required by Park's equations is denoted  $\epsilon'_{xp}$ , then from Equation A.17:

$$K_s K_c = (\epsilon'_p - \epsilon'_{sh}) / (\epsilon'_s + \epsilon'_{at} + \epsilon'_{ss}) \quad \dots (A.18)$$

Designs requiring  $K_s K_c$  to be less than 4.0 were

modified and for the final design the following values resulted:

(i) Centre Panel (Figure A.2(b)):

Equations A.12 to A.16 with  $D = 1.94''$ ,  $A = 26.2 \text{ in}^2$ ,  $T = 17.6^K$  gave

$$\epsilon'_s = .1 \times 10^{-4}$$

$$\epsilon'_{at} = 2.3 \times 10^{-4}$$

$$\epsilon'_{ss} = .6 \times 10^{-4}$$

$$\epsilon'_s + \epsilon'_{at} + \epsilon'_{ss} = 3.0 \times 10^{-4}$$

$$\epsilon'_{sh} = 1.50 \times 10^{-4}$$

and with  $\epsilon'_{xp} = 13.6 \times 10^{-4}$  Equation A.18 gave  $K_s K_c = 4.0$ .

(ii) Centre-edge Panel (Figure A.2(a)):

In this case  $\epsilon'_s = .03 \times 10^{-4}$

$$\epsilon'_{at} = .8 \times 10^{-4} - \text{exterior beam}$$

$$\epsilon'_{at} = 2.3 \times 10^{-4} - \text{interior beam}$$

$$\text{Average } \epsilon'_{at} = 1.6 \times 10^{-4}$$

$$\epsilon'_{ss} = .5 \times 10^{-4}$$

$$\epsilon'_s + \epsilon'_{at} + \epsilon'_{ss} = 2.1 \times 10^{-4}$$

$$\epsilon'_{sh} = 1.5 \times 10^{-4} \text{ as before}$$

With  $\epsilon'_{xp} = 16.3 \times 10^{-4}$ . Equation A.18 gave  $K_s K_c = 7.0$

which could not be reduced without violating minimum reinforcement requirements imposed by CP114.

### A.3 DESIGN OF BEAMS

#### A.3.1 Exterior Beams

##### (a) Design Actions

The critical cases of loading shown in Figure 6.4 (p. 107) gave rise to the design actions shown in Figure A.3. The moments and shears in the beam were calculated from the loading of Figure 6.4 on the assumption that the beam behaved elastically and had uniform flexural stiffness for its whole length.

The mid-point of each span was assumed to be a point of zero torque and the maximum effects at the supports were computed due to the action of the yield moment and eccentric vertical shear at the slab edge. For the end spans this gave the maximum torque,  $M_{tmax} = \frac{1}{2} \cdot L_x m'_x + (\frac{1}{8} \cdot w L_x^2) \cdot \frac{b}{2}$  and for the centre spans:

$$M_{tmax} = \frac{1}{2} \cdot L_y \cdot m'_x + (\frac{1}{8} \cdot w L_x^2 + \frac{1}{2} (L_y - L_x)) \cdot \frac{b}{2}.$$

The development of this torsion caused positive bending moments in the end spans of the adjacent beams at right angles.

##### (b) Size of Cross Section

On the basis of preliminary shear, torsional and flexural strength requirements a section 6" deep and

3½" wide was chosen. The limiting case for flange width as given by ACI 318-63 Clause 906(d) was 1/12 of the span or 4 in.

(c) Allocation of Shear and Torsion Steel

The Australian Code<sup>(33)</sup> gives the nominal concrete stress due to torsion as

$$f_t = \frac{3 M_t}{b^2 d} \quad \dots (A.19)$$

A rectangular section was taken in this case since the torsion was induced by yield moments which developed at the junction of the beam and slab.

For the middle span of the exterior beams the ratio of nominal torsional stress to nominal shear stress (ACI 318-63 Clause 1701) was approximately .7 : .3. This ratio was used in distributing the shear and torsion taken by uncracked concrete sections.

Maximum allowable nominal shear stress in concrete from ACI 318-63 Clause 1701 =  $2\phi \sqrt{f'_c} = 135 \text{ psi } (\phi = .945)$

Shear taken by concrete = 850 lb.

Force in two legs of stirrup = 1000 lb.

$V_u$ 's for vertical stirrups = 6000 lb.in (ACI Equation 17-4)

$V_u$ 's for 45° stirrups = 8500 lb.in (ACI Equation 17.6)

$sM_t$  for vertical torsion stirrups = 12,700 lb.in<sup>2</sup>  
(Australian Code Equation (25) with yield stress

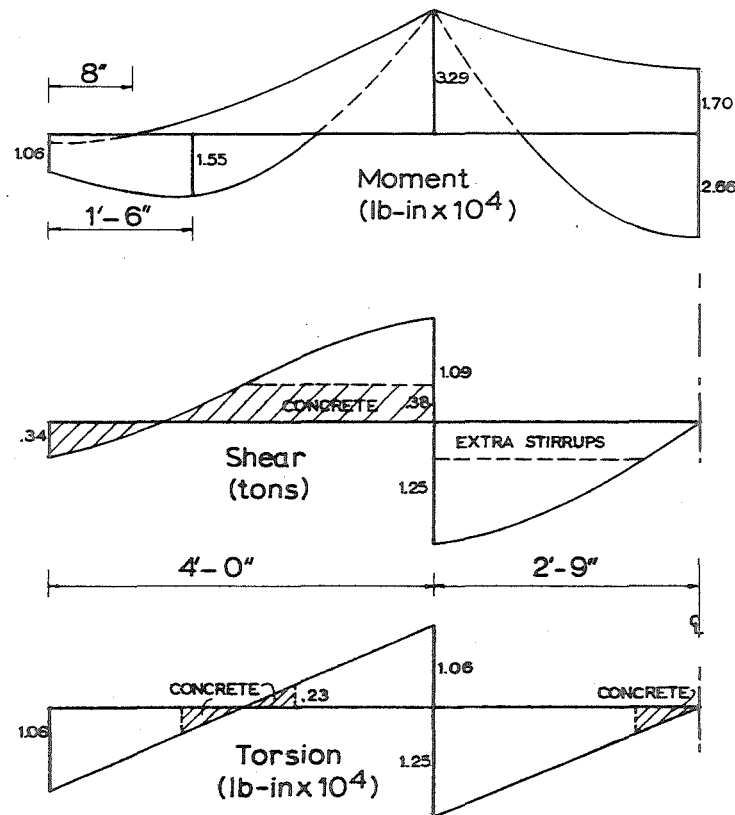


FIGURE A.3 EXTERIOR BEAM ACTIONS

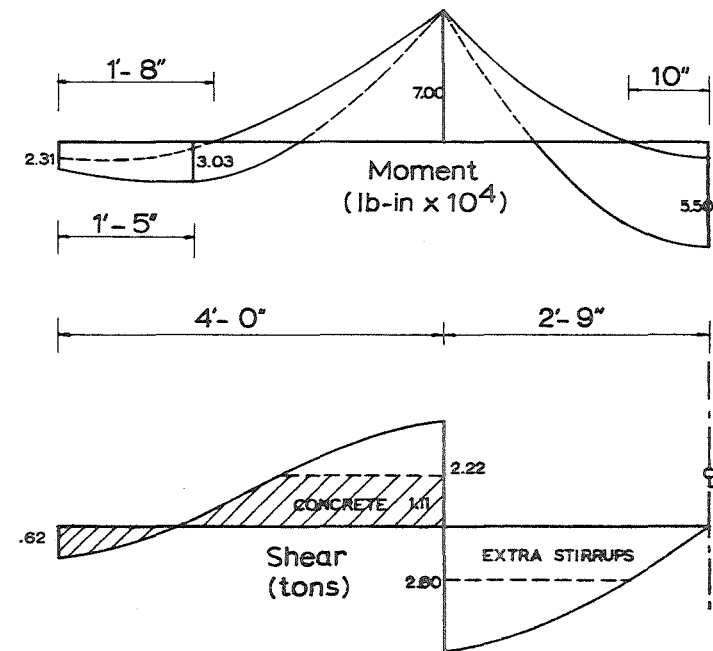


FIGURE A.4 INTERIOR BEAM ACTIONS



used in lieu of permissible stress)

Maximum torque in end spans = 10630 lb-in

Maximum torque in centre spans = 12500 lb-in

Minimum stirrup spacings: end spans:  $s_{\min} = 1.2$  in  
 centre spans:  $s_{\min} = 1.0$  in

Maximum longitudinal steel required for torsion

(Equation 26 of Australian Code),  $A_{sh} = .172 \text{ in}^2$  for  
 end spans,  $A_{sh} = .205 \text{ in}^2$

(d) Allocation of Flexural Steel

(i) In the centre span with tension:

In Equations 4.14 and 4.15:  $b = 3.5$ ",  $b/b_f = .4$ ,

$D = 6.0$ ",  $f'_c = 4200$  psi,  $f_y = 42000$  psi,

At the support:  $T/f'_c b d = .064$ ,  $M/f'_c b d^2 = .089$

Equation 4.14 gave  $p' = 1.28$  per cent,  $A'_s = .25 \text{ in}^2$

Longitudinal torsional steel required at

$$\text{top} = \underline{.10 \text{ in}^2}$$

$$2 \text{ at } \frac{3}{8} \text{ " dia.} + 2 \text{ at } \frac{1}{4} \text{ " dia.} = .32 \text{ in}^2$$

At mid-span:  $M/f'_c b d^2 = .044$ ,  $T/f'_c b d = .064$

Equation 4.15 gave  $p = .85$  per cent,  $A_s = .16 \text{ in}^2$

$$3 \text{ at } \frac{1}{4} \text{ " dia.} = .15 \text{ in}^2$$

(ii) In the end spans (no tension):

At the support  $M = 3.29 \times 10^4 \text{ lb-in}$ , from ACI 318-63

Equation 16-1,  $A_s = .15 \text{ in}^2$

Torsional steel =  $.086 \text{ in}^2$

$$2 \text{ at } \frac{3}{8} \text{ " dia.} = .22 \text{ in}^2$$

But the 2 -  $\frac{1}{4}$ " dia. bars on the other side of the support could not be curtailed and  $A_s$  supplied was  $.32 \text{ in}^2$

At the position of maximum positive moment

$$M = 1.55 \times 10^4 \text{ lb-in, } A_s = .07 \text{ in}^2$$

$$2 \text{ at } \frac{1}{4} \text{ dia.} = .10 \text{ in}^2$$

### A.3.2 Interior Beams

#### (a) Design Actions

Figure A.4 shows the design actions which were obtained as for the exterior beam except that the moment applied at the end due to edge beam torsion was the sum of the yield moments from the adjacent half span on each side of the beam.

#### (b) Size of Cross Section

This was set at 7.5" deep and 3.5" wide.

ACI Clause 906(b) imposed the condition that the maximum flange width should not exceed  $\frac{1}{4}$  of the span which was therefore taken as  $66 \div 4 = 16.5 \text{ in.}$

#### (c) Allocation of Shear Steel

$$\text{Shear taken by concrete} = 2460 \text{ lb}$$

$$\text{Force in two legs of stirrup} = 1000 \text{ lb}$$

$$V_u' \text{ s for vertical stirrups} = 7500 \text{ lb-in}$$

$$V_u' \text{ s for } 45^\circ \text{ stirrups} = 10600 \text{ lb-in}$$

#### (d) Allocation of Flexural Steel

(i) In the centre span with tension:

$$b = 3.5", D = 7.5", b/d_f = .2$$

$$\text{At the support: } M/f_c'bd^2 = .140, T/f_c'bd = .171$$

Equation 4.14 gave  $p' = 2.33$  per cent,  $A'_s = .57 \text{ in}^2$

$$4 \text{ at } \frac{3}{8}'' \text{ dia.} + 2 \text{ at } \frac{1}{4}'' \text{ dia.} = .54 \text{ in}^2$$

At mid-span:  $M/f'_c b d^2 = .034$ ,  $T/f'_c b d = .171$

Equation 4.15 gave  $p = 1.30$  per cent,  $A_x = .32 \text{ in}^2$

$$2 \text{ at } \frac{3}{8}'' \text{ dia.} + 2 \text{ at } \frac{1}{4}'' \text{ dia.} = .32 \text{ in}^2$$

(ii) In the end span:

$$M = 7.00 \times 10^4 \text{ lb-in, } A_s = .24 \text{ in}^2$$

$$2 \text{ at } \frac{3}{8}'' \text{ dia.} = .22 \text{ in}^2$$

However, on the other side 4 at  $\frac{3}{8}'' + 2$  at  $\frac{1}{4}''$  were provided and only 2 at  $\frac{3}{8}''$  were cut off so that  $A_s$  provided =  $.32 \text{ in}^2$ .

At point of maximum positive moment:

$$M = 3.03 \times 10^4 \text{ lb-in, } A_s = .11 \text{ in}^2$$

$$2 \text{ at } \frac{1}{4}'' \text{ dia.} + 1 \text{ at } \frac{1}{8}'' \text{ dia.} = .11 \text{ in}^2$$

### A.3.3 Graphical Allocation of Shear and Torsion Steel

The quantities  $V'_u$ 's and  $M_t$ 's for each stirrup represent an area on the shear force and torsion diagrams respectively. Stirrup spacings were determined by dividing the areas into elements of area  $V'_u$ 's or  $M_t$ 's. For shear the total area covered was that representing the shear not taken by the concrete. For torsion the gross torsional moment was used after the total torque applied exceeded the torsional capacity of the uncracked concrete section.

Maximum spacings as governed by ACI 318-63 Clause 1706 (b) were 3.0 in for the exterior beams and 3.7 in for the interior beams.

Final steel placement is shown in Figure 6.1 (p. 96).

APPENDIX B - MATERIAL PROPERTIES  
AND SLAB DIMENSIONS

B.1 CONCRETE PROPERTIES

B.1.1 Details of Mix

Certified Concrete DD  $\frac{1}{4}$ " mortar mix.

Air 7 per cent

Slump 2"

Aggregate 8700 lb

Cement 1650 lb

Total water 1147 lb

Added water 720 lb

Water/cement ratio = .694

Aggregate grading:

<u>Mesh</u>	<u>Weight</u>	<u>% Retained</u>	<u>Total Re-</u> <u>tained</u>
3/16"	.06	6	6
7	.23	23	29
14	.19	19	48
25	.12	12	60
52	.12	12	72
100	.20	20	92
PAN	.08	8	100

B.1.2 Strength

The results of tests on standard control specimens were as follows:

(a) Cylinder Strength	<u>Age When Tested (Days)</u>	<u>Number Tested</u>	<u>Ave. f' (psi)<sup>c</sup></u>
	24	2	2775
	28	2	3850
	163	4	4350
	181	6	4350
	198	1	4420

(b) Cube Strength	<u>Age</u>	<u>Number</u>	<u>Ave. u</u>
	163	4	5310 psi
	181	5	4890 "
	198	3	4700 "

(c) Modulus of Rupture			
	163	3	710 psi
	181	4	680 "
	198	2	740 "

#### B.1.3 Modulus of Elasticity

Table B.1 gives a summary of readings taken on test specimens to determine the modulus of elasticity of the concrete used.

#### B.1.4 Shrinkage

Readings of shrinkage in the unreinforced specimens are summarised in Table B.2.

### B.2 STEEL PROPERTIES

The results of tensile tests on the reinforcing bars used are given in Table B.3. A Baty extensometer was used to measure extension over a two inch length. All bars were tested without being machined.

TABLE B.1

SUMMARY OF MODULUS OF ELASTICITY RESULTS  
ON MORTAR MIX SPECIMENS

CYLINDERS			PRISMS		
STRESS (psi)	No. 4 ( $\mu$ S)	No. 37 ( $\mu$ S)	STRESS (psi)	No. 1 ( $\mu$ S)	No. 2 ( $\mu$ S)
0000	0000	0000	0000	0000	0000
353	124	102	500	155	145
707	242	216	1000	314	328
1061	366	350	1500	532	514
1414	498	502	2000	688	735
1768	640	624	2500	900	1015
2120	778	774	3000	1124	1308
2475	956	952	3500		1700
2830	1172	1146	3750	1436	1990
3180	1398	1374	4000	1644	2332
3360		1544	4125	1789	2664
3530	1720	1670	4250	2010	3102
3710	1944	1852	4375	2230	
3890	2222	2082			
4070		2312			
4250		2742			

Cylinders were 12" x 6" dia. with 4" demec gauge readings.

Prisms were 18" x 6" x 6" with 8" demec gauge readings.

The above readings are the average of two taken, in each case,  
from opposite sides of the specimen.

Sample 1: Average of 3 readings on 1.94" thick strip.

Sample 2: Average of 6 readings on two blocks 18" x 6" x 3.5".

Sample 3: Average of 6 readings on two blocks 18" x 7.5 x 3.5".

All readings in the above table have been corrected for temperature variations and thus represent the unrestrained shrinkage of the specimens. A value of 8 microstrains per degree Fahrenheit was taken in reducing the readings to an equivalent reading at 68°F.

TABLE B.2

SUMMARY OF SHRINKAGE AND TEMPERATURE MOVEMENT  
READINGS TAKEN ON SAMPLES OF UNREINFORCED  
CONCRETE SPECIMENS

DATE	TEMP.	TIME	SHRINKAGE IN MICROSTRAIN		
			SAMPLE 1	SAMPLE 2	SAMPLE 3
20/12/67	68	1300	0	0	0
21/12/67	66	0900	122	100	93
21/12/67	68	1200	129	108	103
22/12/67	66	0900	171	144	128
22/12/67	69	1700	193	163	151
23/12/67	68	1100	211	184	168
23/12/67	69	1800	219	189	172
24/12/67	63	1300	243	196	175
26/12/67	63	1100	300	258	234
27/12/67	68	1500	346	296	269
29/12/67	66	1200	395	331	300
1/01/68	68	0200	464	356	338
3/01/68	69	1100	583	446	406
4/01/68	72	1600	642	479	449
6/01/68	64	1600	670	488	452
8/01/68	66	0900	745	543	498
9/01/68	66	0900	754	551	505
10/01/68	70	0900	803	597	539
11/01/68	69	0900	790	586	528
12/01/68	70	0900	804	609	551
13/01/68	74	1100	881	644	586
15/01/68	69	1400	907	651	602
17/01/68	73	1500	993	691	658
18/01/68	67	1700	972	693	644
19/01/68	64	1400	945	698	640
23/01/68	70	0900	987	741	681
29/01/68	65	0900	925	739	679
3/02/68	65	1300	974	793	729
7/02/68	67	0900	1068	855	794
21/02/68		1500	1055	900	836
13/03/68	65	0900	1043	935	869
1/04/68		0900	1034	938	875
27/05/68	67	0930	1205	1102	1020

Table B.3. Tensile Tests on Reinforcement.

<u>Steel Type</u>	<u>Nominal Diameter</u>	<u>Yield Force (lb)</u>	<u>No. Tested</u>	<u>Yield Stress (psi)</u>	<u>Modulus of Elasticity</u>	<u>Where Used</u>	<u>s.d. %</u>
A	$\frac{3}{8}$ "	4890	8	44,400	$31.0 \times 10^6$	Beams Only	1.65
A	$\frac{1}{4}$ "	1920	9	40,100	$29.9 \times 10^6$	Beams Only	3.3
A	$\frac{1}{8}$ "	616	8	50,300	$29.8 \times 10^6$	Slab Beams	3.16
B	$\frac{1}{8}$ "	502*	5	39,000	$29.6 \times 10^6$	All Stir-rups	2.4

\* .2% proof stress.

Type A: British steel, lead bath annealed to give extended yield plateau.

Type B: New Zealand soft drawn wire.

### B.3 SLAB DIMENSIONS

#### B.3.1 Level of Top Surface of Floor and Beam and Panel Depths

Readings of level on the top surface before the test are shown in Figure B.1. Panel and beam depth measurements taken before the test are shown in Figure B.2.

Average thicknesses taken from the nine readings per panel were:

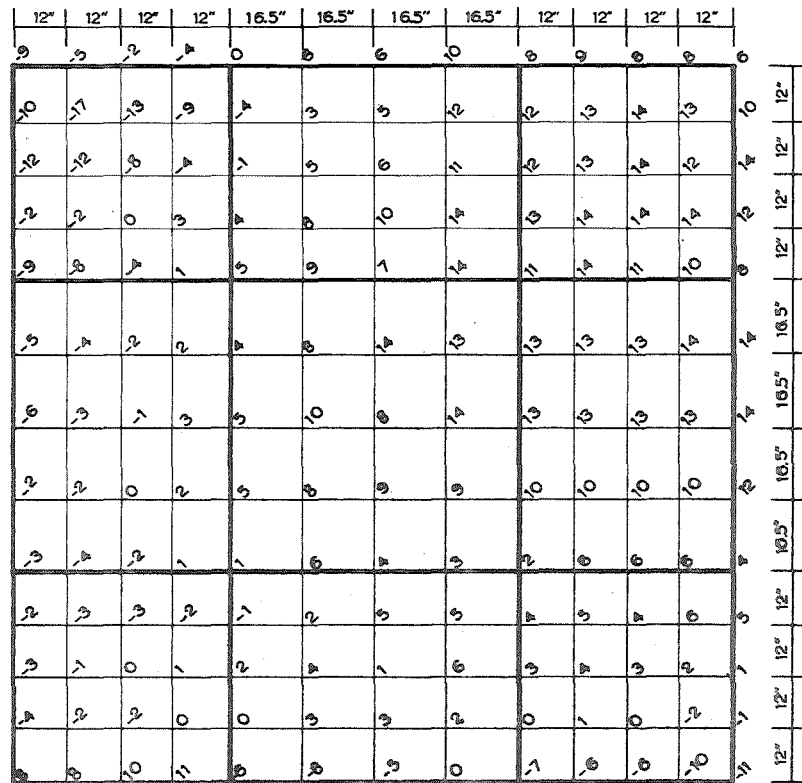


FIGURE B.1 LEVELS ON TOP SURFACE

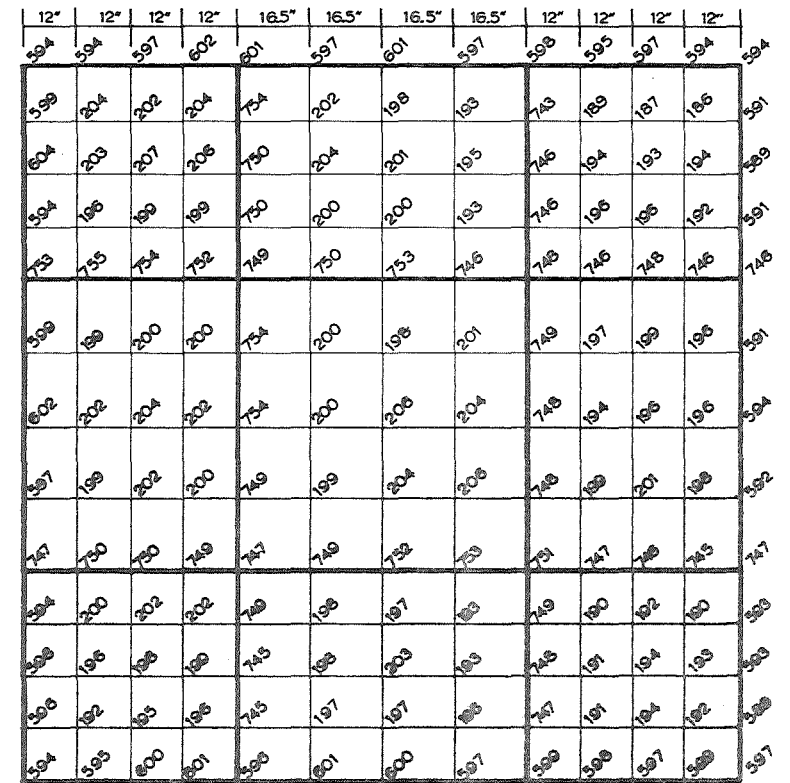


FIGURE B.2 DEPTHS OF BEAMS AND SLABS

All figures in .01 inch units



<u>Panel</u>	A	B	C	D	E	F	G	H	J
Average Thickness (in)	2.02	1.98	1.92	2.01	2.02	1.97	1.98	1.97	1.92
Std. Deviation (in)	.035	.055	.025	.017	.028	.020	.031	.028	.020

Readings taken at the edges of Panels E, H and J after the test gave the following results:

<u>Panel</u>	<u>No. of Readings</u>	<u>Average Thickness (in)</u>	<u>Std. Dev. (in)</u>
E	45	1.937	.031
H	43	1.908	.017
J	36	1.877	.018

### B.3.2 Minimum Cover to Steel

Top steel cover was measured at the following positions:

- (i) Around the edges of the centre panel at every bar
- (ii) Around the edges of Panel H at every bar.
- (iii) Around the edges of Panel J at every bar on two sides; every second bar on two sides.
- (iv) At the interior supports of exterior and interior beams.

Bottom steel cover was checked along the principal cracks of Panels E, H and J and at the mid-span sections of the beams.

Results of the check are given in Table B.4.

Table B.4. Check on Minimum Steel Cover.

<u>Position</u>	<u>No. of</u> <u>Read-</u> <u>ings</u>	<u>Expected</u> <u>Cover</u> <u>1/64th in.</u>	<u>Average</u> <u>Cover</u> <u>1/64th in.</u>	<u>Standard</u> <u>Deviation</u> <u>1/64th in.</u>	<u>Remarks</u>
Centre Panel Edge	28	12	11.6	2.7	EW layer top steel
Centre Panel Edge	28	20	15.5	2.5	NS layer top steel
Panel H Edge	20	12	10.7	1.6	EW layer top steel
Panel H Edge	28	20	16.8	2.2	NS layer top steel
Panel J Edge	15	12	9.6	2.0	EW layer top steel
Panel J Edge	15	20	17.4	2.0	NS layer top steel
Exterior Beam	40	24	24.6	3.9	Support top steel
Interior Beam	16	24	25.6	1.2	Support top steel
Exterior Beam	17	24	23.8	1.7	Centre span bottom steel
Interior Beam	37	24	23.3	1.7	Centre span bottom steel
Panel J	12	20	20.0	1.0	Top layer bottom steel
Panel J	16	12	12.0	.7	Bottom layer bottom steel
Panel E	30	20	21.3	2.3	Top layer bottom steel
Panel E	40	12	13.0	1.7	Bottom layer bottom steel
Panel H	10	20	20.2	.7	Top layer bottom steel
Panel H	33	12	12.0	1.2	Bottom layer bottom steel

# APPENDIX C

## DETAILS OF LOAD INCREMENTS FOR THE TEST ON THE NINE PANEL FLOOR

Column 1 - Load Stage Number.

Column 2-4 - Panel loads in lb/ft.<sup>2</sup>

Column 5 - Temperature.

Column 6 - Time at which load first attained.

Column 7 - Time at which load changed for  
next stage.

LOAD STAGE NO	CENT PNL LOAD	RECT PNL LOAD	CRNR PNL LOAD	TEMP DEG F	TIME ON	TIME OFF
1	75	75	75	71	1340	1400
2	100	100	100	71	1400	1425
3	125	125	125	72	1425	1450
4	150	150	150	71	1450	1515
5	175	175	175	70	1515	1535
6	200	200	200	70	1540	1603
7	225	225	225	70	1605	1640
8	200	200	200	71	1640	1655
9	150	150	150	69	1655	1706
10	75	75	75	69	1708	
13	75	75	75	65		1000
14	100	100	100	67	1005	1020
15	125	125	125	67	1025	1037
16	150	150	150	68	1041	1052
17	175	175	175	69	1057	1109
18	200	200	200	68	1114	1125
19	225	225	225	68	1129	1140
20	200	200	200	68	1143	1153
21	175	175	175	69	1155	1205
22	125	125	125	70	1208	1219
23	75	75	75	70	1222	
26	75	75	75	70	1345	1355
27	100	100	100	71	1400	1410
28	125	125	125	71	1415	1430
29	150	150	150	71	1430	1443
30	175	175	175	71	1445	1500
31	200	200	200	72	1509	1525
32	225	225	225	72	1530	1540
33	200	200	200	72	1545	1557
34	175	175	175	72	1602	1613
35	150	150	150	72	1616	1626
36	125	125	125	72	1626	1642
37	100	100	100	72	1645	1656
38	75	75	75	72	1700	

LOAD STAGE NO	CENT PNL LOAD	RECT PNL LOAD	CRNR PNL LOAD	TEMP DEG F	TIME ON	TIME OFF
91	75	75	75	65		0918
92	75	100	75	67	0925	0942
93	75	125	75		0945	1000
94	75	150	75	68	1005	1015
95	75	175	75	69	1020	1045
96	75	200	75	70	1050	1100
97	75	225	75	70	1105	1120
98	75	200	75	71	1125	1134
99	75	175	75	71	1138	1147
100	75	150	75	71	1152	1205
101	75	125	75	72	1208	1215
102	75	75	75	71	1222	
1A	75	75	75	72		1355
2A	100	100	100	72	1400	1408
3A	125	125	125	72	1412	1422
4A	150	150	150	72	1425	1435
5A	175	175	175	72	1440	1450
6A	200	200	200	72	1455	1502
7A	225	225	225	72	1515	1522
8A	200	200	200	72	1526	1544
9A	175	175	175	73	1547	1554
10A	150	150	150	72	1559	1607
11A	125	125	125	71	1612	1620
12A	100	100	100	72	1624	1630
13A	75	75	75	71	1640	
76	75	75	75	68		0906
77	125	125	125	68	0910	0921
77A	150	150	150	70	0928	0932
78	175	175	175	70	0943	0958
78A	200	200	200	70	1005	1017
79	225	225	225	70	1024	1035
80	250	250	250	70	1040	1100
81	275	275	275	70	1105	1125
82	300	300	300	72	1133	1147
83	325	325	325	72	1155	1207
84	350	350	350	72	1215	1235
85	375	375	375	72	1250	1408
86	350	350	350	72	1415	1432
87	325	325	325	72	1432	1443
88	300	300	300	72	1443	1458
89	275	275	275	72	1458	1518
90	250	250	250	72	1520	1530
91	225	225	225	72	1530	1545
91A	200	200	200	72	1545	1555
92	175	175	175	72	1555	1608
92A	150	150	150	72	1608	1623
93	125	125	125	72	1625	1635
94	75	75	75	72	1640	
95	75	75	75	67		0945
95A	125	125	125	67	0950	1000
96	175	175	175	68	1005	1022
96A	225	225	225	68	1040	1050
97	275	275	275	69	1055	1105
97A	325	325	325	69	1112	1122
97B	350	350	350	70	1128	1135
98	375	375	375	70	1140	1208
99	375	325	325	71	1212	1222
100	375	275	275	71	1225	1350
101	375	225	225	71	1355	1405
102	375	175	175	72	1410	1430
102A	375	150	150	73	1435	1450
103	375	125	125	73	1455	1520
103A	375	100	100	73	1525	1535
104	375	75	75	73	1540	1550
105	325	75	75	73	1600	1608
106	275	75	75	73	1612	1617
107	225	75	75	72	1620	1630
108	150	75	75	71	1635	1645
109	75	75	75	72	1650	

TEST104  
8/5/68

TEST105  
8/5/68

TEST106  
9/5/68

TEST101  
6/5/68

TEST102  
7/5/68

TEST106  
9/5/68

TEST107  
10/5/68

TEST103  
7/5/68

LOAD STAGE NO	CENT PNL LOAD	RECT PNL LOAD	CNR PNL LOAD	TEMP DEG F	TIME ON	TIME OFF
114	175	75	75	66	0920	0915
115	175	75	75	67	0940	0935
116	175	75	75	68	0953	0948
117	225	75	75	68	1010	1005
118	250	75	75	68	1027	1022
119	275	75	75	69	1057	1052
120	300	75	75	70	1103	1102
121	325	75	75	70	1120	1115
122	350	75	75	70	1130	1125
123	375	75	75	71	1150	1145
123A	400	75	75	72	1210	1205
123B	375	75	75	72	1225	1220
124	350	75	75	74	1356	1400
125	325	75	75	74	1415	1425
126	300	75	75	74	1430	1440
127	275	75	75	74	1445	1454
128	250	75	75	75	1457	1504
129	225	75	75	75	1521	1530
130	175	75	75	75	1535	1545
131	125	75	75	75	1550	1600
132	75	75	75	75	1610	
133	75	75	75	72	0940	0930
134	75	125	75	73	0955	1010
135	75	175	75	73	1015	1023
136	75	225	75	73	1028	1040
137	75	250	75	73	1050	1100
137A	200	200	200	74	1105	1118
138	200	275	200	74	1120	1135
139	200	300	200	74	1140	1152
140	200	325	200	74	1157	1207
141	200	350	200	74	1212	1410
142	200	375	200	75	1410	1420
142A	175	375	175	75	1425	1435
142B	150	375	150	75	1440	1450
143	150	350	150	75	1455	1505
144	150	325	150	74	1523	1533
145	150	300	150	75	1538	1547
146	150	275	150	75	1550	1556
147	150	250	150	75	1600	1608
147A	75	250	75	75	1612	1618
148	75	225	75	75	1622	1630
149	75	175	75	76	1636	1645
150	75	125	75	75	1650	
151	75	75	75	75		
152	75	75	75	74	0920	0915
152A	125	125	125	74	0932	0932
153	175	175	175	74	0935	0945
153A	225	225	225	74	0950	1003
154	275	275	275	74	1005	1020
154A	300	300	300	74	1040	1105
154B	325	325	325	74	1110	1120
154C	350	350	350	73	1125	1140
154D	375	375	375	73	1145	1200
155	375	375	375	73	1205	1355
155A	400	400	400	73	1400	1430
156	425	425	425	73	1432	1545
157	450	450	450	72	1550	1600
158	425	425	425	72	1605	1610
159	400	400	400	72	1615	1640
160	375	375	375	71	1405	1418
161	375	375	375	71	1423	1437
162	350	350	350	71	1440	1455
163	325	325	325	72	1500	1520
164	275	275	275	72	1530	1540
165	225	225	225	71	1545	1555
166	175	175	175	71		
167	125	125	125	71		
168	75	75	75	71	1600	1615
169	125	125	125	71	1620	1640
170	175	175	175	71	1645	1650
171	225	225	225	70	1655	16915
172	250	225	225	71	0920	0933
173	275	225	225	71	0938	0947

LOAD STAGE NO	CENT PNL LOAD	RECT PNL LOAD	CNR PNL LOAD	TEMP DEG F	TIME ON	TIME OFF
TEST108 13/5/68	174	300	225	72	0950	1008
	175	325	225	72	1013	1030
	176	350	225	72	1045	1100
	177	375	225	72	1105	1125
	178	350	225	72	1130	1138
	179	325	225	72	1143	1150
	180	300	225	73	1155	1203
	181	275	225	74	1208	1215
	182	250	225	74	1215	1220
	183	225	225	74	1225	1350
	184	250	250	75	1355	1405
	185	275	275	75	1410	1418
	186	300	300	75	1423	1430
	187	325	325	75	1435	1445
	188	350	350	75	1450	1500
	189	375	375	68	1515	1600
TEST109 14/5/68	190	400	400	67	1005	1025
	191	425	425	67	1045	1104
	192	450	450	67	1110	1128
	193	475	475	67	1135	1155
	194	500	500	68	1200	1230
	195	300	300	69	1235	1400
	196	400	400	69	1408	1418
	197	450	450	69	1425	1432
	198	500	500	69	1440	1453
	199	525	525	69	1458	1533
	200	550	550	69	1540	1705
	201	400	400	69	1710	1725
	202	200	200	67	1725	1805
	203	300	300	66	1020	1030
	204	400	400	66	1045	1102
	205	500	500	66	1110	1120
	206	525	525	66	1125	1140
	207	550	550	67	1145	1202
	208	575	575	67	1210	1235
	209	375	375	67	1230	1245
	210	500	500	67	1305	1400
	211	550	550	67	1415	1425
	212	575	575	67	1430	1512
	213	600	600	68	1520	1540
	214	625	625	68	1545	1600
	215	650	650	69	1555	1633
	216	675	675	69	1610	1633
	217	700	700	69	1640	1703
	218	725	725	69	1710	1735
	219	750	750	69	1740	1750
	220	775	775	69	1755	1830
TEST110 15/5/68	221	400	400	62	1830	1840
	222	600	600	62	0945	0955
	223	750	750	63	1000	1020
	224	775	775	63	1025	1045
	225	800	800	65	1050	1108
	226	825	825	65	1115	1135
	227	850	850	67	1140	*
	228	556	556	67	1200	1340
	229	543	543	67	1345	1355
	230	600	600	68	1357	1420
	231	660	660	68	1425	1445
	232	710	710	68	1450	1515
	233	600	825	68	1520	1535
	234	600	850	68	1540	1550
	235	600	875	68	1550	1605
	236	600	900	69	1610	1620
	237	600	925	68	1625	1635
	238	600	950	68	1640	1700
	239	600	966	68		**
		950	1170			***
TEST111 16/5/68						
17/5/68						

\* 850 PSF NOT ATTAINED DUE TO FAILURE OF THE CENTRE PANEL.  
 \*\* FAILURE OF RECTANGULAR PANELS.  
 \*\*\* FAILURE OF CORNER PANELS.

## APPENDIX D

### REDUCED DATA FROM SLAB TEST

#### D.1 DEFLECTIONS

Reduced readings of all deflection gauges with Load Stage 51 as datum are tabulated below. The first column contains the Load Stage Numbers, columns 2, 3 and 4 show the nominal panel loads in psf and the subsequent columns contain the deflection data in .0001 inch units. The numbers at the head of these columns refer to the dial gauge positions as given in Figure D.1.

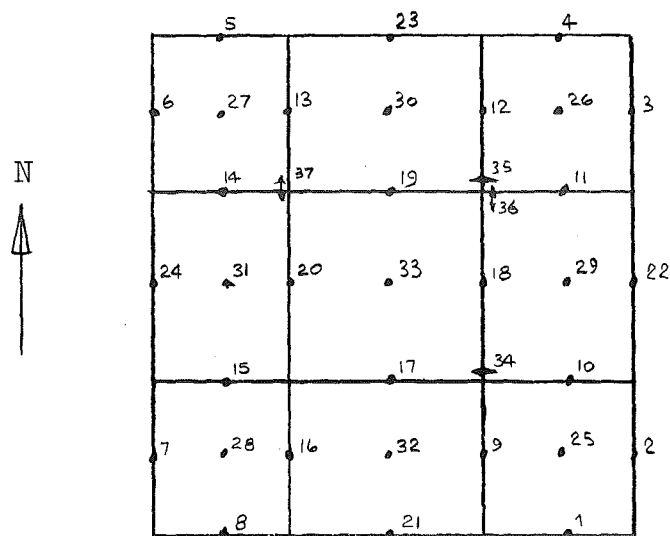


FIGURE D.1. DIAL GAUGE POSITIONS.

STAGE	CNTR	ACTR	CNRR	1	2	3	4	5	6	7	8	9	10	11	12	13
1.0	75.	75.	75.	-47	-	-276	-5	-56	-48	-42	-60	-14	-2	-	-8	-29
2.0	100.	100.	100.	-47	-	-276	-5	-56	-48	-42	-60	-14	-2	-	-8	-29
3.0	125.	125.	125.	-47	-	-276	-5	-56	-48	-42	-60	-14	-2	-	-8	-29
4.0	150.	150.	150.	-24	-	-260	16	-35	-25	-24	-35	-5	-4	-	-1	-1
5.0	175.	175.	175.	-24	-	-260	16	-35	-25	-24	-35	-5	-4	-	-1	-1
6.0	200.	200.	200.	-17	-	-254	19	-29	-18	-24	-29	-5	-4	-	-1	-1
7.0	225.	225.	225.	-3	-	-241	22	-15	-2	-13	-26	-8	-1	-	-1	-1
8.0	250.	250.	250.	-3	-	-241	22	-15	-2	-13	-26	-8	-1	-	-1	-1
9.0	275.	275.	275.	-55	-	-259	-62	-63	-340	-77	-11	-7	-7	-	-1	-1
10.0	300.	300.	300.	-3	-	-241	22	-15	-2	-13	-26	-8	-1	-	-1	-1
11.0	325.	325.	325.	-3	-	-241	22	-15	-2	-13	-26	-8	-1	-	-1	-1
12.0	350.	350.	350.	-6	-	-232	25	-32	-8	-18	-33	-10	-1	-	-1	-1
13.0	375.	375.	375.	-23	-	-219	27	-47	-28	-29	-28	-1	-1	-	-1	-1
14.0	400.	400.	400.	-1	-	-207	29	-4	-4	-4	-4	-1	-1	-	-1	-1
15.0	425.	425.	425.	7	-	-194	32	18	3	-6	-6	-1	-1	-	-1	-1
16.0	450.	450.	450.	14	-	-180	36	18	10	4	-3	-1	-1	-	-1	-1
17.0	475.	475.	475.	21	-	-166	41	15	16	13	-6	-1	-1	-	-1	-1
18.0	500.	500.	500.	27	-	-152	44	25	19	18	-6	-1	-1	-	-1	-1
19.0	525.	525.	525.	34	-	-140	47	25	22	19	-6	-1	-1	-	-1	-1
20.0	550.	550.	550.	39	-	-128	50	27	25	21	-6	-1	-1	-	-1	-1
21.0	575.	575.	575.	44	-	-116	54	28	28	21	-6	-1	-1	-	-1	-1
22.0	600.	600.	600.	49	-	-104	58	30	30	23	-6	-1	-1	-	-1	-1
23.0	625.	625.	625.	55	-	-92	61	33	33	25	-6	-1	-1	-	-1	-1
24.0	650.	650.	650.	60	-	-80	65	35	35	27	-6	-1	-1	-	-1	-1
25.0	675.	675.	675.	66	-	-68	69	37	37	29	-6	-1	-1	-	-1	-1
26.0	700.	700.	700.	71	-	-56	73	39	39	31	-6	-1	-1	-	-1	-1
27.0	725.	725.	725.	77	-	-44	77	41	41	33	-6	-1	-1	-	-1	-1
28.0	750.	750.	750.	82	-	-32	81	43	43	35	-6	-1	-1	-	-1	-1
29.0	775.	775.	775.	88	-	-20	85	45	45	37	-6	-1	-1	-	-1	-1
30.0	800.	800.	800.	93	-	-8	89	47	47	39	-6	-1	-1	-	-1	-1
31.0	825.	825.	825.	99	-	4	93	49	49	41	-6	-1	-1	-	-1	-1
32.0	850.	850.	850.	104	-	12	97	51	51	43	-6	-1	-1	-	-1	-1
33.0	875.	875.	875.	110	-	20	101	53	53	45	-6	-1	-1	-	-1	-

STAGE	CNTR	RCR	CRNK	1	2	3	4	5	6	7	8	9	10	11	12	13
90.0	250.	250.	250.	30	29	37	38	39	38	41	43	44	67	52	46	52
91.0	275.	275.	275.	34	22	37	37	45	32	49	36	36	82	67	62	61
92.0	300.	300.	300.	44	34	46	46	56	43	61	58	58	95	81	89	89
93.0	325.	325.	325.	46	45	44	61	60	51	60	49	59	114	94	92	89
94.0	350.	350.	350.	60	50	57	68	62	54	64	54	64	129	104	108	101
95.0	375.	375.	375.	60	50	57	68	62	51	67	54	64	129	104	108	101
96.0	400.	400.	400.	-5	-7	-2	-2	-2	-7	-7	-7	-7	137	107	114	111
97.0	425.	425.	425.	64	57	58	76	69	55	75	59	59	136	114	118	121
98.0	450.	450.	450.	63	52	58	72	65	55	75	54	54	127	105	114	117
99.0	475.	475.	475.	63	52	58	72	65	55	75	54	54	127	105	114	117
100.0	500.	500.	500.	63	52	58	72	65	55	75	54	54	127	105	114	117
101.0	525.	525.	525.	64	57	58	76	69	55	75	59	59	136	114	118	121
102.0	550.	550.	550.	63	52	58	72	65	55	75	54	54	127	105	114	117
103.0	575.	575.	575.	63	52	58	72	65	55	75	54	54	127	105	114	117
104.0	600.	600.	600.	64	57	58	76	69	55	75	59	59	136	114	118	121
105.0	625.	625.	625.	63	52	58	72	65	55	75	54	54	127	105	114	117
106.0	650.	650.	650.	63	52	58	72	65	55	75	54	54	127	105	114	117
107.0	675.	675.	675.	64	57	58	76	69	55	75	59	59	136	114	118	121
108.0	700.	700.	700.	63	52	58	72	65	55	75	54	54	127	105	114	117
109.0	725.	725.	725.	63	52	58	72	65	55	75	54	54	127	105	114	117
110.0	750.	750.	750.	64	57	58	76	69	55	75	59	59	136	114	118	121
111.0	775.	775.	775.	63	52	58	72	65	55	75	54	54	127	105	114	117
112.0	800.	800.	800.	63	52	58	72	65	55	75	54	54	127	105	114	117
113.0	825.	825.	825.	64	57	58	76	69	55	75	59	59	136	114	118	121
114.0	850.	850.	850.	63	52	58	72	65	55	75	54	54	127	105	114	117
115.0	875.	875.	875.	63	52	58	72	65	55	75	54	54	127	105	114	117
116.0	900.	900.	900.	64	57	58	76	69	55	75	59	59	136	114	118	121
117.0	925.	925.	925.	63	52	58	72	65	55	75	54	54	127	105	114	117
118.0	950.	950.	950.	63	52	58	72	65	55	75	54	54	127	105	114	117
119.0	975.	975.	975.	64	57	58	76	69	55	75	59	59	136	114	118	121
120.0	1000.	1000.	1000.	63	52	58	72	65	55	75	54	54	127	105	114	117

STAGE	CNTR	RCR	CRHR	1	2	3	4	5	6	7	8	9	10	11	12	13
137.0	75.	250.	75.	0	-19	-1	7	9	1	12	-32	71	76	65	82	72
137.1	75.	250.	75.	32	-19	-1	28	41	36	48	-4	84	97	85	92	89
138.0	200.	275.	200.	34	30	29	45	41	32	48	4	97	103	89	101	89
139.0	200.	300.	200.	39	32	32	48	46	31	56	11	110	117	95	104	91
140.0	200.	325.	200.	44	34	34	53	48	26	64	-16	111	118	97	106	94
141.0	200.	350.	200.	49	36	36	57	50	22	72	-16	112	119	100	111	99
142.0	200.	375.	200.	55	37	37	60	52	18	80	-16	113	120	101	112	100
142.1	200.	375.	200.	57	37	37	62	54	16	82	-14	114	121	102	113	101
143.0	150.	375.	150.	62	38	38	64	56	12	90	-21	115	122	103	114	102
144.0	150.	350.	150.	67	39	39	67	58	8	98	-21	116	123	104	115	103
145.0	150.	325.	150.	72	40	40	70	60	5	106	-21	117	124	105	116	104
146.0	150.	275.	150.	77	41	41	73	63	3	114	-21	118	125	106	117	105
147.0	150.	250.	150.	82	42	42	76	66	2	122	-21	119	126	107	118	106
147.1	150.	250.	150.	84	42	42	78	68	1	124	-21	120	127	108	119	107
148.0	75.	225.	75.	-3	-11	-11	7	-15	-14	12	-29	72	77	67	78	71
149.0	75.	175.	75.	5	-9	-9	17	-14	-9	10	-21	62	67	57	68	61
150.0	75.	125.	75.	9	-7	-7	21	-14	-7	6	-14	52	57	47	58	51
151.0	75.	75.	75.	17	8	8	21	-7	6	4	-10	42	47	37	48	41
152.0	15.	75.	15.	17	13	13	17	10	1	3	-10	32	37	27	38	31
153.0	125.	175.	125.	17	15	15	19	12	10	16	-10	22	27	17	28	21
154.0	225.	225.	225.	21	23	23	24	18	16	20	-10	12	17	7	18	11
155.0	275.	275.	275.	26	27	27	29	21	19	24	-10	2	7	2	3	4
156.0	300.	300.	300.	31	30	30	33	24	22	27	-10	1	6	1	2	3
157.0	325.	325.	325.	36	33	33	37	27	25	30	-10	1	10	1	2	3
158.0	350.	350.	350.	41	38	38	42	30	28	34	-10	1	14	1	2	3
159.0	375.	375.	375.	46	40	40	45	33	31	38	-10	1	18	1	2	3
160.0	400.	400.	400.	51	45	45	50	36	34	42	-10	1	22	1	2	3
161.0	425.	425.	425.	56	50	50	55	39	37	46	-10	1	26	1	2	3
162.0	450.	450.	450.	61	55	55	60	42	40	50	-10	1	30	1	2	3
163.0	475.	475.	475.	66	60	60	65	45	43	54	-10	1	34	1	2	3
164.0	500.	500.	500.	71	65	65	70	48	46	60	-10	1	38	1	2	3
165.0	525.	525.	525.	76	70	70	75	51	49	66	-10	1	42	1	2	3
166.0	550.	550.	550.	81	75	75	80	54	52	72	-10	1	46	1	2	3
167.0	575.	575.	575.	86	80	80	85	57	55	78	-10	1	50	1	2	3
168.0	600.	600.	600.	91	85	85	90	60	58	84	-10	1	54	1	2	3
169.0	625.	625.	625.	96	90	90	95	63	61	90	-10	1	58	1	2	3
170.0	650.	650.	650.	101	95	95	100	66	64	96	-10	1	62	1	2	3
171.0	675.	675.	675.	106	100	100	105	69	67	102	-10	1	66	1	2	3
172.0	700.	700.	700.	111	105	105	110	72	70	108	-10	1	70	1	2	3
173.0	725.	725.	725.	116	110	110	115	75	73	114	-10	1	74	1	2	3
174.0	750.	750.	750.	121	115	115	120	78	76	120	-10	1	78	1	2	3
175.0	775.	775.	775.	126	120	120	125	81	79	126	-10	1	82	1	2	3
176.0	800.	800.	800.	131	125	125	130	84	82	132	-10	1	86	1	2	3
177.0	825.	825.	825.	136	130	130	135	87	85	138	-10	1	90	1	2	3
178.0	850.	850.	850.	141	135	135	140	90	88	144	-10	1	94	1	2	3
179.0	875.	875.	875.	146	140	140	145	93	91	150	-10	1	98	1	2	3
180.0	900.	900.	900.	151	145	145	150	96	94	156	-10	1	102	1	2	3
181.0	925.	925.	925.	156	150	150	155	99	97	162	-10	1	106	1	2	3
182.0	950.	950.	950.	161	155	155	160	102	100	168	-10	1	110	1	2	3
183.0	975.	975.	975.	166	160	160	165	105	103	174	-10	1	114	1	2	3
184.0	1000.	1000.	1000.	171	165	165	170	108	106	180	-10	1	118	1	2	3
185.0	275.	275.	275.	55	55	55	57	41	39	48	-10	1	122	1	2	3

STAGE	CNTR	RCR	CRHR	1	2	3	4	5	6	7	8	9	10	11	12	13
186.0	300.	300.	300.	59	60	60	64	43	41	52	-10	1	126	1	2	3
187.0	325.	325.	325.	64	65	65	69	46	44	56	-10	1	130	1	2	3
188.0	350.	350.	350.	69	70	70	74	49	47	60	-10	1	134	1	2	3
189.0	375.	375.	375.	74	75	75	79	52	50	64	-10	1	138	1	2	3
190.0	400.	400.	400.	79	80	80	84	55	53	68	-10	1	142	1	2	3
191.0	425.	425.	425.	84	85	85	89	58	56	72	-10	1	146	1	2	3
192.0	450.	450.	450.	89	90	90	94	61	59	76	-10	1	150	1	2	3
193.0	475.	475.	475.	94	95	95	99	64	62	80	-10	1	154	1	2	3
194.0	500.	500.	500.	99	100	100	104	67	65	84	-10	1	158	1	2	3
195.0	525.	525.	525.	104	105	105	109	70	68	88	-10	1	162	1	2	3
196.0	550.	550.	550.	109	110	110	114	73	71	92	-10	1	166	1	2	3
197.0	575.	575.	575.	114	115	115	119	76	74	96	-10	1	170	1	2	3
198.0	600.	600.	600.	119	120	120	124	79	77	100	-10	1	174	1	2	3
199.0	625.	625.	625.	124	125	125	129	82	80	104	-10	1	178	1	2	3
200.0	650.	650.	650.	129	130	130	134	85	83	108	-10	1	182	1	2	3
201.0	675.	675.	675.	134	135	135	139	88	86	112	-10	1	186	1	2	3
202.0	700.	700.	700.	139	140	140	144	91	89	116	-10	1	190	1	2	3
203.0	725.	725.	725.	144	145	145	149	94	92	120	-10	1	194	1	2	3
204.0	750.	750.	750.	149	150	150	154	97	95	124	-10	1	198	1	2	3
205.0	775.	775.	775.	154	155	155	159	100	98	128	-10	1	202	1	2	3
206.0	800.	800.	800.	159	160	160	164	103	101	132	-10	1	206	1	2	3
207.0	825.	825.	825.	164	165	165	169	106	104	136	-10	1	210	1	2	3
208.0	850.	850.	850.	169	170	170	174	109	107	140	-10	1	214	1	2	3
209.0	875.	875.	875.	174	175	175	179	112	110	144	-10	1	218	1	2	3
210.0	900.	900.	900.	179	180	180	184	115	113	148	-10	1	222	1	2	3
211.0	925.	925.	925.	184	185	185	189	118	116	152	-10	1	226	1	2	3
212.0	950.	950.	950.	189	190	190	194	121	119	156	-10	1	230	1	2	3
213.0	975.	975.	975.	194	195	195	199	124	122	160	-10	1	234	1	2	3
214.0	1000.	1000.	1000.	199	200	200	204	127	125	164	-10	1	238	1	2	3
215.0	600.	600.	600.	82	83	83	86	61	59	72	-10	1	126	1	2	3
216.0	625.	625.	625.	87	88	88	91	64	62	76	-10	1	130	1	2	3
217.0	650.	650.	650.	92	93	93	96	67	65	80	-10	1	134	1	2	3
218.0	675.	675.	675.	97	98	98	101	70	68	84	-10	1	138	1	2	3
219.0	700.	700.	700.	102	103	103	106	73	71	88	-10	1	142	1	2	3
220.0	725.	725.	725.	107	108	108	110	76	74	92	-10	1	146	1	2	3
221.0	750.	750.	750.	112	113	113	115	79	77	96	-10	1	150	1	2	3
222.0	775.	775.	775.	117	118	118	120	82	80	100	-10	1	154	1	2	3
223.0	800.	800.	800.	122	123	123	125	85	83	104	-10	1	158	1	2	3
224.0	825.	825.	825.	127	128	128	130	88	86	108	-10	1	162	1	2	3
225.0	850.	850.	850.	132	133	133	135	91	89	112	-10	1	166	1	2	3
226.0	875.	875.	875.	137	138	138	140	94	92	116</						

STAGE	CNTR	RCTR	CNTR	14	15	16	17	18	19	20	21	22	23	24	25	26
1.0	75.	75.	75.	-56	-46	-17	-58	-100	50	-10	-20	-30	-15	-11	-15	-10
2.0	100.	100.	100.	-46	-33	-10	-40	-70	50	-10	-20	-30	-15	-11	-15	-10
3.0	150.	150.	150.	-33	-21	-3	-30	-40	50	-10	-20	-30	-15	-11	-15	-10
4.0	150.	150.	150.	-18	-3	3	-22	-50	50	-10	-20	-30	-15	-11	-15	-10
5.0	175.	175.	175.	9	9	21	35	5	50	-10	-20	-30	-15	-11	-15	-10
6.0	200.	200.	200.	10	3	36	60	21	50	-10	-20	-30	-15	-11	-15	-10
7.0	225.	225.	225.	-2	-8	38	80	45	50	-10	-20	-30	-15	-11	-15	-10
7.1	255.	255.	255.	-15	-12	-12	-45	-45	50	-10	-20	-30	-15	-11	-15	-10
7.2	255.	255.	255.	-55	-27	-12	-240	-1495	50	-10	-20	-30	-15	-11	-15	-10
7.3	255.	255.	255.	7	17	11	50	11	50	-10	-20	-30	-15	-11	-15	-10
7.4	150.	150.	150.	2	6	6	45	5	50	-10	-20	-30	-15	-11	-15	-10
10.0	75.	75.	75.	-5	-13	-6	-4	-12	-10	-10	-10	-10	-10	-10	-10	-10
13.0	100.	100.	100.	1	1	1	-5	-1	-1	-1	-1	-1	-1	-1	-1	-1
14.0	100.	100.	100.	1	1	1	1	1	1	1	1	1	1	1	1	1
15.0	125.	125.	125.	25	20	1	10	2	10	10	10	10	10	10	10	10
16.0	150.	150.	150.	14	24	27	38	43	48	17	17	17	17	17	17	17
17.0	175.	175.	175.	31	43	43	43	43	43	43	43	43	43	43	43	43
19.0	200.	200.	200.	46	51	60	70	60	42	45	45	45	45	45	45	45
20.0	225.	225.	225.	42	44	55	60	50	30	30	30	30	30	30	30	30
22.0	175.	175.	175.	12	12	21	25	30	18	18	18	18	18	18	18	18
22.1	200.	200.	200.	4	4	7	3	0	0	0	0	0	0	0	0	0
22.2	200.	200.	200.	1	1	3	-16	-10	-10	-10	-10	-10	-10	-10	-10	-10
22.3	175.	175.	175.	13	17	10	10	22	30	30	30	30	30	30	30	30
22.4	100.	100.	100.	16	16	7	7	16	15	15	15	15	15	15	15	15
28.0	125.	125.	125.	20	22	22	22	20	30	30	30	30	30	30	30	30
28.1	150.	150.	150.	22	22	22	22	22	30	30	30	30	30	30	30	30
28.2	175.	175.	175.	22	22	22	22	22	30	30	30	30	30	30	30	30
31.0	200.	200.	200.	22	22	22	22	22	30	30	30	30	30	30	30	30
32.0	225.	225.	225.	22	22	22	22	22	30	30	30	30	30	30	30	30
33.0	250.	250.	250.	22	22	22	22	22	30	30	30	30	30	30	30	30
34.0	175.	175.	175.	22	22	22	22	22	30	30	30	30	30	30	30	30
35.0	150.	150.	150													

STAGE	CNTR	RCR	CRNR	14	15	16	17	18	19	20	21	22	23	24	25	26
80.0	250.	250.	250.	55	57	42	100	120	105	53	62	77	105	108	108	108
81.0	275.	275.	275.	55	57	42	100	120	105	53	62	77	105	108	108	108
82.0	300.	300.	300.	55	57	42	100	120	105	53	62	77	105	108	108	108
83.0	325.	325.	325.	55	57	42	100	120	105	53	62	77	105	108	108	108
84.0	350.	350.	350.	55	57	42	100	120	105	53	62	77	105	108	108	108
85.0	375.	375.	375.	55	57	42	100	120	105	53	62	77	105	108	108	108
86.0	400.	400.	400.	55	57	42	100	120	105	53	62	77	105	108	108	108
87.0	425.	425.	425.	55	57	42	100	120	105	53	62	77	105	108	108	108
88.0	450.	450.	450.	55	57	42	100	120	105	53	62	77	105	108	108	108
89.0	475.	475.	475.	55	57	42	100	120	105	53	62	77	105	108	108	108
90.0	500.	500.	500.	55	57	42	100	120	105	53	62	77	105	108	108	108
91.0	525.	525.	525.	55	57	42	100	120	105	53	62	77	105	108	108	108
92.0	550.	550.	550.	55	57	42	100	120	105	53	62	77	105	108	108	108
93.0	575.	575.	575.	55	57	42	100	120	105	53	62	77	105	108	108	108
94.0	600.	600.	600.	55	57	42	100	120	105	53	62	77	105	108	108	108
95.0	625.	625.	625.	55	57	42	100	120	105	53	62	77	105	108	108	108
96.0	650.	650.	650.	55	57	42	100	120	105	53	62	77	105	108	108	108
97.0	675.	675.	675.	55	57	42	100	120	105	53	62	77	105	108	108	108
98.0	700.	700.	700.	55	57	42	100	120	105	53	62	77	105	108	108	108
99.0	725.	725.	725.	55	57	42	100	120	105	53	62	77	105	108	108	108
100.0	750.	750.	750.	55	57	42	100	120	105	53	62	77	105	108	108	108
101.0	775.	775.	775.	55	57	42	100	120	105	53	62	77	105	108	108	108
102.0	800.	800.	800.	55	57	42	100	120	105	53	62	77	105	108	108	108
103.0	825.	825.	825.	55	57	42	100	120	105	53	62	77	105	108	108	108
104.0	850.	850.	850.	55	57	42	100	120	105	53	62	77	105	108	108	108
105.0	875.	875.	875.	55	57	42	100	120	105	53	62	77	105	108	108	108
106.0	900.	900.	900.	55	57	42	100	120	105	53	62	77	105	108	108	108
107.0	925.	925.	925.	55	57	42	100	120	105	53	62	77	105	108	108	108
108.0	950.	950.	950.	55	57	42	100	120	105	53	62	77	105	108	108	108



STAGE	CNTR	RCR	CRNR	14	15	16	17	18	19	20	21	22	23	24	25	26
137.0	75.	250.	75.	56	63	53	180	190	173	155	110	122	118	129	140	50
137.1	200.	250.	200.	77	90	70	110	125	202	182	82	102	117	117	114	114
137.2	375.	375.	375.	97	97	71	240	240	240	240	240	240	240	240	240	240
139.0	200.	300.	200.	90	92	81	230	245	245	205	102	125	115	115	115	125
140.0	200.	325.	200.	95	92	81	235	247	225	205	111	140	127	115	115	125
141.0	200.	300.	200.	90	92	81	230	245	245	205	102	125	115	115	115	125
141.1	200.	375.	200.	95	101	87	250	285	250	240	141	170	145	115	115	150
142.1	200.	375.	200.	95	101	87	250	285	242	225	141	170	145	115	115	150
142.2	175.	375.	175.	95	92	91	245	265	225	205	152	170	145	115	115	150
143.0	150.	350.	150.	92	92	92	232	255	228	215	151	190	140	115	115	150
144.0	150.	325.	150.	85	87	71	225	255	220	168	139	160	140	115	115	150
144.1	150.	375.	150.	85	87	71	225	255	220	168	139	160	140	115	115	150
146.0	150.	275.	150.	75	75	61	213	234	234	120	120	120	120	120	120	120
147.0	150.	250.	150.	70	74	59	210	225	200	110	110	110	110	110	110	110
147.1	175.	250.	175.	56	64	46	185	205	185	115	115	115	115	115	115	115
148.0	75.	250.	75.	53	62	49	165	183	170	91	91	91	91	91	91	91
149.0	75.	175.	75.	40	53	51	155	165	151	97	97	97	97	97	97	97
150.0	75.	125.	75.	40	44	31	140	166	165	110	110	110	110	110	110	110
151.0	75.	75.	75.	30	37	38	140	146	140	45	45	45	45	45	45	45
151.1	125.	125.	125.	44	51	46	169	175	160	114	114	114	114	114	114	114
153.0	275.	175.	175.	43	43	56	192	200	190	125	125	125	125	125	125	125
154.0	275.	275.	275.	77	77	75	260	265	240	160	160	160	160	160	160	160
154.1	300.	300.	300.	95	95	81	261	275	250	160	160	160	160	160	160	160
154.2	300.	350.	300.	101	101	81	280	285	260	160	160	160	160	160	160	160
155.0	375.	375.	375.	115	115	101	300	315	290	274	274	274	274	274	274	274
155.1	375.	375.	375.	115	115	101	300	315	290	274	274	274	274	274	274	274
156.0	400.	400.	400.	126	132	123	339	365	340	300	300	300	300	300	300	300
157.0	400.	400.	400.	140	140	138	360	386	360	320	320	320	320	320	320	320
157.1	425.	425.	425.	145	144											

STAGE	CNTR	ACTR	CMR	14	15	16	17	18	19	20	21	22	23	24	25	26
186.0	300.0	300.0	300.0	134	129	120	460	405	440	354	270	201	147	338	245	250
187.0	300.0	300.0	300.0	134	129	126	475	415	455	364	281	217	147	338	245	250
188.0	300.0	300.0	300.0	134	129	132	490	430	470	374	292	231	151	342	245	250
189.0	300.0	300.0	300.0	134	129	138	505	445	485	384	303	245	151	342	245	250
190.0	300.0	300.0	300.0	134	129	144	520	460	500	394	314	259	151	342	245	250
191.0	300.0	300.0	300.0	134	129	150	535	475	515	404	325	273	151	342	245	250
192.0	300.0	300.0	300.0	134	129	156	550	490	530	414	336	287	151	342	245	250
193.0	300.0	300.0	300.0	134	129	162	565	505	545	424	347	301	151	342	245	250
194.0	300.0	300.0	300.0	134	129	168	580	520	560	434	358	315	151	342	245	250
195.0	300.0	300.0	300.0	134	129	174	595	535	575	444	369	329	151	342	245	250
196.0	300.0	300.0	300.0	134	129	180	610	550	590	454	380	343	151	342	245	250
197.0	300.0	300.0	300.0	134	129	186	625	565	605	464	391	357	151	342	245	250
198.0	300.0	300.0	300.0	134	129	192	640	580	620	474	402	371	151	342	245	250
199.0	300.0	300.0	300.0	134	129	198	655	595	635	484	413	385	151	342	245	250
200.0	300.0	300.0	300.0	134	129	204	670	610	650	494	424	399	151	342	245	250
201.0	300.0	300.0	300.0	134	129	210	685	625	665	504	435	413	151	342	245	250
202.0	300.0	300.0	300.0	134	129	216	700	640	680	514	446	427	151	342	245	250
203.0	300.0	300.0	300.0	134	129	222	715	655	695	524	457	441	151	342	245	250
204.0	300.0	300.0	300.0	134	129	228	730	670	710	534	468	455	151	342	245	250
205.0	300.0	300.0	300.0	134	129	234	745	685	725	544	479	469	151	342	245	250
206.0	300.0	300.0	300.0	134	129	240	760	700	740	554	490	483	151	342	245	250
207.0	300.0	300.0	300.0	134	129	246	775	715	755	564	501	497	151	342	245	250
208.0	300.0	300.0	300.0	134	129	252	790	730	770	574	512	511	151	342	245	250
209.0	300.0	300.0	300.0	134	129	258	805	745	785	584	523	525	151	342	245	250
210.0	300.0	300.0	300.0	134	129	264	820	760	800	594	534	539	151	342	245	250
211.0	300.0	300.0	300.0	134	129	270	835	775	815	604	545	553	151	342	245	250
212.0	300.0	300.0	300.0	134	129	276	850	790								

STAGE	CNTR	RCR	CRNR	27	28	29	30	31	32	33	34	35	36	37
1.0	75.	75.	75.	-35	-41	5	-40	-65	-17	-89	-70	68		
2.0	100.	100.	100.	-21	-21	3	-20	-40	-25	-52	-13	68		
3.0	125.	125.	125.	-12	-11	110	10	-10	25	51	133	68		
4.0	150.	150.	150.	30	29	495	60	20	47	98	239	68		
5.0	175.	175.	175.	40	45	129	95	80	105	152	330	68		
6.0	200.	200.	200.	61	69	162	123	115	133	206	430	68		
7.0	225.	225.	225.	79	84	190	146	140	152	254	555	68		
8.0	250.	250.	250.	-120	-141	-880	-200	-65	-11	-30	-100	68		
9.0	275.	275.	275.	422	54	120	100	100	110	205	160	68		
10.0	300.	300.	300.	150	150	70	60	53	75	136	277	68		
11.0	325.	325.	325.	26	15	20	-2	-7	15	46	400	68		
12.0	350.	350.	350.	10	7	22	-8	5	15	37	511	68		
13.0	375.	375.	375.	26	17	33	23	25	45	46	611	68		
14.0	400.	400.	400.	40	22	38	45	45	45	51	711	68		
15.0	425.	425.	425.	50	42	75	65	67	65	86	811	68		
16.0	450.	450.	450.	62	35	100	85	95	87	124	911	68		
17.0	475.	475.	475.	75	75	120	105	115	115	155	1011	68		
18.0	500.	500.	500.	83	75	146	125	140	128	186	1111	68		
19.0	525.	525.	525.	89	79	170	140	155	140	217	1211	68		
20.0	550.	550.	550.	94	79	190	155	170	155	248	1311	68		
21.0	575.	575.	575.	99	59	210	170	185	170	279	1411	68		
22.0	600.	600.	600.	104	37	230	185	200	185	310	1511	68		
23.0	625.	625.	625.	109	21	250	200	215	200	341	1611	68		
24.0	650.	650.	650.	114	9	270	215	230	215	372	1711	68		
25.0	675.	675.	675.	119	4	290	230	245	230	403	1811	68		
26.0	700.	700.	700.	124	2	310	245	260	245	434	1911	68		
27.0	725.	725.	725.	129	3	330	260	275	260	465	2011	68		
28.0	750.	750.	750.	134	3	350	275	290	275	496	2111	68		
29.0	775.	775.	775.	139	4	370	290	305	290	527	2211	68		
30.0	800.	800.	800.	144	4	390	305	320	305	558	2311	68		
31.0	825.	825.	825.	149	5	410	320	335	320	589	2411	68		
32.0	850.	850.	850.	154	5	430	335	350	335	620	2511	68		
33.0	875.	875.	875.	159	6	450	350	365	350	651	2611	68		
34.0	900.	900.	900.	164	6	470	365	380	365	682	2711	68		
35.0	925.	925.	925.	169	7	490	380	395	380	713	2811	68		
36.0	950.	950.	950.	174	7	510	395	410	395	744	2911	68		
37.0	975.	975.	975.	179	8	530	410	425	410	775	3011	68		
38.0	1000.	1000.	1000.	184	8	550	425	440	425	806	3111	68		
39.0	1025.	1025.	1025.	189	9	570	440	455	440	837	3211	68		
40.0	1050.	1050.	1050.	194	9	590	455	470	455	868	3311	68		
41.0	1075.	1075.	1075.	199	10	610	470	485	470	899	3411	68		
42.0	1100.	1100.	1100.	204	10	630	485	500	485	930	3511	68		
43.0	1125.	1125.	1125.	209	11	650	500	515	500	961	3611	68		
44.0	1150.	1150.	1150.	214	11	670	515	530	515	992	3711	68		
45.0	1175.	1175.	1175.	219	12	690	530	545	530	1023	3811	68		
46.0	1200.	1200.	1200.	224	12	710	545	560	545	1054	3911	68		
47.0	1225.	1225.	1225.	229	13	730	560	575	560	1085	4011	68		
48.0	1250.	1250.	1250.	234	13	750	575	590	575	1116	4111	68		
49.0	1275.	1275.	1275.	239	14	770	590	605	590	1147	4211	68		
50.0	1300.	1300.	1300.	244	14	790	605	620	605	1178	4311	68		
51.0	1325.	1325.	1325.	249	15	810	620	635	620	1209	4411	68		
52.0	1350.	1350.	1350.	254	15	830	635	650	635	1240	4511	68		
53.0	1375.	1375.	1375.	259	16	850	650	665	650	1271	4611	68		
54.0	1400.	1400.	1400.	264	16	870	665	680	665	1302	4711	68		
55.0	1425.	1425.	1425.	269	17	890	680	695	680	1333	4811	68		
56.0	1450.	1450.	1450.	274	17	910	695	710	695	1364	4911	68		
57.0	1475.	1475.	1475.	279	18	930	710	725	710	1395	5011	68		
58.0	1500.	1500.	1500.	284	18	950	725	740	725	1426	5111	68		
59.0	1525.	1525.	1525.	289	19	970	740	755	740	1457	5211	68		
60.0	1550.	1550.	1550.	294	19	990	755	770	755	1488	5311	68		
61.0	1575.	1575.	1575.	299	20	1010	770	785	770	1519	5411	68		
62.0	1600.	1600.	1600.	304	20	1030	785	800	785	1550	5511	68		
63.0	1625.	1625.	1625.	309	21	1050	800	815	800	1581	5611	68		
64.0	1650.	1650.	1650.	314	21	1070	815	830	815	1612	5711	68		
65.0	1675.	1675.	1675.	319	22	1090	830	845	830	1643	5811	68		
66.0	1700.	1700.	1700.	324	22	1110	845	860	845	1674	5911	68		
67.0	1725.	1725.	1725.	329	23	1130	860	875	860	1705	6011	68		
68.0	1750.	1750.	1750.	334	23	1150	875	890	875	1736	6111	68		
69.0	1775.	1775.	1775.	339	24	1170	890	905	890	1767	6211	68		
70.0	1800.	1800.	1800.	344	24	1190	905	920	905	1798	6311	68		
71.0	1825.	1825.	1825.	349	25	1210	920	935	920	1829	6411	68		
72.0	1850.	1850.	1850.	354	25	1230	935	950	935	1860	6511	68		
73.0	1875.	1875.	1875.	359	26	1250	950	965	950	1891	6611	68		
74.0	1900.	1900.	1900.	364	26	1270	965	980	965	1922	6711	68		
75.0	1925.	1925.	1925.	369	27	1290	980	995	980	1953	6811	68		
76.0	1950.	1950.	1950.	374	27	1310	995	1010	995	1984	6911	68		
77.0	1975.	1975.	1975.	379	28	1330	1010	1025	1010	2015	7011	68		
78.0	2000.	2000.	2000.	384	28	1350	1025	1040	1025	2046	7111	68		
79.0	2025.	2025.	2025.	389	29	1370	1040	1055	1040	2077	7211	68		
80.0	2050.	2050.	2050.	394	29	1390	1055	1070	1055	2108	7311	68		
81.0	2075.	2075.	2075.	399	30	1410	1070	1085	1070	2139	7411	68		
82.0	2100.	2100.	2100.	404	30	1430	1085	1100	1085	2170	7511	68		
83.0	2125.	2125.	2125.	409	31	1450	1100	1115	1100	2201	7611	68		
84.0	2150.	2150.	2150.	414	31	1470	1115	1130	1115	2232	7711	68		
85.0	2175.	2175.	2175.	419	32	1490	1130	1145	1130	2263	7811	68		
86.0	2200.	2200.	2200.	424	32	1510	1145	1160	1145	2294	7911	68		
87.0	2225.	2225.	2225.	429	33	1530	1160	1175	1160	2325	8011	68		
88.0	2250.	2250.	2250.	434	33	1550	1175	1190	1175	2356	8111	68		
89.0	2275.	2275.	2275.	439	34	1570	1190	1205	1190	2387	8211	68		
90.0	2300.	2300.	2300.	444	34	1590	1205	1220	1205	2418	8311	68		
91.0	2325.	2325.	2325.	449	35	1610	1220	1235	1220	2449	8411	68		
92.0	2350.	2350.	2350.	454	35	1630	1235	1250	1235	2480	8511	68		
93.0	2375.	2375.	2375.	459	36	1650	1250	1265	1250	2511	8611	68		
94.0	2400.	2400.	2400.	464	36	1670	1265	1280	1265	2542	8711	68		
95.0	2425.	2425.	2425.	469	37	1690	1280	1295	1280	2573	8811	68		
96.0	2450.	2450.	2450.	474	37	1710	1295	1310	1295	2604	8911	68		
97.0	2475.	2475.	2475.	479	38	1730	1310	1325	1310	2635	9011	68		
98.0	2500.	2500.	2500.	484	38	1750	1325	1340	1325	2666	9111	68		
99.0	2525.	2525.	2525.	489	39	1770	1340	1355	1340	2697	9211	68		
100.0	2550.	2550.	2550.	494	39	1790	1355	1370	1355	2728	9311	68		
101.0	2575.	2575.	2575.	499	40	1810	1370	1385	1370	2759	9411	68		
102.0	2600.	2600.	2600.	504	40	1830	1385	1400	1385	2790	9511	68		
103.0	2625.	26												



## D.2 REACTIONS

At each Load Stage readings of the 16 load cells were taken. These were converted to reaction values in pounds according to the calibration curve (taken as a straight line) for each cell. The following tabulation gives the reactions at the 16 reaction points as shown in Figure D.2. The first four columns are the same as in the table of deflections. The ratio shown in the righthand column is the ratio of the sum of measured reactions to the sum of self weight and nominal applied load.

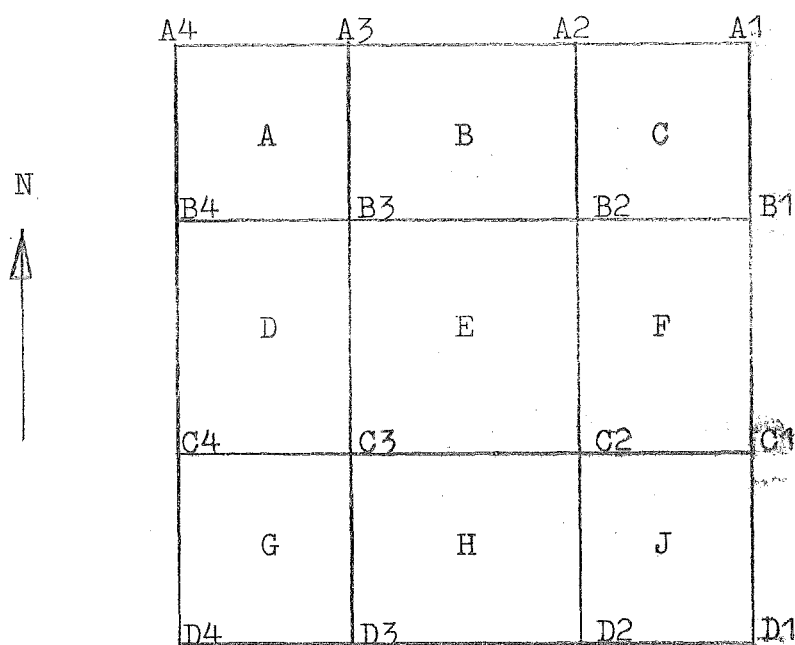


FIGURE D.2. REACTION POINT LOCATION.



STAGE	CNTR	RCTR	CRNR	C3	C2	B2	B3	A2	A3	C4	B4	C1	B1	C2	C3	D1	A4	A1	C4	RATIC
137.0	75.	250.	75.	4826	4925	4544	4905	1928	1855	1873	1896	1843	1856	1755	1872	428	14	62	32	0.9339
137.1	200.	250.	200.	6395	6504	6019	6451	2317	2316	2266	2247	2251	2251	2251	2251	415	15	42	32	0.9339
137.2	350.	350.	350.	7046	7149	6663	7086	2567	2567	2445	2445	2445	2445	2445	2445	435	35	43	32	0.9339
137.3	500.	500.	500.	7398	7487	6950	7393	2697	2697	2556	2556	2556	2556	2556	2556	455	50	43	32	0.9339
137.4	650.	650.	650.	7749	7842	7251	7694	2807	2807	2656	2656	2656	2656	2656	2656	475	65	43	32	0.9339
137.5	800.	800.	800.	8093	8196	7544	7987	3016	3016	2856	2856	2856	2856	2856	2856	495	80	43	32	0.9339
137.6	950.	950.	950.	8438	8541	7824	8267	3225	3225	3056	3056	3056	3056	3056	3056	515	95	43	32	0.9339
137.7	1100.	1100.	1100.	8783	8886	8124	8567	3434	3434	3256	3256	3256	3256	3256	3256	535	110	43	32	0.9339
137.8	1250.	1250.	1250.	9128	9231	8424	8867	3643	3643	3456	3456	3456	3456	3456	3456	555	125	43	32	0.9339
137.9	1400.	1400.	1400.	9473	9576	8712	9155	3852	3852	3656	3656	3656	3656	3656	3656	575	140	43	32	0.9339
138.0	1550.	1550.	1550.	9818	9921	9054	9497	4061	4061	3856	3856	3856	3856	3856	3856	595	155	43	32	0.9339
138.1	1700.	1700.	1700.	10163	10266	9342	9785	4270	4270	4056	4056	4056	4056	4056	4056	615	170	43	32	0.9339
138.2	1850.	1850.	1850.	10508	10611	9687	10130	4479	4479	4256	4256	4256	4256	4256	4256	635	185	43	32	0.9339
138.3	2000.	2000.	2000.	10853	10956	10032	10475	4688	4688	4456	4456	4456	4456	4456	4456	655	200	43	32	0.9339
138.4	2150.	2150.	2150.	11198	11301	10377	10820	4897	4897	4656	4656	4656	4656	4656	4656	675	215	43	32	0.9339
138.5	2300.	2300.	2300.	11543	11646	10722	11165	5106	5106	4856	4856	4856	4856	4856	4856	695	230	43	32	0.9339
138.6	2450.	2450.	2450.	11888	11991	11067	11510	5315	5315	5056	5056	5056	5056	5056	5056	715	245	43	32	0.9339
138.7	2600.	2600.	2600.	12233	12336	11412	11855	5524	5524	5256	5256	5256	5256	5256	5256	735	260	43	32	0.9339
138.8	2750.	2750.	2750.	12578	12681	11757	12200	5733	5733	5456	5456	5456	5456	5456	5456	755	275	43	32	0.9339
138.9	2900.	2900.	2900.	12923	13026	12102	12545	5942	5942	5656	5656	5656	5656	5656	5656	775	290	43	32	0.9339
139.0	3050.	3050.	3050.	13268	13371	12447	12890	6151	6151	5856	5856	5856	5856	5856	5856	795	305	43	32	0.9339
139.1	3200.	3200.	3200.	13613	13716	12792	13235	6360	6360	6056	6056	6056	6056	6056	6056	815	320	43	32	0.9339
139.2	3350.	3350.	3350.	13958	14061	13137	13580	6569	6569	6256	6256	6256	6256	6256	6256	835	335	43	32	0.9339
139.3	3500.	3500.	3500.	14303	14406	13482	13925	6778	6778	6456	6456	6456	6456	6456	6456	855	350	43	32	0.9339
139.4	3650.	3650.	3650.	14648	14751	13827	14270	6987	6987	6656	6656	6656	6656	6656	6656	875	365	43	32	0.9339
139.5	3800.	3800.	3800.	14993	15096	14172	14615	7196	7196	6856	6856	6856	6856	6856	6856	895	380	43	32	0.9339
139.6	3950.	3950.	3950.	15338	15441	14517	14960	7405	7405	7056	7056	7056	7056	7056	7056	915	395	43	32	0.9339
139.7	4100.	4100.	4100.	15683	15786	14862	15305	7614	7614	7256	7256	7256	7256	7256	7256	935	410	43	32	0.9339
139.8	4250.	4250.	4250.	16028	16131	15207	15650	7823	7823	7456	7456	7456	7456	7456	7456	955	425	43	32	0.9339
139.9	4400.	4400.	4400.	16373	16476	15552	16000	8032	8032	7656	7656	7656	7656	7656	7656	975	440	43	32	0.9339
140.0	4550.	4550.	4550.	16718	16821	15897	16340	8241	8241	7856	7856	7856	7856	7856	7856	995	455	43	32	0.9339
140.1	4700.	4700.	4700.	17063	17166	16242	16685	8450	8450	8056	8056	8056	8056	8056	8056	1015	470	43	32	0.9339
140.2	4850.	4850.	4850.	17408	17511	16587	17030	8659	8659	8256	8256	8256	8256	8256	8256	1035	485	43	32	0.9339
140.3	5000.	5000.	5000.	17753	17856	16932	17375	8868	8868	8456	8456	8456	8456	8456	8456	1055	500	43	32	0.9339
140.4	5150.	5150.	5150.	18098	18201	17277	17720	9077	9077	8656	8656	8656	8656	8656	8656	1075	515	43	32	0.9339
140.5	5300.	5300.	5300.	18443	18546	17622	18065	9286	9286	8856	8856	8856	8856	8856	8856	1095	530	43	32	0.9339
140.6	5450.	5450.	5450.	18788	18891	17967	18410	9495	9495	9056	9056	9056	9056	9056	9056	1115	545	43	32	0.9339
140.7	5600.	5600.	5600.	19133	19236	18312	18755	9704	9704	9256	9256	9256	9256	9256	9256	1135	560	43	32	0.9339
140.8	5750.	5750.	5750.	19478	19581	18657	19100	9913	9913	9456	9456	9456	9456	9456	9456	1155	575	43	32	0.9339
140.9	5900.	5900.	5900.	19823	19926	19002	19445	10122	10122	9656	9656	9656	9656	9656	9656	1175	590	43	32	0.9339
141.0	6050.	6050.	6050.	20168	20271	19347	19790	10331	10331	9856	9856	9856	9856	9856	9856	1195	605	43	32	0.9339
141.1	6200.	6200.	6200.	20513	20616	19692	20135	10540	10540	10056	10056	10056	10056	10056	10056	1215	620	43	32	0.9339
141.2	6350.	6350.	6350.	20858	20961	20037	20480	10749	10749	10256	10256	10256	10256	10256	10256	1235	635	43	32	0.9339
141.3	6500.	6500.	6500.	21203	21306	20382	20825	10958	10958	10456	10456	10456	10456	10456	10456	1255	650	43	32	0.9339
141.4	6650.	6650.	6650.	21548	21651	20727	21170	11167	11167	10656	10656	10656	10656	10656	10656	1275	665	43	32	0.9339
141.5	6800.	6800.	6800.	21893	21996	21072	21515	11376	11376	10856	10856	10856	10856	10856	10856	1295	680	43	32	0.9339
141.6	6950.	6950.	6950.	22238	22341	21417	21860	11585	11585	11056	11056	11056	11056	11056	11056	1315	695	43	32	0.9339
141.7	7100.	7100.	7100.	22583	22686	21762	22205	11794	11794	11256	11256	11256	11256	11256	11256	1335	710	43	32	0.9339
141.8	7250.	7250.	7250.	22928	23031	22107	22550	12003	12003	11456	11456	11456	11456	11456	11456	1355	725	43	32	0.9339
141.9	7400.	7400.	7400.	23273	23376	22452	22895	12212	12212	11656	11656	11656	11656	11656	11656	1375	740	43	32	0.9339
142.0	7550.	7550.	7550.	23618	23721	22797	23240	12421	12421	11856	11856	11856	11856	11856	11856	1395	755	43	32	0.9339
142.1	7700.	7700.	7700.	23963	24066	23142	23585	12630	12630	12056	12056	12056	12056	12056	12056	1415	770	43	32	0.9339
142.2	7850.	7850.	7850.	24308	24411	23487	23930	12839	12839	12256	12256	12256	12256	12256	12256	1435	785	43	32	0.9339
142.3	8000.	8000.	8000.	24653	24756	23832	24275	13048	13048	12456	12456	12456	12456	12456	12456	1455	800	43	32	0.9339
142.4	8150.	8150.	8150.	24998	25101	24177	24620	13257	13257	12656	12656	12656	12656	12656	12656	1475	815	43	32	0.9339
142.5	8300.	8300.	8300.	25343	25446	24522	24965	13466	13466	12856	12856	12856	12856	12856	12856	1495	830	43	32	0.9339
142.6	8450.	8450.	8450.	25688	25791	24867	25310	13675	13675	13056	13056	13056	13056	13056	13056	1515	845	43	32	0.9339
142.7	8600.	8600.	8600.	26033	26136	25212	25655	13884	13884	13256	13256	13256	13256	13256	13256	1535	860	43	32	0.9339
142.8	8750.	8750.	8750.	26378	26481	25557	26000	14093	14093	13456	13456	13456	13456	13456	13456	1555	875	43	32	0.9339
142.9	8900.	8900.	8900.	26723	26826	25902	26345	14302	14302	13656	13656	13656	13656	13656	13656	1575	890	43	32	0.9339
143.0	9050.	9050.	9050.	27068	27171	26247	26690	14511	14511	13856	13856	13856	13856	13856	13856	1595	905	43	32	0.9339
143.1	9200.	9200.	9200.	27413	27516	26592	27035	14720	14720	14056	14056	14056	14056	14056	14056	1615	920			

### D.3 STRAINS

The following listing contains the readings in micro-strain units, of all 140 channels of the data logger for all Load Stages during the test. The first column contains the Load Stage numbers and the second column contains numbers which define the load, e.g., at LS32 the number, 220722, is an abbreviation for columns 2, 3 and 4 of the previous tables in Sections D.1 and D.2, and represents a load of 225 psf on the centre panel, 75 psf on the rectangular or centre-edge panels, and 225 psf on the corner panels.

The number at the head of each subsequent column refers to data logger channel to which the gauge was wired. Figures 7.2 and 7.3 show the location of the gauges on the slab. A Philips PR 9249A dummy strain gauge cell was wired to each of channels 1, 21, 41, 61, 81, 101 and 121 to check the performance of the logger. Gauges mounted on the steel in two specially made reinforced blocks were wired to channels 139 and 140 to check the effect of temperature on the steel strain readings.

All readings have LS1 as datum but no other reduction has been made to any reading.

[illegible]

THE LOAD STAGE NUMBER USED AS ZERO FOR THIS RUN IS 1

[illegible]



THE LOAD STAGE NUMBER USED AS ZERO FOR THIS RUN IS 1

[illegible]

THE LOAD STAGE NUMBER USED AS ZERO FOR THIS RUN IS 1

	CHAN	CHAN	CHAN	CHAN	CHAN	CHAN	CHAN	CHAN	CHAN	CHAN	CHAN	CHAN	CHAN	CHAN	CHAN	CHAN	CHAN	CHAN	CHAN			
	1	2	3	4	5	6	7	8	9	10	11	12	13	14	15	16	17	18	19	20		
127	270727	18	-4	0	-4	-7	-10	0.08	-24	-36	74	68	37	-27	32	-39	C	50	49	13	52	-19
128	250725	15	-4	-7	-1	-8	-6	0.86	-37	-40	74	68	37	-27	32	-39	C	50	49	13	52	-19
129	220722	15	-4	-7	-1	-8	-6	0.86	-37	-40	74	68	37	-27	32	-39	C	50	49	13	52	-19
130	170717	17	-3	-4	-11	-12	-15	5.18	-25	-37	79	72	46	-37	36	-43	C	54	53	32	55	-23
131	120712	15	-3	-4	-12	-12	-12	4.73	-25	-40	82	72	46	-37	36	-44	C	52	56	29	56	-27
132	160716	17	-4	-7	-10	-7	-10	0.08	-24	-36	74	68	37	-27	32	-39	C	50	49	13	52	-19
133	70707	17	-4	-3	-7	-11	-14	4.45	-30	-46	90	74	61	-42	34	-42	C	50	57	39	50	-22
134	71207	19	0	-3	-3	-5	-2	4.37	-35	-52	94	75	62	-43	40	-46	C	56	60	45	52	-28
135	71707	16	7	14	13	10	7	4.30	-37	-52	97	84	60	-50	43	-52	C	60	66	47	48	-35
136	7207	17	21	13	12	13	18	4.66	-61	-102	89	61	-55	43	-57	C	65	66	50	49	-35	
137	72507	17	21	13	12	13	18	4.66	-61	-102	89	61	-55	43	-57	C	65	66	50	49	-35	
138	20520	16	18	11	19	18	2	5.18	-46	-62	97	84	39	-55	41	-60	C	58	65	28	45	-36
139	20520	16	18	11	19	18	2	5.18	-46	-62	97	84	39	-55	41	-60	C	58	65	28	45	-36
140	203020	45	19	21	17	17	12	4.47	-66	-103	88	42	-59	50	-62	C	65	70	32	45	-41	
141	203220	18	29	23	20	21	21	5.12	-67	-68	104	89	40	-62	48	-65	C	65	73	31	45	-41
142	203520	17	20	23	20	21	21	5.10	-50	-67	104	89	43	-63	53	-64	C	69	70	34	46	-42
143	203720	20	48	27	23	23	23	5.47	-52	-67	103	88	43	-63	53	-64	C	70	74	34	46	-42
144	173717	13	44	23	27	22	22	5.03	-59	-77	109	92	40	-69	53	-72	C	68	72	32	45	-50
145	153715	19	40	27	32	28	28	4.87	-55	-74	112	95	45	-67	53	-72	C	68	72	36	47	-50
146	153715	19	40	27	32	28	28	4.87	-55	-74	112	95	45	-67	53	-72	C	68	72	36	47	-50
147	153715	19	40	27	32	28	28	4.87	-55	-74	112	95	45	-67	53	-72	C	68	72	36	47	-50
148	153715	19	40	27	32	28	28	4.87	-55	-74	112	95	45	-67	53	-72	C	68	72	36	47	-50
149	153215	20	43	21	23	19	19	4.74	-55	-74	113	94	5									

THE LOAD STAGE NUMBER USED AS ZERO FOR THIS RUN IS 1

	CHAN	CHAN	CHAN	CHAN	CHAN	CHAN	CHAN	CHAN	CHAN	CHAN	CHAN	CHAN	CHAN	CHAN	CHAN	CHAN	CHAN	CHAN	CHAN	CHAN	
	1	2	3	4	5	6	7	8	9	10	11	12	13	14	15	16	17	18	19	20	
1.7A	120000	13	81	-28	-6	1205	-17	-66	117	115	62	-29	5C	-39	C	89	67	25	72	-23	
1.7B	170000	13	23	0	-24	-1	1291	-20	-63	114	54	-32	49	-43	C	86	68	17	69	-26	
1.7C	220000	13	30	0	-18	5	1384	-20	-77	114	54	-32	45	-43	C	86	68	17	62	-29	
1.7D	250000	13	41	107	-5	17	1398	-11	-67	114	110	32	-33	39	-37	C	87	60	-5	62	-12
1.7E	252222	16	37	101	-2	14	1446	-11	-67	114	110	32	-33	39	-37	C	87	60	-5	62	-12
1.7F	272222	17	40	101	-2	12	1445	-10	-72	112	110	32	-33	39	-39	C	86	60	-10	61	-16
1.7G	302222	17	47	95	-17	10	1484	-15	-73	111	110	32	-33	39	-42	C	86	62	-15	60	-17
1.7H	322222	16	31	92	-19	5	1532	-15	-71	111	112	24	-35	36	-42	C	86	62	-15	60	-17
1.7I	352222	13	23	82	-23	-2	1574	-17	-76	109	110	12	-45	33	-46	C	80	60	-24	58	-33
1.7J	372222	17	53	83	-23	-3	1670	-16	-80	104	109	6	-39	38	-45	C	80	61	-33	56	-31
1.7K	322222	20	26	88	-25	0	1635	-15	-82	109	112	16	-43	39	-44	C	83	65	-28	60	-27
1.7L	302222	16	23	81	-27	0	1530	-19	-81	109	110	17	-46	40	-49	C	84	64	-18	63	-39
1.7M	272222	17	23	76	-31	-7	1440	-26	-82	113	115	34	-46	42	-54	C	87	65	-2	66	-42
1.7N	252222	19	53	70	-31	-6	1490	-25	-84	117	118	29	-45	42	-51	C	84	66	-7	62	-40
1.7O	222222	17	23	76	-31	-7	1440	-26	-82	113	115	34	-46	42	-54	C	87	65	-2	66	-42
1.7P	252222	17	52	71	-37	-7	1500	-25	-84	117	118	39	-46	43	-59	C	88	69	4	70	-46
1.7Q	250000	19	28	73	-34	-7	1431	-29	-86	118	119	32	-50	48	-60	C	87	70	-3	68	-49
1.7R	270000	17	37	73	-37	-8	1472	-32	-92	124	129	26	-57	43	-60	C	85	69	-13	65	-59
1.7S	300000	17	33	70	-43	-2	1558	-37	-100	116	120	22	-59	43	-72	C	87	70	-23	62	-60
1.7T	350000	20	49	78	-30	0	1603	-39	-100	117	120	14	-57	46	-74	C	88	70	-23	62	-60
1.7U	370000	17	43	79	-18	3	1656	-36	-102	117	120	9	-59	43	-69	C	85	75	-26	60	-56
1.7V	370000	15	62	143	26	48	1740	-15	-82	118	120	2	-43	40	-28	C	79	64	-28	46	-10
1.7W	370000	15	70	147	27	14	1754	-15	-81	118	120	2	-43	40	-28	C	80	64	-28	46	-10
1.7X	370000	15	76	153	33	55	1808	-11	-79	122	119	1	-44	37	-27	C	80	65	-45	43	-14
1.8A	400000	15	103	181	53	81	2028	-2	-72	110	109	-36	-34	23	-16	C	70	46	-80	34	-2
1.8B	400000	13	71	164	41	70	1673	3	-59	112	106	-13	-26	20	-43	C	70	43	-59	41	-1
1.8C	400000	13	71	164	41	70	1673	3	-59	112	106	-13	-26	20	-43	C	70	43	-59	41	-1
1.8D	400000	13	71	164	41	70	1673	3	-59	112	106	-13	-26	20	-43	C	70	43	-59	41	-1
1.8E	400000	13	71	164	41	70	1673	3	-59	112	106	-13	-26	20	-43	C	70	43	-59	41	-1
1.8F	400000	13	71	164	41	70	1673	3	-59	112	106	-13	-26	20	-43	C	70	43	-59	41	-1
1.8G	400000	13	71	164	41	70	1673	3	-59	112	106	-13	-26	20	-43	C	70	43	-59	41	-1
1.8H	400000	13	71	164	41	70	1673	3	-59	112	106	-13	-26	20	-43	C	70	43	-59	41	-1
1.8I	400000	13	71	164	41	70	1673	3	-59	112	106	-13	-26	20	-43	C	70	43	-59	41	-1
1.8J	400000	13	71	164	41	70	1673	3	-59	112	106	-13	-26	20	-43	C	70	43	-59	41	-1
1.8K	400000	13	71	164	41	70	1673	3	-59	112	106	-13	-26	20	-43	C	70	43	-59	41	-1
1.8L	400000	13	71	164	41	70	1673	3	-59	112	106	-13	-26	20	-43	C	70	43	-59	41	-1
1.8M	400000	13	71	164	41	70	1673	3	-59	112	106	-13	-26	20	-43	C	70	43	-59	41	-1
1.8N	400000	13	71	164	41	70	1673	3	-59	112	106	-13	-26	20	-43	C	70	43	-59	41	-1
1.8O	400000	13	71	164	41	70	1673	3	-59	112	106	-13	-26	20	-43	C	70	43	-59	41	-1
1.8P	400000	13	71	164	41	70	1673	3	-59	112	106	-13	-26	20	-43	C	70	43	-59	41	-1
1.8Q	400000	13	71	164	41	70	1673	3	-59	112	106	-13	-26	20	-43	C	70	43	-59	41	-1
1.8R	400000	13	71	164	41	70	1673	3	-59	112	106	-13	-26	20	-43	C	70	43	-59	41	-1
1.8S	400000	13	71	164	41	70	1673	3	-59	112	106	-13	-26	20	-43	C	70	43	-59	41	-1
1.8T	400000	13	71	164	41	70	1673	3	-59	112	106	-13	-26	20	-43	C	70	43	-59	41	-1
1.8U	400000	13	71	164	41	70	1673	3	-59	112	106	-13	-26	20	-43	C	70	43	-59	41	-1
1.8V	400000	13	71	164	41	70	1673	3	-59	112	106	-13	-26	20	-43	C	70	43	-59	41	-1
1.8W	400000	13	71	164	41	70	1673	3	-59	112	106	-13	-26	20	-43	C	70	43	-59	41	-1
1.8X	400000	13	71	164	41	70	1673	3	-59	112	106	-13	-26	20	-43	C	70	43	-59	41	-1
1.8Y	400000	13	71	164	41	70	1673	3	-59	112	106	-13	-26	20	-43	C	70	43	-59	41	-1
1.8Z	400000	13	71	164	41	70	1673	3	-59	112	106	-13	-26	20	-43	C	70	43	-59	41	-1

THE LOAD STAGE NUMBER USED AS ZERO FOR THIS RUN IS 1

	CHAN	CHAN	CHAN	CHAN	CHAN	CHAN	CHAN	CHAN	CHAN	CHAN	CHAN	CHAN	CHAN	CHAN	CHAN	CHAN	CHAN	CHAN	CHAN	CHAN	
	1	2	3	4	5	6	7	8	9	10	11	12	13	14	15	16	17	18	19	20	
2.05	300000	12	138	831	307	108	7016	-5	-70	124	119	-60	-36	22	-29	C	74	30	-115	2	0
2.06	320000	12	127	835	313	105	7020	-5	-74	124	119	-70	-42	22	-27	C	74	30	-115	2	0
2.07	350000	11	133	871	328	107	7020	-7	-79	123	114	-80	-45	20	-27	C	74	30	-121	-7	-7
2.08	370000	13	145	954	357	113	7020	-8	-83	123	110	-88	-50	20	-32	C	73	30	-132	-10	-10
2.09	370000	13	145	954	357	113	7020	-8	-83	123	110	-88	-50	20	-32	C	73	30	-132	-10	-10
2.10	400000	15	217	1013	378	118	7020	-7	-80	124	109	-86	-46	23	-28	C	75	29	-128	-4	-6
2.11	370000	13	142	912	342	88	7020	-5	-66	123	100	-40	-37	23	-20	C	50	17	-82	7	-1
2.12	370000	13	142	912	342	88	7020	-5	-66	123	100	-40	-37	23	-20	C	50	17	-82	7	-1
2.13	400000	15	217	1013	378	118	7020	-7	-80	124	109	-86	-46	23	-28	C	75	29	-128	-4	-6
2.14	400000	15	217	1013	378	118	7020	-7	-80	124	109	-86	-46	23	-28	C	75	29	-128	-4	-6
2.15	400000	15	217	1013	378	118	7020	-7	-80	124	109	-86	-46	23	-28	C	75	29	-128	-4	-6
2.16	400000	15	217	1013	378	118	7020	-7	-80	124	109	-86	-46	23	-28	C	75	29	-128	-4	-6
2.17	400000	15	217	1013	378	118	7020	-7	-80	124	109	-86	-46	23	-28	C	75	29	-128	-4	-6
2.18	400000	15	217	1013	378	118	7020	-7	-80	124	109	-86	-46	23	-28	C	75	29	-128	-4	-6
2.19	400000	15	217	1013	378	118	7020	-7	-80	124	109	-86	-46	23	-28	C	75	29	-128	-4	-6
2.20	400000	15	217	1013	378	118	7020	-7	-80	124	109	-86	-46	23	-28	C	75	29	-128	-4	-6
2.21	400000	15	217	1013	378	118	7020	-7	-80	124	109	-86	-46	23	-28	C	75	29	-128	-4	-6
2.22	400000	15	217	1013	378	118	7020	-7	-80	124	109	-86	-46	23	-28	C	75	29	-128	-4	-6
2.23	400000	15	217	1013	378	118	7020	-7	-80	124	109	-86	-46	23	-28	C	75	29	-128	-4	-6
2.24	400000	15	217	1013	378	118	7020	-7	-80	124	109	-86	-46	23	-28	C	75	29	-128	-4	-6
2.25	400000	15	217	1013	378	118	7020	-7	-80	124	109	-86	-46	23	-28	C	75	29	-128	-4	-6
2.26	400000	15	217	1013	378	118	7020	-7	-80	124	109	-86	-46	23	-28	C	75	29	-128	-4	-6
2.27	400000	15	217	1013	378	118	7020	-7	-80	124	109	-86	-46	23	-28	C	75	29	-128	-4	-6
2.28	400000	15	217	1013	378	118	7020	-7	-80	124	109	-86	-46	23	-28	C	75	29	-128	-4	-6
2.29	400000	15	217	1013	378	118	7020	-7	-80	124	109	-86	-46	23	-28	C	75	29	-128	-4	-6
2.30	400000	15	217	1013	378	118	7020	-7	-80	124	109	-86	-46	23	-28	C	75	29	-128	-4	-6
2.31	400000	15	217	1013	378	118	7020	-7	-80	124	109	-86	-46	23	-28	C	75	29	-128	-4	-6
2.32	400000	15	217	1013	378	118	7020	-7	-80	124	109	-86	-46	23	-28	C	75	29	-128	-4	-6
2.33	400000	15	217	1013	378	118	7020	-7	-80	124	109	-86	-46	23	-28	C	75	29	-128	-4	-6
2.34	400000	15	217	1013	378	118	7020	-7	-80	124	109	-86	-46	23	-28	C	75	29	-128	-4	-6
2.35	400000	15	217	1013	378	118	7020	-7	-80	124	109	-86	-46	23	-28	C	75	29	-128	-4	-6
2.36	400000	15	217	1013	378	118	7020	-7	-80	124	109	-86	-46	23	-28	C	75	29	-128	-4	-6
2.37	400000	15	217	1013	378	118	7020	-7	-80	124	109	-86	-46	23	-28	C	75	29	-128	-4	-6
2.38	400000	15	217	1013	378	118	7020	-7	-80	124	109	-86	-46	23	-28	C	75	29	-128	-4	-6
2.39	400000	15	217	1013	378	118	7020	-7	-80	124	109	-86	-46	23	-28	C	75	29	-128	-4	-6
2.40	400000	15	217	1013	378	118	7020	-7	-80	124	109	-86	-46	23	-28	C	75	29	-128	-4	-6
2.41	400000	15	217	1013	378	118	7020	-7	-80	124	109	-86	-46	23	-28	C	75	29	-128	-4	-6
2.42	400000	15	217	1013	378	118	7020	-7	-80	124	109	-86	-46	23	-28	C	75	29	-128	-4	-6
2.43	400000	15	217	1013	378	118	7020	-7	-80	124	109	-86	-46	23	-28	C	75	29	-128	-4	-6
2.44	400000	15	217	1013	378	118	7020	-7	-80	124	109	-86	-46	23	-28	C	75	29	-128	-4	-6
2.45	400000	15	217	1013	378	118	7020	-7	-80	124	109	-86	-46	23	-28	C	75	29	-128	-4	-6
2.46	400000	15	217	1013	378	118	7020	-7	-80	124	109	-86	-46	23	-28	C	75	29	-128	-4	-6
2.47	400000	15	217	1013	378	118	7020	-7	-80	124	109	-86	-46	23	-28	C	75	29	-128	-4	-6
2.48	400000	15	217	1013	378	118	7020	-7	-80	124	109	-86	-46	23	-28	C	75	29	-128	-4	-6
2.49	400000	15	217	1013	378	118	7020	-7	-80	124	109	-86	-46	23	-28	C	75	29	-128	-4	-6
2.50	400000	15	217	1013	378	118	7020	-7	-80	124	109	-86	-46	23	-28	C	75	29	-128	-4	-6
2.51	400000	15	217	1013	378	118	7020	-7	-80	124	109	-86	-46	23	-28	C	75	29	-128	-4	-6
2.52	400000	15	217	1013	378	118	7020	-7	-80	124	109	-86	-46	23	-28	C	75	29	-128	-4	-6
2.53	400000	15	217	1013	378	118	7020	-7	-80	124	109	-86	-46	23	-28	C	75	29	-128	-4	-6
2.54	400000	15	217	1013	378	118	7020	-7	-80	124	109	-86	-46	23	-28	C	75	29	-128	-4	-6
2.55	400000	15	217	1013	378	118	7020	-7	-80	124	109	-86	-46	23	-28	C	75	29	-128	-4	-6
2.56	400000	15	217	1013	378	118	7020	-7	-80	124	109	-86	-46	23	-28	C	75	29	-128	-4	-6
2.57	400000	15	217	1013	378	118	7020	-7	-80	124	109	-86	-46	23	-28	C	75	29	-128	-4	-6
2.58	400000	15	217	1013	378	118	7020	-7	-80	124	109	-86	-46	23	-28	C	75	29	-128	-4	-6
2.59	400000	15	217	1013	378	118	7020	-7	-80	124	109	-86	-46	23	-28	C	75	29	-128	-4	-6
2.60	400000	15	217	1013	378	118	7020	-7	-80	124	109	-86	-46	23	-28	C	75	29	-128	-4	-6
2.61	400000	15	217	1013	378	118	7020	-7	-80	124	109	-86	-46	23	-28	C	75	29	-128	-4	-6
2.62	400000	15	217	1013	378	118	7020	-7	-80	124	109	-86	-46	23	-28	C	75	29	-128	-4	-6
2.63	400000	15	217	1013	378	118	7020	-7	-80	124	109	-86	-46	23	-28	C	75	29	-128	-4	-6
2.64	400000	15	217	1013	378	118	7020	-7	-80	124	109	-86	-46	23	-28	C	75	29	-128	-4	-6
2.65	400000	15	217	1013	378	118	7020	-7	-80	124	109	-86	-46	23	-28	C	75	29	-128	-4	-6
2.66	400000	15	217	1013	378	118	7020	-7	-80	124	109	-86	-46	23	-28	C	75	29	-128	-4	-6
2.67	400000	15	217	1013	378	118	7020	-7	-80	124	109	-86	-46	23	-28	C	75	29	-128	-4	-6
2.68	400000	15	217	1013	378	118	7020	-7	-80	124	109	-86	-46	23	-28	C	75	29	-128	-4	-6
2.69	400000	15	217	1013	378	118	7020	-7	-80	124	109	-86	-46	23	-28	C	75	29	-128	-4	-6
2.70	400000	15	217	1013	378	118	7020	-7	-80	124	109	-86	-46	23	-28	C	75	29	-128	-4	-6
2.71	400000	15	217	1013	378	118	7020	-7	-80	124	109	-86	-46	23	-28	C	75	29	-128	-4	-6
2.72	400000	15	217	1013	378	118	7020	-7	-80	124	109	-86	-46	23	-28	C	75	29	-128	-4	-6
2.73	400000	15	217	1013	378	118	7020	-7	-80	124	109	-86	-46	23	-28	C	75	29	-128	-4	-6
2.74	400000	15	217	1013	378	118	7020	-7	-80	124	109	-86	-46	23	-28	C	75	29	-128	-4	-6
2.75	400000	15	217	1013	378	118	7020	-7	-80	124	109	-86	-46	23	-28	C	75	29	-128	-4	-6
2.76	400000	15	217	1013	378	118	7020	-7	-80	124	109	-86	-46	23	-						

THE LOAD STAGE NUMBER USED AS ZERO FOR THIS RUN IS 1

	CHAN	CHAN	CHAN	CHAN	CHAN	CHAN	CHAN	CHAN	CHAN	CHAN	CHAN	CHAN	CHAN	CHAN	CHAN	CHAN	CHAN	CHAN	CHAN	CHAN
	21	22	23	24	25	26	27	28	29	30	31	32	33	34	35	36	37	38	39	40
1A	70707	0	0	0	0	0	0	0	0	0	0	0	0	0	0	0	0	0	0	0
1A	70707	0	0	0	0	0	0	0	0	0	0	0	0	0	0	0	0	0	0	0
2A	101010	1	1	1	1	1	1	1	1	1	1	1	1	1	1	1	1	1	1	1
3A	121212	2	2	2	2	2	2	2	2	2	2	2	2	2	2	2	2	2	2	2
4A	151515	3	3	3	3	3	3	3	3	3	3	3	3	3	3	3	3	3	3	3
5A	171717	4	4	4	4	4	4	4	4	4	4	4	4	4	4	4	4	4	4	4
6A	202020	5	5	5	5	5	5	5	5	5	5	5	5	5	5	5	5	5	5	5
7A	222222	6	6	6	6	6	6	6	6	6	6	6	6	6	6	6	6	6	6	6
8A	252525	7	7	7	7	7	7	7	7	7	7	7	7	7	7	7	7	7	7	7
9A	272727	8	8	8	8	8	8	8	8	8	8	8	8	8	8	8	8	8	8	8
10A	303030	9	9	9	9	9	9	9	9	9	9	9	9	9	9	9	9	9	9	9
11A	333333	10	10	10	10	10	10	10	10	10	10	10	10	10	10	10	10	10	10	10
12A	353535	11	11	11	11	11	11	11	11	11	11	11	11	11	11	11	11	11	11	11
13A	373737	12	12	12	12	12	12	12	12	12	12	12	12	12	12	12	12	12	12	12
14A	404040	13	13	13	13	13	13	13	13	13	13	13	13	13	13	13	13	13	13	13
15A	424242	14	14	14	14	14	14	14	14	14	14	14	14	14	14	14	14	14	14	14
16A	444444	15	15	15	15	15	15	15	15	15	15	15	15	15	15	15	15	15	15	15
17A	474747	16	16	16	16	16	16	16	16	16	16	16	16	16	16	16	16	16	16	16
18A	505050	17	17	17	17	17	17	17	17	17	17	17	17	17	17	17	17	17	17	17
19A	525252	18	18	18	18	18	18	18	18	18	18	18	18	18	18	18	18	18	18	18
20A	555555	19	19	19	19	19	19	19	19	19	19	19	19	19	19	19	19	19	19	19
21A	575757	20	20	20	20	20	20	20	20	20	20	20	20	20	20	20	20	20	20	20
22A	606060	21	21	21	21	21	21	21	21	21	21	21	21	21	21	21	21	21	21	21
23A	626262	22	22	22	22	22	22	22	22	22	22	22	22	22	22	22	22	22	22	22
24A	656565	23	23	23	23	23	23	23	23	23	23	23	23	23	23	23	23	23	23	23
25A	676767	24	24	24	24	24	24	24	24	24	24	24	24	24	24	24	24	24	24	24
26A	707070	25	25	25	25	25	25	25	25	25	25	25	25	25	25	25	25	25	25	25
27A	727272	26	26	26	26	26	26	26	26	26	26	26	26	26	26	26	26	26	26	26
28A	757575	27	27	27	27	27	27	27	27	27	27	27	27	27	27	27	27	27	27	27
29A	777777	28	28	28	28	28	28	28	28	28	28	28	28	28	28	28	28	28	28	28
30A	808080	29	29	29	29	29	29	29	29	29	29	29	29	29	29	29	29	29	29	29
31A	828282	30	30	30	30	30	30	30	30	30	30	30	30	30	30	30	30	30	30	30
32A	858585	31	31	31	31	31	31	31	31	31	31	31	31	31	31	31	31	31	31	31
33A	878787	32	32	32	32	32	32	32	32	32	32	32	32	32	32	32	32	32	32	32
34A	909090	33	33	33	33	33	33	33	33	33	33	33	33	33	33	33	33	33	33	33
35A	929292	34	34	34	34	34	34	34	34	34	34	34	34	34	34	34	34	34	34	34
36A	959595	35	35	35	35	35	35	35	35	35	35	35	35	35	35	35	35	35	35	35
37A	979797	36	36	36	36	36	36	36	36	36	36	36	36	36	36	36	36	36	36	36
38A	100100	37	37	37	37	37	37	37	37	37	37	37	37	37	37	37	37	37	37	37
39A	102102	38	38	38	38	38	38	38	38	38	38	38	38	38	38	38	38	38	38	38
40A	105105	39	39	39	39	39	39	39	39	39	39	39	39	39	39	39	39	39	39	39

THE LOAD STAGE NUMBER USED AS ZERO FOR THIS RUN IS 1

	CHAN	CHAN	CHAN	CHAN	CHAN	CHAN	CHAN	CHAN	CHAN	CHAN	CHAN	CHAN	CHAN	CHAN	CHAN	CHAN	CHAN	CHAN	CHAN	CHAN
	21	22	23	24	25	26	27	28	29	30	31	32	33	34	35	36	37	38	39	40
55	150715	68	24	15	16	33	24	3	27	17	19	14	9	39	15	32	31	21	42	18
56	150715	71	25	16	17	34	25	4	28	18	20	15	10	40	22	32	31	21	43	19
57	150715	74	26	17	18	35	26	5	29	19	21	16	11	12	23	33	32	22	44	20
58	150715	77	27	18	19	36	27	6	30	20	22	17	12	13	24	34	33	23	45	21
59	150715	80	28	19	20	37	28	7	31	21	23	18	13	14	25	35	34	24	46	22
60	150715	83	29	20	21	38	29	8	32	22	24	19	14	15	26	36	35	25	47	23
61	150715	86	30	21	22	39	30	9	33	23	25	20	15	16	27	37	36	26	48	24
62	150715	89	31	22	23	40	31	10	34	24	26	21	16	17	28	38	37	27	49	25
63	150715	92	32	23	24	41	32	11	35	25	27	22	17	18	29	39	38	28	50	26
64	150715	95	33	24	25	42	33	12	36	26	28	23	18	19	30	40	39	29	51	27
65	150715	98	34	25	26	43	34	13	37	27	29	24	19	20	31	41	40	30	52	28
66	150715	101	35	26	27	44	35	14	38	28	30	25	20	21	32	42	41	31	53	29
67	150715	104	36	27	28	45	36	15	39	29	31	26	21	22	33	43	42	32	54	30
68	150715	107	37	28	29	46	37	16	40	30	32	27	22	23	34	44	43	33	55	31
69	150715	110	38	29	30	47	38	17	41	31	33	28	23	24	35	45	44	34	56	32
70	150715	113	39	30	31	48	39	18	42	32	34	29	24	25	36	46	45	35	57	33
71	150715	116	40	31	32	49	40	19	43	33	35	30	25	26	37	47	46	36	58	34
72	150715	119	41	32	33	50	41	20	44	34	36	31	26	27	38	48	47	37	59	35
73	150715	122	42	33	34	51	42	21	45	35	37	32	27	28	39	49	48	38	60	36
74	150715	125	43	34	35	52	43	22	46	36	38	33	28	29	40	50	49	39	61	37
75	150715	128	44	35	36	53	44	23	47	37	39	34	29	30	41	51	50	40	62	38
76	150715	131	45	36	37	54	45	24	48	38	40	35	30	31	42	52	51	41	63	39
77	150715	134	46	37	38	55	46	25	49	39	41	36	31	32	43	53	52	42	64	40
78	150715	137	47	38	39	56	47	26	50	40	42	37	32	33	44	54	53	43	65	41
79	150715	140	48	39	40	57	48	27	51	41	43	38	33	34	45	55	54	44	66	42
80	150715	143	49	40	41	58	49	28	52	42	44	39	34	35	46	56	55	45	67	43
81	150715	146	50	41	42	59	50	29	53	43	45	40	35	36	47	57	56	46	68	44
82	150715	149	51	42	43	60	51	30	54	44	46	41	36	37	48	58	57	47	69	45
83	150715	152	52	43	44	61	52	31	55	45	47	42	37	38	49	59	58	48	70	46
84	150715	155	53	44	45	62	53	32	56	46	48	43	38	39	50	60	59	49	71	47
85	150715	158	54	45	46	63	54	33	57	47	49	44	39	40	51	61	60	50	72	48
86	150715	161	55	46	47	64	55	34	58	48	50	45	40	41	52	62	61	51	73	49
87	150715	164	56	47	48	65	56	35	59	49	51	46	41	42	53	63	62	52	74	50
88	150715	167	57	48	49	66	57	36	60	50	52	47	42	43	54	64	63	53	75	51
89	150715	170	58	49	50	67	58	37	61	51	53	48	43	44	55	65	64	54	76	52
90	150715	173	59	50	51	68	59	38	62	52	54	49	44	45	56	66	65	55	77	53
91	150715	176	60	51	52	69	60	39	63	53	55	50	45	46	57	67	66	56	78	54
92	150715	179	61	52	53	70	61	40	64	54	56	51	46	47	58	68	67	57	79	55
93	150715	182	62	53	54	71	62	41	65	55	57	52	47	48	59	69	68	58	80	56
94	150715	185	63	54	55	72	63	42	66	56	58	53	48	49	60	70	69	59	81	57
95	150715	188	64	55	56	73	64	43	67	57	59	54	49	50	61	71	70	60	82	58
96	150715	191	65	56	57	74	65	44	68	58	60	55	50	51	62	72	71	61	83	59
97	150715	194	66	57	58	75	66	45	69	59	61	56	51	52	63	73	72	62	84	60
98	150715	197	67	58	59	76	67	46	70	60	62	57	52	53	64	74	73	63	85	61
99	150715	200	68	59	60	77	68	47	71	61	63	58	53	54	65	75	74	64	86	62
100	150715	203	69	60	61	78	69	48	72	62	64	59	54	55	66	76	75	65	87	63
101	150715	206	70	61	62	79	70	49	73	63	65	60	55	56	67	77	76	66	88	64
102	150715	209	71	62	63	80	71	50	74	64	66	61	56	57	68	78	77	67	89	65
103	150715	212	72	63	64	81	72	51	75	65	67	62	57	58	69	79	78	68	90	66
104	150715	215	73	64	65	82	73	52	76	66	68	63	58	59	70	80	79	69	91	67
105	150715	218	74	65	66	83	74	53	77	67	69	64	59	60	71	81	80	70	92	68
106	150715	221	75	66	67	84	75	54	78	68	70	65	60	61	72	82	81	71	93	69
107	150715	224	76	67	68	85	76	55	79	69	71	66	61	62	73	83	82	72	94	70
108	150715	227	77	68	69	86	77	56	80	70	72	67	62	63	74	84	83	73	95	71
109	150715	230	78	69	70	87	78	57	81	71	73	68	63	64	75	85	84	74	96	72
110	150715	233	79	70	71	88	79	58	82	72	74	69	64	65	76	86	85	75	97	73
111	150715	236	80	71	72	89	80	59	83	73	75	70	65	66	77	87	86	76	98	74
112	150715	239	81	72	73	90	81	60	84	74	76	71	66	67	78	88	87	77	99	75
113	150715	242	82	73	74	91	82	61	85	75	77	72	67	68	79	89	88	78	100	76
114	150715	245	83	74	75	92	83	62	86	76	78	73	68	69	80	90	89	79	101	77
115	150715	248	84	75	76	93	84	63	87	77	79	74	69	70	81	91	90	80	102	78
116	150715	251	85	76	77	94	85	64	88	78	80	75	70	71	82	92	91	81	103	79
117	150715	254	86	77	78	95	86	65	89	79	81	76	71	72	83	93	92	82	104	80
118	150715	257	87	78	79	96	87	66	90	80	82	77	72	73	84	94	93	83	105	81
119	150715	260	88	79	80	97	88	67	91	81	83	78	73	74	85	95	94	84	106	82
120	150715	263	89	80	81	98	89	68	92	82	84	79	74	75	86	96	95	85	107	83
121	150715	266	90	81	82	99	90	69	93	83	85	80	75	76	87	97	96	86	108	84
122	150715	269	91	82	83	100	91	70	94	84	86	81	76	77	88	98	97	87	109	85
123	150715	272	92	83	84	101	92	71	95	85	87	82	77	78	89	99	98	88	110	86
124	150715	275	93	84	85	102	93	72	96	86	88	83	78	79	90	100	99	89	111	87
125	150715	278	94	85	86	103	94	73	97	87	89	84	79	80	91	101	100	90	112	88
126	150715	281	95	86	87	104	95	74	98	88	90	85	80	81	92	102	101	91	113	89
127	150715	284	96	87	88	105	96	75	99	89	91	86	81	82	93	103	102	92	114	90
128	150715	287	97	88	89	106	97	76	100	90	92	87	82	83	94	104	103	93	115	91
129	150715	290	98	89	90	107	98	77	101	91	93	88	83	84	95	105	104	94	116	92
130	150715	293	99	90	91	108	99	78	102	92	94	89	84	85	96	106	105	95	117	93
131	150715	296	100	91	92	109	100	79	103	93	95	90	85	86	97	107	106	96	118	94
132	150715	299																		

THE LOAD STAGE NUMBER USED AS ZERO FOR THIS RUN IS 1

	CHAN	CHAN	CHAN	CHAN	CHAN	CHAN	CHAN	CHAN	CHAN	CHAN	CHAN	CHAN	CHAN	CHAN	CHAN	CHAN	CHAN	CHAN	CHAN		
	21	22	23	24	25	26	27	28	29	30	31	32	33	34	35	36	37	38	39	40	
177	353535	116	38	3	-1	56	47	-12	48	4	3	41	23	6	44	17	37	24	9	80	7
178	353535	103	39	4	-1	55	49	-12	49	4	3	41	23	6	44	17	37	24	9	80	7
179	373737	116	38	3	-1	56	47	-12	48	4	3	41	23	6	44	17	37	24	9	80	7
180	373737	102	37	6	-3	56	49	-18	53	4	3	42	25	9	45	19	37	21	11	80	5
181	353535	103	39	4	-1	55	49	-12	49	4	3	41	23	6	44	17	37	24	9	80	7
182	323232	96	46	3	-1	46	51	-13	50	5	1	40	24	7	44	20	37	19	13	77	6
183	303030	115	42	3	-2	52	44	-8	47	5	2	39	27	4	44	16	39	25	7	79	8
184	272727	654	37	7	-1	54	44	-3	47	5	2	39	27	4	44	16	39	25	7	79	8
185	252525	23	32	3	-1	50	42	-2	42	8	2	33	28	4	42	12	36	34	8	80	7
186	202020	25	32	3	-1	50	44	-2	44	8	2	33	30	4	44	13	39	36	10	81	10
187	171717	25	32	3	-1	50	44	-2	44	8	2	33	30	4	44	13	39	36	10	81	10
188	151515	25	32	3	-1	50	44	-2	44	8	2	33	30	4	44	13	39	36	10	81	10
189	121212	25	32	3	-1	50	44	-2	44	8	2	33	30	4	44	13	39	36	10	81	10
190	707070	28	33	7	-1	48	41	-1	38	6	7	30	31	4	45	16	41	45	13	83	10
191	707070	28	33	7	-1	48	41	-1	38	6	7	30	31	4	45	16	41	45	13	83	10
192	121212	25	32	3	-1	50	44	-2	44	8	2	33	30	4	44	13	39	36	10	81	10
193	121212	25	32	3	-1	50	44	-2	44	8	2	33	30	4	44	13	39	36	10	81	10
194	171717	25	32	3	-1	50	44	-2	44	8	2	33	30	4	44	13	39	36	10	81	10
195	222222	25	32	3	-1	50	44	-2	44	8	2	33	30	4	44	13	39	36	10	81	10
196	222222	25	32	3	-1	50	44	-2	44	8	2	33	30	4	44	13	39	36	10	81	10
197	272727	654	37	7	-1	54	44	-3	47	5	2	39	27	4	44	16	39	25	7	79	8
198	323232	96	46	3	-1	46	51	-13	50	5	1	40	24	7	44	20	37	19	13	77	6
199	353535	116	38	3	-1	56	47	-12	48	4	3	41	23	6	44	17	37	24	9	80	7
200	373737	116	38	3	-1	56	47	-12	48	4	3	41	23	6	44	17	37	24	9	80	7
201	373737	102	37	6	-3	56	49	-18	53	4	3	42	25	9	45	19	37	21	11	80	5
202	353535	103	39	4	-1	55	49	-12	49	4	3	41	23	6	44	17	37	24	9	80	7
203	323232	96	46	3	-1	46	51	-13	50	5	1	40	24	7	44	20	37	19	13	77	6
204	303030	115	42	3	-2	52	44	-8	47	5	2	39	27	4	44	16	39	25	7	79	8
205	272727	654	37	7	-1	54	44	-3	47	5	2	39	27	4	44	16	39	25	7	79	8
206	252525	23	32	3	-1	50	42	-2	42	8	2	33	28	4	42	12	36	34	8	80	7
207	202020	25	32	3	-1	50	44	-2	44	8	2	33	30	4	44	13	39	36	10	81	10
208	171717	25	32	3	-1	50	44	-2	44	8	2	33	30	4	44	13	39	36	10	81	10
209	151515	25	32	3	-1	50	44	-2	44	8	2	33	30	4	44	13	39	36	10	81	10
210	121212	25	32	3	-1	50	44	-2	44	8	2	33	30	4	44	13	39	36	10	81	10
211	707070	28	33	7	-1	48	41	-1	38	6	7	30	31	4	45	16	41	45	13	83	10
212	707070	28	33	7	-1	48	41	-1	38	6	7	30	31	4	45	16	41	45	13	83	10
213	121212	25	32	3	-1	50	44	-2	44	8	2	33	30	4	44	13	39	36	10	81	10
214	121212	25	32	3	-1	50	44	-2	44	8	2	33	30	4	44	13	39	36	10	81	10
215	171717	25	32	3	-1	50	44	-2	44	8	2	33	30	4	44	13	39	36	10	81	10
216	222222	25	32	3	-1	50	44	-2	44	8	2	33	30	4	44	13	39	36	10	81	10
217	222222	25	32	3	-1	50	44	-2	44	8	2	33	30	4	44	13	39	36	10	81	10
218	272727	654	37	7	-1	54	44	-3	47	5	2	39	27	4	44	16	39	25	7	79	8
219	323232	96	46	3	-1	46	51	-13	50	5	1	40	24	7	44	20	37	19	13	77	6
220	353535	116	38	3	-1	56	47	-12	48	4	3	41	23	6	44	17	37	24	9	80	7
221	373737	116	38	3	-1	56	47	-12	48	4	3	41	23	6	44	17	37	24	9	80	7
222	373737	102	37	6	-3	56	49	-18	53	4	3	42	25	9	45	19	37	21	11	80	5
223	353535	103	39	4	-1	55	49	-12	49	4	3	41	23	6	44	17	37	24	9	80	7
224	323232	96	46	3	-1	46	51	-13	50	5	1	40	24	7	44	20	37	19	13	77	6
225	303030	115	42	3	-2	52	44	-8	47	5	2	39	27	4	44	16	39	25	7	79	8
226	272727	654	37	7	-1	54	44	-3	47	5	2	39	27	4	44	16	39	25	7	79	8
227	252525	23	32	3	-1	50	42	-2	42	8	2	33	28	4	42	12	36	34	8	80	7
228	202020	25	32	3	-1	50	44	-2	44	8	2	33	30	4	44	13	39	36	10	81	10
229	171717	25	32	3	-1	50	44	-2	44	8	2	33	30	4	44	13	39	36	10	81	10
230	151515	25	32	3	-1	50	44	-2	44	8	2	33	30	4	44	13	39	36	10	81	10
231	121212	25	32	3	-1	50	44	-2	44	8	2	33	30	4	44	13	39	36	10	81	10
232	707070	28	33	7	-1	48	41	-1	38	6	7	30	31	4	45	16	41	45	13	83	10
233	707070	28	33	7	-1	48	41	-1	38	6	7	30	31	4	45	16	41	45	13	83	10
234	121212	25	32	3	-1	50	44	-2	44	8	2	33	30	4	44	13	39	36	10	81	10
235	121212	25	32	3	-1	50	44	-2	44	8	2	33	30	4	44	13	39	36	10	81	10
236	171717	25	32	3	-1	50	44	-2	44	8	2	33	30	4	44	13	39	36	10	81	10
237	222222	25	32	3	-1	50	44	-2	44	8	2	33	30	4	44	13	39	36	10	81	10
238	222222	25	32	3	-1	50	44	-2	44	8	2	33	30	4	44	13	39	36	10	81	10
239	272727	654	37	7	-1	54	44	-3	47	5	2	39	27	4	44	16	39	25	7	79	8
240	323232	96	46	3	-1	46	51	-13	50	5	1	40	24	7	44	20	37	19	13	77	6
241	353535	116	38	3	-1	56	47	-12	48	4	3	41	23	6	44	17	37	24	9	80	7
242	373737	116	38	3	-1	56	47	-12	48	4	3	41	23	6	44	17	37	24	9	80	7
243	373737	102	37	6	-3	56	49	-18	53	4	3	42	25	9	45	19	37	21	11	80	5
244	353535	103	39	4	-1	55	49	-12	49	4	3	41	23	6	44	17	37	24	9	80	7
245	323232	96	46	3	-1	46	51	-13	50	5	1	40	24	7	44	20	37	19	13	77	6
246	303030	115	42	3	-2	52	44	-8	47	5	2	39	27	4	44	16	39	25	7	79	8
247	272727	654	37	7	-1	54	44	-3	47	5	2	39	27	4	44	16	39	25	7	79	8
248	252525	23	32	3	-1	50	42	-2	42	8	2	33	28	4	42	12	36	34	8	80	7
249	202020	25	32	3	-1	50	44	-2	44	8	2	33	30	4	44	13	39	36	10	81	10
250	171717	25	32	3	-1	50	44	-2	44	8	2	33	30	4	44	13	39	36	10	81	10
251	151515	25	32	3	-1	50	44	-2	44	8	2	33	30	4	44	13	39	36	10	81	10
252	121212	25	32	3	-1	50	44	-2	44	8	2	33	30	4	44	13	39	36	10	81	10
253	7																				

\*\*\*\*\*

[illegible]

THE LOAD STACK NUMBER USED AS ZERO FOR THIS RUN IS 1

[illegible]

THE LOAD STAGE NUMBER USED AS ZERO FOR THIS RUN IS 1

[illegible]

THE LOAD STAGE NUMBER USED AS ZERO FOR THIS RUN IS 1

[illegible]

[illegible]





THE LOAD STAGE NUMBER USED AS ZERO FOR THIS RUN IS 1

	CHAN	CHAN	CHAN	CHAN	CHAN	CHAN	CHAN	CHAN	CHAN	CHAN	CHAN	CHAN	CHAN	CHAN	CHAN	CHAN	CHAN	CHAN	CHAN	
	61	62	63	64	65	66	67	68	69	70	71	72	73	74	75	76	77	78	79	80
100	17	-7	81	67	66	77	-2	12	7	473	440	333	233	-43	-45	-4	-3	-22	-26	-32
101	17	18	97	65	66	77	-2	15	3	477	442	338	236	-42	-47	-4	-4	-22	-26	-32
102	17	-3	94	72	71	83	-5	10	2	498	467	373	256	-52	-52	-13	-7	-27	-26	-34
103	17	-16	95	75	70	84	-6	13	3	500	469	377	256	-51	-53	-13	-7	-27	-28	-36
104	17	-16	90	67	68	78	-5	13	3	485	457	372	249	-41	-47	-5	0	-22	-26	-32
105	17	-14	83	55	53	70	0	13	5	468	440	360	236	-40	-48	-2	0	-22	-22	-31
106	17	0	76	55	53	65	19	9	452	427	349	227	-36	-40	1	9	-18	-19	-27	
107	17	3	71	53	50	60	5	13	435	410	335	225	-28	-34	19	10	-10	-10	-17	
108	17	5	67	48	48	53	22	18	416	392	323	201	-24	-32	18	10	-10	-10	-17	
109	17	11	57	40	40	40	11	24	16	399	376	310	194	-18	-26	19	20	-8	-5	-16
110	17	10	51	38	36	40	12	26	20	380	360	296	182	-11	-16	26	24	0	3	-10
111	17	12	50	34	30	37	11	30	27	363	342	282	157	0	-10	38	34	9	7	-3
112	17	14	41	32	23	27	31	31	27	343	322	267	157	0	-10	38	34	9	7	-3
113	17	21	33	20	18	26	24	33	30	325	304	252	144	4	-5	44	40	12	10	2
114	17	27	20	16	16	22	22	30	35	283	262	218	118	14	4	44	40	12	10	2
115	17	33	34	17	16	20	32	41	33	315	307	246	145	11	3	53	48	12	10	2
116	17	28	46	23	34	57	24	38	31	345	339	270	164	3	-6	62	43	20	36	6
117	17	22	54	28	37	64	22	33	27	377	363	292	185	3	-13	54	36	12	27	-3
118	17	18	65	42	49	74	18	31	20	414	400	325	215	-15	-23	41	30	4	17	-17
119	17	18	77	53	59	72	11	28	17	451	432	354	237	-27	-32	42	32	19	7	-17
120	17	14	87	63	64	89	5	23	10	484	467	389	261	-39	-39	19	12	-13	-5	-27
121	17	3	95	67	68	95	2	20	9	504	488	409	277	-42	-47	11	11	-16	-14	-30
122	17	7	102	74	71	102	2	20	13	530	510	440	295	-46	-52	10	10	-27	-17	-28
123	17	16	81	53	56	77	7	23	13	526	507	448	295	-43	-47	4	6	-28	-14	-30
124	17	10	66	35	40	59	14	28	19	515	497	443	288	-40	-43	4	6	-27	-17	-28
125	17	10	61	27	30	38	14	30	19	512	497	443	288	-40	-43	4	6	-27	-17	-28
126	17	10	57	29	28	37	12	31	20	512	490	437	282	-39	-46	5	9	-28	-20	-27
127	17	14	39	13	15	30	17	36	27	505	481	433	254	-33	-39	8	12	-27	-19	-27
128	17	14	39	13	15	30	17	36	27	505	481	433	254	-33	-39	8	12	-27	-19	-27
129	17	23	26	0	1	22	30	43	35	495	471	432	247	-31	-38	10	12	-27	-20	-27
130	17	23	26	0	1	22	30	43	35	495	471	432	247	-31	-38	10	12	-27	-20	-27
131	17	23	26	0	1	22	30	43	35	495	471	432	247	-31	-38	10	12	-27	-20	-27
132	17	23	26	0	1	22	30	43	35	495	471	432	247	-31	-38	10	12	-27	-20	-27
133	17	23	26	0	1	22	30	43	35	495	471	432	247	-31	-38	10	12	-27	-20	-27
134	17	23	26	0	1	22	30	43	35	495	471	432	247	-31	-38	10	12	-27	-20	-27
135	17	23	26	0	1	22	30	43	35	495	471	432	247	-31	-38	10	12	-27	-20	-27
136	17	23	26	0	1	22	30	43	35	495	471	432	247	-31	-38	10	12	-27	-20	-27
137	17	23	26	0	1	22	30	43	35	495	471	432	247	-31	-38	10	12	-27	-20	-27
138	17	23	26	0	1	22	30	43	35	495	471	432	247	-31	-38	10	12	-27	-20	-27
139	17	23	26	0	1	22	30	43	35	495	471	432	247	-31	-38	10	12	-27	-20	-27
140	17	23	26	0	1	22	30	43	35	495	471	432	247	-31	-38	10	12	-27	-20	-27
141	17	23	26	0	1	22	30	43	35	495	471	432	247	-31	-38	10	12	-27	-20	-27
142	17	23	26	0	1	22	30	43	35	495	471	432	247	-31	-38	10	12	-27	-20	-27
143	17	23	26	0	1	22	30	43	35	495	471	432	247	-31	-38	10	12	-27	-20	-27
144	17	23	26	0	1	22	30	43	35	495	471	432	247	-31	-38	10	12	-27	-20	-27
145	17	23	26	0	1	22	30	43	35	495	471	432	247	-31	-38	10	12	-27	-20	-27
146	17	23	26	0	1	22	30	43	35	495	471	432	247	-31	-38	10	12	-27	-20	-27
147	17	23	26	0	1	22	30	43	35	495	471	432	247	-31	-38	10	12	-27	-20	-27
148	17	23	26	0	1	22	30	43	35	495	471	432	247	-31	-38	10	12	-27	-20	-27
149	17	23	26	0	1	22	30	43	35	495	471	432	247	-31	-38	10	12	-27	-20	-27
150	17	23	26	0	1	22	30	43	35	495	471	432	247	-31	-38	10	12	-27	-20	-27
151	17	23	26	0	1	22	30	43	35	495	471	432	247	-31	-38	10	12	-27	-20	-27
152	17	23	26	0	1	22	30	43	35	495	471	432	247	-31	-38	10	12	-27	-20	-27
153	17	23	26	0	1	22	30	43	35	495	471	432	247	-31	-38	10	12	-27	-20	-27
154	17	23	26	0	1	22	30	43	35	495	471	432	247	-31	-38	10	12	-27	-20	-27
155	17	23	26	0	1	22	30	43	35	495	471	432	247	-31	-38	10	12	-27	-20	-27
156	17	23	26	0	1	22	30	43	35	495	471	432	247	-31	-38	10	12	-27	-20	-27
157	17	23	26	0	1	22	30	43	35	495	471	432	247	-31	-38	10	12	-27	-20	-27
158	17	23	26	0	1	22	30	43	35	495	471	432	247	-31	-38	10	12	-27	-20	-27
159	17	23	26	0	1	22	30	43	35	495	471	432	247	-31	-38	10	12	-27	-20	-27
160	17	23	26	0	1	22	30	43	35	495	471	432	247	-31	-38	10	12	-27	-20	-27

THE LOAD STAGE NUMBER USED AS ZERO FOR THIS RUN IS 1

	CHAN	CHAN	CHAN	CHAN	CHAN	CHAN	CHAN	CHAN	CHAN	CHAN	CHAN	CHAN	CHAN	CHAN	CHAN	CHAN	CHAN	CHAN	CHAN	CHAN
	61	62	63	64	65	66	67	68	69	70	71	72	73	74	75	76	77	78	79	80
127	2707277	12	-2	44	18	26	26	36	52	55	371	345	338	203	19	6	97	74	16	15
128	2507277	12	3	37	13	20	22	37	52	57	361	332	325	3190	44	22	68	76	17	18
129	1207177	12	5	32	10	15	16	37	52	56	350	319	310	184	24	10	79	21	20	20
130	1207177	13	17	26	0	15	7	42	55	60	328	296	293	170	33	108	83	30	23	23
131	1207172	12	25	16	4	0	-2	47	53	63	308	282	249	147	42	108	83	30	23	23
132	7070777	9	7	-6	-11	44	60	6	63	64	302	286	272	130	39	126	92	46	46	25
133	7070777	9	45	4	-1	-10	-3	52	52	52	52	52	52	52	52	52	52	52	52	52
134	7120777	18	49	7	-17	-6	2	45	62	63	314	298	283	161	10	136	86	41	43	19
135	7170777	14	54	17	-13	-4	4	59	60	329	314	311	303	161	10	136	86	41	43	19
136	7207777	14	54	17	-13	-4	4	59	60	329	314	311	303	161	10	136	86	41	43	19
137	7250777	11	60	120	-7	1	3	58	58	56	352	337	313	184	24	121	78	39	37	0
137A	2025200	14	60	40	32	13	20	24	32	50	405	382	356	218	49	-6	128	68	21	20
138	2025200	14	60	40	32	13	20	24	32	50	405	382	356	218	49	-6	128	68	21	20
139	2030200	16	43	42	16	20	25	30	51	50	420	398	369	229	7	-7	100	65	22	-3
140	2032200	16	44	47	17	21	29	30	51	48	431	409	378	233	4	-10	99	64	22	-8
141	2035200	14	51	55	23	27	27	27	51	47	445	431	395	244	8	-13	96	60	51	-1
142	2035200	10	43	55	20	21	22	22	46	45	432	427	389	238	-1	-17	90	59	19	-12
142A	1737177	10	43	55	20	21	22	22	46	45	432	427	389	238	-1	-17	90	59	19	-12
142B	1537175	13	53	44	18	11	18	26	51	47	445	422	386	244	8	-10	95	61	19	-10
142C	1537175	13	53	44	18	11	18	26	51	47	445	422	386	244	8	-10	95	61	19	-10
143	1535155	14	55	37	10	14	14	14	59	53	449	410	372	219	9	-6	104	66	25	-7
144	1532155	14	54	36	9	10	10	8	53	52	401	399	365	217	7	-5	103	66	27	-4
145	1530155	15	52	37	7	7	6	6	33	33	385	380	353	206	11	-3	101	66	27	0
146	1527155	15	52	37	7	7	6	6	33	33	385	380	353	206	11	-3	101	66	27	0
147	1525155	15	51	25	4	0	2	2	36	60	57	375	368	344	176	11	124	73	27	0
147A	7207777	18	63	16	-14	-10	-10	-10	62	60	332	327	310	179	20	125	83	38	30	10
148	7207777	15	59	-2	-18	-16	-24	42	65	65	314	305	297	159	33	130	86	42	32	16
149	7170777	15	59	-2	-18	-16	-24	42	65	65	314	305	297	159	33	130	86	42	32	16
150	7120777	17	48	-3	-22	-20	-38	60	70	70	295	286	279	149	21	131	89	44	36	20
151	7070777	14	50	-4	-19	-17	-26	59	76	76	288	269	268	138	47	34	159	111	51	43
152	7070777	14	50	-4	-19	-17	-26	59	76	76	288	269	268	138	47	34	159	111	51	43
152A	1200000	16	42	17	6	-4	-4	4	72	72	346	346	340	163	39	25	149	102	42	37
153	2000000	16	42	17	6	-4	-4	4	72	72	346	346	340	163	39	25	149	102	42	37
153A	2000000	16	42	32	11	5	42	7	70	65	397	384	363	209	19	7	126	86	29	20
154	2700000	16	42	32	11	5	42	7	70	65	397	384	363	209	19	7	126	86	29	20
154A	3000000	18	43	55	18	23	16	13	58	60	435	415	390	236	9	-3	141	79	11	-2
154B	3000000	18	43	55	18	23	16	13	58	60	435	415	390	236	9	-3	141	79	11	-2
154C	3000000	18	43	55	18	23	16	13	58	60	435	415	390	236	9	-3	141	79	11	-2
154D	3000000	18	43	55	18	23	16	13	58	60	435	415	390	236	9	-3	141	79	11	-2
155	3700000	19	29	77	47	47	51	22	43	49	575	518	493	296	-16	-22	86	54	-3	-11
156	4000000	17	25	80	54	48	67	16	42	44	592	577	527	280	-33	-37	69	46	-15	-38
156A	4000000	17	25	80	54	48	67	16	42	44	592	577	527	280	-33	-37	69	46	-15	-38
157	4000000	19	29	77	47	47	51	22	43	49	575	518	493	296	-16	-22	86	54	-3	-11
158	4500000	19	15	116	57	64	64	12	27	750	783	680	577	-73	-72	56	26	-49	-48	-48
159	4500000	19	15	116	57	64	64	12	27	750	783	680	577	-73	-72	56	26	-49	-48	-48
160	4500000	19	15	116	57	64	64	12	27	750	783	680	577	-73	-72	56	26	-49	-48	-48
161	3700000	18	23	97	43	54	49	19	18	35	699	731	630	541	-57	-52	76	45	-37	-38
161A	3700000	18	23	97	43	54	49	19	18	35	699	731	630	541	-57	-52	76	45	-37	-38
161B	3700000	18	23	97	43	54	49	19	18	35	699	731	630	541	-57	-52	76	45	-37	-38
161C	3700000	18	23	97	43	54	49	19	18	35	699	731	630	541	-57	-52	76	45	-37	-38
161D	3700000	18	23	97	43	54	49	19	18	35	699	731	630	541	-57	-52	76	45	-37	-38
162	3500000	14	30	108	61	73	70	22	13	39	695	722	635	548	-46	-39	102	71	-18	-25
163	3200000	16	31	97	54	71	64	22	12	40	673	701	617	530	-48	-35	101	69	-14	-6
164	3200000	16	31	97	54	71	64	22	12	40	673	701	617	530	-48	-35	101	69	-14	-6
165	2200000	12	44	64	33	56	43	32	22	52	593	612	545	468	-14	-15	137	94	6	-2
166	1700000	14	51	67	30	50	34	37	25	55	544	561	500	428	0	0	153	106	22	28
167	1200000	14	58	47	18	43	22	29	62	495	512	460	394	16	1	168	120	32	46	29
168	1200000	14	58	47	18	43	22	29	62	495	512	460	394	16	1	168	120	32	46	29
169	1200000	14	51	52	26	41	26	39	58	483	500	499	446	385	19	11	167	123	38	42



[illegible]

THE LOAD STAGE NUMBER USED AS ZERO FOR THIS RUN IS 1

	CHAN	CHAN	CHAN	CHAN	CHAN	CHAN	CHAN	CHAN	CHAN	CHAN	CHAN	CHAN	CHAN	CHAN	CHAN	CHAN	CHAN	CHAN	CHAN		
	81	82	83	84	85	86	87	88	89	90	91	92	93	94	95	96	97	98	99	100	
94H	353535	14	-26	153	117	107	28	11	14	6	165	155	246	233	122	-40	31	31	214	155	138
94C	353535	16	-26	153	117	107	29	11	14	6	167	154	249	233	121	-40	28	31	218	155	137
95	373737	15	-28	168	125	114	30	11	16	6	187	174	279	268	129	-48	31	34	240	174	148
95A	373737	17	-27	168	125	116	29	11	16	5	186	173	281	270	131	-49	31	32	242	174	149
96	393939	16	-24	160	119	109	28	10	18	5	181	166	270	264	120	-41	31	30	236	170	141
97	323232	15	-22	151	110	104	25	8	12	4	171	155	256	243	111	-33	26	25	225	161	135
97A	323232	15	-22	152	110	105	26	8	12	3	161	146	265	255	101	-27	26	25	224	161	135
98	303030	14	-19	142	105	95	25	8	10	3	151	146	241	235	101	-27	26	25	214	155	128
99	272727	15	-11	133	89	82	22	4	9	3	131	125	206	205	81	-11	20	20	176	129	102
99A	272727	15	-11	133	89	82	22	4	9	3	131	125	206	205	81	-11	20	20	176	129	102
100	202020	16	-3	104	73	67	18	3	3	3	122	104	168	170	62	16	16	16	165	119	97
100A	202020	16	-3	104	73	67	18	3	3	3	122	104	168	170	62	16	16	16	165	119	97
101	171717	16	-10	94	63	57	15	1	3	3	113	97	149	154	53	18	17	17	152	106	86
101A	171717	16	-10	94	63	57	15	1	3	3	113	97	149	154	53	18	17	17	152	106	86
102	151515	16	-12	85	55	49	15	0	2	1	103	81	127	135	42	18	12	12	137	101	78
102A	151515	16	-12	85	55	49	15	0	2	1	103	81	127	135	42	18	12	12	137	101	78
103	121212	16	-10	74	47	42	15	0	2	1	93	73	108	117	31	23	11	15	125	90	67
103A	121212	16	-10	74	47	42	15	0	2	1	93	73	108	117	31	23	11	15	125	90	67
104	707070	14	-3	54	29	22	11	0	10	3	76	53	88	86	18	46	41	41	117	72	49
104A	707070	14	-3	54	29	22	11	0	10	3	76	53	88	86	18	46	41	41	117	72	49
105	121212	16	-10	74	47	42	15	0	2	1	93	73	108	117	31	23	11	15	125	90	67
105A	121212	16	-10	74	47	42	15	0	2	1	93	73	108	117	31	23	11	15	125	90	67
106	171717	16	-10	94	63	57	15	1	3	3	117	97	149	154	53	18	17	17	152	106	86
106A	171717	16	-10	94	63	57	15	1	3	3	117	97	149	154	53	18	17	17	152	106	86
107	222222	15	-12	141	105	102	36	18	22	22	157	154	208	214	88	-11	41	41	204	153	119
107A	222222	15	-12	141	105	102	36	18	22	22	157	154	208	214	88	-11	41	41	204	153	119
108	323232	14	-20	160	121	112	38	18	22	20	182	182	249	250	108	-108	41	41	234	172	138
108A	323232	14	-20	160	121	112	38	18	22	20	182	182	249	250	108	-108	41	41	234	172	138
109	153545	12	-25	171	129	124	42	24	24	22	196	169	231	274	119	-24	42	42	275	193	147
109A	153545	12	-25	171	129	124	42	24	24	22	196	169	231	274	119	-24	42	42	275	193	147
110	373737	14	-22	168	122	117	32	11	16	13	201	164	208	208	118	-28	34	34	257	191	142
110A	373737	14	-22	168	122	117	32	11	16	13	201	164	208	208	118	-28	34	34	257	191	142
111	323232	16	-17	151	104	104	29	10	14	12	182	148	259	282	108	-34	32	32	234	171	122
111A	323232	16	-17	151	104	104	29	10	14	12	182	148	259	282	108	-34	32	32	234	171	122
112	373737	14	-17	144	100	99	22	7	14	4	178	145	258	258	103	-36	25	25	226	169	120
112A	373737	14	-17	144	100	99	22	7	14	4	178	145	258	258	103	-36	25	25	226	169	120
113	323232	13	-17	148	99	96	22	6	4	3	179	147	268	278	103	-34	25	25	227	166	120
113A	323232	13	-17	148	99	96	22	6	4	3	179	147	268	278	103	-34	25	25	227	166	120
114	373737	15	-11	130	85	84	20	1	4	4	160	129	253	263	98	-28	23	23	204	150	103
114A	373737	15	-11	130	85	84	20	1	4	4	160	129	253	263	98	-28	23	23	204	150	103
115	373737	14	-8	109	68	65	13	1	3	0	137	103	233	246	83	-28	13	13	172	124	79
115A	373737	14	-8	109	68	65	13	1	3	0	137	103	233	246	83	-28	13	13	172	124	79
116	373737	14	-1	97	53	52	10	1	1	1	122	103	231	243	81	-28	13	13	167	124	80
116A	373737	14	-1	97	53	52	10	1	1	1	122	103	231	243	81	-28	13	13	167	124	80
117	373737	14	-1	97	53	52	10	1	1	1	122	103	231	243	81	-28	13	13	167	124	80
117A	373737	14	-1	97	53	52	10	1	1	1	122	103	231	243	81	-28	13	13	167	124	80
118	373737	14	-1	97	53	52	10	1	1	1	122	103	231	243	81	-28	13	13	167	124	80
118A	373737	14	-1	97	53	52	10	1	1	1	122	103	231	243	81	-28	13	13	167	124	80
119	373737	14	-1	97	53	52	10	1	1	1	122	103	231	243	81	-28	13	13	167	124	80
119A	373737	14	-1	97	53	52	10	1	1	1	122	103	231	243	81	-28	13	13	167	124	80
120	373737	14	-1	97	53	52	10	1	1	1	122	103	231	243	81	-28	13	13	167	124	80
120A	373737	14	-1	97	53	52	10	1	1	1	122	103	231	243	81	-28	13	13	167	124	80
121	373737	14	-1	97	53	52	10	1	1	1	122	103	231	243	81	-28	13	13	167	124	80
121A	373737	14	-1	97	53	52	10	1	1	1	122	103	231	243	81	-28	13	13	167	124	80
122	373737	14	-1	97	53	52	10	1	1	1	122	103	231	243	81	-28	13	13	167	124	80
122A	373737	14	-1	97	53	52	10	1	1	1	122	103	231	243	81	-28	13	13	167	124	80
123	373737	14	-1	97	53	52	10	1	1	1	122	103	231	243	81	-28	13	13	167	124	80
123A	373737	14	-1	97	53	52	10	1	1	1	122	103	231	243	81	-28	13	13	167	124	80
124	373737	14	-1	97	53	52	10	1	1	1	122	103	231	243	81	-28	13	13	167	124	80
124A	373737	14	-1	97	53	52	10	1	1	1	122	103	231	243	81	-28	13	13	167	124	80
125	373737	14	-1	97	53	52	10	1	1	1	122	103	231	243	81	-28	13	13	167	124	80
125A	373737	14	-1	97	53	52	10	1	1	1	122	103	231	243	81	-28	13	13	167	124	80
126	373737	14	-1	97	53	52	10	1	1	1	122	103	231	243	81	-28	13	13	167	124	80

THE LOAD STAGE NUMBER USED AS ZERO FOR THIS RUN IS 1

	CHAN	CHAN	CHAN	CHAN	CHAN	CHAN	CHAN	CHAN	CHAN	CHAN	CHAN	CHAN	CHAN	CHAN	CHAN	CHAN	CHAN	CHAN	CHAN	CHAN	
	81	82	83	84	85	86	87	88	89	90	91	92	93	94	95	96	97	98	99	100	
127	270727	12	25	133	70	67	15	-11	-6	-12	142	125	156	175	31	33	-22	0	156	114	95
127A	250727	12	26	123	65	60	12	-11	-10	-12	136	116	148	169	26	33	-20	-4	152	110	60
128	220722	10	24	115	57	52	-1	-16	-16	-17	130	108	138	158	19	33	-25	-6	145	104	60
128A	220722	10	24	115	57	52	-1	-16	-16	-17	130	108	138	158	19	33	-25	-6	145	104	60
129	170717	16	29	102	47	41	-4	-19	-18	-19	120	96	123	144	13	35	-27	-6	141	100	59
129A	170717	16	29	102	47	41	-4	-19	-18	-19	120	96	123	144	13	35	-27	-6	141	100	59
131	120712	12	30	77	34	31	-1	-21	-23	-22	110	85	103	119	4	53	-26	-8	126	95	48
131A	70707	13	30	82	22	22	-1	-24	-26	-26	100	72	86	125	4	55	-26	-8	126	95	48
133	70707	13	30	77	34	31	-1	-24	-26	-26	100	72	86	125	4	55	-26	-8	126	95	48
133A	70707	13	30	77	34	31	-1	-24	-26	-26	100	72	86	125	4	55	-26	-8	126	95	48
134	71207	12	31	75	55	54	-2	-18	-15	-15	94	64	78	120	7	55	-3	11	144	103	50
134A	71207	12	31	75	55	54	-2	-18	-15	-15	94	64	78	120	7	55	-3	11	144	103	50
135	71707	12	31	83	30	29	-2	-23	-20	-18	103	71	102	140	7	46	-1	11	159	115	50
136	72207	13	31	89	30	30	-2	-23	-20	-18	103	71	102	140	7	46	-1	11	159	115	50
136A	72207	13	31	89	30	30	-2	-23	-20	-18	103	71	102	140	7	46	-1	11	159	115	50
137A	202520	14	9	122	61	59	4	-19	-18	-17	147	116	156	179	21	31	-1	18	189	140	84
138	202770	14	16	128	67	64	4	-19	-18	-17	147	116	156	179	21	31	-1	18	189	140	84
138A	202770	14	16	128	67	64	4	-19	-18	-17	147	116	156	179	21	31	-1	18	189	140	84
140	203220	15	11	135	72	69	4	-21	-19	-23	171	134	216	244	24	35	12	15	251	161	103
141	203520	15	11	136	73	71	4	-21	-19	-23	171	134	216	244	24	35	12	15	251	161	103
141A	203520	15	11	136	73	71	4	-21	-19	-23	171	134	216	244	24	35	12	15	251	161	103
142A	173717	12	9	142	77	75	3	-26	-23	-20	179	147	221	261	26	36	6	4	266	244	126
142B	153715	12	9	137	69	67	3	-28	-25	-23	182	150	244	278	27	33	-5	3	266	244	126
142C	153715	12	9	137	69	67	3	-28	-25	-23	182	150	244	278	27	33	-5	3	266	244	126
143	153515	12	9	126	62	63	-5	-27	-26	-30	176	136	238	273	27	33	-1	7	293	244	138
144	153215	13	1	126	57	61	-5	-27	-26	-30	170	121	211	252	27	13	-6	9	276	231	120
144A	153015	16	1	123	57	53	-5	-27	-26	-30	164	118	211	252	27	13	-6	9	263	215	106
146	152515	16	9	115	47	51	-5	-29	-27	-30	151	106	181	217	40	26	-5	3	241	205	100
147A	72507	14	17	122	30	34	-8	-33	-33	-33	133	88	131	197	35	35	-16	3	227	196	80
147B	72507	14	17	122	30	34	-8	-33	-33	-33	133	88	131	197	35	35	-16	3	227	196	80
149	71707	16	23	82	18	22	-11	-37	-33	-34	114	91	119	137	6	50	-5	5	194	171	57
150	71207	16	23	86	10	16	-11	-37	-33	-36	102	63	94	135	7	60	-30	-2	171	153	57
151	70707	16	23	86	10	16	-11	-37	-33	-36	102	63	94	135	7	60	-30	-2	171	153	57
152	70707	16	23	86	10	16	-11	-37	-33	-36	102	63	94	135	7	60	-30	-2	171	153	57
152A	120000	15	31	104	17	24	-10	-36	-32	-33	112	73	96	142	7	61	-31	-7	178	165	53
153	70000	16	12	115	2	2	-10	-36	-32	-34	107	74	140	218	11	42	-29	-7	190	170	77
153A	70000	16	12	115	2	2	-10	-36	-32	-34	107	74	140	218	11	42	-29	-7	190	170	77
154	270000	16	12	153	66	74	-2	-28	-23	-30	185	143	222	259	53	17	-4	269	244	107	
154A	300000	16	15	174	79	93	-2	-27	-17	-25	210	160	255	290	60	10	-3	299	266	123	
154B	300000	16	15	174	79	93	-2	-27	-17	-25	210	160	255	290	60	10	-3	299	266	123	
154C	300000	16	15	174	79	93	-2	-27	-17	-25	210	160	255	290	60	10	-3	299	266	123	
155	350000	17	1	203	103	116	10	-21	-14	-15	265	238	311	350	81	3	-5	351	331	153	
156	400000	17	4	219	113	132	16	-19	-11	-12	292	272	346	398	102	-3	-2	414	383	172	
156A	400000	17	4	219	113	132	16	-19	-11	-12	292	272	346	398	102	-3	-2	414	383	172	
157	420000	17	21	276	130	172	19	-13	-6	-10	382	351	375	466	113	4	22	457	464	240	
157A	420000	17	21	276	130	172	19	-13	-6	-10	382	351	375	466	113	4	22	457	464	240	
158	450000	17	26	295	140	188	19	-16	-4	-10	406	385	391	510	126	-17	6	483	490	368	
158A	450000	17	26	295	140	188	19	-16	-4	-10	406	385	391	510	126	-17	6	483	490	368	
159	450000	15	21	508	591	463	30	-11	7	11	852	778	687	800	677	-68	26	60	653	635	385
159A	450000	17	17	498	580	453	29	-11	7	10	836	768	665	787	671	-57	26	60	636	625	377
160	470000	17	17	510	570	432	25	-13	2	10	868	797	686	800	677	-68	26	60	653	635	385
161	370000	16	13	474	557	432	25	-13	2	10	802	741	625	729	650	-42	17	55	611	604	352
161A	370000	17	12	473	558	432	25	-13	2	10	807	746	623	729	650	-42	17	55	610	603	359
161B	370000	17	12	473	558	432	25	-13	2	10	807	746	623	729	650	-42	17	55	610	603	359
161C	370000	17	12	473	558	432	25	-13	2	10	807	746	623	729	650	-42	17	55	610	603	359
161D	370000	17	12	473	558	432	25	-13	2	10	807	746	623	729	650	-42	17	55	610	603	359
161E	370000	17	12	473	558	432	25	-13	2	10	807	746	623	729	650	-42	17	55	610	603	359
161F	370000	17	12	473	558	432	25	-13	2	10	807	746	623	729	650	-42	17	55	610	603	359
162	320000	14	-10	493	580	449	27	-11	6	15	812	752	620	729	652	-14	18	54	619	616	382
164	270000	16	-5	468	554	424	25	-13	-1	16	777	722	577	696	633	15	2	589	596	366	
165	270000	16	-5	468	554	424	25	-13	-1	16	777	722	577	696	633	15	2	589	596	366	
166	170000	16	15	414	490	370	18	-19	-6	8	693	651	468	605	583	32	3	42	529	543	320
167	120000	17	26	386	463	342	12	-22	-12	7	651	618	410	507	560	47	-2	37	497	516	295
168	120000	17	26	386	463	342	12	-22	-12	7	651	618	410	507	560	47	-2	37	497	516	295
169	120000	13	23	376	455	337	10	-21	-13	3	642	611	391	537	547	49	-4	35	494	509	291

THE LOAD STAGE NUMBER USED AS ZERO FOR THIS RUN IS 1

CHAN	CHAN	CHAN	CHAN	CHAN	CHAN	CHAN	CHAN	CHAN	CHAN	CHAN	CHAN	CHAN	CHAN	CHAN	CHAN	CHAN	CHAN	CHAN			
91	92	93	94	95	96	97	98	99	100	91	92	93	94	95	96	97	98	99	100		
170A	120000	13	25	371	468	334	14	-20	-11	3	841	610	386	538	542	47	-3	37	494	510	270
170B	170000	13	18	307	407	311	13	-20	-11	3	841	610	386	538	542	47	-3	37	494	510	270
171A	220000	16	10	427	510	389	22	-17	-4	12	722	689	491	630	593	21	6	43	567	566	334
171B	220000	16	8	443	549	404	25	-7	4	20	742	706	508	638	607	22	15	53	586	582	349
172A	272222	14	7	445	547	404	26	-9	-2	16	741	707	524	644	609	24	11	51	586	581	350
172B	272222	14	5	445	547	404	25	-13	-3	16	741	706	524	644	609	24	11	51	586	581	350
173A	302222	15	6	443	545	403	24	-13	-3	13	740	703	535	655	612	25	7	45	584	574	349
173B	302222	15	6	443	545	403	24	-16	-6	11	740	707	549	661	616	15	5	44	578	573	347
174A	372222	14	1	444	543	406	0	-21	-13	0	742	704	581	676	623	18	9	38	576	572	347
174B	372222	14	1	444	543	406	0	-21	-13	0	742	704	581	676	623	18	9	38	576	572	347
175A	402222	16	2	444	549	411	15	-19	-10	4	749	716	587	697	649	10	1	42	579	573	346
175B	402222	16	2	444	549	411	15	-19	-10	4	749	716	587	697	649	10	1	42	579	573	346
176A	472222	14	1	444	543	406	0	-21	-13	0	742	704	581	676	623	18	9	38	576	572	347
176B	472222	14	1	444	543	406	0	-21	-13	0	742	704	581	676	623	18	9	38	576	572	347
177A	502222	15	4	444	540	401	12	-22	-14	-3	742	708	551	674	637	11	-8	40	575	568	342
177B	502222	15	4	444	540	401	12	-22	-14	-3	742	708	551	674	637	11	-8	40	575	568	342
178A	572222	16	3	436	537	399	9	-26	-19	-2	739	708	543	664	630	23	-10	35	573	566	343
178B	572222	16	3	436	537	399	9	-26	-19	-2	739	708	543	664	630	23	-10	35	573	566	343
179A	602222	16	3	436	537	399	9	-26	-19	-2	739	708	543	664	630	23	-10	35	573	566	343
179B	602222	16	3	436	537	399	9	-26	-19	-2	739	708	543	664	630	23	-10	35	573	566	343
180A	672222	14	12	424	527	386	2	-27	-23	-14	730	701	511	642	618	26	-19	25	562	560	336
180B	672222	14	12	424	527	386	2	-27	-23	-14	730	701	511	642	618	26	-19	25	562	560	336
181A	702222	15	4	436	539	399	11	-21	-14	-2	739	708	543	664	630	23	-10	35	573	566	343
181B	702222	15	4	436	539	399	11	-21	-14	-2	739	708	543	664	630	23	-10	35	573	566	343
182A	772222	16	3	436	537	399	9	-26	-19	-2	739	708	543	664	630	23	-10	35	573	566	343
182B	772222	16	3	436	537	399	9	-26	-19	-2	739	708	543	664	630	23	-10	35	573	566	343
183A	802222	16	3	436	537	399	9	-26	-19	-2	739	708	543	664	630	23	-10	35	573	566	343
183B	802222	16	3	436	537	399	9	-26	-19	-2	739	708	543	664	630	23	-10	35	573	566	343
184A	872222	14	12	424	527	386	2	-27	-23	-14	730	701	511	642	618	26	-19	25	562	560	336
184B	872222	14	12	424	527	386	2	-27	-23	-14	730	701	511	642	618	26	-19	25	562	560	336
185A	902222	15	4	436	539	399	11	-21	-14	-2	739	708	543	664	630	23	-10	35	573	566	343
185B	902222	15	4	436	539	399	11	-21	-14	-2	739	708	543	664	630	23	-10	35	573	566	343
186A	972222	16	3	436	537	399	9	-26	-19	-2	739	708	543	664	630	23	-10	35	573	566	343
186B	972222	16	3	436	537	399	9	-26	-19	-2	739	708	543	664	630	23	-10	35	573	566	343
187A	1000000	16	3	436	537	399	9	-26	-19	-2	739	708	543	664	630	23	-10	35	573	566	343
187B	1000000	16	3	436	537	399	9	-26	-19	-2	739	708	543	664	630	23	-10	35	573	566	343
188A	1070000	14	-14	408	507	417	10	-26	-19	-12	809	777	603	725	657	-2	-10	33	631	616	382
188B	1070000	14	-14	408	507	417	10	-26	-19	-12	809	777	603	725	657	-2	-10	33	631	616	382
189A	1100000	14	-14	408	507	417	10	-26	-19	-12	809	777	603	725	657	-2	-10	33	631	616	382
189B	1100000	14	-14	408	507	417	10	-26	-19	-12	809	777	603	725	657	-2	-10	33	631	616	382
190A	1170000	14	-11	521	644	491	12	-23	-13	-14	837	833	670	779	713	-19	-6	32	684	671	417
190B	1170000	14	-11	521	644	491	12	-23	-13	-14	837	833	670	779	713	-19	-6	32	684	671	417
191A	1200000	16	2	444	549	411	15	-19	-10	4	749	716	587	697	649	10	1	42	579	573	346
191B	1200000	16	2	444	549	411	15	-19	-10	4	749	716	587	697	649	10	1	42	579	573	346
192A	1270000	14	1	444	543	406	0	-21	-13	0	742	704	581	676	623	18	9	38	576	572	347
192B	1270000	14	1	444	543	406	0	-21	-13	0	742	704	581	676	623	18	9	38	576	572	347
193A	1300000	15	4	444	540	401	12	-22	-14	-3	742	708	551	674	637	11	-8	40	575	568	342
193B	1300000	15	4	444	540	401	12	-22	-14	-3	742	708	551	674	637	11	-8	40	575	568	342
194A	1370000	16	3	436	537	399	9	-26	-19	-2	739	708	543	664	630	23	-10	35	573	566	343
194B	1370000	16	3	436	537	399	9	-26	-19	-2	739	708	543	664	630	23	-10	35	573	566	343
195A	1400000	16	3	436	537	399	9	-26	-19	-2	739	708	543	664	630	23	-10	35	573	566	343
195B	1400000	16	3	436	537	399	9	-26	-19	-2	739	708	543	664	630	23	-10	35	573	566	343
196A	1470000	14	12	424	527	386	2	-27	-23	-14	730	701	511	642	618	26	-19	25	562	560	336
196B	1470000	14	12	424	527	386	2	-27	-23	-14	730	701	511	642	618	26	-19	25	562	560	336
197A	1500000	15	4	436	539	399	11	-21	-14	-2	739	708	543	664	630	23	-10	35	573	566	343
197B	1500000	15	4	436	539	399	11	-21	-14	-2	739	708	543	664	630	23	-10	35	573	566	343
198A	1570000	16	3	436	537	399	9	-26	-19	-2	739	708	543	664	630	23	-10	35	573	566	343
198B	1570000	16	3	436	537	399	9	-26	-19	-2	739	708	543	664	630	23	-10	35	573	566	343
199A	1600000	16	3	436	537	399	9	-26	-19	-2	739	708	543	664	630	23	-10	35	573	566	343
199B	1600000	16	3	436	537	399	9	-26	-19	-2	739	708	543	664	630	23	-10	35	573	566	343
200A	1670000	14	12	424	527	386	2	-27	-23	-14	730	701	511	642	618	26	-19	25	562	560	336
200B	1670000	14	12	424	527	386	2	-27	-23	-14	730	701	511	642	618	26	-19	25	562	560	336
201A	1700000	15	4	436	539	399	11	-21	-14	-2	739	708	543	664	630	23	-10	35	573	566	343
201B	1700000	15	4	436	539	399	11	-21	-14	-2	739	708	543	664	630	23	-10	35	573	566	343
202A	1770000	16	3	436	537	399	9	-26	-19	-2	739	708	543	664	630	23	-10	35	573	566	343
202B	1770000	16	3	436	537	399	9	-26	-19	-2	739	708	543	664	630	23	-10	35	573	566	343
203A	1800000	16	3	436	537	399	9	-26	-19	-2	739	708	543	664	630	23	-10	35	573	566	343
203B	1800000	16	3	436	537	399	9	-26	-19	-2	739	708	543	664	630	23	-10	35	573	566	343
204A	1870000	14	12	424	527	386	2	-27	-23	-14	730	701	511	642	618	26	-19	25	562	560	336



THE LOAD STAGE NUMBER USED AS ZERO FOR THIS RUN IS 1

	CHAN	CHAN	CHAN	CHAN	CHAN	CHAN	CHAN	CHAN	CHAN	CHAN	CHAN	CHAN	CHAN	CHAN	CHAN	CHAN	CHAN	CHAN	CHAN	CHAN	
	101	102	103	104	105	106	107	108	109	110	111	112	113	114	115	116	117	118	119	120	
34H	353535	15	136	86	136	164	-38	118	-32	224	146	171	114	8	147	-15	187	-40	184	-33	70
44C	353535	18	138	90	137	164	-37	118	-32	226	144	170	114	7	149	-12	190	-37	186	-33	71
45A	373737	14	148	96	152	172	-41	134	-36	257	167	189	132	6	164	-12	232	-45	217	-39	73
46	353535	15	141	92	147	168	-33	132	-29	220	156	180	137	14	195	-9	233	-33	225	-28	73
47	323232	15	127	84	133	155	-30	124	-25	206	144	169	131	15	184	-8	208	-28	201	-24	72
48	303030	15	119	78	124	144	-21	116	-19	192	134	154	124	15	174	-5	205	-27	196	-17	72
49	272727	16	113	76	114	135	-18	112	-15	179	121	144	119	22	167	10	192	-13	184	-7	72
50	242424	13	103	66	103	123	-11	104	-14	162	109	129	113	26	154	16	175	-5	172	-4	62
51	222222	15	91	60	92	110	-6	95	-3	150	96	118	104	38	145	23	165	4	156	6	62
52	202020	15	81	52	82	99	-4	88	-2	142	84	103	99	41	135	36	155	9	146	8	62
53	171717	15	75	49	76	87	-3	82	0	120	71	89	91	33	124	31	129	28	120	24	69
54	151515	15	64	42	63	77	12	74	4	102	56	75	84	36	109	39	113	36	112	30	70
55	121212	17	51	35	52	64	19	67	2	84	44	64	77	38	99	41	95	36	99	69	69
56	101010	11	41	28	40	53	37	54	15	64	32	47	67	34	76	62	61	60	63	65	77
57	070707	11	31	21	32	43	27	41	9	47	24	37	57	27	64	56	61	46	68	79	79
58	040404	11	21	14	21	30	18	27	6	32	16	24	40	20	50	44	42	30	46	39	79
59	010101	13	10	7	10	13	9	12	3	16	8	11	18	11	25	16	20	16	15	23	83
60	000000	13	10	7	10	13	9	12	3	16	8	11	18	11	25	16	20	16	15	23	83
61	000000	13	10	7	10	13	9	12	3	16	8	11	18	11	25	16	20	16	15	23	83
62	000000	13	10	7	10	13	9	12	3	16	8	11	18	11	25	16	20	16	15	23	83
63	000000	13	10	7	10	13	9	12	3	16	8	11	18	11	25	16	20	16	15	23	83
64	000000	13	10	7	10	13	9	12	3	16	8	11	18	11	25	16	20	16	15	23	83
65	000000	13	10	7	10	13	9	12	3	16	8	11	18	11	25	16	20	16	15	23	83
66	000000	13	10	7	10	13	9	12	3	16	8	11	18	11	25	16	20	16	15	23	83
67	000000	13	10	7	10	13	9	12	3	16	8	11	18	11	25	16	20	16	15	23	83
68	000000	13	10	7	10	13	9	12	3	16	8	11	18	11	25	16	20	16	15	23	83
69	000000	13	10	7	10	13	9	12	3	16	8	11	18	11	25	16	20	16	15	23	83
70	000000	13	10	7	10	13	9	12	3	16	8	11	18	11	25	16	20	16	15	23	83
71	000000	13	10	7	10	13	9	12	3	16	8	11	18	11	25	16	20	16	15	23	83
72	000000	13	10	7	10	13	9	12	3	16	8	11	18	11	25	16	20	16	15	23	83
73	000000	13	10	7	10	13	9	12	3	16	8	11	18	11	25	16	20	16	15	23	83
74	000000	13	10	7	10	13	9	12	3	16	8	11	18	11	25	16	20	16	15	23	83
75	000000	13	10	7	10	13	9	12	3	16	8	11	18	11	25	16	20	16	15	23	83
76	000000	13	10	7	10	13	9	12	3	16	8	11	18	11	25	16	20	16	15	23	83
77	000000	13	10	7	10	13	9	12	3	16	8	11	18	11	25	16	20	16	15	23	83
78	000000	13	10	7	10	13	9	12	3	16	8	11	18	11	25	16	20	16	15	23	83
79	000000	13	10	7	10	13	9	12	3	16	8	11	18	11	25	16	20	16	15	23	83
80	000000	13	10	7	10	13	9	12	3	16	8	11	18	11	25	16	20	16	15	23	83
81	000000	13	10	7	10	13	9	12	3	16	8	11	18	11	25	16	20	16	15	23	83
82	000000	13	10	7	10	13	9	12	3	16	8	11	18	11	25	16	20	16	15	23	83
83	000000	13	10	7	10	13	9	12	3	16	8	11	18	11	25	16	20	16	15	23	83
84	000000	13	10	7	10	13	9	12	3	16	8	11	18	11	25	16	20	16	15	23	83
85	000000	13	10	7	10	13	9	12	3	16	8	11	18	11	25	16	20	16	15	23	83
86	000000	13	10	7	10	13	9	12	3	16	8	11	18	11	25	16	20	16	15	23	83
87	000000	13	10	7	10	13	9	12	3	16	8	11	18	11	25	16	20	16	15	23	83
88	000000	13	10	7	10	13	9	12	3	16	8	11	18	11	25	16	20	16	15	23	83
89	000000	13	10	7	10	13	9	12	3	16	8	11	18	11	25	16	20	16	15	23	83
90	000000	13	10	7	10	13	9	12	3	16	8	11	18	11	25	16	20	16	15	23	83
91	000000	13	10	7	10	13	9	12	3	16	8	11	18	11	25	16	20	16	15	23	83
92	000000	13	10	7	10	13	9	12	3	16	8	11	18	11	25	16	20	16	15	23	83
93	000000	13	10	7	10	13	9	12	3	16	8	11	18	11	25	16	20	16	15	23	83
94	000000	13	10	7	10	13	9	12	3	16	8	11	18	11	25	16	20	16	15	23	83
95	000000	13	10	7	10	13	9	12	3	16	8	11	18	11	25	16	20	16	15	23	83
96	000000	13	10	7	10	13	9	12	3	16	8	11	18	11	25	16	20	16	15	23	83
97	000000	13	10	7	10	13	9	12	3	16	8	11	18	11	25	16	20	16	15	23	83
98	000000	13	10	7	10	13	9	12	3	16	8	11	18	11	25	16	20	16	15	23	83
99	000000	13	10	7	10	13	9	12	3	16	8	11	18	11	25	16	20	16	15	23	83
100	000000	13	10	7	10	13	9	12	3	16	8	11	18	11	25	16	20	16	15	23	83
101	000000	13	10	7	10	13	9	12	3	16	8	11	18	11	25	16	20	16	15	23	83
102	000000	13	10	7	10	13	9	12	3	16	8	11	18	11	25	16	20	16	15	23	83
103	000000	13	10	7	10	13	9	12	3	16	8	11	18	11	25	16	20	16	15	23	83
104	000000	13	10	7	10	13	9	12	3	16	8	11	18	11	25	16	20	16	15	23	83
105	000000	13	10	7	10	13	9	12	3	16	8	11	18	11	25	16	20	16	15	23	83
106	000000	13	10	7	10	13	9	12	3	16	8	11	18	11	25	16	20	16	15	23	83
107	000000	13	10	7	10	13	9	12	3	16	8	11	18	11	25	16	20	16	15	23	83
108	000000	13	10	7	10	13	9	12	3	16	8	11	18	11	25	16	20	16	15	23	83
109	000000	13	10	7	10	13	9	12	3	16	8	11	18	11	25	16	20	16	15	23	83
110	000000	13	10	7	10	13	9	12	3	16	8	11	18	11	25	16	20	16	15	23	83
111	000000	13	10	7	10	13	9	12	3	16	8	11	18	11	25	16	20	16	15	23	83
112	000000	13	10	7	10	13	9	12	3	16	8	11	18	11	25	16	20	16	15	23	83
113	000000	13	10	7	10	13	9	12	3	16	8	11	18	11	25	16	20	16	15	23	83
114	000000	13	10	7	10	13	9	12	3	16	8	11	18	11	25	16	20	16	15	23	83
115	000000	13	10	7	10	13	9	12	3	16	8	11	18	11	25	16	20	16	15	23	83
116	000000	13	10	7	10	13	9	12	3	16	8	11	18	11	25	16	20	16	15	23	83
117	000000	13	10	7	10																



THE LOAD STAGE NUMBER USED AS ZERO FOR THIS RUN IS 1

	CHAN	CHAN	CHAN	CHAN	CHAN	CHAN	CHAN	CHAN	CHAN	CHAN	CHAN	CHAN	CHAN	CHAN	CHAN	CHAN	CHAN	CHAN	CHAN	CHAN
	101	102	103	104	105	106	107	108	109	110	111	112	113	114	115	116	117	118	119	120
1700000	14	267	122	420	553	61	288	37	707	771	695	835	31	839	115	813	97	821	82	244
1700000	17	304	138	460	478	50	305	26	777	838	781	886	28	929	111	906	83	904	69	244
1710000	15	311	154	461	600	39	320	19	854	915	870	946	26	1029	101	1005	70	994	54	245
1710000	14	323	161	473	612	40	327	19	873	926	878	954	26	1048	101	1025	70	1013	54	245
1720000	15	322	162	464	600	39	320	16	917	976	929	992	23	1089	102	1066	65	1056	51	254
1720000	13	322	162	470	624	39	331	17	917	976	927	993	24	1091	105	1067	64	1056	51	254
1730000	15	317	158	463	627	37	333	14	940	999	954	1006	20	1115	100	1092	60	1080	41	255
1740000	16	317	158	463	627	34	333	14	946	1027	984	1036	18	1115	100	1092	60	1080	41	255
1740000	16	316	153	469	634	30	348	14	996	1047	1015	1043	18	1183	91	1158	50	1143	33	260
1750000	14	315	144	470	650	27	341	10	1027	1078	1052	1061	15	1217	86	1190	47	1178	30	263
1770000	15	318	155	470	666	22	357	9	1057	1115	1092	1081	18	1249	84	1227	40	1214	23	265
1770000	15	319	161	472	665	22	357	9	1057	1115	1092	1081	18	1249	84	1227	40	1214	23	265
1770000	17	317	157	475	658	27	354	11	1007	1068	1045	1056	16	1262	91	1179	50	1168	32	258
1800000	15	314	144	468	650	31	349	12	977	1043	1019	1043	18	1172	91	1151	55	1143	38	254
1810000	15	316	144	464	644	35	346	15	945	1015	988	1026	18	1142	101	1084	61	1113	44	254
1830000	15	316	144	464	644	35	346	15	945	1015	988	1026	18	1142	101	1084	61	1113	44	254
1830000	17	303	147	464	635	40	348	19	886	957	925	994	26	1076	110	1048	70	1047	57	254
1830000	15	406	138	462	629	39	334	20	876	948	915	986	27	1072	110	1045	72	1046	57	253
1840000	17	316	144	472	631	42	340	11	904	974	947	1006	26	1071	107	1084	60	1076	41	254
1860000	17	316	144	472	631	42	340	11	904	974	947	1006	26	1071	107	1084	60	1076	41	254
1860000	17	311	155	465	660	20	355	4	969	1033	1018	1049	21	1184	95	1166	50	1154	30	253
1870000	14	345	165	511	673	13	363	-4	1005	1066	1057	1070	13	1226	91	1207	43	1191	24	254
1870000	17	357	180	524	698	8	409	-9	1041	1100	1083	1095	14	1264	89	1249	43	1234	14	254
1870000	16	357	180	524	698	8	409	-9	1041	1100	1083	1095	14	1264	89	1249	43	1234	14	254
1870000	16	351	404	559	730	0	427	-12	1089	1155	1160	1123	18	1308	88	1295	34	1276	12	254
1890000	13	431	457	591	755	-2	400	-20	1147	1198	1189	1149	12	1326	88	1306	31	1298	14	257
1890000	11	436	455	594	762	-8	431	-24	1144	1198	1183	1154	8	1324	78	1315	20	1297	1	260
1890000	11	462	488	619	790	-2	458	-22	1185	1231	1213	1179	7	1356	88	1335	20	1307	9	272
1890000	13	466	489	622	785	-1	456	-20	1185	1239	1215	1181	8	1359	81	1350	28	1330	10	272
1890000	13	464	489	624	797	-1	466	-20	1193	1251	1228	1185	8	1371	85	1363	28	1343	8	272
1890000	14	464	489	624	797	-1	466	-20	1193	1251	1228	1185	8	1371	85	1363	28	1343	8	272
1890000	12	468	495	632	1126	-1	473	-22	1201	1258	1238	1191	8	1378	85	1370	31	1350	8	273
1890000	12	471	500	634	113	-1	483	-25	1206	1264	1244	1173	11	1383	88	1374	32	1351	5	271
1900000	14	481	516	649	837	-10	504	-29	1241	1306	1289	1213	6	1417	84	1410	32	1400	1	271
1900000	9	507	545	682	844	-22	548	-39	1317	1395	1375	1254	6	1507	74	1500	14	1443	-15	273
1930000	11	521	577	704	935	-30	578	-43	1370	1452	1484	1291	-13	1567	69	1550	8	1480	-21	274
1930000	10	527	583	706	937	-28	578	-44	1375	1457	1491	1292	-13	1569	68	1550	8	1480	-21	274
1940000	12	547	593	733	958	-36	598	-50	1425	1526	1557	1330	-36	1642	62	1608	0	1526	-26	276
1950000	11	466	554	684	888	16	574	-10	1113	1252	1247	1173	-20	1283	104	1250	56	1172	30	270
1960000	11	558	648	698	93	-10	605	-24	1260	1387	1415	1226	-30	1464	85	1433	27	1351	-12	274
1960000	11	561	648	698	93	-10	605	-24	1260	1387	1415	1226	-30	1464	85	1433	27	1351	-12	274
1960000	11	565	646	753	1019	-34	663	-47	1301	1555	1641	1337	-56	1665	66	1623	0	1531	-28	278
1990000	11	591	683	797	1077	-43	714	-51	1489	1633	1695	1385	-82	1741	58	1687	-7	1586	-37	278
1990000	8	510	705	827	1060	-43	743	-54	1500	1650	1705	1394	-59	1767	55	1696	-12	1574	-37	282
1990000	13	607	646	753	1019	-34	663	-47	1301	1555	1641	1337	-56	1665	66	1623	0	1531	-28	278
1990000	13	687	776	874	1194	-53	858	-59	1625	1845	1728	1465	-117	1859	45	1807	-27	1684	-56	282
2000000	11	630	805	874	1247	-57	922	-59	1659	1916	1735	1499	-138	1956	36	1843	-30	1721	-58	282
2000000	11	699	847	981	1293	-63	1082	-65	1686	1978	1760	1438	-153	2021	31	1897	-33	1752	-59	280
2000000	13	716	707	739	1444	-63	1201	-43	1751	1970	1772	1486	-169	2123	43	1992	-32	1821	-59	284
2000000	13	720	754	762	1494	-67	1257	-40	1751	1972	1774	1536	-189	2255	44	1988	-27	1901	-55	284
2000000	13	721	766	765	1493	-62	1267	-38	1747	1971	1773	1543	-184	2262	43	1980	-27	1901	-55	284
2000000	14	655	705	752	1003	-57	1274	-40	1751	1972	1774	1536	-189	2255	44	1988	-27	1901	-55	284
2020000	14	655	706	753	1432	-20	1247	-14	1457	1697	1441	1355	-166	1939	74	1683	6	1631	-16	280
2020000	13	527	783	753	1190	30	1153	18	1407	1333	841	1013	-115	1422	113	1246	67	1172	41	272
2020000	10	537	778	749	1160	30	1149	18	1387	1217	835	1002	-115	1422	113	1246	67	1172	41	272
2040000	13	692	792	871	1344	-21	1212	-17	1414	1643	1355	1345	-161	1926	76	1658	10	1583	-13	276

THE LOAD STAGE NUMBER USED AS ZERO FOR THIS RUN IS 1

[illegible]

THE LOAD STAGE NUMBER USED AS ZERO FOR THIS RUN IS 1

[illegible]

THE LOAD STAGE NUMBER USED AS ZERO FOR THIS RUN IS 1

[illegible]

THE LOAD STAGE NUMBER USED AS ZERO FOR THIS RUN IS 1

	CHAN	CHAN	CHAN	CHAN	CHAN	CHAN	CHAN	CHAN	CHAN	CHAN	CHAN	CHAN	CHAN	CHAN	CHAN	CHAN	CHAN	CHAN	CHAN		
	121	122	123	124	125	126	127	128	129	130	131	132	133	134	135	136	137	138	139	140	
84B	123535	14	74	67	90	84	75	77	-87	-13	-63	84	94	65	-24	-51	101	82	-53	-8	13
84C	123535	14	74	67	90	84	75	77	-87	-13	-63	84	94	65	-24	-51	101	82	-53	-8	13
85	123737	14	82	68	87	93	79	83	-95	-17	-71	94	104	72	-28	-56	112	88	-62	-10	16
85A	123737	14	83	70	89	93	86	83	-95	-18	-71	89	103	73	-29	-57	111	88	-62	-10	16
86	123535	14	79	67	83	80	79	83	-88	-9	-64	83	100	70	-24	-57	100	87	-57	-13	15
87	123737	14	75	64	80	84	73	76	-92	-5	-55	78	96	67	-14	-40	102	84	-57	-13	15
87A	123737	14	71	56	72	77	71	73	-77	-5	-46	78	88	64	-14	-40	94	79	-40	-13	15
89	123737	16	66	54	72	73	67	69	-75	-15	-37	74	85	63	-8	-32	94	77	-32	-11	15
90	123737	16	62	49	65	67	63	65	-75	-15	-37	74	85	63	-8	-32	94	77	-32	-11	15
91	123737	16	58	44	62	63	54	54	-75	-15	-37	74	85	63	-8	-32	94	77	-32	-11	15
91A	123737	16	54	40	58	56	50	54	-48	-35	-15	61	68	48	-10	-17	74	61	-12	-16	14
92	123737	16	49	34	52	54	46	41	-48	-35	-15	61	68	48	-10	-17	74	61	-12	-16	14
92A	123737	16	44	28	44	44	41	41	-48	-35	-15	61	68	48	-10	-17	74	61	-12	-16	14
93	121212	17	42	27	38	42	37	37	-23	-58	-5	42	50	37	18	9	57	42	13	-13	15
94	123737	17	32	22	31	31	26	29	-7	-63	-15	32	39	29	57	17	48	42	23	-13	15
95	123737	17	28	22	28	28	22	22	-7	-63	-15	32	39	29	57	17	48	42	23	-13	15
95A	121212	17	28	22	28	28	22	22	-7	-63	-15	32	39	29	57	17	48	42	23	-13	15
96	121212	17	28	22	28	28	22	22	-7	-63	-15	32	39	29	57	17	48	42	23	-13	15
96A	121212	17	28	22	28	28	22	22	-7	-63	-15	32	39	29	57	17	48	42	23	-13	15
97	123737	16	71	61	65	87	67	66	-36	-39	-15	90	98	72	24	-36	104	82	-17	-16	14
97A	123737	16	71	61	65	87	67	66	-36	-39	-15	90	98	72	24	-36	104	82	-17	-16	14
97B	123737	16	71	61	65	87	67	66	-36	-39	-15	90	98	72	24	-36	104	82	-17	-16	14
97C	123737	16	71	61	65	87	67	66	-36	-39	-15	90	98	72	24	-36	104	82	-17	-16	14
98	123737	16	71	61	65	87	67	66	-36	-39	-15	90	98	72	24	-36	104	82	-17	-16	14
98A	123737	16	71	61	65	87	67	66	-36	-39	-15	90	98	72	24	-36	104	82	-17	-16	14
98B	123737	16	71	61	65	87	67	66	-36	-39	-15	90	98	72	24	-36	104	82	-17	-16	14
98C	123737	16	71	61	65	87	67	66	-36	-39	-15	90	98	72	24	-36	104	82	-17	-16	14
99	123737	16	71	61	65	87	67	66	-36	-39	-15	90	98	72	24	-36	104	82	-17	-16	14
99A	123737	16	71	61	65	87	67	66	-36	-39	-15	90	98	72	24	-36	104	82	-17	-16	14
99B	123737	16	71	61	65	87	67	66	-36	-39	-15	90	98	72	24	-36	104	82	-17	-16	14
99C	123737	16	71	61	65	87	67	66	-36	-39	-15	90	98	72	24	-36	104	82	-17	-16	14
100	123737	16	71	61	65	87	67	66	-36	-39	-15	90	98	72	24	-36	104	82	-17	-16	14
100A	123737	16	71	61	65	87	67	66	-36	-39	-15	90	98	72	24	-36	104	82	-17	-16	14
100B	123737	16	71	61	65	87	67	66	-36	-39	-15	90	98	72	24	-36	104	82	-17	-16	14
100C	123737	16	71	61	65	87	67	66	-36	-39	-15	90	98	72	24	-36	104	82	-17	-16	14
101	123737	16	71	61	65	87	67	66	-36	-39	-15	90	98	72	24	-36	104	82	-17	-16	14
101A	123737	16	71	61	65	87	67	66	-36	-39	-15	90	98	72	24	-36	104	82	-17	-16	14
101B	123737	16	71	61	65	87	67	66	-36	-39	-15	90	98	72	24	-36	104	82	-17	-16	14
101C	123737	16	71	61	65	87	67	66	-36	-39	-15	90	98	72	24	-36	104	82	-17	-16	14
102	123737	16	71	61	65	87	67	66	-36	-39	-15	90	98	72	24	-36	104	82	-17	-16	14
102A	123737	16	71	61	65	87	67	66	-36	-39	-15	90	98	72	24	-36	104	82	-17	-16	14
102B	123737	16	71	61	65	87	67	66	-36	-39	-15	90	98	72	24	-36	104	82	-17	-16	14
102C	123737	16	71	61	65	87	67	66	-36	-39	-15	90	98	72	24	-36	104	82	-17	-16	14
103	123737	16	71	61	65	87	67	66	-36	-39	-15	90	98	72	24	-36	104	82	-17	-16	14
103A	123737	16	71	61	65	87	67	66	-36	-39	-15	90	98	72	24	-36	104	82	-17	-16	14
103B	123737	16	71	61	65	87	67	66	-36	-39	-15	90	98	72	24	-36	104	82	-17	-16	14
103C	123737	16	71	61	65	87	67	66	-36	-39	-15	90	98	72	24	-36	104	82	-17	-16	14
104	123737	16	71	61	65	87	67	66	-36	-39	-15	90	98	72	24	-36	104	82	-17	-16	14
104A	123737	16	71	61	65	87	67	66	-36	-39	-15	90	98	72	24	-36	104	82	-17	-16	14
104B	123737	16	71	61	65	87	67	66	-36	-39	-15	90	98	72	24	-36	104	82	-17	-16	14
104C	123737	16	71	61	65	87	67	66	-36	-39	-15	90	98	72	24	-36	104	82	-17	-16	14
105	123737	16	71	61	65	87	67	66	-36	-39	-15	90	98	72	24	-36	104	82	-17	-16	14
105A	123737	16	71	61	65	87	67	66	-36	-39	-15	90	98	72	24	-36	104	82	-17	-16	14
105B	123737	16	71	61	65	87	67	66	-36	-39	-15	90	98	72	24	-36	104	82	-17	-16	14
105C	123737	16	71	61	65	87	67	66	-36	-39	-15	90	98	72	24	-36	104	82	-17	-16	14
106	123737	16	71	61	65	87	67	66	-36	-39	-15	90	98	72	24	-36	104	82	-17	-16	14
106A	123737	16	71	61	65	87	67	66	-36	-39	-15	90	98	72	24	-36	104	82	-17	-16	14
106B	123737	16	71	61	65	87	67	66	-36	-39	-15	90	98	72	24	-36	104	82	-17	-16	14
106C	123737	16	71	61	65	87	67	66	-36	-39	-15	90	98	72	24	-36	104	82	-17	-16	14
107	123737	16	71	61	65	87	67	66	-36	-39	-15	90	98	72	24	-36	104	82	-17	-16	14
107A	123737	16	71	61	65	87	67	66	-36	-39	-15	90	98	72	24	-36	104	82	-17	-16	14
107B	123737	16	71	61	65	87	67	66	-36	-39	-15	90	98	72	24	-36	104	82	-17	-16	14
107C	123737	16	71	61	65	87	67	66	-36	-39	-15	90	98	72	24	-36	104	82	-17	-16	14
108	123737	16	71	61	65	87	67	66	-36	-39	-15	90	98	72	24	-36	104	82	-17	-16	14
108A	123737	16	71	61	65	87	67	66	-36	-39	-15	90	98	72	24	-36	104	82	-17	-16	14
108B	123737	16	71	61	65	87	67	66	-36	-39	-15	90	98	72	24	-36	104	82	-17	-16	14
108C	123737	16	71	61	65	87	67	66	-36	-39	-15	90	98	72	24	-36	104	82	-17	-16	14
109	123737	16	71	61	65	87	67	66	-36	-39	-15	90	98	72	24	-36	104	82	-17	-16	14
109A	123737	16	71	61	65	87	67	66	-36	-39	-15	90	98	72	24	-36	104	82	-17	-16	14
109B	123737	16	71	61	65	87	67	66	-36	-39	-15	90	98	72	24	-36	104	82	-17	-16	14
109C	123737	16	71	61	65	87	67	66	-36	-39	-15	90	98	72	24	-36	104	82	-17	-16	14
110	123737	16	71	61	65	87	67	66	-36	-39	-15	90	98	72	24	-36	104	82	-17	-16	14
110A	123737	16	71	61	65	87	67	66	-36	-39	-15	90	98	72							



APPENDIX E - COMPUTER PROGRAMME DESCRIPTION

### E.1 PROGRAMME TO CALCULATE ACTIONS ON A REINFORCED CONCRETE SECTION

This programme is described in Sections 7.3.3 and 7.3.4.

The values of steel strain and concrete strain measured at any section defined a linear strain profile from which the strains at the top and bottom surface could be calculated for input into subroutines CONACT and STEEL which were used to compute the concrete and steel actions within the section.

### E.2 SUBROUTINES CONACT AND STEEL

The following assumptions were made in deriving the subroutines:

- (i) The strain profile was linear across the section.
- (ii) When the neutral axis lay within the section, all concrete subject to tensile strain was assumed to carry no tensile stress once the maximum tensile strain in the concrete exceeded the fracture strain.
- (iii) When strain across the section was tensile at all points in the section, all concrete subject to a strain greater than the fracture strain was assumed to carry no tension.
- (iv) The stress-strain relationship for steel was tri-linear as defined by Figure E.1(a).

- (v) The stress-strain curve for concrete in tension was linear up to a tensile fracture strain of  $\epsilon_{ct}$  at which the fracture stress was  $f'_c/Q$  (see Figure E.1(b)).
- (vi) The stress-strain curve for concrete in compression was that proposed by Hogenstad et al.,<sup>(2)</sup> and shown in Figure E.1(c).
- (vii) The section was, in general, that of a T-beam.
- (viii) Moments were considered as acting about the mid-depth of the section where the net axial force was considered to act.

#### E.2.1 Subroutine STEEL

Section properties were known and the strain at the levels of top and bottom steel were calculated from the two known values of strain at the top and bottom surface. Stresses could therefore be found from the assumed stress-strain relationship.

#### E.2.2 Subroutine CONACT

Knowledge of the top and bottom surface strains enabled the determination of concrete actions by use of the assumed stress-strain relationships for concrete in tension and compression.

Subroutine CONACT was written as four separate cases depending on the sign of top and bottom strains:

- CASEA - Both top and bottom strains tensile
- CASEB - Top strain compressive, bottom strain tensile

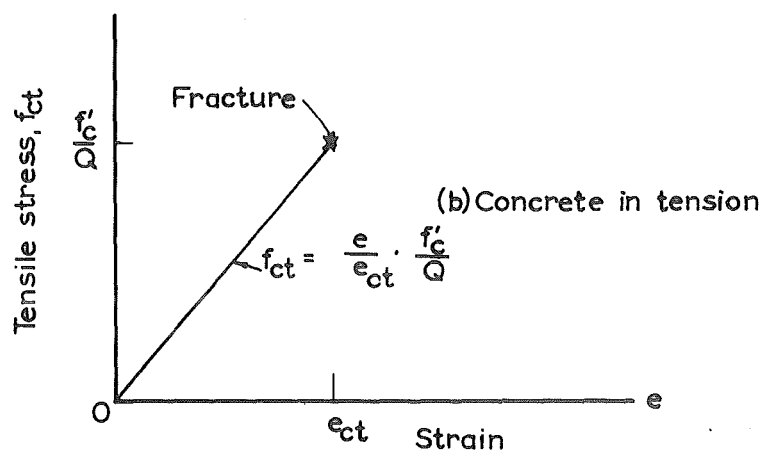
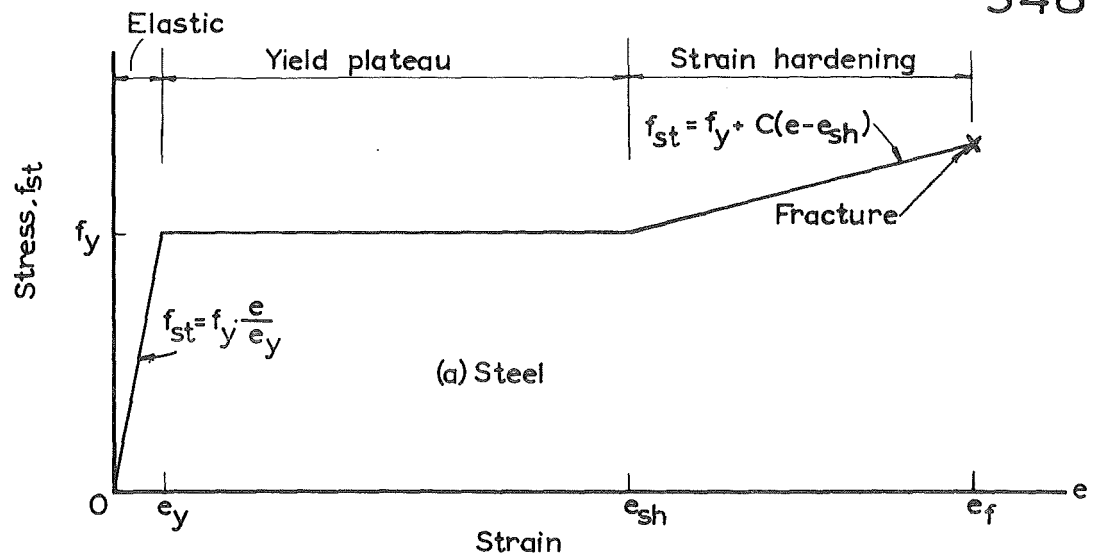
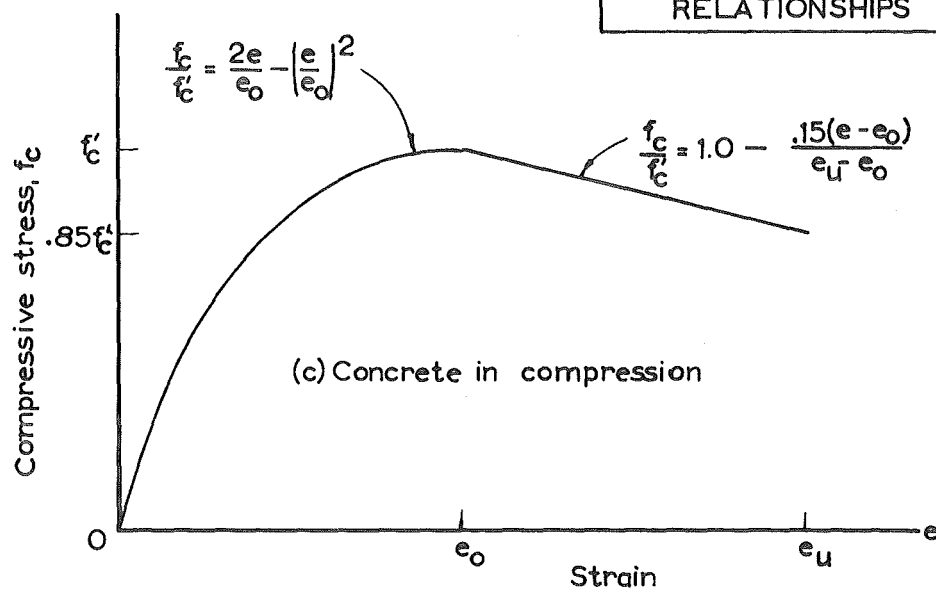


FIGURE E.1 ASSUMED  
STRESS-STRAIN  
RELATIONSHIPS



CASEC - Both top and bottom strains compressive  
 CASED - Top strain tensile, bottom strain compressive.

For each case integration of the stress-strain curve over the appropriate range of strains was performed analytically and the results used in the subroutines for the relevant case.

In computation the flange overhangs of T- or L-beams were ignored initially and the actions on the rectangular portion of the section were found.

To calculate the flange contributions, the strain at the level of the bottom of the flange was used in place of the strain at the bottom of the beam. The flange section was then considered as a rectangular section of different depth and breadth. The subroutines were then used to calculate the moment and force in the flange as related to its mid-depth which were transformed to equivalent actions at the mid-depth of the beam.

Values of the parameters defining the stress-strain curves used in computation were as follows (notation referring to Figure E.1):

$$f'_c = 4350 \text{ psf}, f_y/f'_c = 9.78 \text{ (beam steel)}, = 11.82 \text{ (slab steel)}$$

$$e_y = .0014 \text{ (beam steel)} = .00169 \text{ (slab steel)}$$

$$e_{ct} = .0028, Q = 1.85, e_o = .0028, e_u = .004$$

$$e_{sh} = .0100, e_f = .0101, C = 0.$$



APPENDIX F - RESULTS OF TESTS ON  
CONCRETE SLAB STRIPS

F.1 DESCRIPTION OF TABULATED RESULTS

The results of the tests on three slab strip specimens are tabulated below. The quantities listed are:

- LSN        =   Load Stage Number
- DVT        =   Vertical deflection at mid-span in .0001" units
- DHZ        =   Horizontal movement of the free end in .0001" units.
- CST        =   The average of the two concrete strains in microstrain. The values listed include a correction of -20 microstrain to account for initial loading.
- SST        =   The average of the two steel strains in microstrain. The values listed have included a correction of +15 microstrain for initial load.
- PRF        =   Total load, in pounds, applied to the strip through the proving ring.
- NAPLD      =   The sum of the forces, in pounds, measured in the tie rods used to apply the axial compression to the section.
- NCALC      =   Axial compression calculated from strain readings.

MAPLD = Total moment about mid-depth applied to  
the mid-span section.

MCALC = Moment calculated from strain readings.

Actions from the strain readings were computed using the subroutines CONACT and STEEL. The values of the parameters defining the stress-strain curves are given in the table and correspond to those given in Figure E.1. The variable, SR, is defined by

$$SR = f_y / f'_c = FY / FCDASH$$

SLAB STRP NC.1 JULY 1968

ECT= 0.800E-03 EC = 0.250E-02 EU = 0.650E-02 Q = 0.5000  
 EY= 0.169E-02 EP = 0.200E-01 FF = 0.100E-01 C = 0.0  
 SR = 11.400FC DASH = 4400.0

LSN	DVT	DHZ	CST	SST	PRF	NAPLD	NCALC	MAPLD	MCALC
1	0	0	-20	15	0.	0	101.	323	333.
2	0	-2	-44	0	0.	1007	1164.	323	450.
3	0	-11	-61	-24	0.	2019	2363.	323	370.
4	10	-11	-83	-40	0.	2995	3434.	324	422.
5	10	-11	-103	-52	0.	3993	4469.	326	541.
6	15	-11	-121	-63	0.	5005	5581.	319	937.
7	15	-11	-138	-73	50.	4987	5581.	613	888.
8	15	-11	-155	-83	50.	3999	4591.	607	849.
9	15	-11	-172	-93	50.	2999	3501.	603	801.
10	15	-11	-189	-103	50.	1999	2528.	597	716.
11	20	-11	-206	-113	50.	8999	1124.	598	716.
12	20	-11	-223	-123	50.	34	199.	598	716.
13	20	-11	-240	-133	100.	32	235.	598	716.
14	20	-11	-257	-143	100.	1016	1233.	598	716.
15	20	-11	-274	-153	100.	2031	2221.	598	716.
16	20	-11	-291	-163	100.	3033	3229.	598	716.
17	20	-11	-308	-173	100.	4013	4371.	598	716.
18	20	-11	-325	-183	100.	5011	5540.	598	716.
19	20	-11	-342	-193	100.	6000	6464.	598	716.
20	20	-11	-359	-203	100.	3999	4411.	598	716.
21	20	-11	-376	-213	100.	3015	3455.	598	716.
22	20	-11	-393	-223	100.	2003	2340.	598	716.
23	20	-11	-410	-233	100.	1015	1301.	598	716.
24	20	-11	-427	-243	100.	1148	1266.	598	716.
25	20	-11	-444	-253	100.	1183	1558.	598	716.
26	20	-11	-461	-263	100.	1173	1490.	598	716.
27	20	-11	-478	-273	100.	1164	1440.	598	716.
28	20	-11	-495	-283	100.	1155	1358.	598	716.
29	20	-11	-512	-293	100.	1148	1266.	598	716.
30	20	-11	-529	-303	100.	1139	1197.	598	716.
31	20	-11	-546	-313	100.	1130	1124.	598	716.
32	20	-11	-563	-323	100.	1121	1051.	598	716.
33	20	-11	-580	-333	100.	1112	978.	598	716.
34	20	-11	-597	-343	100.	1103	905.	598	716.
35	20	-11	-614	-353	100.	1094	832.	598	716.
36	20	-11	-631	-363	100.	1085	759.	598	716.
37	20	-11	-648	-373	100.	1076	686.	598	716.
38	20	-11	-665	-383	100.	1067	613.	598	716.
39	20	-11	-682	-393	100.	1058	540.	598	716.
40	20	-11	-699	-403	100.	1049	467.	598	716.
41	20	-11	-716	-413	100.	1040	394.	598	716.
42	20	-11	-733	-423	100.	1031	321.	598	716.
43	20	-11	-750	-433	100.	1022	248.	598	716.
44	20	-11	-767	-443	100.	1013	175.	598	716.
45	20	-11	-784	-453	100.	1004	102.	598	716.
46	20	-11	-801	-463	100.	995	29.	598	716.
47	20	-11	-818	-473	100.	986	-44.	598	716.
48	20	-11	-835	-483	100.	977	-117.	598	716.
49	20	-11	-852	-493	100.	968	-190.	598	716.
50	20	-11	-869	-503	100.	959	-263.	598	716.
51	20	-11	-886	-513	100.	950	-336.	598	716.
52	20	-11	-903	-523	100.	941	-409.	598	716.

LSN	DVT	DHZ	CST	SST	PRF	NAPLD	NCALC	MAPLD	MCALC
53	225	4	-254	97	400.	4041	3851.	2613	3327.
54	235	-5	-281	72	400.	5042	4846.	2641	3454.
55	255	-4	-293	87	450.	5047	4934.	2627	3381.
56	255	3	-277	103	450.	4041	3954.	2699	3687.
57	250	10	-256	120	450.	3062	2954.	2874	3630.
58	241	19	-232	137	450.	2038	1902.	2847	3535.
59	240	25	-211	156	450.	1046	862.	2823	3486.
60	240	32	-192	180	450.	32	-241.	2769	3490.
61	4129	395	-105	2150	300.	55	-151.	1935	1771.
62	3940	396	-79	1840	300.	54	-190.	1444	1397.
63	3680	382	-53	1458	100.	56	-514.	893	1244.
64	3358	389	-26	1044	0.	58	-491.	342	800.
65	2812	399	-78	559	0.	1038	398.	614	919.
66	2640	371	-124	178	0.	2030	1143.	1038	1047.
67	2030	270	-168	-322	0.	3023	1956.	1031	1081.
68	700	-7	-176	-722	0.	4029	2320.	605	917.
69	419	-575	-195	-813	0.	5035	2574.	533	1004.
70	510	-555	-245	-733	150.	5023	3012.	1404	1410.
71	649	-538	-300	-562	300.	5061	3420.	2301	1901.
72	1065	-468	-361	-41	450.	5086	3615.	333	1632.
73	430	-362	-198	-75	0.	476	2987.	330	1632.
74	1678	-279	-36	346	0.	-42	-293.	315	708.
75	1679	-262	-30	830	0.	-42	-293.	315	708.
76	1290	-63	325	0.	0.	957	476.	446	716.
77	695	-485	-105	-297	0.	1776	1297.	460	932.
78	-482	-137	-566	0.	0.	2941	1816.	517	917.
79	421	-52	-51	73	0.	3971	2198.	430	815.
80	391	-562	-183	-797	0.	4969	2503.	517	969.
81	423	-659	-776	50.	50.	4959	6838.	807	4883.
82	452	-558	-226	-754	100.	4951	2837.	1096	1264.
83	485	-552	-243	-728	150.	4947	2984.	1387	1406.
84	515	-543	-261	-698	200.	4945	3077.	1677	1549.
85	468	-543	-261	-698	200.	3967	2577.	1058	1411.
86	532	-525	-175	-525	100.	2983	2166.	1031	1022.
87	1018	-429	-143	109	100.	1930	1384.	1069	1149.
88	1641	-331	-106	716	100.	1032	569.	969	1220.
89	2385	-172	-63	1208	0.	25	-229.	217	1277.
90	355	-621	-196	-811	0.	4979	2573.	1660	1564.
91	478	-703	-598	-237	200.	3948	2831.	1624	1433.
92	511	-598	-237	-598	200.	2964	2158.	104	1603.
93	951	-500	-213	2	200.	1953	1353.	1750	1753.
94	1679	-382	-181	672	200.	921	520.	1446	1786.
95	2429	-355	-135	1184	200.	4969	2573.	1660	1564.
96	3125	-198	-307	1924	300.	3929	2892.	2346	2059.
97	638	-658	-282	-69	300.	2944	2108.	2305	2210.
98	950	-588	-282	-69	300.	1934	1283.	2305	2210.
99	1653	-450	-251	581	300.	4953	3614.	2305	2210.
100	2755	-320	-217	1253	300.	4961	3558.	2305	2210.
101	3355	-248	-170	1723	300.	4961	3558.	2305	2210.
102	1030	-610	-351	-92	400.	2932	2067.	3401	2650.
103	1470	-921	-321	371	400.	1973	1658.	3215	2623.
104	2995	-342	-299	1274	400.	949	819.	2960	2491.
105	3512	-351	-255	1712	400.	4936	3648.	2936	2491.
106	4605	-242	-202	2239	400.	3971	2900.	4228	3824.
107	1419	-667	-380	1237	450.	2941	2655.	378	354.
108	3602	-660	-384	1237	450.	195	-184.	324	354.
109	2027	-615	-41	1276	450.	1000	576.	1121	1121.
110	5038	-230	-228	977	0.	1042	576.	1029	1384.
111	4346	-590	-51	977	0.	1095	594.	1346	1632.
112	3959	-661	-100	622	0.	1145	592.	1346	1632.
113	4138	-660	-117	898	50.	1213	664.	1346	1632.
114	4320	-651	-134	1069	100.	1279	773.	1346	1632.
115	4722	-646	-149	1279	150.	1305	823.	1346	1632.
116	4722	-646	-149	1279	150.	1305	823.	1346	1632.
117	4971	-622	-184	1709	250.	1346	1632.	1346	1632.
118	5197	-615	-202	1921	300.	1346	1632.	1346	1632.
119	5379	-609	-217	2097	350.	1346	1632.	1346	1632.
120	5655	-607	-234	2278	400.	1346	1632.	1346	1632.
121	6065	-605	-256	2312	450.	1346	1632.	1346	1632.
122	6400	-607	-274	2304	381.	1346	1632.	1346	1632.
123	6808	-572	-247	2293	370.	1346	1632.	1346	1632.
124	7309	-540	-248	2384	355.	1346	1632.	1346	1632.
125	8255	-588	-243	2141	302.	1346	1632.	1346	1632.
126	8922	-554	-234	2066	301.	1346	1632.	1346	1632.
127	9579	-525	-224	1761	281.	1346	1632.	1346	1632.
128	10366	-754	-201	1570	281.	1346	1632.	1346	1632.
129	11140	-754	-181	1399	296.	1346	1632.	1346	1632.
130	12508	-797	-149	1487	339.	1346	1632.	1346	1632.
131	13370	-890	-143	1462	347.	1346	1632.	1346	1632.
132	16000	-1221	-141	1314	356.	1346	1632.	1346	1632.

SLAB

STRP

NC.3

JULY

1968

ECT= 0.800E-03 EC = 0.250E-02 EU = 0.650E-02 O = 0.5000  
EY= 0.169E-02 EF = 0.200E-01 EF = 0.100E-01 C = 0.0  
SR = 11.400FCDASH = 4400.0

LSN	DVT	DHZ	CST	SST	PRF	NAPLD	NCALC	NAPLC	NCALC
1	0	0	-20	15	0.	0	101.	323	333.
2	20	3	-35	29	50.	113.	598	600.	600.
3	38	4	-49	41	100.	8	98.	873	856.
4	55	5	-64	54	150.	109.	109.	1145	1122.
5	72	8	-77	62	200.	128.	128.	1423	1402.
6	95	9	-94	75	250.	169	169.	1698	1652.
7	114	10	-110	95	300.	113.	113.	1973	1941.
8	131	10	-123	109	350.	8	53.	2248	2193.
9	150	10	-140	123	400.	10	42.	2523	2489.
10	170	11	-157	137	450.	11	87.	2798	2778.
11	189	13	-173	156	500.	13	-54.	3073	3101.
12	209	16	-190	180	550.	16	-294.	3348	3471.
13	570	130	-610	1751	202.	66	2591.	1437	4105.
14	373	121	-231	1041	0.	40	1257.	324	2275.
15	51	83	-165	-129	0.	5020	8319.	343	284.
16	71	83	-186	-113	50.	5018	8330.	343	660.
17	94	83	-205	-94	100.	5016	8194.	620	1048.
18	115	83	-224	-79	150.	5016	8177.	1205	1397.
19	138	83	-247	-60	200.	5014	8118.	1492	1829.
20	158	83	-270	-39	250.	5012	8026.	1777	2272.
21	179	83	-298	-14	300.	5007	7944.	2062	2784.
22	200	83	-325	13	350.	5006	7884.	2348	3197.
23	225	76	-362	54	400.	5008	7882.	2633	3653.
24	251	75	-406	102	450.	5012	8031.	2923	4103.
25	285	78	-464	169	500.	5018	8320.	3216	4628.
26	321	80	-530	249	550.	5028	8677.	3509	5171.
27	368	81	-616	350	600.	5043	9264.	3808	5844.
28	419	85	-716	469	650.	5065	9992.	4110	6584.
29	470	90	-811	569	700.	5096	10550.	4412	7235.
30	70	50	-207	-126	0.	4992	9239.	357	745.
31	60	75	-184	-99	0.	4003	7822.	347	797.
32	81	79	-204	-78	50.	4003	7658.	630	1214.
33	101	80	-222	-60	100.	4004	7522.	913	1586.
34	124	81	-242	-40	150.	4008	7379.	1197	1995.
35	145	81	-265	-16	200.	4011	7209.	1481	2460.
36	170	83	-294	16	250.	4009	7052.	1768	2927.
37	199	86	-337	129	300.	4014	7074.	2036	3436.
38	225	89	-385	129	350.	4022	7193.	2339	3901.
39	265	90	-452	211	400.	4034	7499.	2629	4469.
40	308	95	-531	309	450.	4054	8014.	2922	5095.
41	359	100	-623	432	500.	4081	8599.	3219	5777.
42	409	105	-712	557	550.	4109	9142.	3516	6403.
43	470	114	-814	719	600.	4151	9645.	3818	7065.
44	61	73	-191	-99	0.	4008	7989.	347	868.
45	55	79	-166	-75	0.	3007	6638.	333	1573.
46	76	80	-186	-55	50.	3003	6477.	630	1754.
47	100	80	-207	-31	100.	3003	6244.	903	2113.
48	121	81	-235	7	150.	3010	5994.	1184	2413.
49	150	84	-273	48	200.	3013	5875.	1468	2810.
50	181	83	-322	123	250.	3024	5955.	1752	3352.
51	230	93	-415	341	300.	3047	6399.	2043	3899.
52	282	100	-500	372	350.	3079	6944.	2334	4762.

LSN	DVT	DHZ	CST	SST	PRF	NAPLD	NCALC	NAPLC	NCALC
53	348	109	-611	533	400.	3120	7525.	2631	5488.
54	408	116	-702	694	450.	3156	7941.	2926	6079.
55	470	121	-796	869	500.	3203	8345.	3223	6662.
56	56	80	-168	-73	0.	3011	6607.	339	910.
57	59	88	-153	-32	0.	1933	4945.	334	1211.
58	82	89	-184	4	50.	1998	4636.	614	1842.
59	116	90	-233	73	100.	2014	4434.	896	2423.
60	145	98	-318	202	150.	2035	4773.	1181	3127.
61	231	105	-419	374	200.	2077	5249.	1470	3861.
62	302	115	-520	565	250.	2125	5710.	1762	4541.
63	381	126	-622	771	300.	2179	6160.	2056	5198.
64	440	132	-695	933	350.	2216	6426.	2345	5640.
65	505	141	-780	1113	400.	2266	6766.	2637	6155.
66	58	89	-161	-24	0.	2006	4877.	336	1382.
67	105	100	-209	191	0.	2006	4877.	336	1382.
68	183	112	-306	408	50.	993	2658.	333	1979.
69	259	124	-391	610	100.	1047	3024.	807	2189.
70	335	135	-478	813	150.	1099	3377.	901	2485.
71	406	145	-560	1010	200.	1157	3781.	1186	3766.
72	479	158	-645	1208	250.	1204	4145.	1471	4298.
73	548	163	-727	1399	300.	1250	4536.	1757	4844.
74	610	168	-804	1570	350.	1294	4907.	2043	5362.
75	692	170	-903	1766	400.	1337	5272.	2329	5846.
76	170	116	-266	267	0.	1397	5861.	2619	6433.
77	340	159	-343	550	0.	1063	3185.	341	2450.
78	431	171	-444	1203	50.	44	1600.	324	2420.
79	506	181	-528	1423	100.	49	2036.	335	3112.
80	589	192	-609	1661	150.	49	2445.	875	3753.
81	702	202	-693	1943	200.	51	3133.	1151	4181.
82	840	221	-773	2216	250.	51	3502.	1426	4536.
83	1005	239	-859	2523	300.	48	3502.	1702	4844.
84	1200	255	-958	2836	350.	45	3863.	1977	5159.
85	1408	278	-1029	4900	400.	53	4339.	2254	5547.
86	1772	312	-1159	5350	450.	78	2836.	2359	4500.
87	2004	332	-1262	7900	500.	181	3374.	2497	4958.
88	2516	370	-1500	11500	550.	279	2585.	2504	4367.
89	3008	404	-1758	3020	600.	279	2585.	2842	4367.
90	3502	435	-2017	3020	650.	525	*****	3099	*****
91	4012	462	-2297	3020	700.	779	14275.	3282	4725.
92	4505	490	-2575	3020	750.	1026	16819.	3302	10254.
93	5000	512	-2863	3020	800.	1257	19404.	3513	11639.
94	5550	521	-3150	3020	850.	1449	21772.	3777	12799.
95	6010	529	-3389	3020	900.	1625	23970.	3912	13711.
96	6500	530	-3626	3020	950.	1791	25922.	4042	14399.
97	6750	529	-3749	3020	1000.	1894	27393.	4120	14830.
98	7010	529	-3859	3020	1050.	1979	28722.	4255	15153.
99	725	529	-3982	3020	1100.	2017	29368.	4255	15153.
100	7505	529	-4046	3020	1150.	2046	29921.	4255	15153.
101	7755	529	-4133	3020	1200.	2066	30420.	4255	15153.
102	8014	529	-4228	3020	1250.	2079	30823.	4255	15153.
103	8120	529	-4275	3020	1300.	2090	31234.	4255	15153.
104	8260	528	-4323	3020	1350.	2089	31627.	4255	15153.
105	8489	528	-4395	3020	1400.	2089	31828.	4255	15153.
106	9001	524	-4634	3020	1450.	2078	32031.	4255	15153.
107	9490	524	-4655	3020	1500.	2065	32327.	4255	15153.
108	10004	522	-4788	3020	1550.	2016	32877.	4191	15707.
109	10529	522	-4822	3020	1600.	1941	33343.	4074	15721.
110	11530	521	-5075	3020	1650.	1832	33823.	3988	15724.
111	13459	521	-5075	3020	1700.	1678	34289.	3799	15715.
112	17460	520	-5075	3020	1750.	1313	34792.	3486	15692.
113	0	0	-2630	3020	1800.	374	34846.	3241	15689.
						17	36870.	2588	15425.
						-2115	1232.	323	-965.

LSN	DVT	DHZ	CST	SST	PRF	NAPLC	NALC	MAPLC	MCALC	SLAH	STRP	NC.2	JULY	1968
1	0	0	-20	15	0.	0	101.	323	333.					
2	0	0	-38	2	0.	998	934.	323	412.					
3	5	-11	-60	-14	0.	1998	2010.	323	470.					
4	8	-18	-80	0.	0.	2997	3114.	323	474.					
5	13	-21	-100	43	0.	4011	4234.	323	563.					
6	19	-25	-127	-64	0.	5006	5319.	323	604.					
7	40	-22	-144	50	0.	4998	5332.	323	617.					
8	21	-159	-191	100	0.	4987	5319.	323	617.					
9	18	-70	-175	-26	100	4983	5319.	323	617.					
10	9	-18	-191	-14	200	4979	5335.	323	617.					
11	11	-15	-206	-3	200	4974	5352.	323	617.					
12	132	-12	-222	9	300	4968	5375.	323	617.					
13	150	-10	-239	22	300	4966	5376.	323	617.					
14	170	-9	-253	34	400	4953	5381.	323	617.					
15	29	-25	-271	47	0.	4950	5403.	323	617.					
16	35	-20	-286	-34	50	4028	4331.	323	617.					
17	52	-10	-300	-11	150	4022	4329.	323	617.					
18	70	-15	-315	1	200	4014	4350.	323	617.					
19	89	-12	-330	13	250	4012	4351.	323	617.					
20	105	-10	-344	25	300	4014	4353.	323	617.					
21	122	-8	-359	37	350	4018	4354.	323	617.					
22	140	-1	-374	50	400	4018	4351.	323	617.					
23	160	-22	-389	62	400	4036	4316.	323	617.					
24	20	-11	-404	74	0.	3022	3269.	323	617.					
25	35	-10	-419	86	0.	3015	3225.	323	617.					
26	52	-10	-434	98	0.	3016	3283.	323	617.					
27	70	-4	-449	110	0.	3015	3292.	323	617.					
28	89	-4	-464	122	0.	3011	3304.	323	617.					
29	105	-1	-479	134	0.	3009	3294.	323	617.					
30	122	3	-494	146	0.	3009	3294.	323	617.					
31	140	3	-509	158	0.	3005	3285.	323	617.					
32	160	3	-524	170	0.	3023	3250.	323	617.					
33	19	-3	-539	182	0.	2027	2122.	323	617.					
34	35	-11	-554	194	0.	2028	2233.	323	617.					
35	52	-6	-569	206	0.	2028	2233.	323	617.					
36	70	-4	-584	218	0.	2028	2233.	323	617.					
37	89	-4	-599	230	0.	2028	2233.	323	617.					
38	105	-1	-614	242	0.	2028	2233.	323	617.					
39	122	3	-629	254	0.	2028	2233.	323	617.					
40	140	3	-644	266	0.	2028	2233.	323	617.					
41	160	3	-659	278	0.	2028	2233.	323	617.					
42	19	-3	-674	290	0.	2028	2233.	323	617.					
43	35	-11	-689	302	0.	2028	2233.	323	617.					
44	52	-6	-704	314	0.	2028	2233.	323	617.					
45	70	-4	-719	326	0.	2028	2233.	323	617.					
46	89	-4	-734	338	0.	2028	2233.	323	617.					
47	105	-1	-749	350	0.	2028	2233.	323	617.					
48	122	3	-764	362	0.	2028	2233.	323	617.					
49	140	3	-779	374	0.	2028	2233.	323	617.					
50	160	3	-794	386	0.	2028	2233.	323	617.					
51	19	-3	-809	398	0.	2028	2233.	323	617.					
52	35	-11	-824	410	0.	2028	2233.	323	617.					
53	52	-6	-839	422	0.	2028	2233.	323	617.					
54	70	-4	-854	434	0.	2028	2233.	323	617.					
55	89	-4	-869	446	0.	2028	2233.	323	617.					
56	105	-1	-884	458	0.	2028	2233.	323	617.					
57	122	3	-899	470	0.	2028	2233.	323	617.					
58	140	3	-914	482	0.	2028	2233.	323	617.					
59	160	3	-929	494	0.	2028	2233.	323	617.					
60	19	-3	-944	506	0.	2028	2233.	323	617.					
61	35	-11	-959	518	0.	2028	2233.	323	617.					
62	52	-6	-974	530	0.	2028	2233.	323	617.					
63	70	-4	-989	542	0.	2028	2233.	323	617.					
64	89	-4	-1004	554	0.	2028	2233.	323	617.					
65	105	-1	-1019	566	0.	2028	2233.	323	617.					
66	122	3	-1034	578	0.	2028	2233.	323	617.					
67	140	3	-1049	590	0.	2028	2233.	323	617.					
68	160	3	-1064	602	0.	2028	2233.	323	617.					
69	19	-3	-1079	614	0.	2028	2233.	323	617.					
70	35	-11	-1094	626	0.	2028	2233.	323	617.					
71	52	-6	-1109	638	0.	2028	2233.	323	617.					
72	70	-4	-1124	650	0.	2028	2233.	323	617.					
73	89	-4	-1139	662	0.	2028	2233.	323	617.					
74	105	-1	-1154	674	0.	2028	2233.	323	617.					
75	122	3	-1169	686	0.	2028	2233.	323	617.					
76	140	3	-1184	698	0.	2028	2233.	323	617.					
77	160	3	-1199	710	0.	2028	2233.	323	617.					
78	19	-3	-1214	722	0.	2028	2233.	323	617.					
79	35	-11	-1229	734	0.	2028	2233.	323	617.					
80	52	-6	-1244	746	0.	2028	2233.	323	617.					
81	70	-4	-1259	758	0.	2028	2233.	323	617.					
82	89	-4	-1274	770	0.	2028	2233.	323	617.					
83	105	-1	-1289	782	0.	2028	2233.	323	617.					
84	122	3	-1304	794	0.	2028	2233.	323	617.					
85	140	3	-1319	806	0.	2028	2233.	323	617.					
86	160	3	-1334	818	0.	2028	2233.	323	617.					
87	19	-3	-1349	830	0.	2028	2233.	323	617.					
88	35	-11	-1364	842	0.	2028	2233.	323	617.					
89	52	-6	-1379	854	0.	2028	2233.	323	617.					
90	70	-4	-1394	866	0.	2028	2233.	323	617.					
91	89	-4	-1409	878	0.	2028	2233.	323	617.					
92	105	-1	-1424	890	0.	2028	2233.	323	617.					
93	122	3	-1439	902	0.	2028	2233.	323	617.					
94	140	3	-1454	914	0.	2028	2233.	323	617.					
95	160	3	-1469	926	0.	2028	2233.	323	617.					
96	19	-3	-1484	938	0.	2028	2233.	323	617.					
97	35	-11	-1499	950	0.	2028	2233.	323	617.					
98	52	-6	-1514	962	0.	2028	2233.	323	617.					
99	70	-4	-1529	974	0.	2028	2233.	323	617.					
100	89	-4	-1544	986	0.	2028	2233.	323	617.					

FCT= 0.800E-03 EC = 0.250E-02 EU = 0.650E-02 O = 0.5000  
 EY= 0.169E-02 EH = 0.200E-01 EF = 0.100E-01 C = 0.0  
 SR = 11.400FCDA5H = 4400.0

LSN	DVT	DHZ	CST	SST	PRF	NAPLC	NALC	MAPLC	MCALC
99	460	38	-431	667	700.	3942	3753.	4354	3519.
100	493	43	-453	739	750.	3950	3903.	4642	3708.
101	540	51	-478	846	800.	3967	4053.	4937	3938.
102	676	76	-471	1169	839.	4051	7968.	5213	7151.
103	85	-20	-159	10	0.	3983	1617.	326	1211.
104	71	-20	-133	24	0.	2981	1346.	344	1026.
105	95	-17	-150	37	50.	2982	1505.	626	1161.
106	116	-15	-166	53	100.	2980	1652.	907	1290.
107	139	-11	-184	84	150.	2978	1812.	1193	1471.
108	163	-9	-204	124	200.	2975	1980.	1471	1607.
109	189	-2	-225	171	250.	2987	2138.	1757	1799.
110	241	-2	-249	244	300.	2999	2305.	2045	2025.
111	257	-1	-275	341	350.	3018	2458.	2334	2232.
112	282	21	-293	448	400.	3037	2582.	2623	2457.
113	380	30	-316	595	450.	3061	2725.	2914	2681.
114	429	39	-339	698	500.	3083	2869.	3205	2902.
115	478	48	-362	797	550.	3104	3014.	3493	3185.
116	520	55	-385	900	600.	3126	3126.	3785	3337.
117	570	65	-409	1016	650.	3138	3294.	4076	3569.
118	639	79	-431	1182	690.	3183	3377.	4300	3814.
119	89	-19	-139	62	0.	2958	1049.	349	1026.
120	78	-11	-108	62	0.	1938	1066.	338	860.
121	100	-10	-124	87	50.	1946	1208.	617	996.
122	129	-7	-142	141	100.	1954	1361.	898	1167.
123	153	-3	-163	232	150.	1959	1495.	1181	1368.
124	220	10	-186	333	200.	1999	1646.	1466	1567.
125	273	20	-204	463	250.	2022	1733.	1753	1802.
126	328	30	-226	591	300.	2031	1856.	2040	2035.
127	376	39	-248	698	350.	2040	1979.	2232	2185.
128	428	50	-271	814	400.	2059	2132.	2612	2487.
129	478	59	-291	922	450.	2113	2247.	2899	2692.
130	529	70	-315	1050	500.	2148	2385.	3175	2935.
131	589	85	-339	1221	550.	2183	2548.	3493	3200.
132	100	-2	-107	122	0.	1980	1026.	342	876.
133	108	3	-86	156	0.	952	803.	333	771.
134	160	11	-127	257	50.	84	769.	639	990.
135	218	21	-121	437	100.	1010	909.	995	1191.
136	271	31	-136	572	150.	1039	964.	1176	1372.
137	328	41	-152	710	200.	1064	1036.	1457	1560.
138	381	51	-168	833	250.	1092	1186.	1708	1808.
139	440	61	-184	963	300.	1120	1299.	2022	2088.
140	493	73	-204	1089	350.	1147	1474.	2304	2306.
141	565	89	-223	1273	400.	1190	1526.	2590	2549.
142	639	100	-246	1500	450.	1219	1661.	2914	2914.
143	718	40	-263	1620	500.	126	151.	323	699.
144	282	46	-82	746	90.	29	985.	598	904.
145	340	56	-100	878	100.	27	185.	737	1117.
146	400	66	-107	1029	150.	26	206.	1149	1361.
147	460	80	-122	1184	200.	42	389.	1424	1609.
148	272	50	-36	719	0.	23	-150.	323	690.
149	96	-4	-72	163	0.	2016	700.	342	635.
150	150	10	-118	298	100.	10	1036.	342	635.
151	243	20	-151	409	200.	2061	1246.	1473	1380.
152	370	45	-205	708	300.	2128	1565.	2051	1949.
153	440	66	-226	833	400.	2188	1828.	2630	2485.
154	509	88	-252	1118	450.	2253	2093.	2914	2688.
155	605	98	-300	1255	500.	2243	2090.	3208	2946.
156	673	100	-326	1391	550.	2277	2235.	3501	3212.
157	741	120	-350	1500	600.	2315	2385.	3814	3522.
158	901	148	-379	1829	650.	2425	2627.	4116	3822.
159	1065	178	-434	2082	700.	2534	3035.	4442	4125.
160	1188	196	-498	2216	650.	2015	2701.	4125	3879.
161	1551	270	-443	2444	690.	2351	3118.	4503	4185.
162	1681	285	-455	2535	687.	2445	3579.	4513	2419.
163	1811	300	-468	2671	709.	2535	4012.	4513	2419.
164	3602	480	-658	5166	714.	3519	6171.	5517	5010.
165	4340	536	-820	5545	692.	3708	8747.	5779	4726.
166	4350	538	-829	5560	693.	3769	8993.	5843	4888.
167	4370	540	-837	5572	694.	3809	9209.	5917	4949.
168	4801	569	-897	5521	629.	3922	9343.	5665	5109.
169	5000	581	-914	5504	624.	3979	9474.	5722	5294.
170	5250	602	-935	5440	644.	4043	9626.	5768	5424.
171	5499	628	-961	5368	667.	4114	9774.	5817	5579.
172	5752	650	-981	5434	667.	4144	9943.	5825	5715.
173	6255	686	-1019	5381	511.	4213	10413.	5884	5772.
174	6500	701	-1035	5372	512.	4243	10304.	5896	5804.
175	6750	715	-1051	5372	513.	4273	10154.	5908	5836.
176	7000	723	-1025	5360	470.	4275	9933.	5899	6224.
177	7259	736	-1028	5370	443.	4280	9621.	5848	6510.
178	7641	773	-1067	5373	443.	4310	9403.	5848	6510.
179	7979	1761	-1653	2021	250.	4987	3414.	4532	5559.
180	1551	PSA	-777	11610	333.	12	1552.	2174	3022.

REFERENCES

1. THOMAS, F.G. "Studies in Reinforced Concrete, Part VIII, The Strength and Deformation of Some Reinforced Concrete Slabs Subjected to Concentrated Loading". D.S.I.R. Building Research Station Technical Paper No. 25, H.M.S.O., 1939.
2. JOHANSEN, K.W. "Yield-Line Theory". Cement and Concrete Association, London, 1962.
3. OCKLESTON, A.J. "Load Tests on a Three-Storey Reinforced Concrete Building in Johannesburg". Structural Engineer, Vol. 33, October, 1955.
4. OCKLESTON, A.J. "Arching Action in Reinforced Concrete Slabs". Structural Engineer, Vol. 36, June, 1958.
5. OCKLESTON, A.J. "Loading Tests on Reinforced Concrete Slabs Spanning in Two Directions". Paper No. 6, Portland Cement Institute, Richmond, Johannesburg, 1958.
6. POWELL, D.S. "The Ultimate Strength of Concrete Panels Subjected to Uniformly Distributed Loads". Cambridge University Thesis, 1956.
7. WOOD, R.H. "Plastic and Elastic Design of Slabs and Plates". Thames and Hudson, 1961.
8. LIEBENBERG, A.C. "Arch Action in Concrete Slabs" Pretoria, South Africa, CSIR Research Report 234, 1966.
9. LIEBENBERG, A.C. "Arch Action in Reinforced Concrete Slabs" Proceedings. South African Institution of Civil Engineers, Jubilee Issue, 1963.
10. CHRISTIANSEN, K.P. "The Effect of Membrane Stresses on the Ultimate Strength of the Interior Panel in a Reinforced Concrete Slab". Structural Engineer. Vol. 41, August 1963.
11. PARK, R. "The Ultimate Strength of Uniformly Loaded Laterally Restrained Rectangular Two-Way Slabs". Ph.D. Thesis, University of Bristol, 1964.

12. PARK, R. "Ultimate Strength of Rectangular Concrete Slabs Under Short-Term Uniform Loading With Edges Restrained Against Lateral Movement". Proc. Instn civ. Engrs, Vol. 28, June, 1964.
13. PARK, R. "The Ultimate Strength and Long-Term Behaviour of Uniformly Loaded Two-Way Concrete Slabs With Partial Lateral Restraint at All Edges." Magazine of Concrete Research, Vol. 16, No. 48, September 1964.
14. TAYLOR, R. "A Note on a Possible Basis for a New Method of Ultimate Load Design of Reinforced Concrete Slabs". Magazine of Concrete Research, Vol. 17, No. 53, December, 1965.
15. BROTHIE, J.F., JACOBSON, A., and OKUBO, S. "Effect of Membrane Action on Slab Behaviour". Research Report R65-25, School of Engineering, Massachusetts Institute of Technology, August, 1965.
16. GURFINKEL, G.R. "Analysis of Behaviour of Reinforced Concrete Beams Restrained at the Ends Against Longitudinal Displacements". Ph.D. Thesis, University of Illinois, Urbana, Illinois, 1966.
17. KEMP, K.O. "Yield of a Square Reinforced Concrete Slab on Simple Supports Allowing For Membrane Forces." Structural Engineer, Vol. 45, July, 1967.
18. MORLEY, C.T. "Yield-line Theory For Reinforced Concrete Slabs at Moderately Large Deflexions." Magazine of Concrete Research, Vol. 19, No. 61. December, 1967.
19. HAYES, B. "Allowing for Membrane Action in the Plastic Analysis of Rectangular Reinforced Concrete Slabs." Magazine of Concrete Research, Vol. 20, No. 65. December, 1968.
20. HOGNESTAD, E., HANSON, N.W., and McHENRY, D. "Concrete Stress Distribution in Ultimate Strength Design". Journal of the American Concrete Institute, Vol. 52, December, 1955.
21. CARR, A.J. "Refined Finite Element Analysis of Thin Shells Including Dynamic Loadings". Ph.D. Dissertation, University of California, Berkeley, 1967.
22. PARK, R. "Limit Design of Beams for Two-Way Reinforced Concrete Slabs". Structural Engineer, Vol. 46, September, 1968.

23. ALAMI, Z.Y., and FERGUSON, P.M. "Accuracy of Models Used in Research on Reinforced Concrete". Journal of the A.C.I. Vol. 60, September, 1963.
24. GAMBLE, W.L., SOZEN, M.A., and Siess, C.P. "An Experimental Study of a Reinforced Concrete Two-Way Floor Slab." Structural Research Series No. 211, University of Illinois, Urbana, Illinois, June, 1961.
25. HATCHER, D.S., SOZEN, M.A., and SIESS, C.P. "A Study of Tests on a Flat Plate and Flat Slab." Structural Research Series No. 217. University of Illinois, Urbana, Illinois, July 1961.
26. VANDERBILT, M.D., SOZEN, M.A., and SIESS, C.P. "An Experimental Study of a Reinforced Concrete Two-Way Floor Slab With Shallow Beams." Structural Research Series No. 228, University of Illinois, Urbana, Illinois. October, 1961.
27. BASE, G.D., READ, J.B., BEEBY, A.W., and TAYLOR, H.P.J. "An Investigation of the Crack Control Characteristics of Various Types of Bar in Reinforced Concrete Beams." Cement and Concrete Association. Research Report 18, Part 2, December, 1966.
28. LITTLE, W.A., and PAPARONI, M. "Size Effect in Small Scale Models of Reinforced Concrete Beams". Journal of the A.C.I. Vol 63, November, 1966.
29. KAAR, P.H. and MATTOCK, A.H. "High Strength Bars as Concrete Reinforcement: Part 4 - Control of Cracking". Journal of the Portland Cement Association, Vol. 5, No. 1, January 1963.
30. COMITE EUROPEEN DU BETON. "Recommendations for an International Code of Practice for Reinforced Concrete." ACI - C and CA, London, 1964.
31. KAAR, P.H. "High Strength Bars as Concrete Reinforcement. Part 8: Similitude in Flexural Cracking of T-Beam Flanges". Journal of the PCA, Vol. 8, No. 2, May 1966.
32. GERGELY, P. and LUTZ, L.A. "Maximum Crack Width in Reinforced Concrete Flexural Members." Causes, Mechanism, and Control of Cracking in Concrete, ACI Publication SP-20, 1968.



- 33. - "SAA Code for Concrete Buildings". Standards Association of Australia, Sydney, Australian Standard No. CA2 - 1958.
- 34. - "Building Code Requirements for Reinforced Concrete" (ACI 318-63). American Concrete Institute, June, 1963.
- 35. - "The Structural Use of Reinforced Concrete in Buildings". British Standard Code of Practice CP 114, 1957.
- 36. - "Basic Design Loads". New Zealand Standard Model Building ByLaw, Chapter 8, December 1965.
- 37. SAWCZUK, A. "Plastic Behaviour of Simply Supported Reinforced Concrete Plates at Moderately Large Deflections". International Journal of Solids and Structures, Vol. 1. No. 1, February, 1965.
- 38. MAGURA, D.D. "Structural Model Testing - Reinforced and Prestressed Mortar Beams". Journal of the PCA, Vol. 9, No. 1, January, 1967.
- 39. BEHERA, U., RAJAGOPALAN, K.S., and FERGUSON, P.M. "Reinforcement for Torque in Spandrel L-Beams". Paper presented at the ASCE National Meeting on Water Resources Engineering, New Orleans, Louisiana, February, 1969.

- oOo -